

A THREE-CHANNEL MICROCOMPUTER SYSTEM FOR QUANTITATIVE
ANALYSIS
OF THE PHONOCARDIOGRAM, ELECTROCARDIOGRAM, AND CAROTID PULSE
SIGNALS

by

Richard J. Lehner

A thesis
presented to the University of Manitoba
in partial fulfillment of the
requirements for the degree of
Master of Science
in
Department of Electrical Engineering

Winnipeg, Manitoba

(c) Richard J. Lehner, 1985

A THREE-CHANNEL MICROCOMPUTER SYSTEM FOR QUANTITATIVE ANALYSIS
OF THE PHONOCARDIOGRAM, ELECTROCARDIOGRAM, AND
CAROTID PULSE SIGNALS

BY

RICHARD J. LEHNER

A thesis submitted to the Faculty of Graduate Studies of
the University of Manitoba in partial fulfillment of the requirements
of the degree of

MASTER OF SCIENCE

© 1985

Permission has been granted to the LIBRARY OF THE UNIVERSITY OF MANITOBA to lend or sell copies of this thesis, to the NATIONAL LIBRARY OF CANADA to microfilm this thesis and to lend or sell copies of the film, and UNIVERSITY MICROFILMS to publish an abstract of this thesis.

The author reserves other publication rights, and neither the thesis nor extensive extracts from it may be printed or otherwise reproduced without the author's written permission.

ABSTRACT

Most diseases of the heart cause changes in the heart sounds and additional murmurs long before other symptoms appear, and hence heart sound analysis by auscultation is the primary test conducted by physicians. The heart sound signal (or phonocardiogram), however, has much more information, which, if analyzed quantitatively in a proper manner could lead to important diagnostic results. A microprocessor-based system is proposed to perform quantitative analysis of the phonocardiogram. The heart sounds are recorded from locations on the chest along with the electrocardiogram (ECG) and carotid pulse signals. The phonocardiogram is segmented into systole and diastole using the ECG and carotid pulse as references. The phonocardiogram is quantified into four parameters representing the time and frequency domain characteristics of the signal. Results of the application of the methods to 47 phonocardiogram signals are presented. This work shows that the parameters of phonocardiogram signals with systolic or diastolic murmurs differ from those of normal signals and hence aid in the detection of murmurs.

ACKNOWLEDGMENTS

I would like to thank Dr. Rangaraj Rangayyan for providing guidance and encouragement and for acting as my thesis supervisor. Dr. Rangayyan's dedication and support is sincerely appreciated.

I would also like to thank Dr. George Collins, Laverne Hastman, R.T. and the staff of the Variety Childrens Heart Centre at the Health Sciences Centre. These people provided an invaluable resource of experience and expertise. The co-operation of the many patients is also acknowledged. Thanks also to Messrs. Jack Sill and Ken Biegen of the Electrical Engineering Department for their assistance in the hardware aspects of the project. I am indebted to many colleagues for their help, particularly Messrs. Jim Slipec, Randall Dembowski, Ken Lam, Dwayne Burek, and J. Winston Brown.

The financial support of this research by the Natural Sciences and Engineering Research Council is also gratefully acknowledged.

CONTENTS

ABSTRACT	v
ACKNOWLEDGMENTS	vi
<u>Chapter</u>	<u>page</u>
I. INTRODUCTION	1
Proposed Method	5
Thesis Outline	7
II. HEART SOUNDS AND PHONOCARDIOGRAPHY	8
Cardiac Physiology	8
The Electrocardiogram	8
The Cardiac Cycle	9
Normal Heart Sounds	12
Murmurs	15
The Carotid Pulse	16
Phonocardiography	20
Auditory Perception of Heart Sounds	20
Relationship Between Heart Sounds, ECG, and Carotid Pulse	21
PCG and Pulse Recording Procedures	22
Review of PCG Signal Processing Techniques	25
Review of ECG and Pulse Signal Processing Techniques	28
III. SYSTEM HARDWARE DESCRIPTION	30
Introduction	30
MC68000 Educational Computer Board	31
Interfacing to the ECB	35
ECB-to-SAAB Interface	37
Data Acquisition System	39
Intel 8231A Arithmetic Processing Unit	48
Digital-to-Analog Conversion Circuitry	53
IV. SIGNAL PROCESSING TECHNIQUES AND SOFTWARE DESCRIPTION	56
Introduction	56
System Initialization	60
Analog-to-Digital Conversion	61
Detection of the QRS-Complex in the ECG	64

Detection of the Dicrotic Notch in the Carotid Pulse	68
PCG Signal Processing	72
Segmentation of PCG into Systole and Diastole	72
PCG Energy Curve	79
PCG Energy Spectrum	80
PCG Energy Distribution Coefficient	87
Summary	88
V. DISCUSSION OF RESULTS	90
VI. CONCLUSIONS AND RECOMMENDATIONS FOR FURTHER STUDY	106
Conclusions	106
Recommendations	107
REFERENCES	109
 <u>Appendix</u>	
A. SAAB SCHEMATIC DIAGRAMS	119
B. SOFTWARE LISTING	126

LIST OF TABLES

<u>Table</u>	<u>page</u>
3.1. Educational Computer Board Memory Map	34
3.2. MC68230 Timer Address Map	34
3.3. MC68000 Memory Enable Signal Address Map	36
3.4. Data Acquisition Control Signal Address Map	41
3.5. Function Table for Multiplexer Control Signals . .	43
3.7. APU Function Table	51
3.8. D/A Control Signal Address Map	54
4.1. Delay Between Second Heart Sound and Dicrotic Notch	77
4.2. Typical Execution Times of the PCG Analysis System Routines	89
5.1. EDC Errors Incurred From Segmentation Errors . . .	94
5.2. Average EDC_t and EDC_f Values	103
5.3. Mean and SD of EDC_t and EDC_f Values	105
A.1. Device Reference	120
A.2. Device Reference	121

LIST OF FIGURES

<u>Figure</u>	<u>page</u>
2.1. Typical Normal ECG Lead	11
2.2. Anterior View of the Opened Heart	11
2.3. The Etiology of Heart Sounds	14
2.4. Phonocardiogram of Patient with Severe Aortic Stenosis	17
2.5. PCG of Patient with Mitral Stenosis	18
2.6. Typical Normal Carotid Pulse Tracing	18
2.7. Normal Phonocardiogram, ECG, and Carotid Pulse Tracings	19
2.8. Locations For Surface Heart Sound Pickups	24
2.9. Block Diagram of the HP1514B ECG/Phono System . .	24
3.1. Block Diagram of PCG Analysis System	32
3.2. MC68000 Memory Enable Signal Decode Logic	36
3.3. ECB DTACK* Signal Generation	38
3.4. Block Diagram of Data Acquisition System	40
3.5. Data Acquisition Control Signal Decode Logic	40
3.6. Active Lowpass Butterworth Filter	41
3.7. Schematic Diagram of LF398 Sample-Hold Unit . . .	43
3.8. Schematic Diagram of CD4051 Analog Multiplexer . .	44
3.9. Schematic Diagram of ADC1210 A/D Converter	46
3.10. A/D Operational Timing Diagram	47
3.11. ADTACK* Signal Generation	47
3.12. ADTACK* Timing Diagram	48

3.13.	Schematic Diagram of INTEL 8231A APU	50
3.14.	APUDTACK* Signal Generation	51
3.15.	APUDTACK* Timing Diagrams	52
3.16.	D/A Circuitry Decode Logic	54
3.17.	Schematic Diagram of DAC1210 D/A Converter	55
4.1.	Signal Processing Flowchart	59
4.2.	MC68000 Status Register	61
4.3.	Analog-to-Digital Conversion Flowchart	63
4.4.	ECG and ECG Transform $g(n)$	66
4.5.	Carotid Pulse and ECG Transform $g(n)$	67
4.6.	Carotid Pulse and Transform $s(n)$	71
4.7.	PCG signal and Corresponding ECG Transform $g(n)$	75
4.8.	PCG signal and Corresponding Carotid Transform $s(n)$	76
4.9.	PCG Segmented into Systole and Diastole	78
4.10.	FFT FORTRAN Source Code	84
4.11.	Square Wave and Corresponding 1024-point DFT	85
4.12.	Pulse and Corresponding 1024-point DFT	86
5.1.	Normal PCG with Simulated Segmentation Errors . .	92
5.2.	PCG with Systolic Murmur and Simulated Segmentation Errors	93
5.3.	Normal PCG and Corresponding Energy Curves and Energy Spectra	95
5.4.	PCG with VSD and Corresponding Energy Curves and Energy Spectra	97
5.5.	PCG with PEM and Corresponding Energy Curves and Energy Spectra	98
5.6.	PCG with MI and Corresponding Energy Curves and Energy Spectra	99

5.7.	PCG with AS and Corresponding Energy Curves and Energy Spectra	100
A.1.	SAAB Schematic Diagram (sheet 1 of 3)	122
A.2.	SAAB Schematic Diagram (sheet 2 of 3)	123
A.3.	SAAB Schematic Diagram (sheet 3 of 3)	124
A.4.	USER ROM Schematic Diagram	125

Chapter I

INTRODUCTION

After a half-century of steady increases in heart disease fatalities in the United States, the rate now appears to be on the decline. Unfortunately, heart disease is still by far the nation's leading killer. Cardiologists admit they aren't sure why the death rates are falling. Most of them agree, however, that technology is aiding in the process [1].

The advent of a new generation of early diagnostic technologies such as coronary angiography, digital radiography, computed tomography, radio-nuclide emission imaging, nuclear magnetic resonance (NMR) imaging, and ultrasound techniques [2] are partly responsible for the decline. Presently, coronary angiography is the "gold standard of coronary diagnosis" despite its invasiveness, its use of small but significant radiation doses, and its slight (0.2% or less) risk of provoking a heart attack [1]. However, angiography is not foolproof. The arteries may be obscured by other organs, and image interpretation is sometimes difficult, especially of the smaller vessels. Ultrasound techniques provide views of the cardiac valves and chambers, and with its real-time capabilities, study of the heart valves in motion is possible.

However, due to its persistent problems in resolution and contrast, ultrasound has almost reached its limits as a cardiac tool [1]. NMR imaging provides images of the heart with high clarity and resolution, although interpretation of the images is still quite difficult. NMR imaging is still in its infancy thus it is still very expensive and is something of a wildcard in diagnostic technology [1].

With the arrival of the early diagnostic technology, many basic and fundamental techniques used in clinical practice have been neglected and abandoned in less-than-perfect stages. In particular, the age-old art of heart sound analysis by auscultation suffers from a lack of quantitative analysis techniques. Much needs to be done in order to bring the analysis of the phonocardiogram to a state comparable to that of the electrocardiogram (ECG), the electromyogram (EMG), or the electroencephalogram (EEG).

Frequently, murmurs or alterations in the heart sounds are the only definitive signs of some types of heart disease, appearing long before stress on the cardiovascular system is sufficient to produce other signs and symptoms [3]. Detection and recognition of heart murmurs is a valuable source of information concerning the functioning of heart valves. Auscultation of the heart is presently the primary test performed by cardiologists to assess the condition of the heart. This technique provides beneficial information to the clinician concerning the functional integrity

of the heart. However, the technique is plagued by an insufficient understanding of the genesis of heart sounds and any diagnosis based solely on auscultation is questionable and is, in fact, seldom practised. This is due to the wide diversity of opinion concerning the theories that attempt to explain the origin of heart sounds and murmurs [4-20]. Further, from a study of the physical characteristics of heart sounds and human hearing, it is seen that the human ear is poorly suited for cardiac auscultation, thus limiting the capacity of the physician [21]. In addition, auscultation is a subjective test and is prone to interpreter variations and errors [22,23].

This has led to many attempts towards automated analysis of the heart sound signal using the phonocardiograph. The phonocardiogram (PCG), which is a graphic recording of the heart sounds, allows the physician to compare the temporal relationships between the heart sounds and the mechanical and electrical events of the cardiac cycle. While qualitative descriptors used by physicians, such as 'muffled component' of a sound, 'musical murmur', 'rumble', or 'whiff', may be hard to measure or quantify, other features of the PCG can be measured more accurately by quantitative methods. The important features of the PCG are:

1. Frequency content of murmurs and sounds.
2. Maximum intensity of sounds and intensity pattern of murmurs.

3. Timing sequence of murmurs and sounds.
4. Location of the maximum intensity point and the transmission pattern of murmurs and sounds on the precordium.

The need for noninvasive methods has always been present, and phonocardiography could be of great use in achieving this goal. Even though phonocardiography has been available for more than 60 years it has been mainly used by physicians in a qualitative manner. The PCG contains valuable information, which, if analyzed quantitatively in a proper manner, could lead to important diagnostic results. The PCG is currently used in the diagnosis of cardiac malformations and pulmonary hypertension in infants. Noninvasive and passive methods are needed in pediatric cardiology. The small size of the thorax and the presence of fewer intervening structures aids heart sound analysis in infants.

A few automatic diagnostic systems for the PCG have been developed. Presently, the PCG is being used to test the functional and structural integrity of cardiac prosthetic valves. However, there still exists the need for a simple and efficient method to quantify the PCG signal into parameters aiding the detection of murmurs. A system performing such a task would be extremely useful for screening purposes as well as in routine diagnosis. Such a system would also be useful for further heart sound research.

1.1 PROPOSED METHOD

Since only short segments of the PCG are usually examined, and few real time constraints are involved in processing the data, a microcomputer based system could adequately perform the time and frequency domain analysis techniques encountered in phonocardiographic studies. Furthermore, because of its low cost, the system could be dedicated entirely to PCG applications. In this work, a three-channel prototype system, designed to process the PCG, ECG, and carotid pulse signals, is presented. The microcomputer system, hereafter referred to as the PCG analysis system, is used to perform quantitative analysis of the phonocardiogram for the detection of murmurs.

The Motorola 4 MHz MC68000 microprocessor is the central processing unit (CPU) of the PCG analysis system. The system includes 32K bytes of random access memory (RAM), 32K bytes of read only memory (ROM), and input/output (I/O) facilities to provide interfaces to a terminal and host computer. System hardware is also comprised of a three-channel data acquisition system, an Intel 8231A arithmetic processing unit (APU), and a signal display section using three digital-to-analog (D/A) converters. The D/A converters can be connected to an oscilloscope or strip chart recorder. The approximate cost of this prototype system is \$1500.00. The system can be easily expanded if additional analog channels or increased processing capabilities are required. The system software is written in MC68000 macro assembly language.

The PCG analysis system is used to implement methods for the time and frequency domain analysis of the systolic and diastolic segments of the PCG signal. A technique for the segmentation of the PCG into systole and diastole using the ECG and carotid pulse as timing references is carried out. Using a QRS-complex detection algorithm based on a smoothed difference of the ECG and a transformation based on a smoothed second difference of the carotid pulse, the PCG can be segmented into systole and diastole. Quantification of the time and frequency domain characteristics of each PCG segment is conducted by first computing the energy curve. An important point involved in the design of a dedicated PCG analysis system is the implementation of a FFT algorithm in assembly language in order to provide the basic core of spectral analysis techniques. Using the FFT routine, the energy spectrum of the PCG is computed. A quantity known as the Energy Distribution Coefficient (EDC) is used to quantify the energy curve and energy spectrum. The PCG signal can then be represented by the systolic and diastolic time and frequency EDC parameters which give an indication of the location of murmurs in time and the frequency content of the signal.

1.2 THESIS OUTLINE

Following a brief description on cardiac physiology and the production of heart sounds and murmurs, the characteristics of the phonocardiogram are outlined and a review of the various signal processing techniques that have been applied to the analysis of the PCG, ECG, and carotid pulse signals is then given. The system hardware and the signal processing techniques developed for this work are then discussed in detail. Following these, a discussion of the results obtained is given along with conclusions and recommendations for further research. Details of hardware used and program listings are given in the appendices.

Chapter II

HEART SOUNDS AND PHONOCARDIOGRAPHY

2.1 CARDIAC PHYSIOLOGY

2.1.1 The Electrocardiogram

The electrocardiogram (ECG) is a manifestation of the electrical activity within the heart. The ECG signal may be recorded by measuring the potential difference between two points on the body. These two points constitute an ECG lead. The triangular lead arrangement known as Einthoven's triangle is normally used, whereby electrodes are placed on the right arm (RA), the left arm (LA), and the left leg (LL). An electrode is also placed on the right leg (RL) and is grounded or used as the reference voltage. The resulting three leads are lead I, LA to RA; lead II, LL to RA; and lead III, LL to LA. Figure 2.1 shows a normal ECG lead along with the conventional terms used in describing the deflections and intervals in the tracing.

2.1.2 The Cardiac Cycle

To understand the physiological aspects of heart sound production, a brief review on the phases of the cardiac cycle is given [24]. Figure 2.2 is an anterior view of the heart showing the cardiac chambers and valves. The human heart has four chambers. The atria are the receiving chambers of the heart. The systemic veins empty into the right atrium and the pulmonary veins empty into the left atrium. The ventricles are the pumping chambers of the heart. The ventricles receive blood from their respective atria and pump it into the major arteries of the pulmonary and systemic circulations. The right ventricle pumps into the pulmonary artery and the left ventricle into the aorta. The atria and ventricles are separated on the right side by the tricuspid valve and on the left side by the mitral valve. Together, the tricuspid and mitral valves are referred to as the atrioventricular (AV) valves. The valves situated at the ventricular outflows are the semilunar valves. The pulmonary valve opens into the pulmonary artery and the aortic valve opens into the aorta.

The period of ventricular relaxation, during which the ventricles become filled with blood, is called diastole and the period of ventricular contraction is called systole. The P wave of the ECG, which occurs during late diastole, represents electrical excitation of the atria. In approximately 100 msec atrial contraction commences, causing a

slight rise in both atrial and ventricular pressures. At this stage the AV valves are open. Ventricular depolarization then occurs, marked by the onset of the QRS-complex of the ECG, and ventricular contraction begins shortly. As the ventricles contract, the intraventricular pressure rises, closing the AV valves. The semilunar valves are also closed at this time. This phase, termed the the isovolumic contraction phase continues for about 50 msec. The intraventricular pressure increases until this pressure is greater than the pressure in the pulmonary artery and aorta. At this point the semilunar valves open and blood is ejected from the ventricles.

Ventricular systole lasts approximately 300 msec; the ventricles then begin to relax and their pressures drop rapidly, closing the semilunar valves. After semilunar valve closure, the isovolumic relaxation phase continues for about 80 msec and ends with the opening of the AV valves, occurring when ventricular pressures fall below atrial pressures. The phase of rapid filling begins when the AV valves open. During systole, blood accumulates in the atria and the atrial pressures increase. When ventricular pressures become less than atrial pressures, blood moves down from the atria to the ventricles. This process lasts for 100 msec. The final phase of the cardiac cycle is the phase of slow filling or diastasis. This phase lasts about 200 msec and is caused by continued venous return and is terminated by atrial systole.

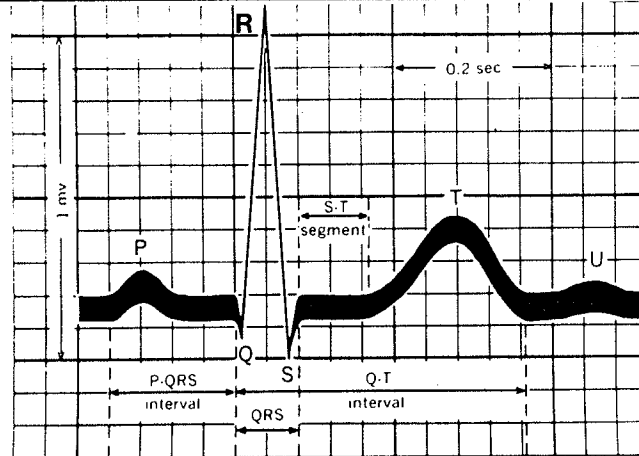


Figure 2.1: Typical Normal ECG Lead

Significant features are the P,Q,R,S, and T waves, the duration of each wave, and time intervals such as the QRS,S-T, and Q-T intervals (From reference [24], p.52)

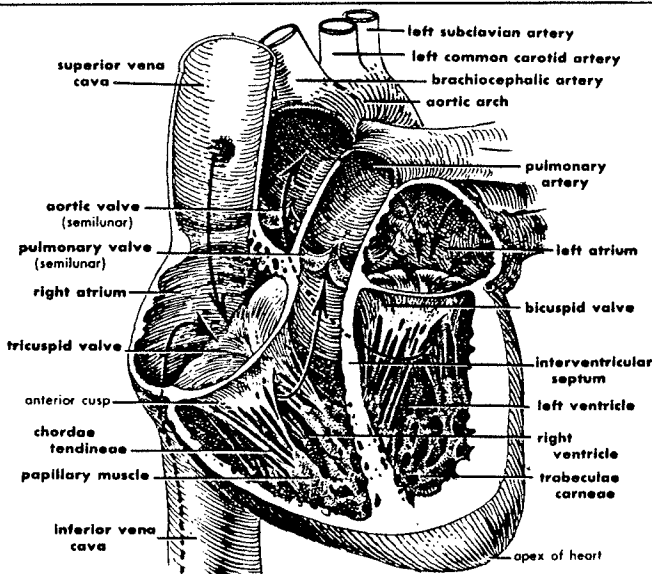


Figure 2.2: Anterior View of the Opened Heart

This figure shows the cardiac chambers and valves. The arrows indicate direction of flow through the heart. (From reference [24], p.28).

2.1.3 Normal Heart Sounds

Heart sounds are generally believed to be caused by the acceleration or deceleration of blood in the heart chambers [3]. There are two major heart sounds that occur during the sequence of one complete cardiac cycle (Figure 2.3).

The first heart sound (S1) can be divided into four components. The first component arises at the onset of ventricular contraction when blood is accelerated in the ventricle, surging blood toward the atrioventricular valves [3]. The frequency and intensity of the first component are very low since the ventricles are relaxed and the acceleration of blood is not high. This movement of blood closes and applies tension to the atrioventricular valves before ventricular pressure rises.

The second component of the first heart sound begins with abrupt tension of the closed AV valves decelerating the moving blood [3]. The frequency of these vibrations is greater than that in the first component. The intensity of the vibrations is dependent upon the velocity of the blood and the abruptness with which it is decelerated.

The third component of the first heart sound occurs during ventricular contraction. The pressure in the ventricle rises above that in the corresponding artery and blood moves toward the semilunar valves [3]. The frequency and intensity of these vibrations is similar to those produced in the sec-

ond component. The fourth component probably represents vibrations due to turbulence in blood flowing rapidly through the ascending aorta and pulmonary artery [3].

The closure of the semilunar valves gives rise to the second heart sound (S2). Although the primary vibrations occur in the arteries, they are also transmitted to the ventricles and atria by movement of the blood, valves, and valve rings [3]. The frequency of the second sound is usually higher than that of the first sound and is normally split into two components (A2,P2), reflecting the fact that the aortic valve normally closes before the pulmonary valve. Pathological conditions may cause this gap to widen, or may also reverse the order of occurrence of A2 and P2.

In some cases a third heart sound (S3) may be heard, corresponding to sudden termination of the ventricular rapid filling phase. These vibrations are of low frequency and the sound is generally inaudible in the normal adult, but is frequently heard in children. In late diastole, a fourth heart sound (S4) may be sometimes heard, caused by atrial contractions displacing blood into the distended ventricles. In addition to these sounds, valvular clicks and snaps are occasionally heard.

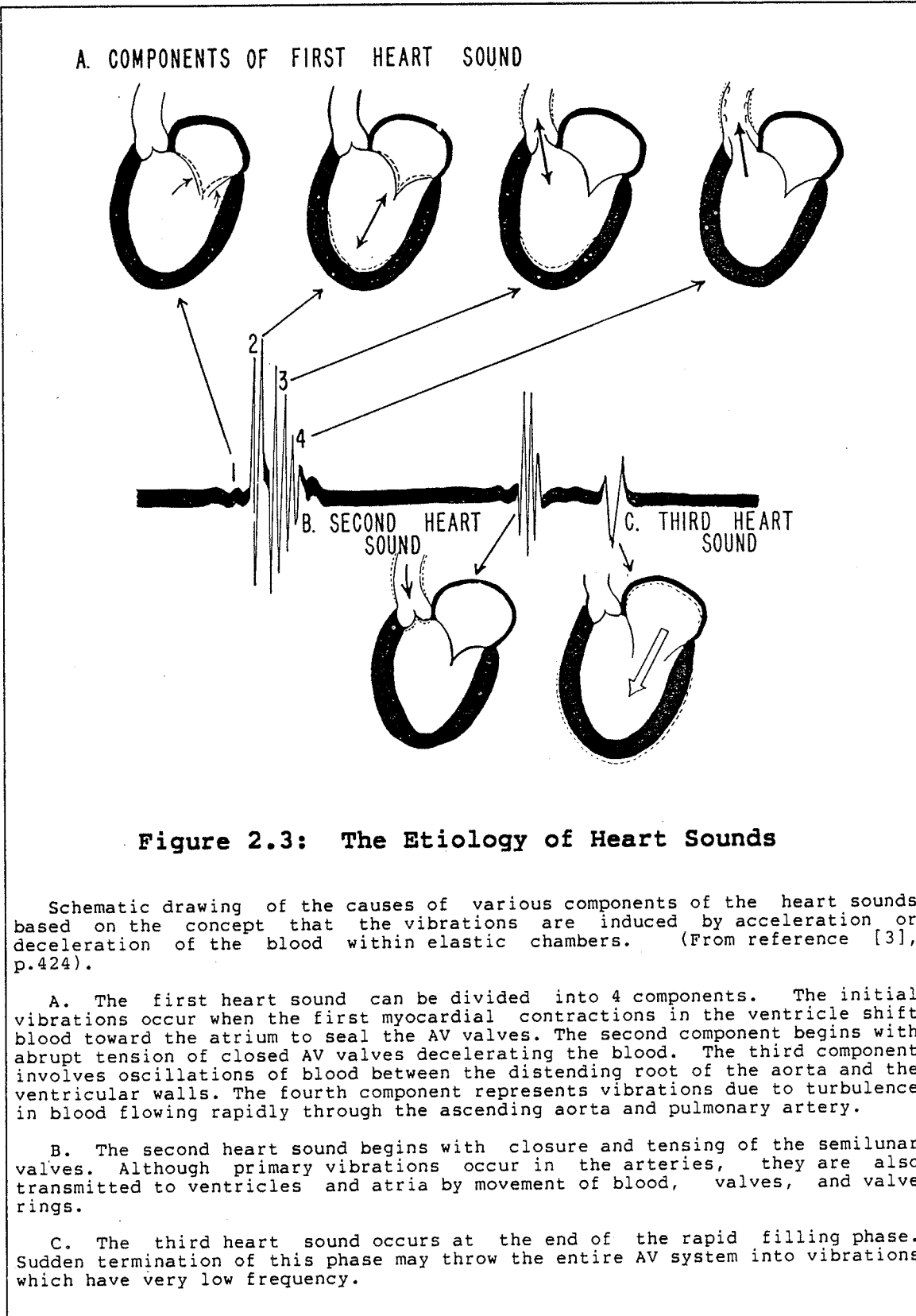


Figure 2.3: The Etiology of Heart Sounds

Schematic drawing of the causes of various components of the heart sounds based on the concept that the vibrations are induced by acceleration or deceleration of the blood within elastic chambers. (From reference [3], p.424).

A. The first heart sound can be divided into 4 components. The initial vibrations occur when the first myocardial contractions in the ventricle shift blood toward the atrium to seal the AV valves. The second component begins with abrupt tension of closed AV valves decelerating the blood. The third component involves oscillations of blood between the distending root of the aorta and the ventricular walls. The fourth component represents vibrations due to turbulence in blood flowing rapidly through the ascending aorta and pulmonary artery.

B. The second heart sound begins with closure and tensing of the semilunar valves. Although primary vibrations occur in the arteries, they are also transmitted to ventricles and atria by movement of blood, valves, and valve rings.

C. The third heart sound occurs at the end of the rapid filling phase. Sudden termination of this phase may throw the entire AV system into vibrations which have very low frequency.

2.1.4 Murmurs

The intervals between S1 and S2, and S2 and S1 of the next cardiac cycle (corresponding to ventricular systole and diastole) are normally silent. Murmurs, which are caused by certain cardiovascular defects and diseases, occur in these intervals. Murmurs are high frequency noise-like sounds which arise when the blood velocity becomes high in the presence of an irregularity through which the blood flows. Typical conditions in the cardiovascular system which cause blood flow turbulence include valvular stenosis and valvular insufficiency.

Systolic murmurs (SM) are caused by conditions such as ventricular septal defect (VSD), aortic stenosis (AS), pulmonary stenosis (PS), mitral insufficiency (MI), and tricuspid insufficiency (TI). While semilunar stenosis (AS,PS) causes an obstruction in the path of blood being ejected during systole, AV valvular insufficiency (MI, TI) causes regurgitation of blood to the atria during ventricular contraction. Diastolic murmurs (DM) are caused by such conditions as aortic and pulmonary insufficiency (AI, PI) and mitral and tricuspid stenosis (MS, TS). Other conditions causing murmurs are atrial septal defect (ASD), patent ductus arteriosus (PDA), as well as certain functional conditions due to vigorous exercises, which increases cardiac output and blood velocity.

Although murmurs are noise-like, certain features aid in distinguishing between different causes. For example, AS causes a diamond shaped midsystolic murmur, while MS causes a decrescendo-crescendo type diastolic-presystolic murmur. See Figures 2.4 and 2.5 for tracings of such signals.

2.1.5 The Carotid Pulse

The carotid artery in the neck is the point of the arterial system closest to the heart where external sensing can be performed. The carotid pulse tracing (Figure 2.6) begins to rise abruptly with aortic ejection and reaches its initial peak at the time ejection is probably at its maximum [25]. The first peak, called the percussion wave (P), is usually followed by a plateau or secondary wave, called the tidal wave (T), late in systole [25]. The pulse then falls smoothly to a point in which the dicrotic notch (D) is inscribed. The tidal wave represents primarily the reflected pulse returning from the upper body. The dicrotic notch is produced by abrupt completion of aortic valve closure [25]. In early diastole a small positive wave designated as the dicrotic wave (DW) occurs, which represents the reflected pulse from the lower body [25]. Figure 2.7 shows the important intervals of the carotid waveform.

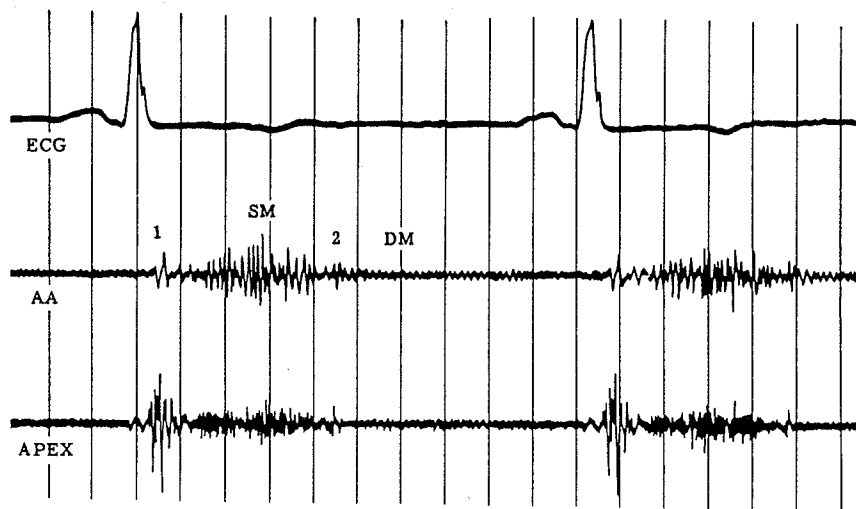


Figure 2.4: Phonocardiogram of Patient with Severe Aortic Stenosis

The ECG signal is also shown. Note the systolic murmur with peak intensity in midsystole (diamond shaped envelope). (From reference [25], p.132).

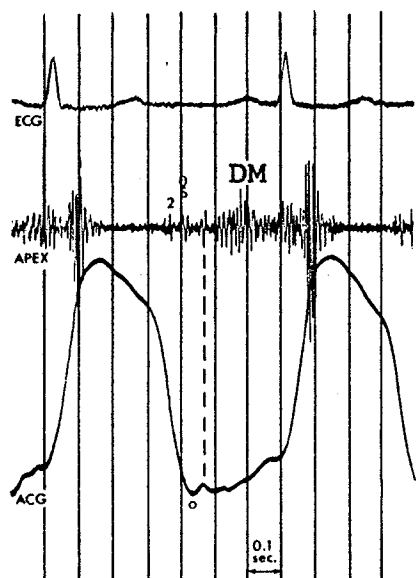


Figure 2.5: PCG of Patient with Mitral Stenosis

The ECG signal and apexcardiogram are also shown. Note the pre-systolic accentuation of the diastolic murmur. (From reference [25], p.152).

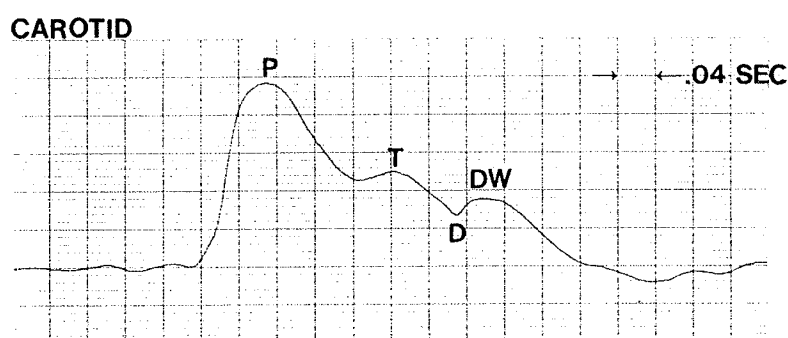


Figure 2.6: Typical Normal Carotid Pulse Tracing

Percussion wave P occurs approximately at maximum carotid ejection. Tidal wave T follows late in systole. Dicrotic notch D indicates closure of aortic valve. In diastole the dicrotic wave DW occurs.

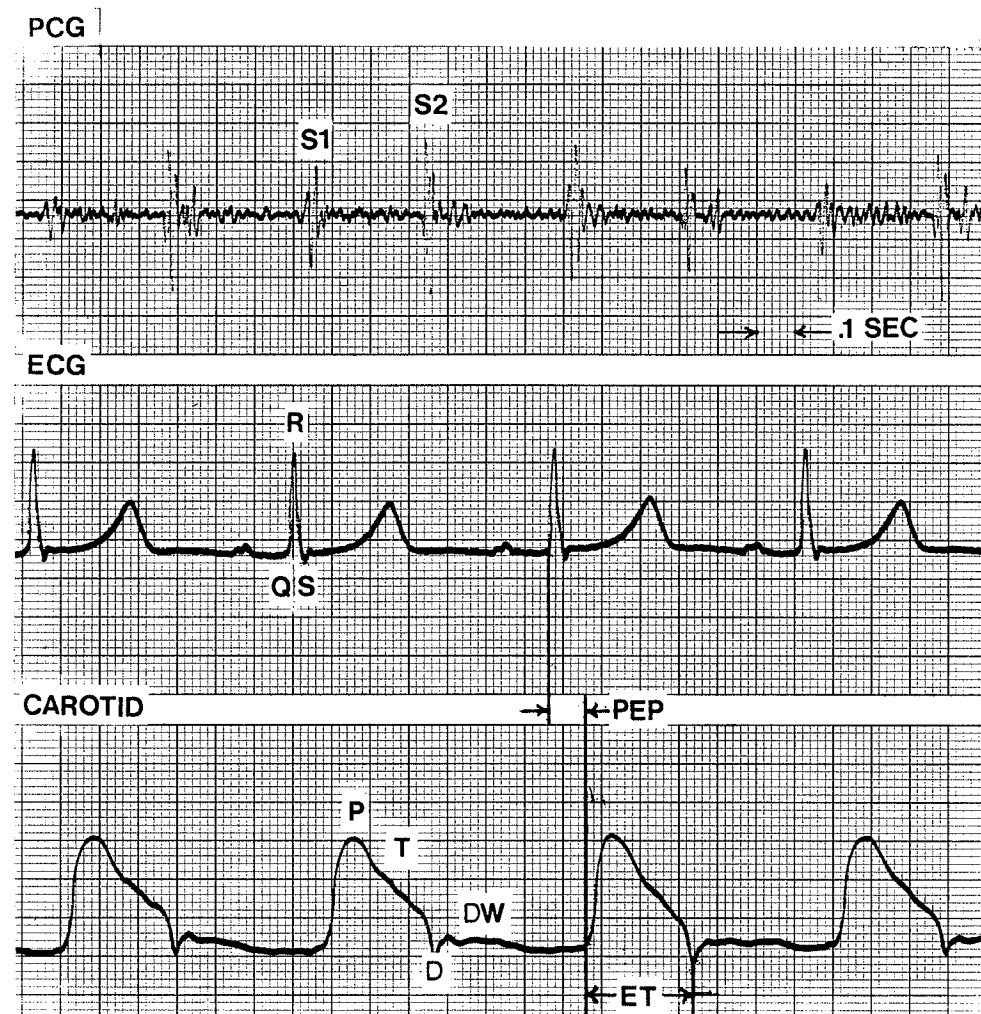


Figure 2.7: Normal Phonocardiogram, ECG, and Carotid Pulse Tracings

The pre-ejection period PEP is measured from the Q wave of the ECG to the onset of carotid upstroke. The ejection time ET is the interval from the start of carotid upstroke to the dicrotic notch. Note that the first heart sound occurs at the end of the QRS complex. The second heart sound occurs just before dicrotic notch.

2.2 PHONOCARDIOGRAPHY

2.2.1 Auditory Perception of Heart Sounds

Due to the varying threshold of audibility of the human auditory system with frequency of sound presented, and the low frequency nature of heart sounds, only a portion of the cardiohemic vibrations is audible [3]. The maximum sensitivity of human auditory perception lies in the 1000 Hz to 2000 Hz region, which is above the usual range of cardiac sounds. Normal heart sounds usually lie in the 20 Hz to 200 Hz range while the maximum frequency of murmurs is 600 Hz [3].

From a study of the physical characteristics of heart sounds and human hearing, it is seen that the human ear is poorly suited for cardiac auscultation [21]. Certain details such as the presence of murmurs, which are of much higher frequency than the normal sounds, can be detected easily by auscultation. However, it has been shown that auscultation is a subjective test and is prone to interpreter variations and errors [22,23].

Although the training and experience of the cardiologist do improve results attained by auscultation, the heart signal has much more information. This has led to many attempts towards automated analysis of the heart sound signal using the phonocardiograph.

2.2.2 Relationship Between Heart Sounds, ECG, and Carotid Pulse

The phonocardiograph [26], which consists of microphones, selective filters and amplifiers, and a recording unit, gives a graphic recording of heart sounds and murmurs (called a phonocardiogram or PCG). It is valuable in that it eliminates the subjective interpretation of these sounds. Additional channels are also provided for the recording of reference tracings so that the evaluation of heart sounds and murmurs with respect to the electrical and mechanical events in the cardiac cycle can be conducted.

The relationship between the PCG, ECG, and carotid pulse can be seen in Figure 2.7. The ECG can be used as a reference in identifying the first heart sound. The beginning of the QRS-complex provides a sharp reference which can be used to accurately determine the onset of ventricular contraction. Thus the R wave can be used to determine the start of the first heart sound.

Although variable, the beginning of the steep ascent of the carotid pulse usually coincides with the fourth component of the first heart sound [25]. The dicrotic notch follows A2 (aortic component of the second heart sound) by the time required to travel to the recording site in the neck. This usually amounts to 10 - 50 msec and is dependent upon the distance of the recording site from the heart and the pulse-wave velocity [25].

2.2.3 PCG and Pulse Recording Procedures

Since heart sounds and murmurs are of low amplitude, extraneous sounds must be minimized in the vicinity of the patient. Thus it is a standard procedure to record the phonocardiogram in a room that is as quiet as possible. The patient is placed in a supine position with the head on a pillow. ECG leads are placed on all four extremities and a standard Lead II is recorded throughout the procedure. There are optimal recording sites for various heart sounds, sites at which the intensity of sound is the highest because the sound is being transmitted through solid tissue or through a minimal thickness of inflated lung [27]. An HP21050A contact sensor is strapped firmly to the patient at one of the heart sound pickup areas on the chest shown in Figure 2.8. These locations are as follows:

1. Aortic area: second right intercostal space.
2. Pulmonary area: second left intercostal space.
3. Tricuspid area: fourth left intercostal space.
4. Mitral area: near the apex of the heart.

The HP21050A contact sensor has a relatively flat response from 0.05 Hz to 1000 Hz with an equal attenuation of about 5 dB over the entire range. This makes it equally suitable to record the first and second heart sounds (below 200 Hz) and high frequency murmurs (up to 600 Hz).

The HP21281A pulse transducer kit is used to record the carotid pulse. A trained technician locates the site where the carotid pulsation in the neck is the strongest and the pickup pressure cup is applied firmly. This transducer has a frequency response of approximately dc to 1000 Hz.

A three-channel HP1514B ECG/Phono system is used to obtain an amplified and filtered phonocardiogram with simultaneous ECG and carotid pulse reference signals. Channel 1 records a filtered heart sound. In this work, the PCG was obtained using a highpass filter (cutoff frequency of 25 Hz). Channel 2 is used to record a Lead II ECG as a timing reference. Any lead could be used as long as a suitable reference QRS-complex is obtained. Channel 3 is used to record a highpass filtered carotid pulse with a cutoff frequency of 1 Hz. Figure 2.9 shows a block diagram of the HP1514B ECG/Phono recording system as it is used to record the PCG and carotid pulse in this project.

A four-channel HP3960 FM instrumentation recorder is used to simultaneously record the PCG, ECG, and carotid pulse waveforms. The signals are recorded for a duration of 10 seconds.¹

¹ The recording time of 10s is sufficient to diagnose heart diseases from the PCG. It is desirable to reduce recording time to a few seconds, especially for children, since the patient's breath is held during recording.

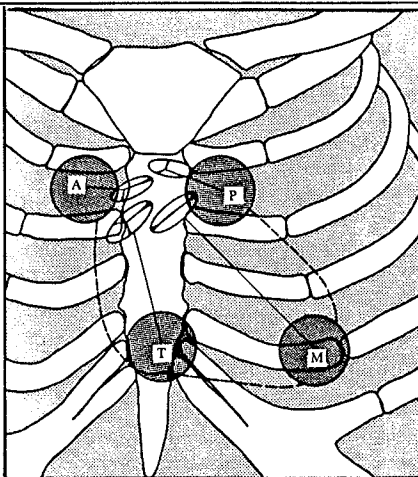


Figure 2.8: Locations For Surface Heart Sound Pickups

A, aortic area: second right intercostal space; P, pulmonary area: second left intercostal space; T, tricuspid area: fourth left intercostal space; M, mitral area: near apex of heart. (From reference [28], p.357)

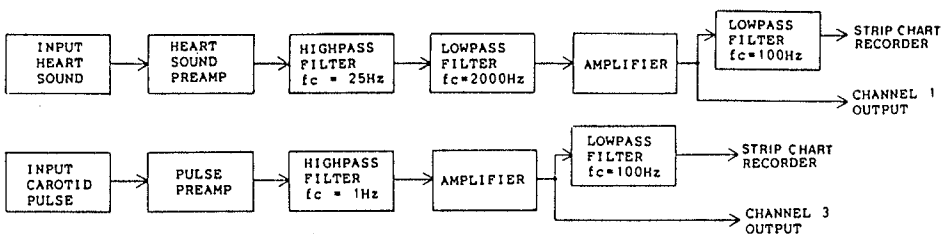


Figure 2.9: Block Diagram of the HP1514B ECG/Phono System

Note that the heart sound signal and carotid pulse are highpass filtered at 25 Hz and 1 Hz, respectively. The signals are lowpass filtered at 100 Hz and directed to a strip chart recorder. The unfiltered signals are directed to the respective output channels.

2.3 REVIEW OF PCG SIGNAL PROCESSING TECHNIQUES

Many signal processing techniques have been tried to quantify the PCG signal. The time-envelope of energy of the PCG signal is clinically significant as murmurs of specific envelope shapes occur in certain parts of the cardiac cycle. For example, aortic stenosis causes a diamond shaped systolic murmur, while mitral stenosis leads to a decrescendo-crescendo type diastolic-presystolic murmur. Early techniques to extract the sound envelope employed demodulation and synchronized averaging of the envelope of the cardiac sounds [29]. Complex demodulation and power spectrum estimation techniques have been conducted to extract the 'envelopogram' of the PCG signal [30]. In another method, the average power in contiguous 10 msec segments was plotted to obtain a 'power curve' [31]. Maximum amplitude and zero crossing measurements of the PCG signal have been attempted [32]. The use of wave analyzers and bandpass filter banks to improve detection of aortic stenosis in the presence of mitral insufficiency has also been reported [33]. In addition, cardiac screening systems have been designed based on measurements of frequency content, amplitude, energy, and timing of heart sounds [34-36].

Analysis of the PCG signal in the frequency domain has also been extensively researched [37-52]. A sound spectrograph, in which sound intensity is displayed in gray shades against time and frequency coordinates is discussed in ref-

erence [37]. Three dimensional contour plots of the PCG involving contours of equal intensity against time and frequency coordinates have been conducted [38]. Fast Fourier transform analysis of PCG signals has been attempted [42-49]. Other techniques of spectral analysis on the PCG are discussed in references [50-52].

Linear predictive analysis has been used to extract the spectral patterns from the PCG signal [53]. These parameters are used as features for pattern classification. The linear predictive method was also used to derive an algorithm for detection and segmentation of the first and second heart sounds based on the frequency domain characteristics of the heart sounds [54]. A spectral analysis technique using selective linear prediction coding to determine the spectral distribution of the second heart sound is described in reference [55].

In addition, images of sound distribution produced from multiple PCGs recorded on the chest wall have been used to compute chest wall maps showing the varying distribution patterns of sounds and murmurs over the passage of time [56]. Statistical analysis of heart sounds has been performed using the first two statistical moments to classify the heart sounds into deterministic and nondeterministic sounds and to segment the heart sound components [57,58].

The phonocardiogram has also been used to test the functional and structural integrity of cardiac prosthetic valves [59-68]. Parametric pole-zero modelling methods for frequency domain feature extraction [69] and FFT techniques for spectral analysis [70,71] have been reported for prosthetic valve sound analysis.

Digital signal processing techniques such as homomorphic filtering have been applied to the PCG with limited success [72-75]. Pole-zero modelling by Shanks' method was also attempted with some success [72,74-76]. Procedures for quantitative analysis of the PCG in the time and frequency domain have been proposed using the energy curve and power spectrum [77,78,79]. The application of speech signal processing techniques to the analysis of the PCG has been discussed in reference [80].

An overview of the methods tried illustrates that there have been many attempts at the analysis of the PCG. However, there still exists a need for a simple and efficient method to quantify the subjective features of the PCG and classify the various types of murmurs. A system performing such a task, realizable for online analysis, would be extremely useful for screening purposes, as well as in routine diagnosis and further heart sound research.

2.4 REVIEW OF ECG AND PULSE SIGNAL PROCESSING TECHNIQUES

The ECG and carotid pulse can be used as reference signals for the identification of features in the PCG. In particular, the QRS-complex of the ECG provides a sharp reference which can be used to identify the first heart sound (start of systole). The dicrotic notch in the carotid pulse can be used to approximate the onset of the second heart sound (start of diastole).

The application of signal processing techniques to the analysis of the ECG has been quite extensive; see, for example, references [81-86]. A thorough review of the digital analysis of the ECG can be found in reference [87]. Reported techniques have used a transform based on the first difference of the ECG signal as a reference for the PCG [88,89]. A single peak corresponding to the QRS-complex is found and used to identify the first heart sound.

The waveshape for the carotid pulse is essentially the same as for the aortic pulse and, as such, many of the arterial pulse wave analysis techniques reported can be applied directly to the carotid pulse. Reviews of some of these methods are given in references [87] and [90].

The use of specially designed filters that selectively exaggerate the feature sought, as well as minimize noise, has been reported [91]. An application of the AZTEC preprocessing program [92] has been used to initiate the search

for important points, such as systolic upstroke and onset of dicrotic notch, in the central arterial pressure wave [93].

Pattern recognition techniques have also been used to identify the features of arterial pulse waves. An algorithm for the automatic identification of the important points in brachial pulse waves is described in references [94,95]. A waveform parsing technique has been used to detect and measure structural variations of the carotid pulse wave [96].

A real time pressure algorithm has been developed using data reduction analysis and specific selectable thresholds to filter noise and detect critical points [97]. A method for the processing of the arterial pressure wave involving a series of algorithms to identify the major events of the aortic pressure wave is reported in [98].

Most reported pulse analysis techniques have been for real-time analysis and are concerned with data reduction techniques and the identification of all major events in the pressure cycle. In this study, real-time processing of the carotid pulse is not necessary. One cardiac cycle of the carotid pulse, in which the dicrotic notch is localized, need only be extracted. A transform based on the second derivative of the carotid pulse is computed to provide a reference point for the identification of the second heart sound.

Chapter III

SYSTEM HARDWARE DESCRIPTION

3.1 INTRODUCTION

The Motorola MC68000 microprocessor is the central processing unit of the prototype PCG analysis system. A detailed operational description of the MC68000 processor is available in the MC68000 User's Manual [99]. The analysis system consists of two computer boards; the Motorola Educational Computer Board (ECB) and a Signal Acquisition and Analysis Board (SAAB). The ECB consists of the microprocessor, memory, timer, and input/output (I/O) facilities. The user interface to the ECB is provided by connecting the board to a terminal via an RS-232 interface. A second serial port is provided to connect the ECB to a host computer system. A complete hardware description of the ECB is provided in the ECB User's Manual [100].

The SAAB, designed to be directly interfaced to the ECB, consists of the following:

1. A three-channel data acquisition system including anti-aliasing filters, sample/hold units, an analog multiplexer, and an analog-to-digital (A/D) converter.

2. An arithmetic processing unit (APU) to provide extended signal processing capabilities.
3. Three digital-to-analog (D/A) converters to display the various output signals on an oscilloscope or strip chart recorder.

Figure 3.1 shows a block diagram of the PCG analysis system. The SAAB schematic diagrams are included in Appendix A.

This chapter provides a brief description of the MC68000 Educational Computer Board hardware including the MC68230 Peripheral Interface/Timer and ECB interfacing techniques. Following this a detailed description of the signal acquisition and analysis board will be given including the data acquisition system, the APU and the D/A circuitry. In this discussion, active low signals are designated by an asterisk (*) following the signal name.

3.2 MC68000 EDUCATIONAL COMPUTER BOARD

The ECB includes a 4 MHz MC68000 16-bit microprocessor, 32K bytes of dynamic random access memory (RAM), 16K bytes of firmware read-only memory (ROM), two serial communication ports (RS-232 compatible), a parallel port, a 24-bit programmable timer, and a wire-wrap area.

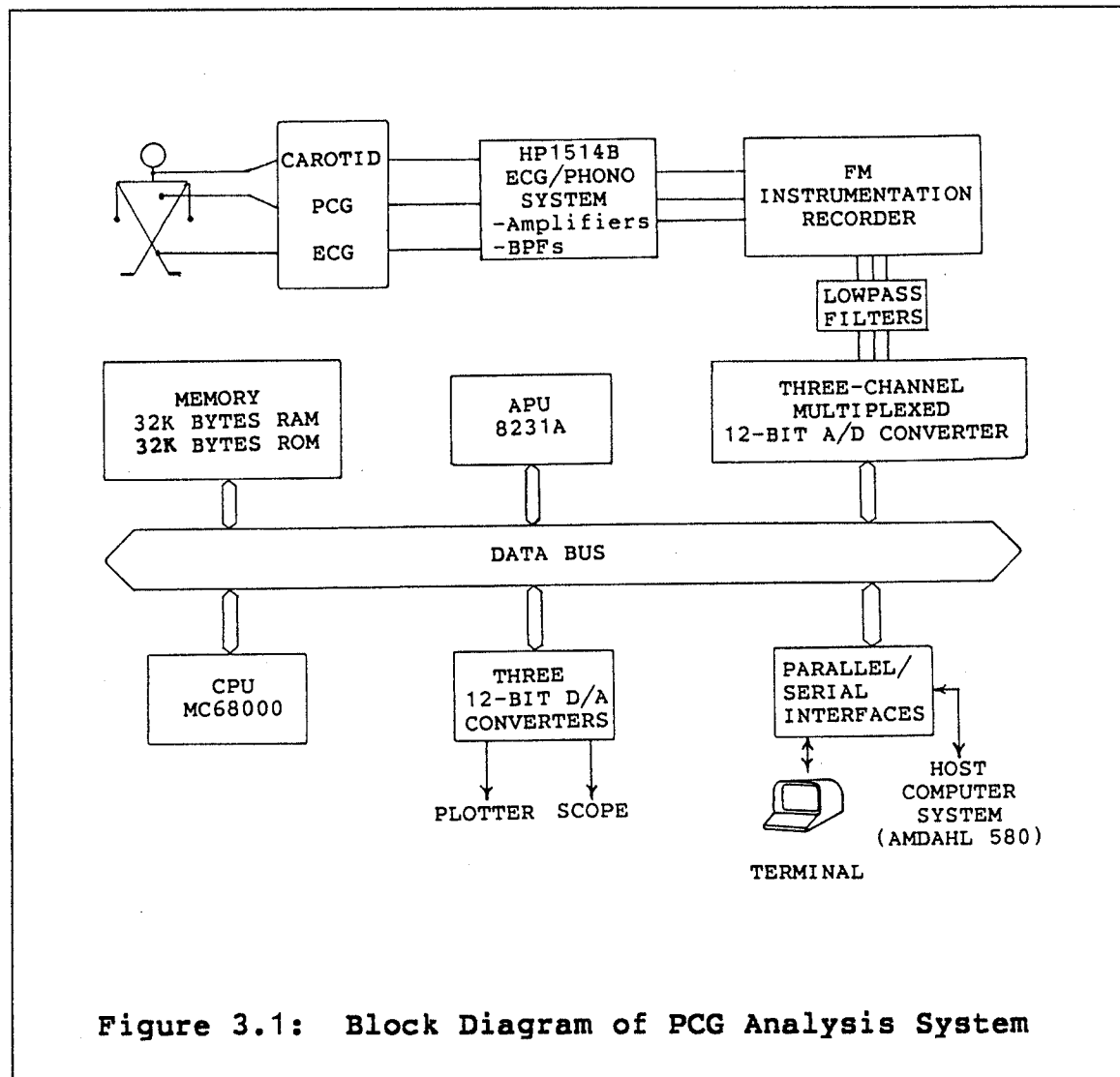


Figure 3.1: Block Diagram of PCG Analysis System

The ECB memory map is shown in Table 3.1. The RAM is addressed at the bottom of the memory map (\$000007-\$007FFF) and consists of sixteen MCM4116B devices. The user area of RAM extends from \$000900-\$007FFF. The firmware ROM is located at \$008000-\$00BFFF. The system firmware is stored in two MCM68A364 devices. All I/O devices are mapped into the same 64K byte page at \$010000-\$01FFFF. Redundant mapping occurs since the address is not fully decoded (i.e. the same device appears at several addresses).

Two MC6850 asynchronous communications interface adapters (ACIAs) provide the bus interface for the two serial ports. One of the ACIAs is used for connecting a terminal to ECB Port 1 and the other ACIA is used to connect a host computer system to ECB Port 2. A baud rate generator provides the transmit and receive clocks for both ACIAs. Both serial ports are RS-232 compatible.

The ECB includes an MC68230 peripheral interface/timer (PI/T) device. This device consists of two parallel interface ports, 8 general purpose I/O pins, and a 24-bit programmable timer. Table 3.2 shows the address map for the MC68230 timer. For complete details regarding the timer registers and programmable options available to the timer, refer to the MC68230 PI/T Data Sheet [101].

TABLE 3.1
Educational Computer Board Memory Map

Function	Address
System Memory	\$000000-\$0008FF
Vector Table	\$000000-\$0003FF
User Memory	\$000900-\$007FFF
Tutor Firmware	\$008000-\$00BFFF
I/O Devices	\$010000-\$01FFFF
PI/T	\$010000-\$01003F
ACIAs	\$010040-\$010043
Not Used	\$020000-\$02FFFF
M6800 Page	\$030000-\$03FFFF
Not Used	\$040000-\$FFFFFF

TABLE 3.2
MC68230 Timer Address Map

Address	PI/T Register
\$010021	Timer Control Register (TCR)
\$010023	Timer Interrupt Vector Register (TIVR)
\$010027	Counter Preload Register High (CPRH)
\$010029	Counter Preload Register Middle (CPRM)
\$01002B	Counter Preload Register Low (CPRL)
\$01002F	Counter Register High (CNTRH)
\$010031	Counter Register Middle (CNTRM)
\$010033	Counter Register Low (CNTRL)
\$010035	Timer Status Register (TSR)

3.2.1 Interfacing to the ECB

A small wirewrap area is provided directly on the ECB. In addition to the wire wrap area, the ECB has a connection area which gives access to 46 of the MC68000 bus and system timing signals and has provision for an auxiliary 50 pin I/O header.

Five connections on the ECB, denoted E1*-E5*, are provided, giving active-low enable signals for unused areas of the MC68000 memory map. Figure 3.2 shows the decode logic for these enable signals and Table 3.3 shows the memory map for the signals.

When interfacing to the ECB, special care must be taken with the Data Transfer Acknowledge signal (DTACK*). This input indicates that the data transfer between the processor and a device is completed. It may be used as a handshake line when the MC68000 is used in asynchronous operations. The processor DTACK* is generated by ANDing DTACK PIT*, DTACK RAM*, and DTACK ROM*, as shown in Figure 3.3. The processor DTACK* goes low whenever any of these go low. Another signal can not be added to the processor DTACK* since the signal is not an open collector output. The USER DTACK* is connected to the system via ECB connection E7. The DTACK PIT* is turned off when not used and the USER DTACK* can be bussed at this point. The USER DTACK* must be an open-collector or three-state driver.

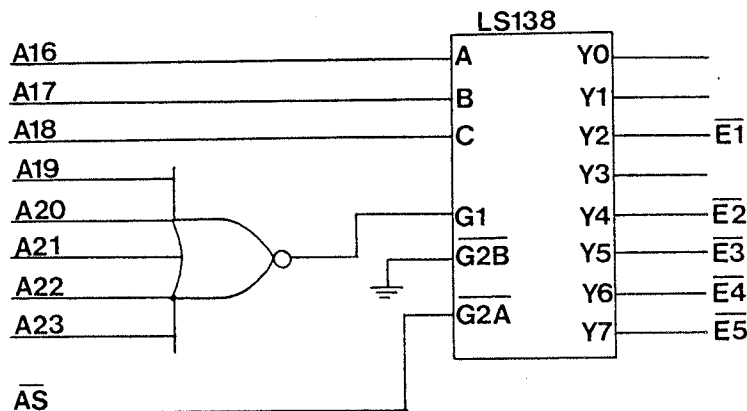


Figure 3.2: MC68000 Memory Enable Signal Decode Logic

TABLE 3.3
MC68000 Memory Enable Signal Address Map

Enable Signal	Address Segment
E1*	\$020000-\$02FFFF
E2*	\$040000-\$04FFFF
E3*	\$050000-\$05FFFF
E4*	\$060000-\$06FFFF
E5*	\$070000-\$07FFFF

3.2.2 ECB-to-SAAB Interface

Individual wirewrap pins are soldered into the connections provided on the ECB. Signals from these pins are wirewrapped to a 50-pin right angle header, which is inserted into the auxiliary I/O header location on the ECB. The SAAB has a similar 50-pin header. The interface between the ECB and the SAAB is provided via a 50-conductor ribbon cable. Four extra signals are connected to the header, these being the memory enable signals E1*, E2*, E3*, and the USER DTACK* connection E7.

The MC68000 data bus and address bus are buffered using 74LS245 and 74LS241 devices, respectively. These buffers are enabled only when devices on the SAAB are addressed and when the MC68000 ADDRESS STROBE (AS*) is asserted, indicating there is a valid address on the address bus. The MC68000 READ/WRITE (R/W*) signal is used to define the data bus transfer as a read or write cycle.

The SAAB USER DTACK* is provided by ANDing the respective DTACKs* from the data acquisition system, arithmetic processing unit, and digital-to-analog conversion circuitry. This signal goes low indicating completion of data transfer.

The MC68000 microprocessor can handle seven levels of interrupts. Interrupt requests to the ECB are restricted to an M6800 type autovectored priority level 4 interrupt. The ECB provides an autovectored interrupt request designated

6800 IRQ*. The 6800 IRQ* signal is generated by ANDing the interrupt request signals from the data acquisition system (ADIRQ*) and the APU (APUIRQ*). When either of these signals goes low the 6800 IRQ* line is asserted, generating the level 4 interrupt on the MC68000.

The ECB wirewrap area is used to provide 16K bytes of user ROM, using two 2764 devices. The ROM is mapped into memory segment \$070000-\$07FFFF. Connection E5* from the ECB is used in the decoding scheme. The USEROM DTACK* signal is generated using a 74LS175 device. Schematic diagrams of the ECB-to-SAAB interface and the ROM circuitry are found in Appendix A.

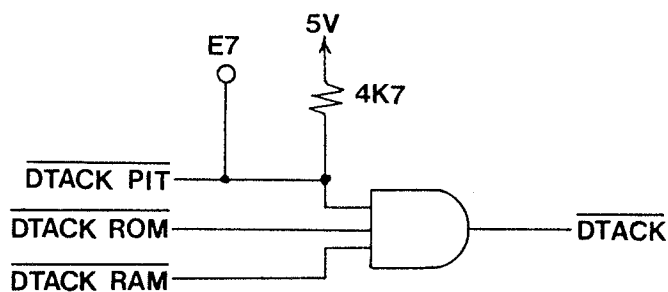


Figure 3.3: ECB DTACK* Signal Generation

3.3 DATA ACQUISITION SYSTEM

A block diagram of the data acquisition system is shown in Figure 3.4. In this system, data is taken from the analog inputs at the same instant of time, requiring a sample-hold unit per channel ahead of the analog multiplexer. All sample-holds are given the hold command simultaneously. The multiplexer then sequentially switches to each sample-hold output while the analog-to-digital (A/D) converter converts the signal into digital form.

The data acquisition system is mapped into memory segment \$020000-\$02FFFF. Data acquisition control is accomplished using a 74LS138 3- to 8-line decoder. Connection E1* from the ECB and MC68000 address lines A1-A3 are used in the decoding scheme, as shown in Figure 3.5. Table 3.4 shows the address map for the data acquisition control signals.

The PCG, ECG, and carotid pulse signals are directed through anti-aliasing filters using the active lowpass Butterworth filter shown in Figure 3.6. These lowpass filters (one per channel) are constructed using MC741 operational amplifiers. The lowpass filter cutoff frequency (f_c) for the PCG signal is 500 Hz. The cutoff frequency for the ECG signal and the carotid pulse is 100 Hz.

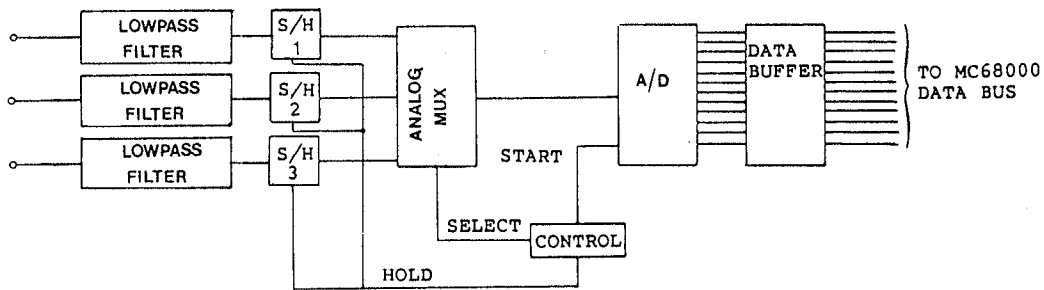


Figure 3.4: Block Diagram of Data Acquisition System

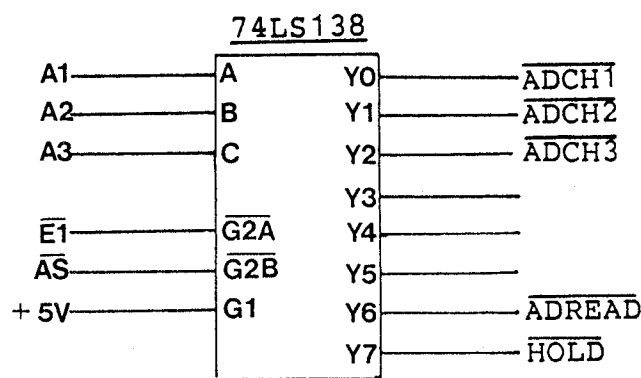


Figure 3.5: Data Acquisition Control Signal Decode Logic

TABLE 3.4
Data Acquisition Control Signal Address Map

Address	Function
\$020001	Select ECG channel of multiplexer (ADCH1)
\$020003	Select PCG channel of multiplexer (ADCH2)
\$020005	Select Carotid channel of multiplexer (ADCH3)
\$020006	Not Used
\$020008	Not Used
\$02000A	Not Used
\$02000C	Read A/D Converter (ADREAD)
\$02000E	Initiate hold state of S/H devices (HOLD)

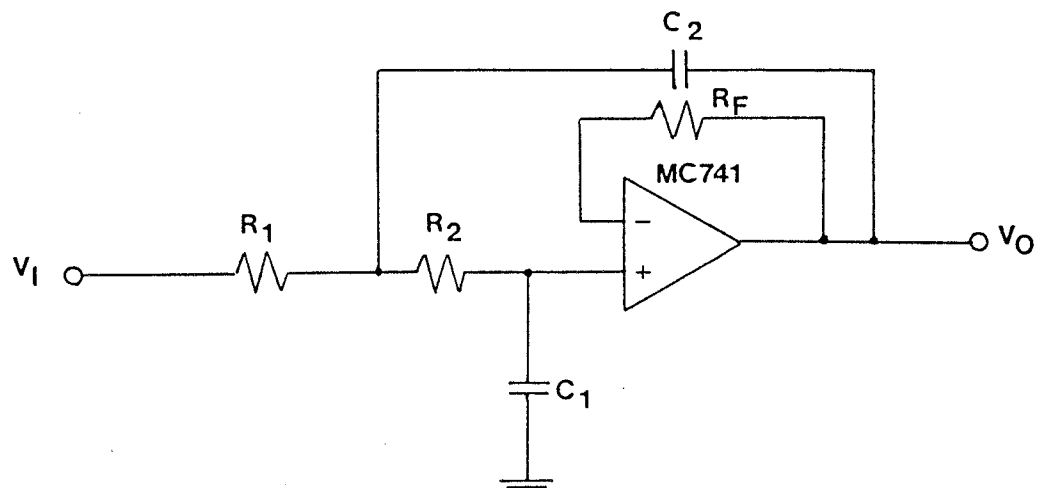


Figure 3.6: Active Lowpass Butterworth Filter

Lowpass filter designed such that $R = R_1 = R_2$, $R_f = 2R$, $C_2 = 2C_1$ and $C_1 = .707/\omega_c R$.

Three National Semiconductor LF398 Sample and Hold Circuits are used to hold the three signals at the same instant of time. Figure 3.7 shows a schematic diagram of a sample/hold unit as it is configured in the data acquisition system. The hold mode is initiated by taking the logic input of each device high. This is accomplished by asserting the HOLD* signal. The MC555 timer is set up in monostable mode resulting in a 5.0 volt, 30.0 μ sec pulse whenever HOLD* is asserted. With a hold capacitor of 0.01 μ F, typical acquisition time is 20.0 μ sec.

A National Semiconductor CD4051 device is employed in this system as a 3-channel multiplexer with three control inputs A, B, and C. The three control signals select 1 of 3 channels to be turned "ON" and connect the input to the output. The function table for the three select inputs is shown in Table 3.5. A schematic diagram of the multiplexer as it is configured in this system is shown in Figure 3.8. To simplify multiplexer control the filtered ECG, PCG and Carotid pulse signals are connected to the multiplexer input channels 6, 5, and 3, respectively. Control of channel selection is accomplished using a 74LS175 device in conjunction with the ADCH1*, ADCH2*, and ADCH3* signals and the CONVERSION COMPLETE (CC*) signal from the A/D converter.

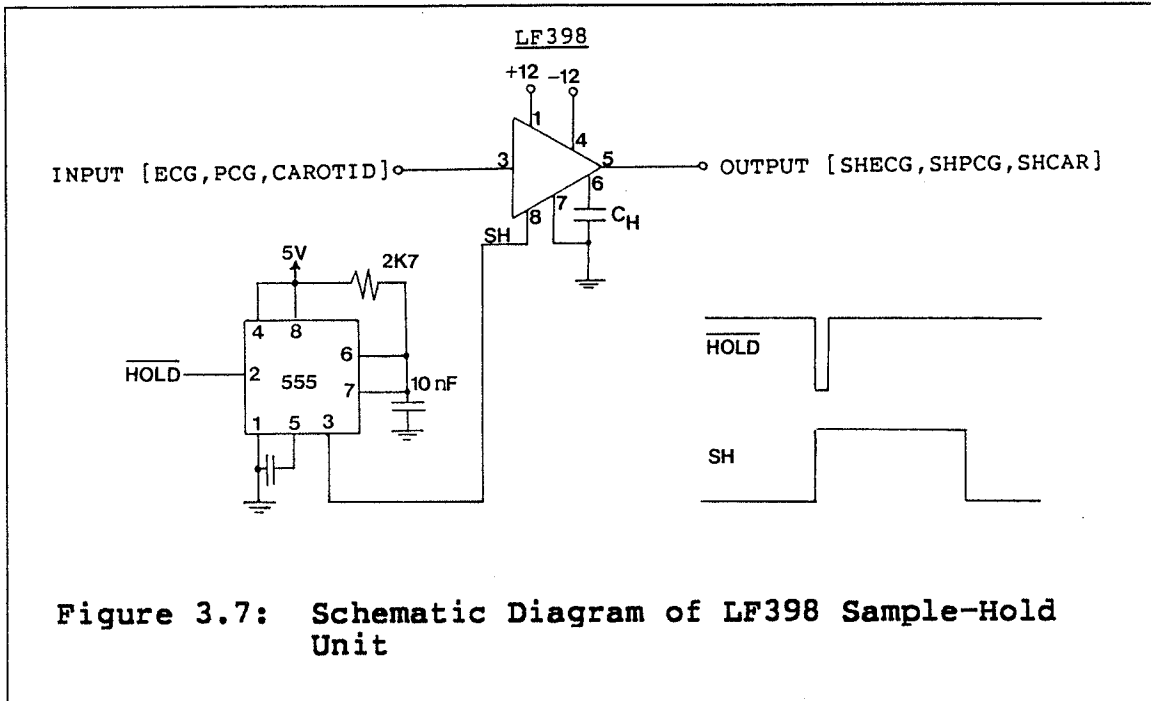


TABLE 3.5			
Function Table for Multiplexer Control Signals			
Input States			"ON" Channels
C	B	A	
0	0	0	0
0	0	1	1
0	1	0	2
0	1	1	3
1	0	0	4
1	0	1	5
1	1	0	6
1	1	1	7

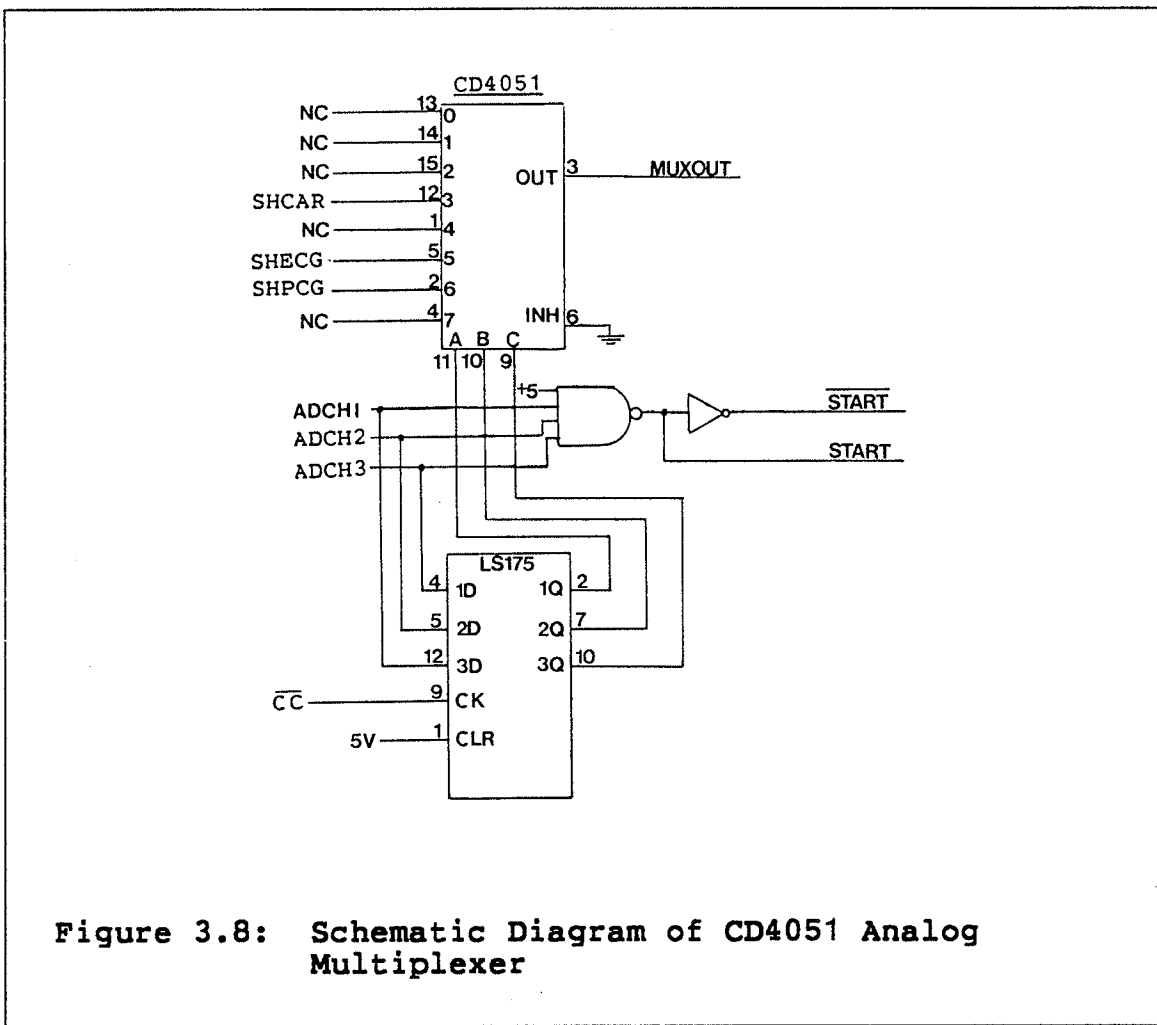


Figure 3.8: Schematic Diagram of CD4051 Analog Multiplexer

The National Semiconductor ADC1210 is a CMOS device used to perform 12-bit successive approximation (SA) analog-to-digital conversion. The A/D converter operates at a clock frequency of 125 KHz. This clock is derived by dividing the ECB 1MHZ CLOCK signal by 8 using a 74LS93 4-bit binary counter. The A/D is configured to convert analog inputs in the \pm 2.5 volt range. The outputs of the ADC1210 are buffered using 74C901 hex inverting TTL buffers and are then connected to the inputs of 74LS373 latches.

A schematic diagram of the A/D converter is shown in Figure 3.9. To start conversion, the START CONVERSION (SC*) pin is taken low by asserting ADCH1*, ADCH2*, or ADCH3*. This causes the SA register to reset synchronously on the next clock cycle low-to-high transition. Conversion begins on the next low-to-high transition of the clock pulse. After completing the conversion, the CC* signal is asserted. This output, together with a 74121 monostable multivibrator, generates the ADIRQ* signal. The timing diagram of the A/D operation is shown in Figure 3.10. Asserting ADREAD* latches the A/D output data to the MC68000 data bus.

The ADTACK* signal is generated using the circuit shown in Figure 3.11. There are two cases in which this signal is generated. The first case arises when the HOLD* or ADREAD* signals are asserted. These signals operate synchronously with the processor. Using the 74LS175 device, a delay corresponding to 4 clock cycles of the ECB 8MHZ CLOCK signal is

incurred before ADTACK* is sent to USER DTACK*. The second case arises as a result of the asynchronous operation of the A/D converter and the processor. The ADTACK* signal is asserted only when the A/D converter SA register has been reset and the converter is about to start its conversion process. The timing diagram for this case is shown in Figure 3.12.

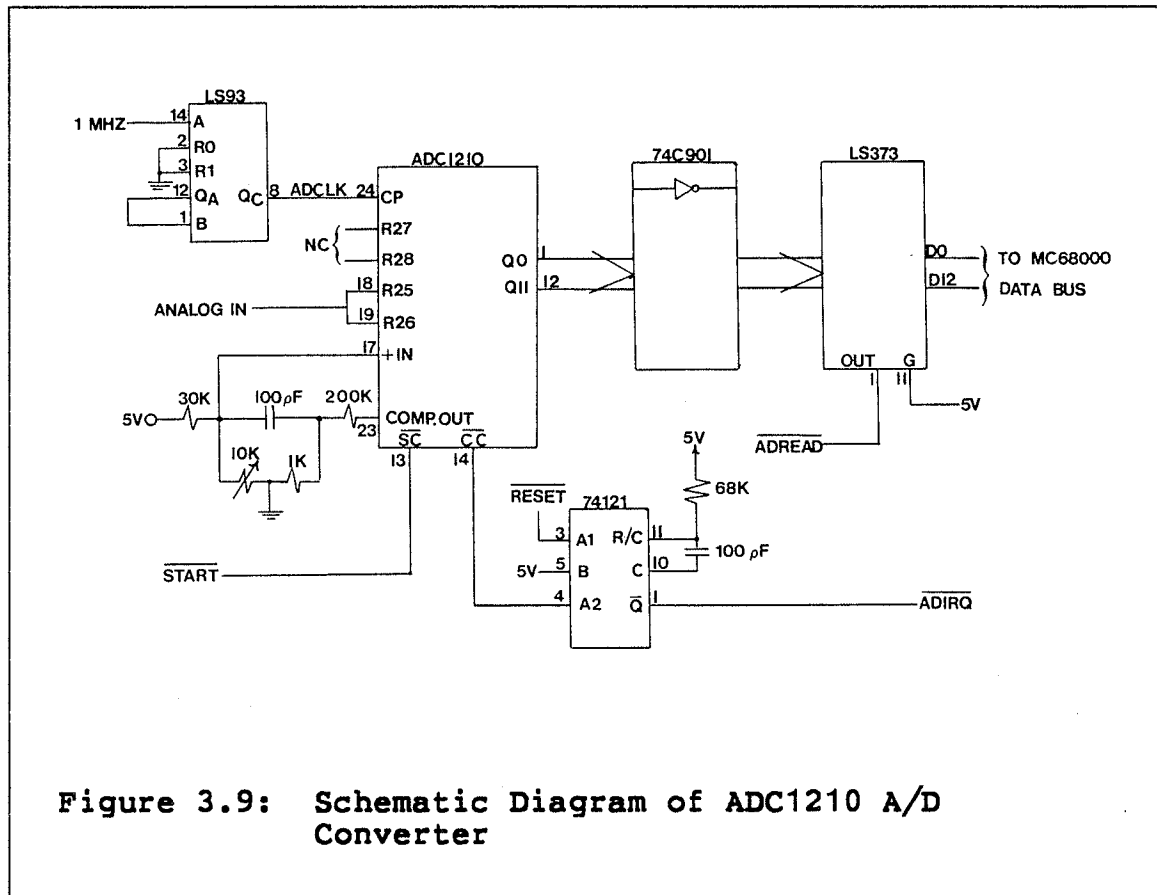
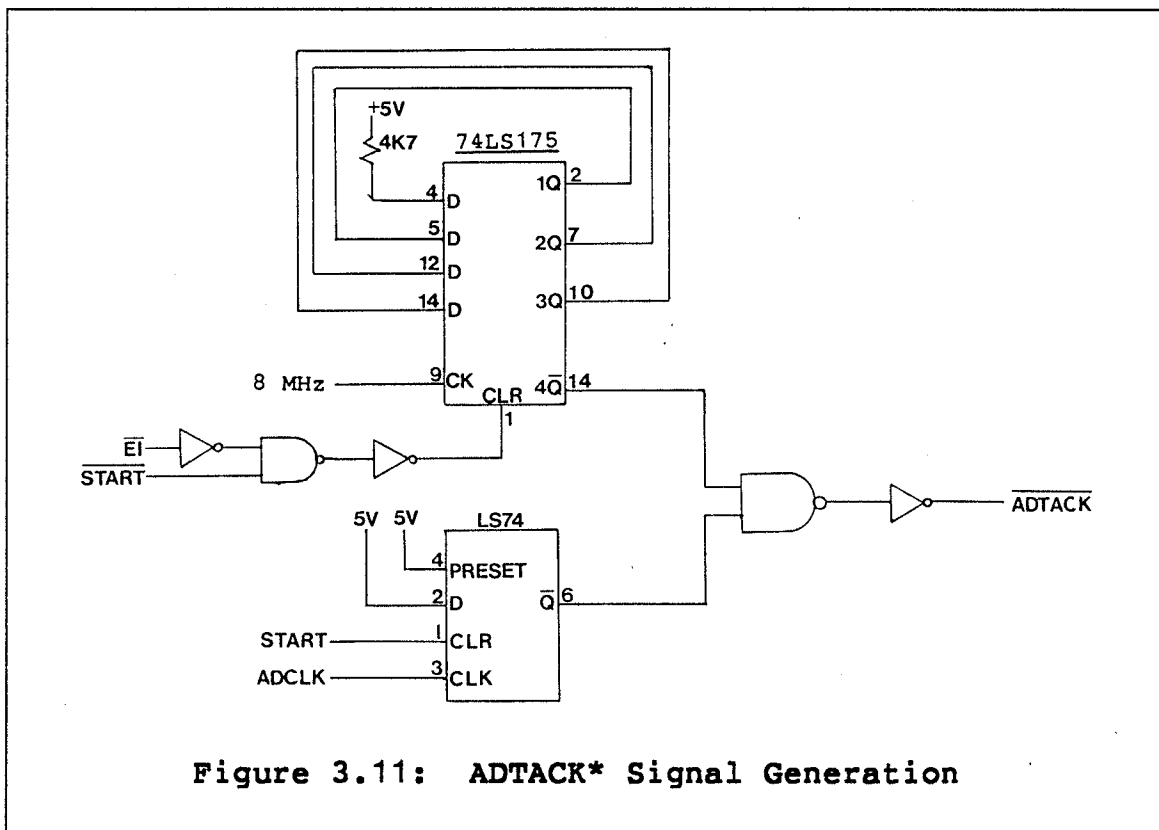
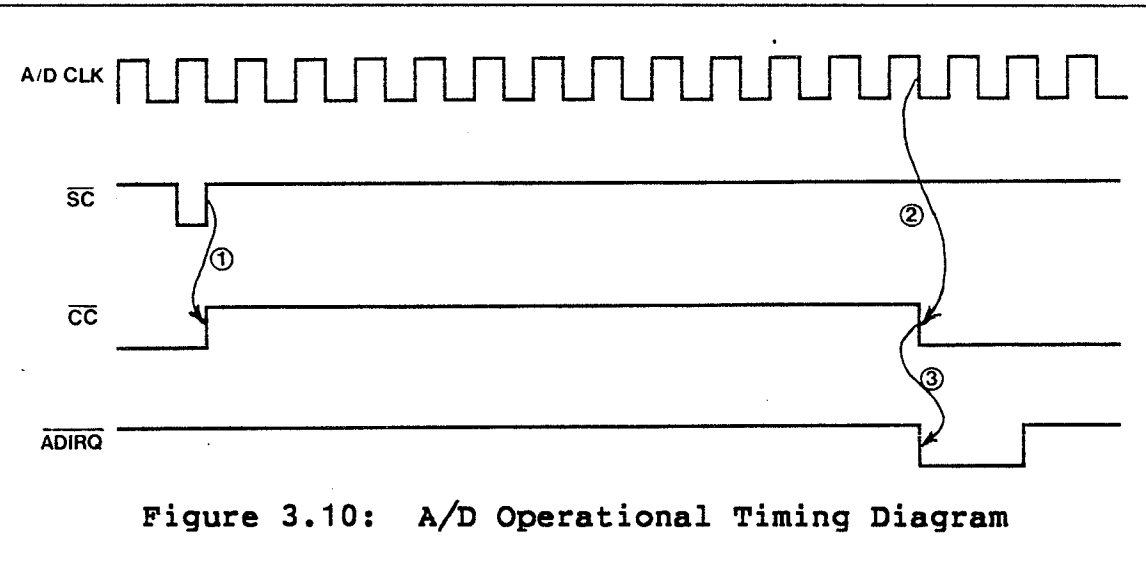
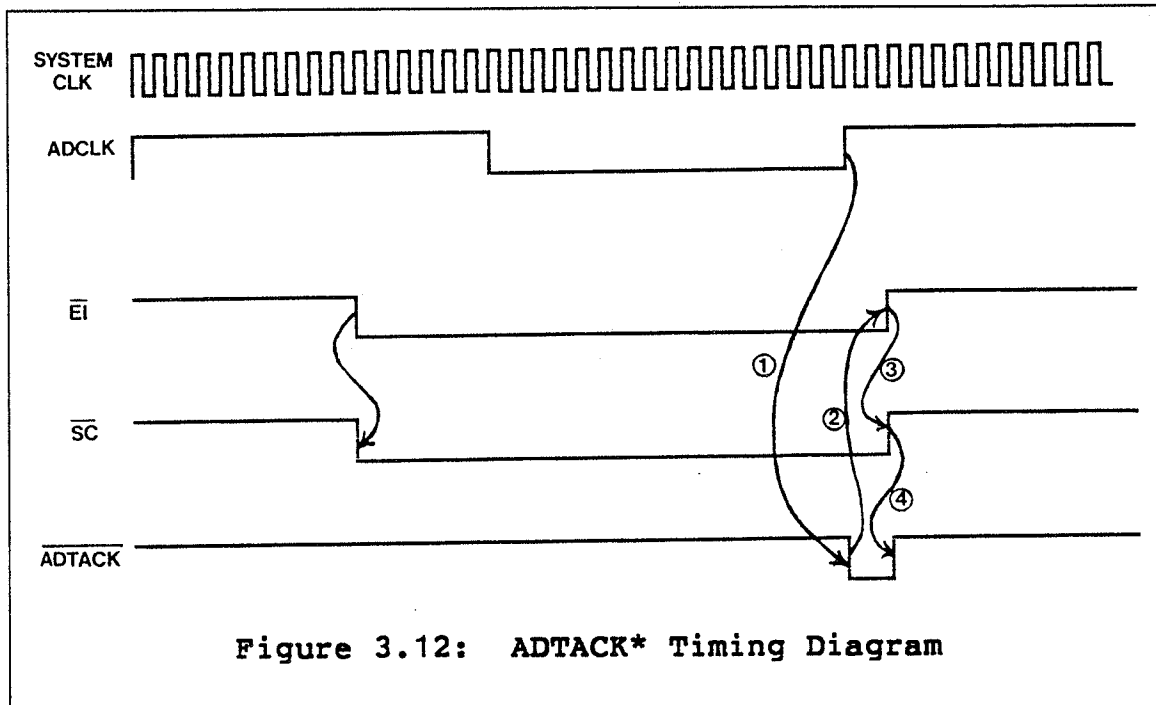


Figure 3.9: Schematic Diagram of ADC1210 A/D Converter





3.4 INTEL 8231A ARITHMETIC PROCESSING UNIT

The 4 MHz Intel 8231A (also Advanced Micro Devices Am9511) arithmetic processing unit (APU) performs fixed and floating point arithmetic and floating point trigonometric and mathematical operations. All transfers take place over an 8-bit bidirectional data bus. Operands are pushed onto an internal stack and a command is issued to perform operations on the data in the stack. Results are then available on the stack or additional operations may be performed. Transfers to and from the APU are handled by the MC68000 over data lines D0-D7. These data lines are buffered using a 74LS245 device.

The APU is mapped into memory segment \$050000-\$05FFFF. ECB connection E3* and MC68000 address line A4 are used in the decoding scheme. The resulting addresses generated are \$50001 for the operand entry address and \$50011 for the command entry address.

A schematic diagram of the APU is shown in Figure 3.13. The C/D*, RD*, and WR* lines are used to determine the type of data transfer to be performed over the data bus. Table 3.7 describes the functions available and the corresponding signals on the C/D*, RD*, and WR* lines needed to provide these functions. A command may be issued after the required operands have been positioned on the stack. Upon completion of command execution, the END* output goes low. This signal is used to generate the APUIRQ* signal, informing the MC68000 that execution of the command is completed. The MC68000 sends an interrupt acknowledge signal to the APU by asserting APUEACK*. This signal resets the END* output on the APU.

The APUDTACK* signal is generated using a 74LS175 and 74LS74 device, as shown in Figure 3.14. The READY* output is used as a handshake signal during read or write transactions. A low on this output indicates the APU has not yet completed its information transfer with the MC68000. For read operations, after RD* and CS* go low, READY* will go low and remain low until the data bus contains valid data, then goes high. The READY* pulse low duration (TPPWR) can

be a minimum of 0.9 μ sec and a maximum of 3.05 μ sec. For write operations, after WR* and CS* go low, READY* goes low for a very short duration. The READY* pulse low duration is a minimum of zero and a maximum of 50 nsec. This signal may not go low at all for very fast devices. The APUDTACK* circuitry handles these cases. The timing diagrams for the APU read and write operations are shown in Figure 3.15.

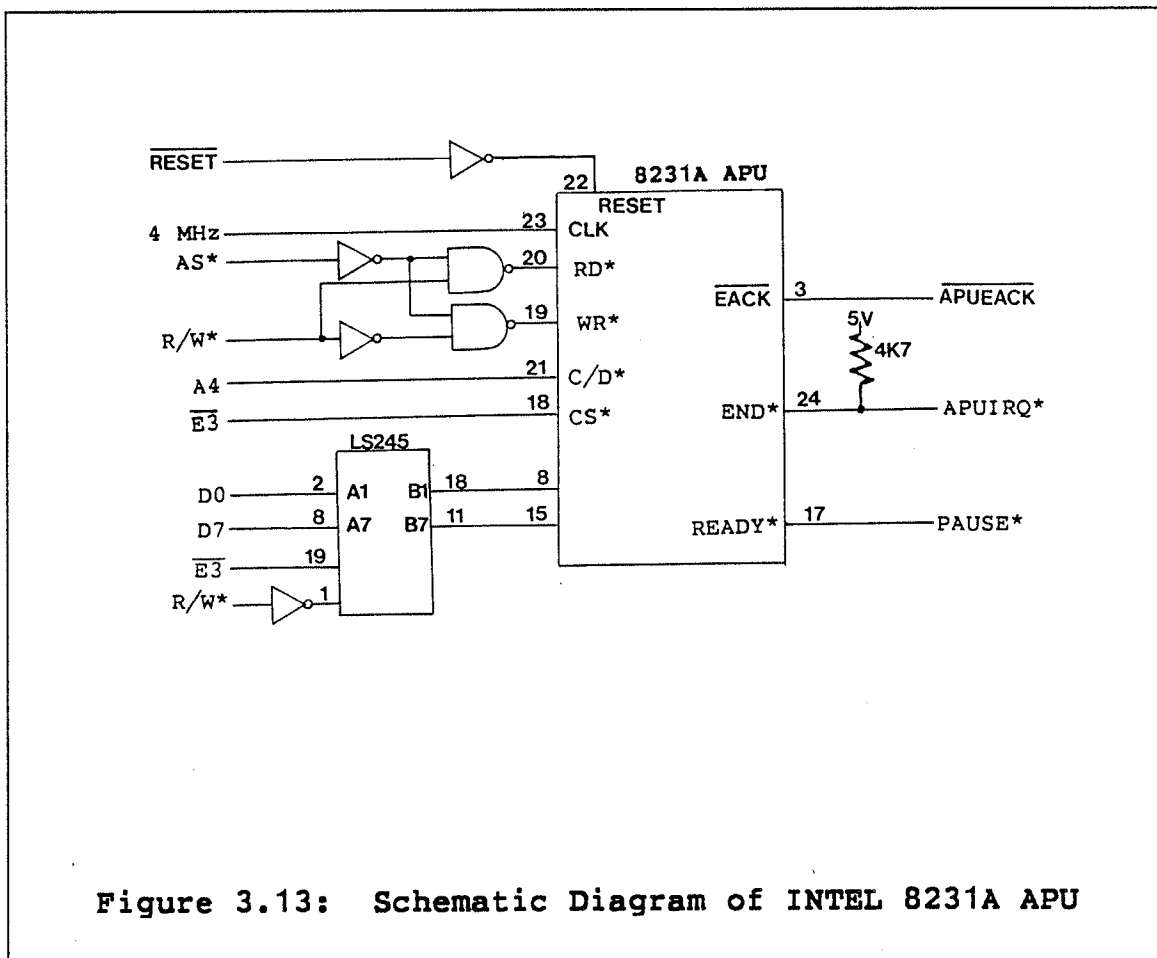


Figure 3.13: Schematic Diagram of INTEL 8231A APU

TABLE 3.7
APU Function Table

C/D*	RD*	WR*	Function
L	H	L	Push data byte onto stack
L	L	H	Pop data byte from stack
H	H	L	Enter command byte from data bus
H	L	H	Read status
X	L	L	Undefined

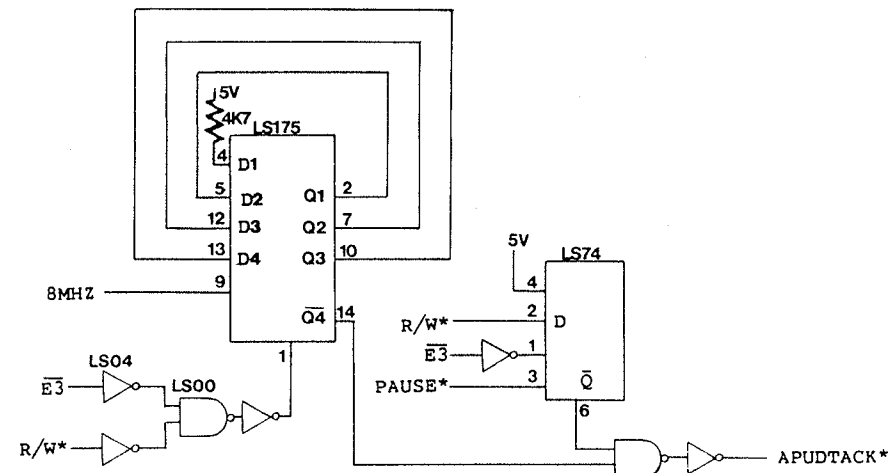
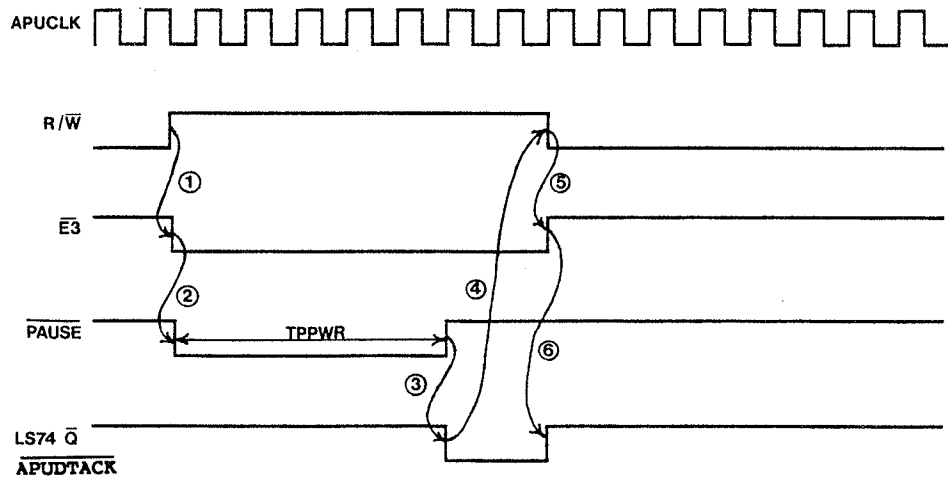


Figure 3.14: APUDTACK* Signal Generation

read:



write:

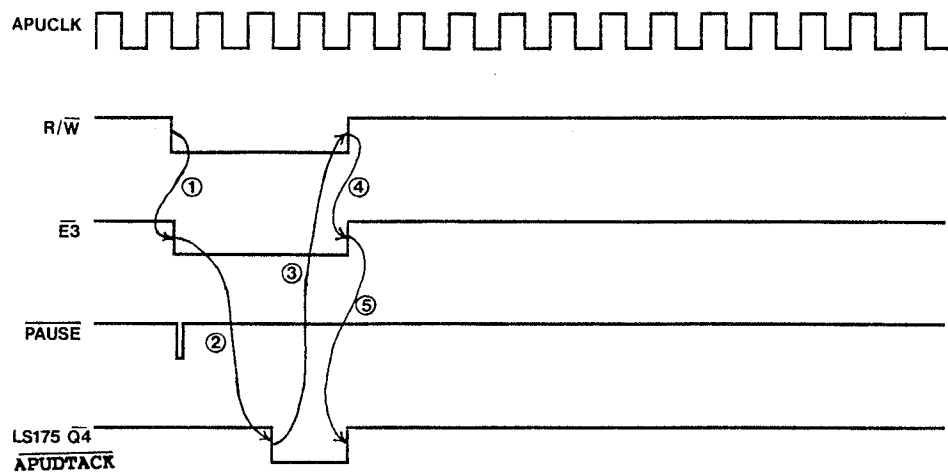


Figure 3.15: APUDTACK* Timing Diagrams

3.5 DIGITAL-TO-ANALOG CONVERSION CIRCUITRY

The digital-to-analog (D/A) converters are mapped in memory segment \$040000-\$04FFFF. Control of the D/A converters is provided with a 74LS138 3- to 8-line decoder. Connection E2* from the ECB and MC68000 address lines A1-A3 are used in the decoding scheme, as shown in Figure 3.16. Table 3.8 shows the D/A control signal address map.

Three National Semiconductor DAC1210 12-bit D/A converters are interfaced directly to the MC68000 data bus. These devices are configured to appear as one-word addresses in the I/O space. Conversion of a 12-bit digital word to an analog signal is performed by writing the data to D/A memory location DACHx (where x = 1, 2, or 3). The output of the D/A converter is a current (IOUT1); thus a current-to-voltage converter circuit using an MC741 operational amplifier is used to provide an output voltage in the range 0.0-5.0 volts. A schematic diagram of one of D/A converters as it is configured in this system is shown in Figure 3.17.

The DADTACK* signal is generated using the 74LS175 configuration similar to that shown in Figure 3.11. The E1* signal is replaced by E2* and a delay corresponding to 4 clock cycles of the ECB 8MHZ CLOCK signal is incurred before the DADTACK* signal is sent to the USER DTACK* circuitry.

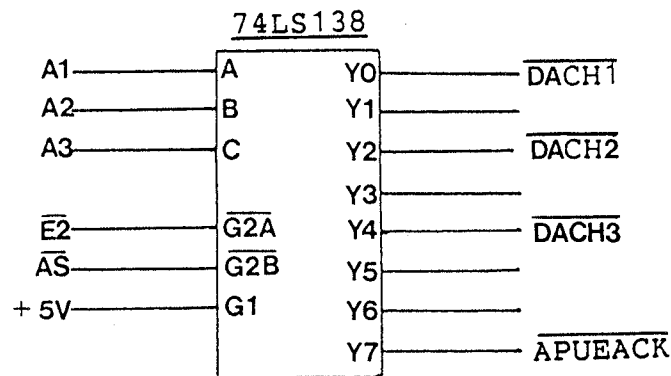
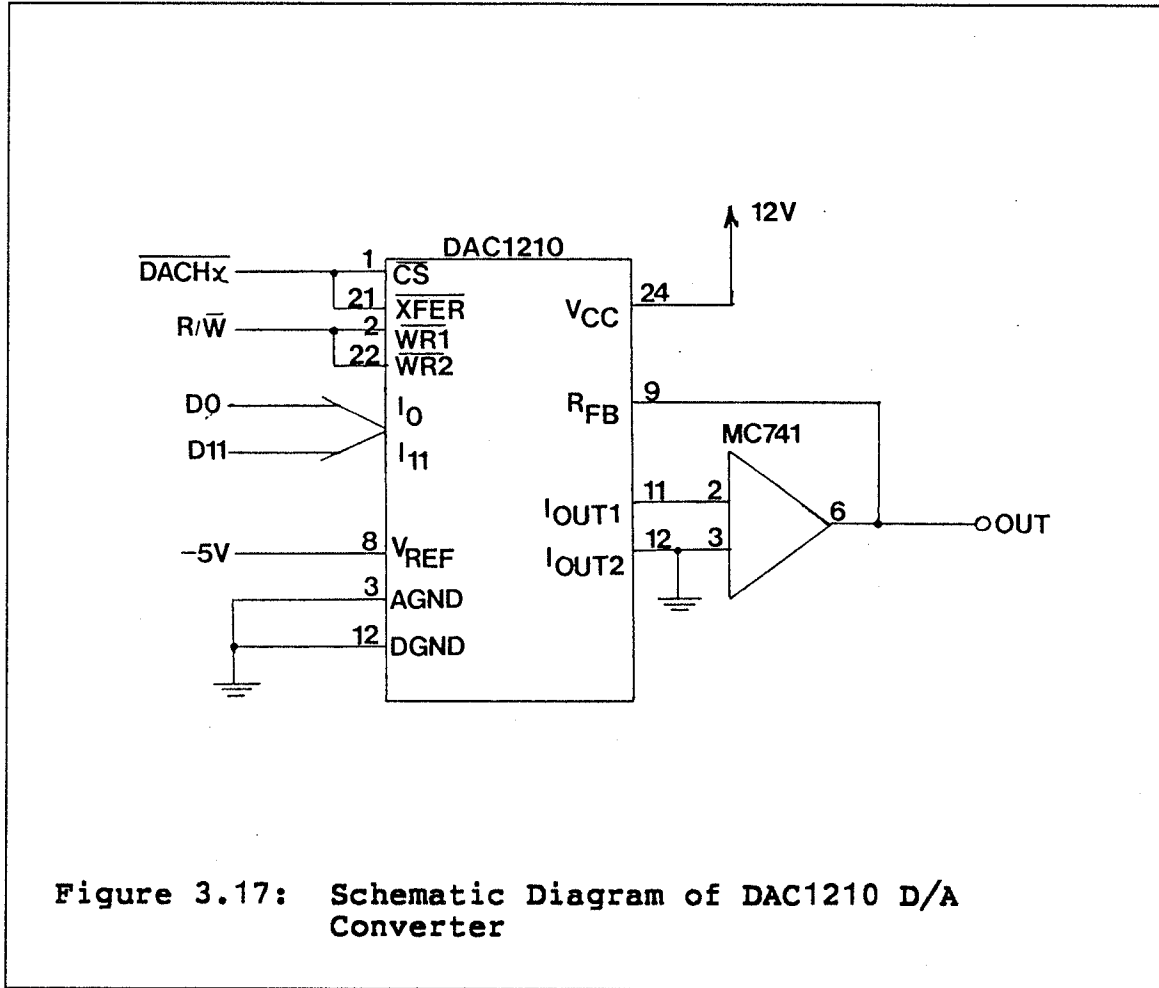


Figure 3.16: D/A Circuitry Decode Logic

TABLE 3.8
D/A Control Signal Address Map

Address	Function
\$040000	Perform D/A conversion on channel 1 (DACH1)
\$040002	Not used
\$040004	Perform D/A conversion on channel 2 (DACH2)
\$040006	Not Used
\$040008	Perform D/A conversion on channel 3 (DACH3)
\$04000A	Not used
\$04000C	Not used
\$04000E	APU Interrupt Acknowledge (APUEACK)



Chapter IV

SIGNAL PROCESSING TECHNIQUES AND SOFTWARE DESCRIPTION

4.1 INTRODUCTION

Frequently, murmurs or alterations in the heart sounds are the only definitive signs of some types of heart disease, appearing long before stress on the cardiovascular system is sufficient to produce other signs and symptoms [3]. Presently, auscultation is the primary test performed to assess the condition of the heart; however, this test is prone to interpreter variations and errors [22,23]. The primary aim in automated PCG analysis is the quantification of the subjective features of the signal. The important features of the PCG signal are the intensity and timing sequence of murmurs and sounds, and the location, frequency content, and envelope shape of murmurs, if present. Currently, there exists the need for a simple and efficient method to quantify the PCG signal into parameters aiding the detection of murmurs. Such a system would be extremely useful for screening purposes and routine diagnosis.

In this chapter, methods for the time and frequency domain analysis of the systolic and diastolic segments of the phonocardiogram (PCG) signal are presented. A technique for

the segmentation of the PCG into systole and diastole is also discussed. The electrocardiogram (ECG) and the carotid pulse signals are used as timing references for the first and second heart sounds. Using a QRS-complex detection algorithm based on a smoothed difference of the ECG signal, the RR interval, corresponding to one cardiac cycle, can be established. The beginning of the cardiac cycle coincides with the start of the first heart sound (start of systole). A transformation based on a smoothed second difference of the carotid pulse is applied to locate the dicrotic notch in the carotid pulse. Using the location of the dicrotic notch, the beginning of the second heart sound (start of diastole) can be determined.

Upon segmenting the PCG into systole and diastole, quantification of the time and frequency domain characteristics is conducted. The energy curve and energy spectrum of each segment are computed and are then quantified using the concept of an Energy Distribution Coefficient (EDC).

The signal processing software is written in MC68000 assembly language using the MC68000 two-pass Cross Macro Assembler resident on the Amdahl 580/5850 computer system. This assembler provides access to the host computer's resources including the text editor and filing system. For a complete description of the assembler and an instruction set summary refer to the assembler reference manual [102].

For debugging purposes, the software can be downloaded from the host computer system into the Educational Computer Board (ECB) memory. The ECB operates under control of "TUTOR" firmware. TUTOR is the system monitor which controls communication with the terminal and host computer and provides debug capabilities, line assembly/disassembly, and I/O control. Upon completion of the debugging process, the software can be programmed into an erasable programmable read only memory (EPROM).

The signal processing software can be divided into the following major categories (Figure 4.1):

1. System Initialization
2. Analog-to-Digital Conversion
3. Detection of the QRS-Complex in the ECG
4. Detection of the Dicrotic Notch in the Carotid Pulse
5. Segmentation of the PCG into Systole and Diastole
6. Computation of the PCG Energy Curves
7. Computation of the PCG Energy Spectra
8. Computation of the Energy Distribution Coefficients

This chapter provides a detailed description of the signal analysis theory and techniques and the signal processing software. A program listing is included in Appendix B. In this discussion numbers in hexadecimal form are represented with a preceding '\$'.

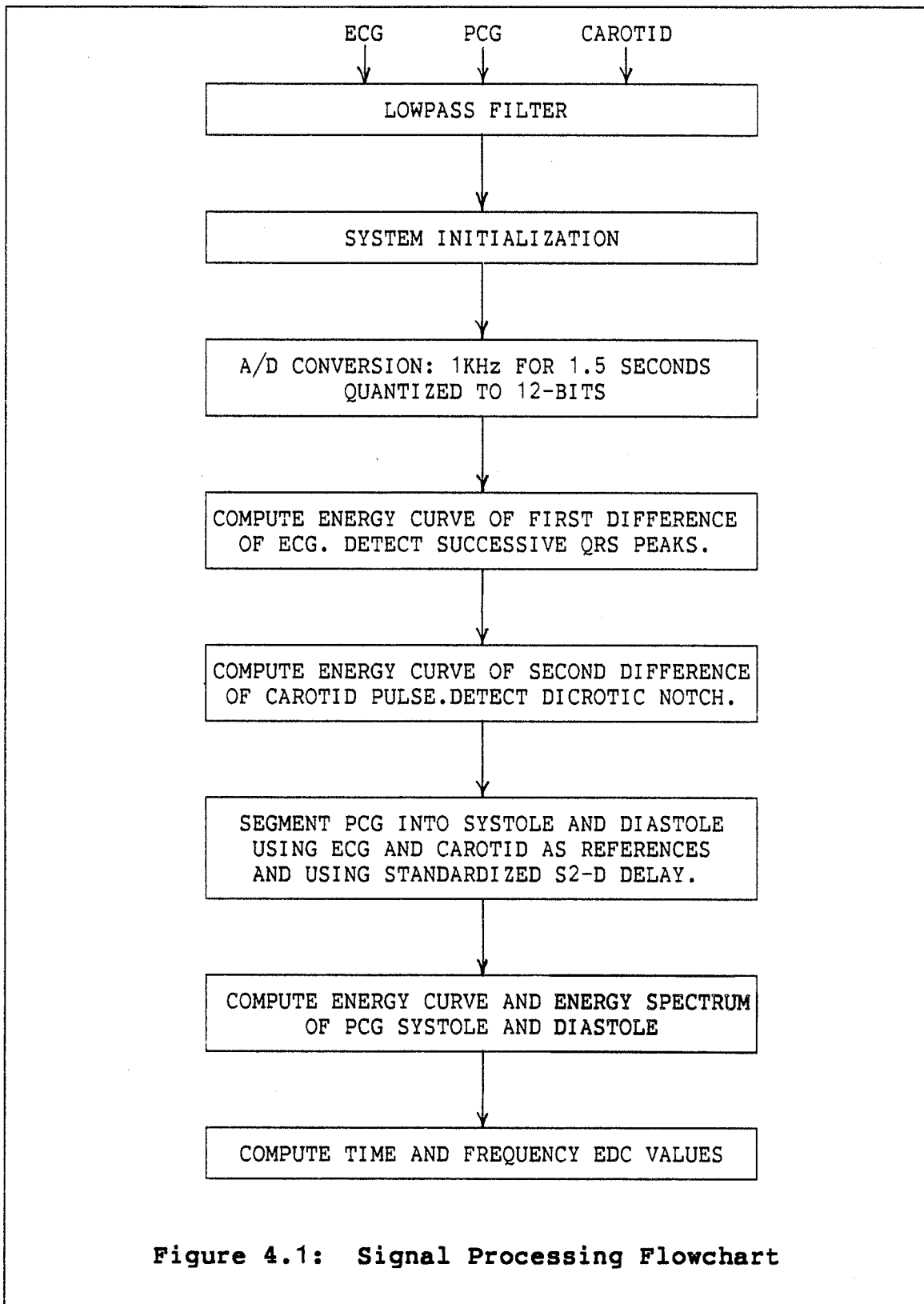


Figure 4.1: Signal Processing Flowchart

4.2 SYSTEM INITIALIZATION

The MC68000 microprocessor contains a 16-bit status register (Figure 4.2) which contains the interrupt mask as well as the following condition codes: extend, negative, zero, overflow, and carry. Additional status bits indicate that the processor is in a trace mode and in one of two states of privilege: the supervisor state or the user state. The initialization procedure begins with selecting the supervisor state for the MC68000. The supervisor state is the higher state of privilege in which all instructions can be executed. The interrupt mask of the status register is initialized to allow level 4 interrupts or higher.

Since the processor is in the supervisor state, the 32-bit supervisor stack pointer is set to a valid RAM address. The seven 32-bit address registers and eight 32-bit data registers are initialized as necessary throughout the program.

Initialization of the starting address of the A/D and APU interrupt service routines (ISR) is also required. Interrupt vectors are memory locations from which the processor fetches the address of a routine which will handle the interrupt. A vector number is an 8-bit number which, when multiplied by four, gives the address of an interrupt vector. When the M6800 IRQ* signal is asserted a level 4 interrupt acknowl-

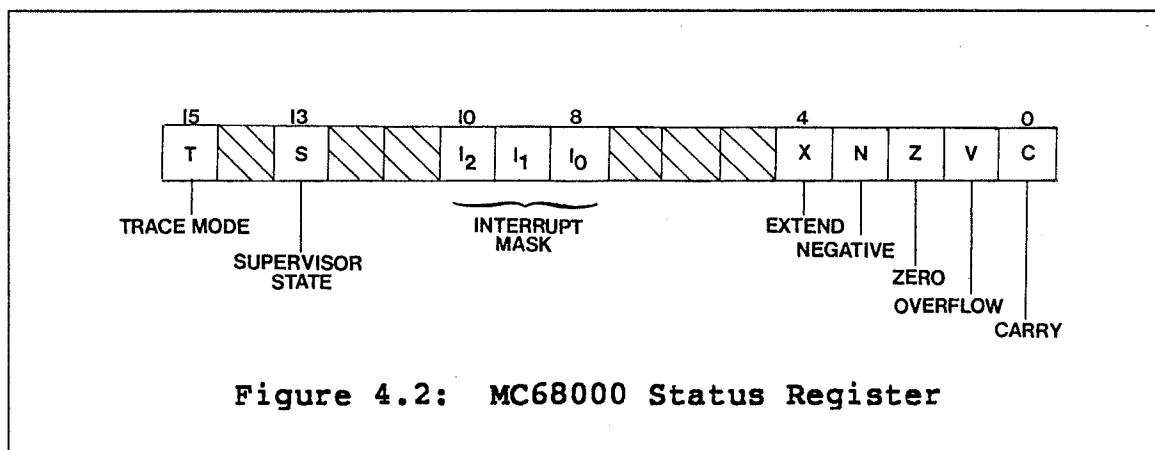


Figure 4.2: MC68000 Status Register

edge cycle from the MC68000 causes an autovectored response with the vector number equal to 28. Autovectoring is used when the interrupting device can not provide the processor with the vector number. The address of the A/D and the APU interrupt service routines is thus stored in the interrupt vector at address \$000070.

4.3 ANALOG-TO-DIGITAL CONVERSION

The PCG, ECG, and carotid pulse signals are sampled at a rate of 1024 Hz. The sampling period is controlled using the timer in the PI/T. The timer is initialized by writing the sampling period to the Counter Preload Register (CPR). The timer is set up to load the Counter Register (CR) from the CPR and to begin decrementing the CR. At the start of the sampling period, the S/H device hold state is initiated by performing a 'dummy' write to address HOLD. During each sampling period, data from the three analog channels are digi-

tized and stored in RAM. A flowchart of the A/D process is shown in Figure 4.3. The following events are carried out for each analog channel:

1. A 'dummy' write to address ADCH1, ADCH2, or ADCH3 is conducted to connect the analog multiplexer input to the output and to start the A/D converter.
2. The processor stops fetching and executing instructions until the CONVERSION COMPLETE* signal is received from the A/D converter (via the M6800 IRQ* level 4 interrupt).
3. The A/D ISR address is fetched from the level 4 interrupt vector and the program enters the ISR. The digitized data is read from address ADREAD and stored in the system memory.

After the three analog signals have been digitized, the processor waits until the sampling period is over (CR equals zero). Upon reaching zero, the CR is loaded from the CPR and resumes counting and the sampling process continues. Approximately 1.5 seconds of data are acquired and stored in RAM, upon which the timer is disabled.

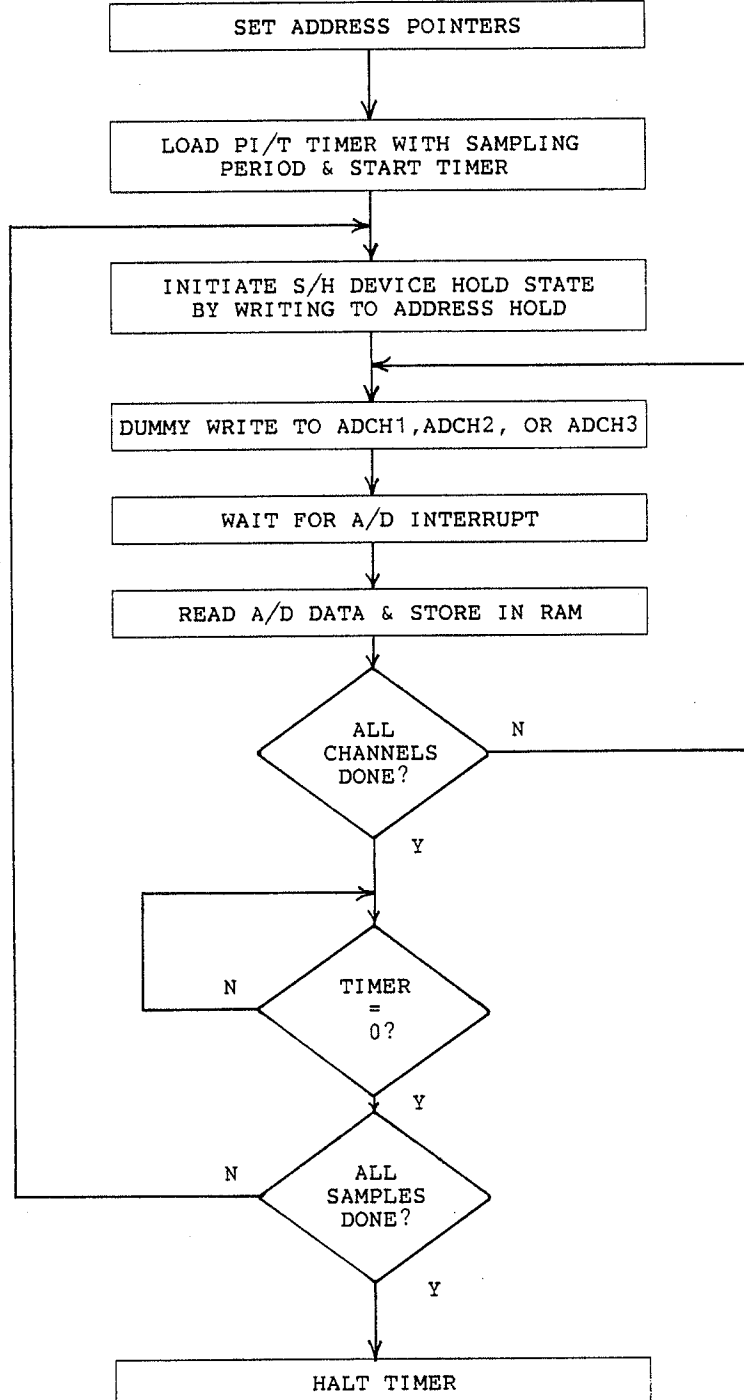


Figure 4.3: Analog-to-Digital Conversion Flowchart

4.4 DETECTION OF THE QRS-COMPLEX IN THE ECG

The digitized ECG signal is first downsampled to an effective sampling rate of 256 Hz by taking every fourth sample. A QRS-complex detection routine based on a smoothed difference of the digitized ECG signal is used to determine the RR interval [88,89]. With $x(n)$ representing the digitized ECG signal, the following transformation is applied to compute the smoothed energy curve of the first difference of the ECG signal:

$$g(n) = \sum_{k=1}^M [x(n-k+1) - x(n-k)]^2 w(k) \quad (4.1)$$

Here $w(k)$ is a weighting sequence or window which selects a segment of $x(n)$, M is the number of samples in the window, and n is the running index of the signal and its transform. The purpose of the window is to attach lower weight to samples which occurred further back in time. Thus $w(k)$ tends to zero monotonically as k increases. We define $w(k) = (M-k+1)$, where $k = 1, 2, \dots, M$. This process, in effect, convolves the ECG difference signal with a decreasing weighting sequence.

The ECG transform $g(n)$ yields a single positive peak for each cardiac cycle with maximum value occurring near the end of the QRS-complex. An ECG signal and its corresponding transform $g(n)$ with $M=16$ are shown in Figure 4.4. In this figure note that the ECG signal is corrupted with low amplitude 60 Hz noise. This noise was picked up during the recording procedures. The low level noise, however, does not

affect $g(n)$. Since the amplitude of the noise is minimal in comparison with the amplitude of the QRS-complex, the noise is effectively smoothed out during the convolution process.

A simple peak detecting routine is used to detect successive QRS end points (Q_1, Q_2) from $g(n)$. The ECG transform is scanned and a threshold is set at half the maximum transform value. The transform data is scanned a second time to search for the QRS end points. A sample in $g(n)$ is considered a QRS end point peak if the sample value at that point is greater than the threshold and is greater than the ten previous sample values and the ten following sample values. This search is continued until two peaks are found, representing the start and end of one cardiac cycle.

Figure 4.5 shows the carotid pulse and the ECG transform $g(n)$. After detecting two successive peaks in $g(n)$, denoted Q_1 and Q_2 , point C_1 is identified on the carotid pulse. This point corresponds to the start of the cardiac cycle. The di-crotic notch is searched for in a region starting at C_1 .

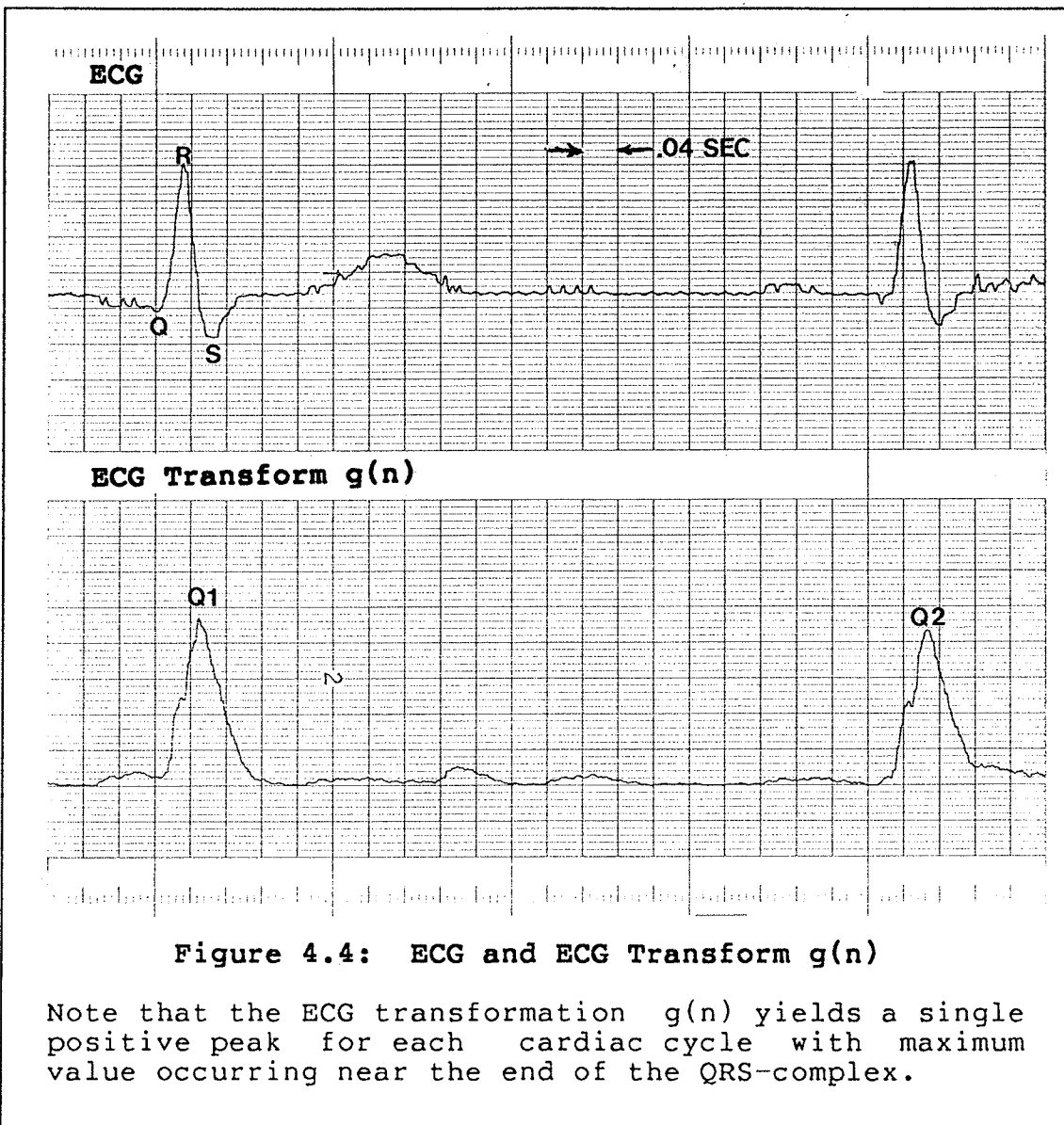


Figure 4.4: ECG and ECG Transform $g(n)$

Note that the ECG transformation $g(n)$ yields a single positive peak for each cardiac cycle with maximum value occurring near the end of the QRS-complex.

The 32-bit $g(n)$ sample values have been truncated to 12-bits for display purposes.

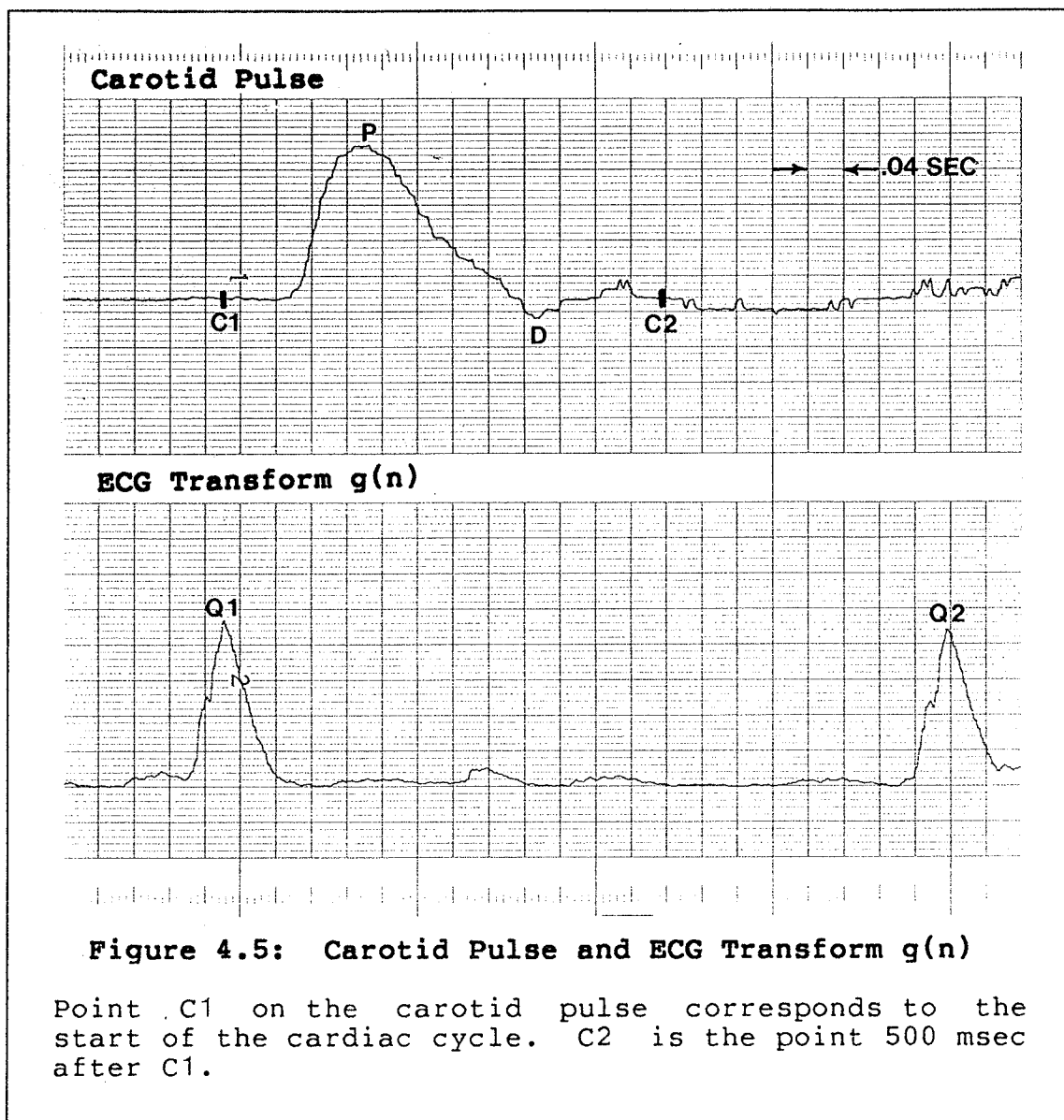


Figure 4.5: Carotid Pulse and ECG Transform $g(n)$

Point C1 on the carotid pulse corresponds to the start of the cardiac cycle. C2 is the point 500 msec after C1.

The 32-bit $g(n)$ sample values have been truncated to 12-bits for display purposes.

4.5 DETECTION OF THE DICROTIC NOTCH IN THE CAROTID PULSE

The carotid pulse can be characterized by measuring the important intervals of the waveform. The pre-ejection period (PEP) is the period from the beginning of the QRS-complex of the ECG to the onset of the carotid upstroke as indicated in Figure 2.7. The following equation may be used to approximate the true PEP interval [25]:

$$\text{PEPC} = \text{PEP} + 0.4(\text{HR}) \quad (4.2)$$

Here PEPC is the rate-corrected pre-ejection period (normally 131 ± 13 msec), PEP is the actual pre-ejection period, and HR is the heart rate in beats per minute (bpm). It should be noted that this is only an approximate relation which depends on, among other factors, age, sex, and physiological condition of the heart.

Another indirect measurement is the ejection time (ET), which is the interval from the onset of carotid upstroke to the dicrotic notch, as indicated in Figure 2.7. In the normal resting individual, this interval is dependent upon heart rate. Using the following equation, the true ejection time (ET) can be approximated by [25]:

$$\text{ETC} = \text{ET} + 1.6(\text{HR}) \quad (4.3)$$

Here ETC is the rate-corrected ejection time, ET is the actual ejection time, and HR is the heart rate in bpm. The normal value for ETC is 395 ± 13 msec for males and 415 ± 11

msec for females. It should be noted that although these equations yield only approximate time intervals, they can be used to localize the dicrotic notch in a general area.

Using equation (4.2), the maximum interval between the end of the QRS-complex and the onset of carotid upstroke can be determined. Using a maximum PEPC of 144 msec and a minimum heart rate of 60 bpm, the PEP is 120 msec. It should be noted that equation (4.1) yields a peak near the end of the QRS-complex, therefore the interval between the S-wave of the ECG and the onset of carotid upstroke is 90 msec (using a minimum QRS width of 30 msec). The ejection time of the carotid pulse is the time interval from the onset of upstroke to the dicrotic notch. Equation (4.3) can be used to approximate the region in which the dicrotic notch will fall. Using a minimum heart rate of 60 bpm and a maximum ETC of 425 msec, the ET is 325 msec. Using the PEP and ET intervals, the maximum interval between the QRS-complex and the dicrotic notch is 380 msec. To take into account variational factors, such as abnormal PEP or ET intervals and formula approximations, it was decided to search for the dicrotic notch in an area between C1 and a point 500 msec after C1. This point is designated C2 on Figure 4.5.

The digitized carotid pulse is first downsampled to 256 Hz. The dicrotic notch is defined as the point of minimum pressure occurring after the percussion wave, in the region of the maximum second derivative. A least squares estimate of the second derivative [98] is obtained from

$$p(n) = [2y(n-2) - y(n-1) - 2y(n) - y(n+1) + 2y(n+2)] \quad (4.4)$$

where $y(n)$ represents the digitized carotid pulse waveform, and $p(n)$ is the second derivative evaluated at the n th data point. The following transformation is then applied to obtain a smoothed energy curve of the second derivative of the digitized carotid pulse:

$$s(n) = \sum_{k=1}^{M-2} p(n-k)w(k) \quad (4.5)$$

Here $w(k)$ is a window which selects a segment of $p(n)$, M is the number of samples in the window and n is the running index of the signal and its transform. The window $w(k)$ was selected such that $w(k) = (M-k+1)$, as for the ECG.

This transformation yields two positive peaks with local maxima occurring at points corresponding to the onset of carotid upstroke and the dicrotic notch. The carotid pulse and its corresponding transform with $M=16$ are shown in Figure 4.6. The first peak (T_1) represents the onset of upstroke. After T_1 is detected, the search for T_2 , the peak corresponding to the dicrotic notch, is undertaken. A peak detecting routine, similar to that presented in the previous section, is used to locate both peaks. To locate the dicrotic notch, the local minimum which occurs on the carotid pulse within a ± 20 msec region of the maximum second derivative (T_2) is determined.

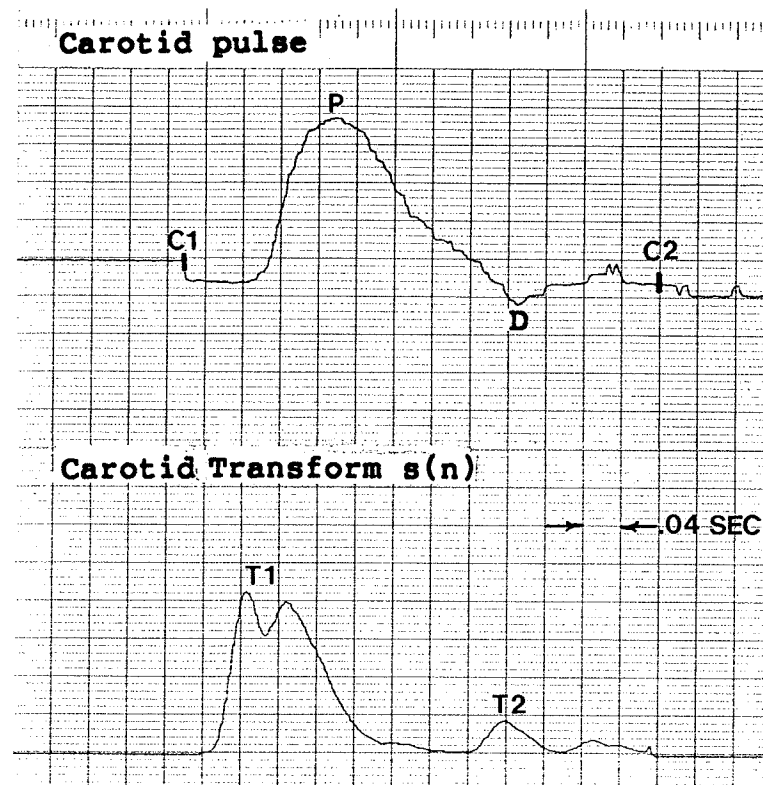


Figure 4.6: Carotid Pulse and Transform $s(n)$

The carotid transform $s(n)$ results in two relative maxima. Peak T1 corresponds to the onset of carotid upstroke and peak T2 corresponds to the dicrotic notch.

The 32-bit $s(n)$ sample values have been truncated to 12-bits for display purposes.

4.6 PCG SIGNAL PROCESSING

4.6.1 Segmentation of PCG into Systole and Diastole

The ECG transform $g(n)$ is used to identify the start and end of one PCG cycle. Figure 4.7 shows the PCG signal and the corresponding $g(n)$. The peaks in $g(n)$ provide a sharp reference which can be used to determine the start of the first heart sound and thus the start of the cardiac cycle. The PCG cycle ends at the beginning of the next first heart sound. The start and end points of one cardiac cycle are labelled P1 and P3, respectively, on the PCG signal.

The dicrotic notch in the carotid pulse is used to identify the start of the second heart sound (S2). With the start of S2 determined, segmentation of the PCG into systole and diastole is possible. Figure 4.8 shows a PCG signal and the corresponding carotid transform $s(n)$. As can be seen in the figure, there is a time delay between the start of S2 and the dicrotic notch (T2 on carotid transform - this interval will be referred to as the S2-D delay). This time delay must be properly determined in order to correctly identify the start of S2.

The S2-D delay is dependent upon the distance of the recording site from the heart and the pulse-wave velocity. Since the recording site of the carotid pulse is kept relatively constant, it was decided to use a measurement based on a standardized S2-D interval in order to correctly locate

the start of S2 [103,104]. For the cases tested the S2-D delay was initially measured from a strip chart recording of the signals. This delay is reflected in column 1 of Table 4.1. Column 2 contains the heart rate of the patient. The range of the S2-D delay is quite small, ranging from a minimum of 35 msec to a maximum of 54 msec. For the signals analyzed in this study the mean delay was found to be 42.6 msec with a standard deviation of 5.0 msec. The mean delay and the standard deviation of the S2-D delay are used to compute the standardized S2-D interval.

The mean S2-D delay is subtracted from the computed location of the dicrotic notch. To prevent the likelihood that any portion of S2 is included in the systolic segment, a value equal to two standard deviations of the mean delay (in this work 10 msec) is further subtracted. This point, which identifies the start of S2, is labelled P2 on the PCG signal (Figure 4.8).

To summarize, the standardized S2-D interval is equal to the mean delay plus two standard deviations of the mean delay. In this work the interval is 53 msec. This value is subtracted from the computed location of the dicrotic notch to give the location of the start of the second heart sound. Figure 4.9 shows a PCG signal separated into its systolic and diastolic segments. Qualitatively, the PCG segmentation is quite accurate, as can be seen in this figure. Minor problems which may result in this method and an analysis of

the PCG quantification error resulting from this procedure are discussed in the following chapter.

We believe this procedure to be quite accurate for quantifying the time and frequency domain characteristics of the systolic and diastolic segments of the PCG. This method is computationally simpler than other methods presented for PCG segmentation and analysis of the first and second heart sounds [40,42,45,54,55,57,58,67]. The minimal computation time makes it very useful for online analysis using a dedicated microcomputer system. In most reported cases, the exact location of the start of S2 is not used; rather, a window which selects the approximate location of S2 is used in the analysis [40,42,45,67]. Other reported methods involving linear prediction coding [57,58] are not suited for this type of microcomputer system, while statistical methods [57,58] require many cardiac cycles to perform PCG segmentation and are thus time consuming.

The procedure proposed in this work requires a third signal - the carotid pulse, which is a useful diagnostic tool recommended to be recorded with the PCG and ECG signals [105]. The use of the standardized S2-D interval simplifies the problem of accurate S2 location. This procedure has been successively implemented on the PCG analysis system and is used to segment the PCG into systole and diastole in order that time and frequency domain analysis can be performed on both PCG segments.

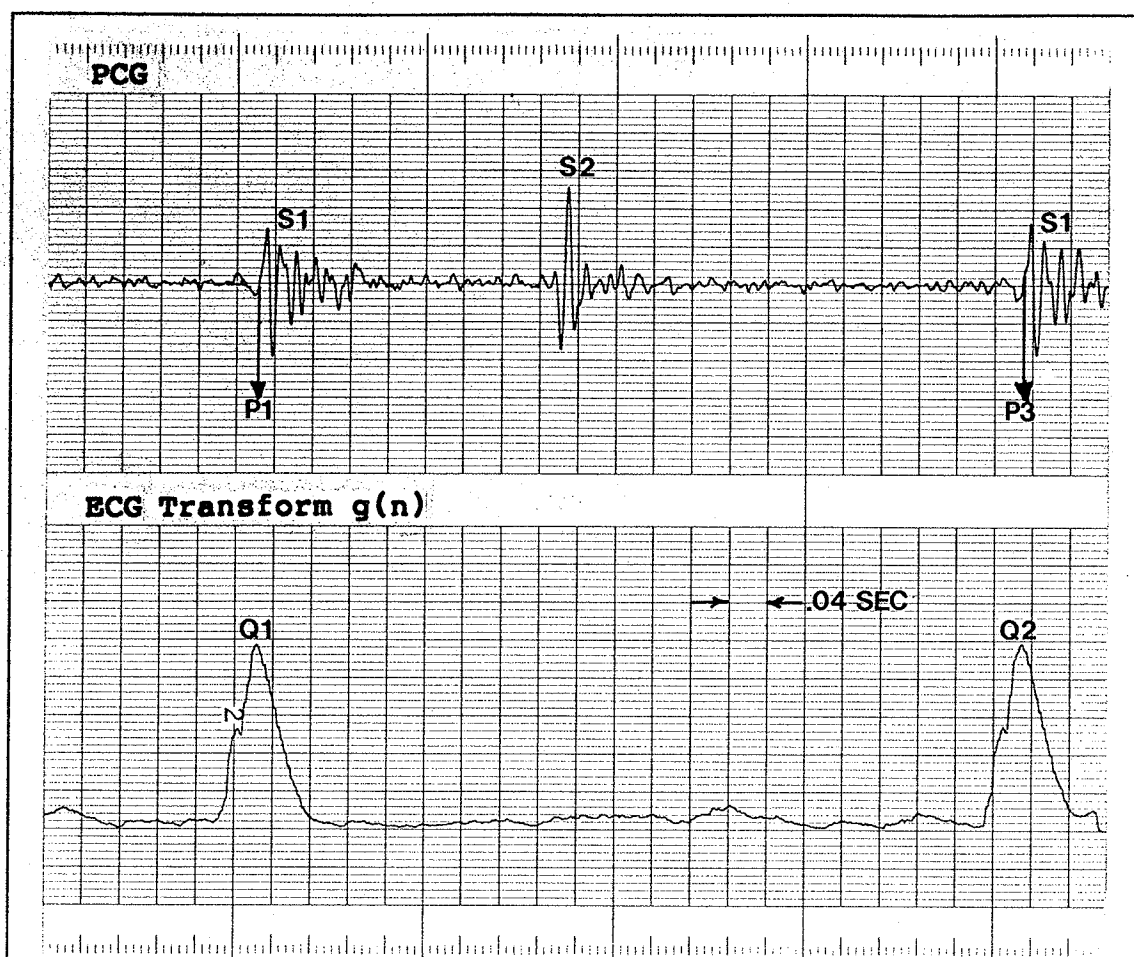
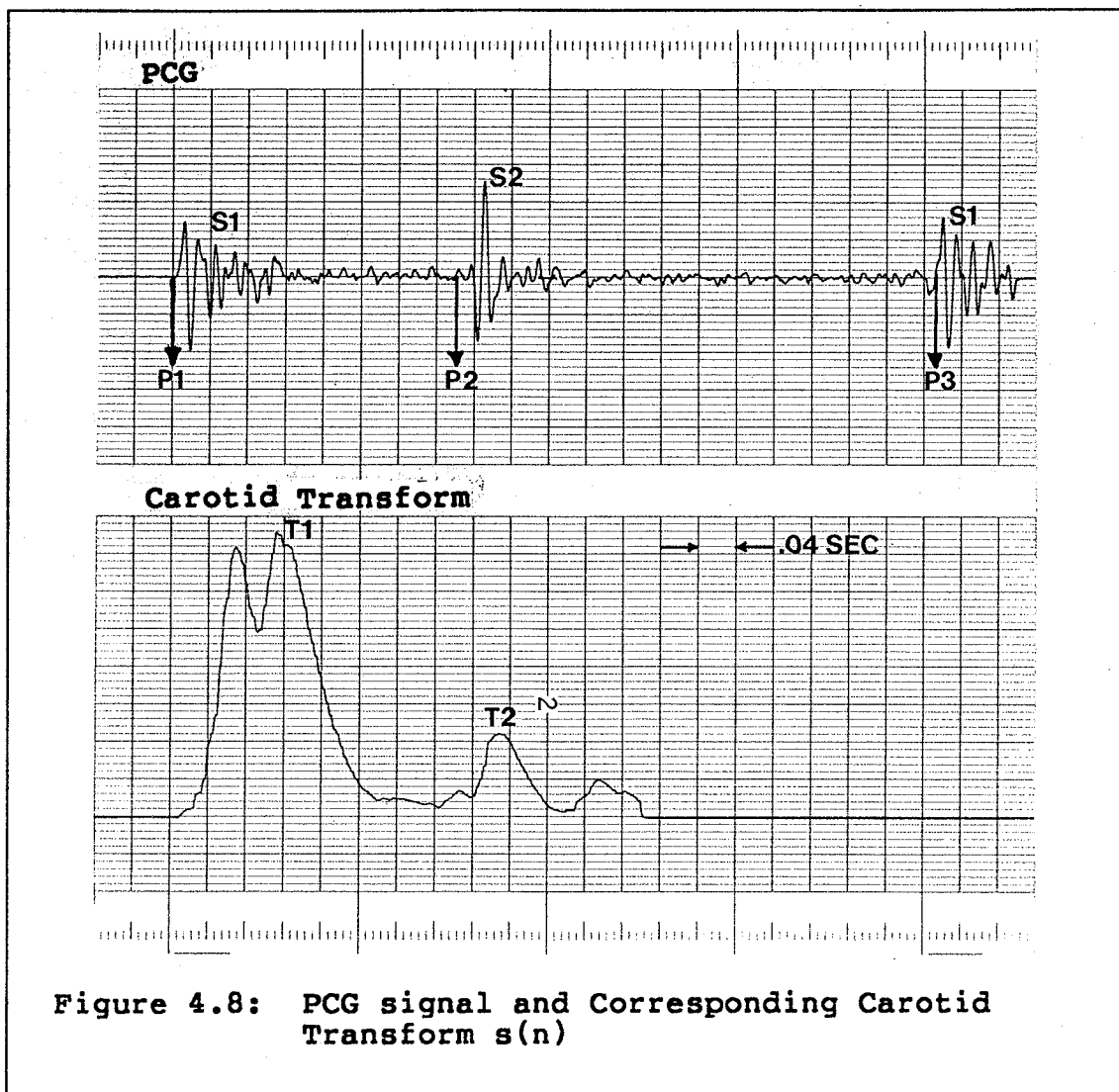


Figure 4.7: PCG signal and Corresponding ECG Transform $g(n)$

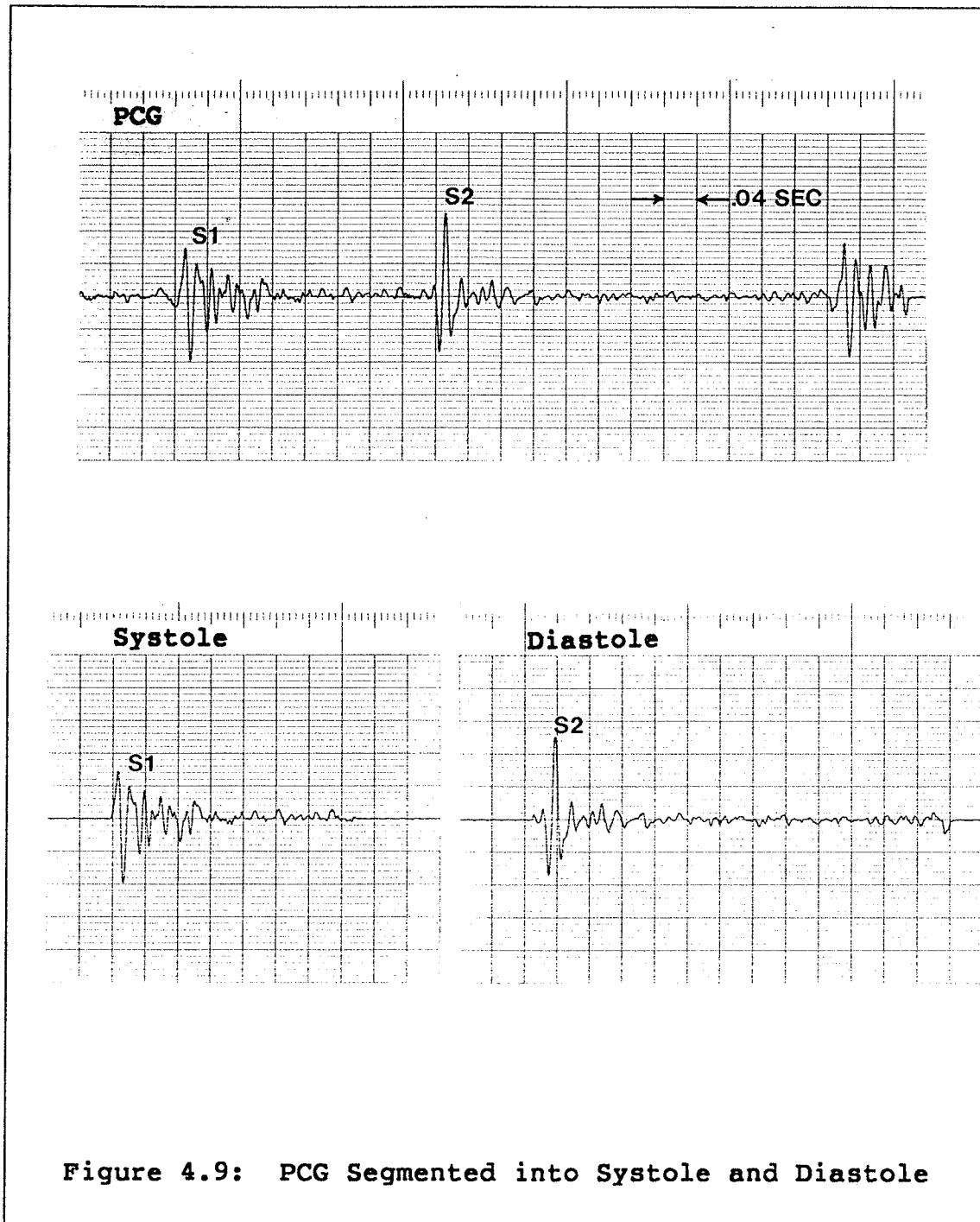
The 32-bit $g(n)$ sample values have been truncated to 12-bits for display purposes.



The 32-bit $s(n)$ sample values have been truncated to 12-bits for display purposes.

TABLE 4.1
Delay Between Second Heart Sound and Dicrotic Notch

Patient	S2-D Delay (msec)	Heartrate (bpm)
A	45	61
B	46	73
C	44	70
1a	42	77
1b	43	76
1c	44	76
2a	53	75
2b	53	75
2c	54	72
3a	41	87
3b	39	85
3c	38	83
4a	43	111
4b	44	117
5	38	82
6	39	84
7a	40	83
7b	44	83
8a	52	62
8b	50	60
9a	41	92
9b	39	94
10	41	77
11a	47	82
11b	45	93
13	47	82
14a	46	80
14b	48	80
15b	42	74
15c	44	78
16a	35	130
17a	44	76
18a	39	90
20	35	67
21	36	82
22a	35	45
22b	41	51
22c	41	51
24a	35	54
24b	41	58



4.6.2 PCG Energy Curve

The pattern of energy distribution of the PCG signal is very important in the diagnosis of valvular and septal defects, which cause murmurs of characteristic envelope shapes in particular locations of the cardiac cycle. This work employs the method of computing energy covered by a moving window, which is commonly used in speech signal processing [106].

The energy of a signal is an easily extractable parameter. In the case of a real discrete time signal $x(n)$, the energy is defined in general as [106]

$$E = \sum_{n=-\infty}^{\infty} x(n)^2 \quad (4.6)$$

For nonstationary signals such as the PCG, a time-varying energy calculation can be used as follows:

$$E(n) = \sum_{k=1}^{M} x(n-k)w(k) \quad (4.7)$$

where $w(k)$ is a decreasing weighting sequence which selects a segment of $x(n)$ and M is the number of samples in the window. The sequence $E(n)$ displays the time-varying energy characteristics of the signal $x(n)$. The selection of a suitable window $w(k)$ and appropriate window width M is very important in obtaining useful energy measurements. The window $w(k)$ is taken as a decreasing function so that PCG samples which occurred further back in time will have lower weight attached with them. The choice of M depends on the nature of

the signal and the sampling rate used. If M is too small there will be many ripples in $E(n)$ making it appear noisy; however, if M is too large $E(n)$ will become featureless [106]. With a sampling rate of 1024 Hz, M is chosen to be 32 and the window function is defined as $w(k) = M+1-k$.

This method is used to obtain the time-varying amplitude characteristics of the systolic and diastolic segments of the PCG signal for one cardiac cycle. The significance of $E(n)$ is that it provides a good measure for separating the heart sounds and murmurs from the silent periods during the cardiac cycle. Thus, the presence of murmurs is indicated when significant energy appears after the first heart sound in the systolic segment or after the second heart sound in the diastolic segment.

4.6.3 PCG Energy Spectrum

The frequency content of the PCG is one of the easiest features that can be assessed by auscultation. It is also an important factor in the detection of murmurs. A normal PCG lies in the 0 - 200 Hz frequency band. The frequency content of murmurs may be as high as 600 Hz; however the frequency content depends upon the pressure gradient across the defect, which depends upon the extent of the defect. The energy spectrum of the signal, which is the square of the Fourier transform, gives useful information by providing the distribution of energy versus frequency.

Physically, the Fourier transform $X(k)$ represents the distribution of signal strength with frequency. The fast Fourier transform (FFT) is a method for computing the discrete Fourier transform (DFT). With $x(n)$ representing the signal, the DFT is defined by [107]

$$X(k) = \sum_{n=0}^{N-1} x(n) W_N^{nk} \quad (4.8)$$

for $k = 0, 1, \dots, N-1$. The term $X(k)$ is the k th coefficient of the DFT and $x(n)$ is the n th sample of the time series, consisting of N samples. The term $W_N = \exp(-j2\pi/N)$. The inverse discrete Fourier transform (IDFT) is given by

$$x(n) = \frac{1}{N} \sum_{k=0}^{N-1} X(k) W_N^{-nk} \quad (4.9)$$

A typical FORTRAN source code of a radix-2 decimation in time FFT is shown in Figure 4.10. The FFT subroutine implemented in MC68000 assembly language is based on this algorithm [108]. To facilitate understanding of the assembly language version, each FORTRAN statement is reproduced in the comment field of the corresponding block of MC68000 instructions (See Appendix B).

The first part of the program, which is equivalent to the DO 3 loop, performs the in-place bit reversal shuffling of the input vector. The second part, equivalent to the nested DO loops, performs the actual FFT computations. Loop DO 4 I=J,N,LE evaluates the butterflies which have the same coefficient W_N^k in a given stage. Loop DO 5 I,LE1 computes and

keeps track of which coefficient w_N^k is being evaluated in a given stage, while loop DO 5 L=1,LN runs through all M stages.

The 8231A APU performs 16- and 32-bit fixed-point operations, as well as 32-bit floating-point arithmetic. In addition to the basic arithmetic operations (add, subtract, multiply, divide) the APU also evaluates logarithmic and trigonometric functions. The APU commands operate on operands located at the top of the APU stack (TOS) and next on stack (NOS) and results are returned to the stack at NOS and then popped to TOS. Operands are entered into the stack least significant byte first and most significant byte last by writing to the APU operand entry address APUOPER. The APU stack can accommodate four floating-point quantities. After the operands are positioned on the stack, a command can be issued by writing to the APU command entry address APUCOM. An interrupt request from the APU signals the current command execution is completed. At this time, the result from an operation can be read from TOS or a new command can be given.

The time required to compute a 1024-point FFT is approximately 4.3 seconds. All calculations are done in floating-point arithmetic to eliminate scaling and rounding of values, and to provide a greater dynamic range. Figures 4.11 and 4.12 show examples of typical time signals and their respective transforms computed using the PCG analysis system.

Since the digitized PCG segment $x(n)$ is of finite length, the data is multiplied by a Hamming window $w(n)$ to improve the spectral quality of the output. This process convolves the Fourier transforms of $x(n)$ and $w(n)$. The Hamming window equation is as follows [109]:

$$w(n) = \begin{cases} .54 + (.46)\cos(2\pi n/N), & |n| < (N-1)/2 \\ 0 & , \text{ otherwise} \end{cases} \quad (4.10)$$

Here N is the number of samples in the segment.

The FFT routine is used to compute the Fourier transform of the systolic and diastolic segments of the PCG signal over one cardiac cycle. The energy spectrum, which is the square of the Fourier transform, is computed for both segments to obtain the distribution of energy versus the frequency. This method is used to obtain the frequency domain characteristics of the PCG for one cardiac cycle. An indication of the presence of high frequency murmurs is obtained when the energy spectrum displays significant energy beyond 200 Hz.

```

SUBROUTINE FFT(F,LN)
COMPLEX F(1024),U,W,T,CMPLX
PI=3.141593
N=2**LN

C
C     START BIT REVERSAL
C
      NV2=N/2
      NM1=N-1
      J=1
      DO 3 I = 1,NM1
      IF (I .GE. J) GO TO 1
      T = F(J)
      F(J) = F(I)
      F(I) = T
      1   K=NV2
      2   IF (K .GE. J) GO TO 3
      J = J-K
      K=K/2
      GO TO 2
      3   J=J+K

C
C     FFT COMPUTATION
C
      DO 5 L=1,LN
      LE=2**L
      LE1=LE/2
      U=(1.0,0.0)
      W=CMPLX(COS(PI/LE1),-SIN(PI/LE1))
      DO 5 J=1,LE1
      DO 4 I=J,N,LE
      IP=I+LE1
      T=F(IP)*U
      F(IP)=F(I)-T
      F(I)=F(I)+T
      4   U=U*W
      5   RETURN
      END

```

Figure 4.10: FFT FORTRAN Source Code

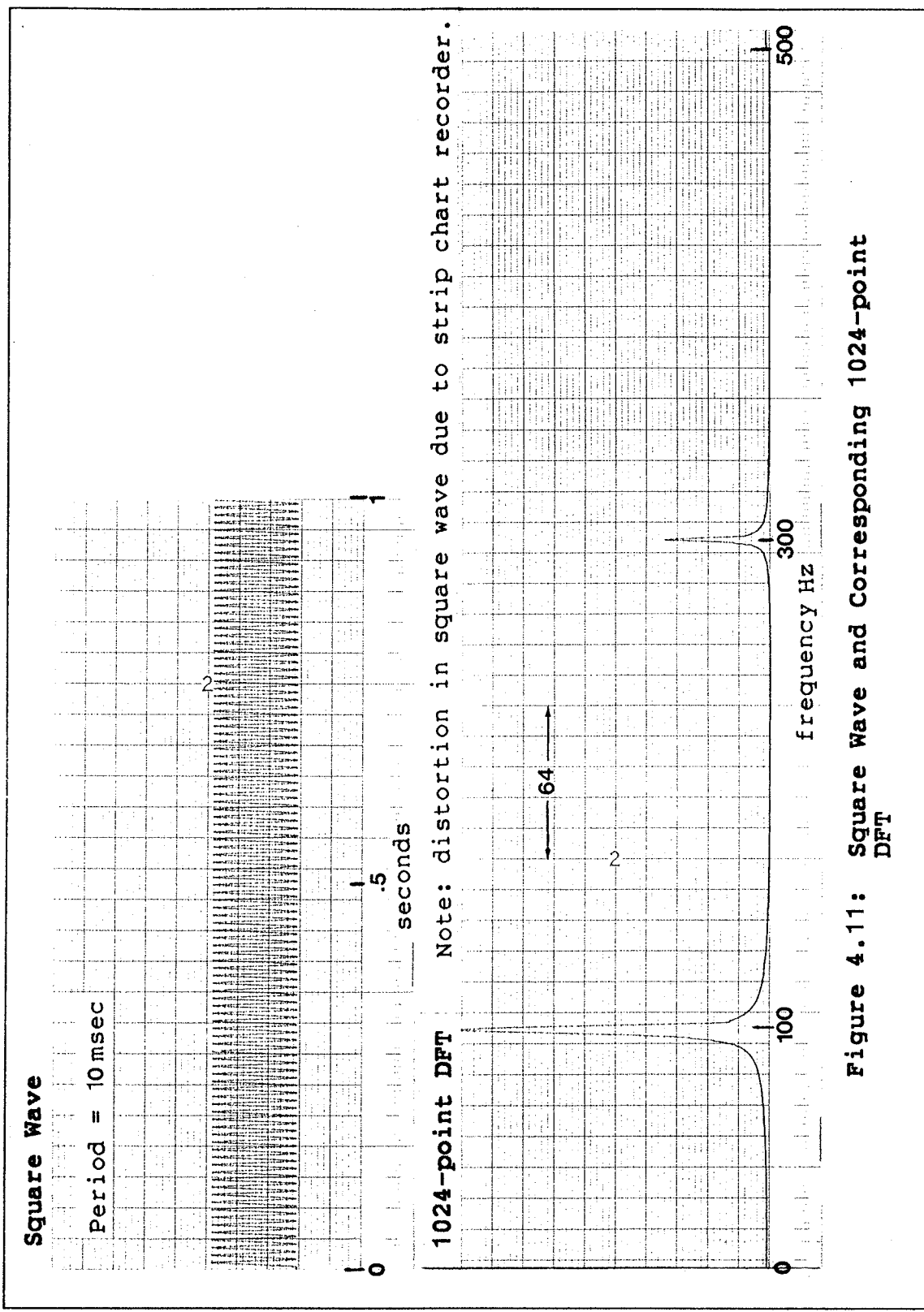


Figure 4.11: Square Wave and Corresponding 1024-point DFT

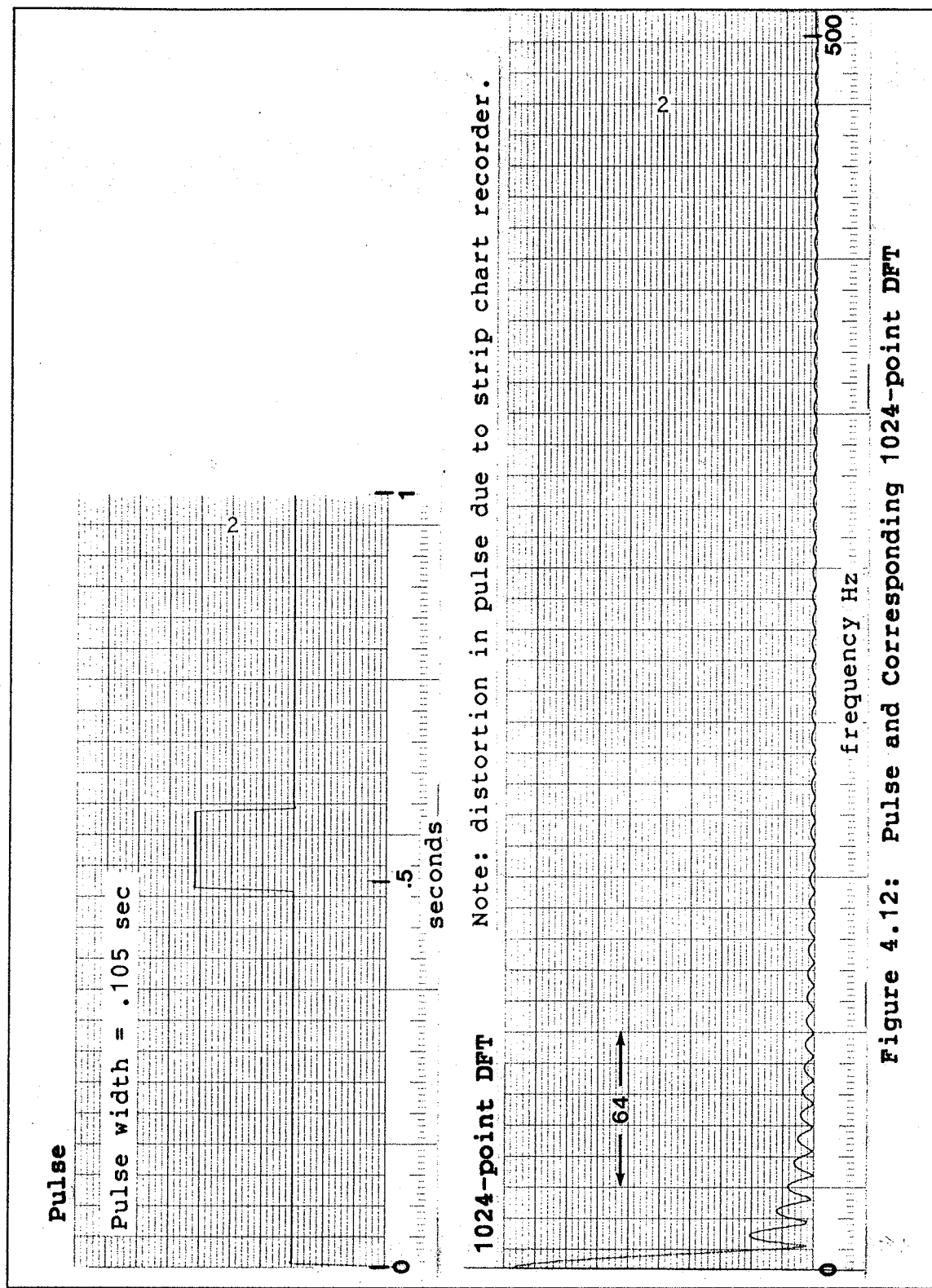


Figure 4.12: Pulse and Corresponding 1024-point DFT

4.6.4 PCG Energy Distribution Coefficient

To quantify the energy curve, a quantity which depends on the distribution of energy over the duration of the signal is used. This quantity is the Energy Distribution Coefficient [77] and is defined as

$$\text{EDC}_t = \frac{\sum_{n=1}^L a(n)E(n)}{\sum_{n=1}^L E(n)} \quad (4.11)$$

where $E(n)$ is the energy curve, L is the number of samples in $E(n)$, $a(n)$ is a nondecreasing weighting sequence, and the subscript t denotes the time domain. In this work, we define $a(n) = n$. Additional subscripts s and d denote the systolic and diastolic segments, respectively. A similar quantity EDC_f is defined for the frequency domain with $E(n)$ in the above equation replaced by the energy spectrum. The denominator is a normalization factor.

From the above equation, it is apparent that due to the progressively heavier weighting PCG signals with systolic and/or diastolic murmurs will have larger EDC_{ts} and/or EDC_{td} values than a normal PCG signal with no murmurs. Also, signals with higher frequency components can be expected to have higher EDC_{fs} and EDC_{fd} values as their energy spectra will have larger values at frequencies away from the origin. Thus the PCG signal can be represented by the four quantities EDC_{ts} , EDC_{td} , EDC_{fs} , and EDC_{fd} which give an indication of the location of murmurs in the cardiac cycle and the frequency content of the signal. To compare different

records of varying durations, a correction factor must be applied to the quantity EDC. In this work, the EDC_t values are corrected by dividing by the number of samples and multiplying by a factor of 1024. A correction factor is not necessary for EDC_f as the duration L of the energy spectrum is common to all signals, equal to one half the number of points used for the computation of the FFT.

4.7 SUMMARY

To summarize, an MC68000 microprocessor based system has been designed to analyze the time and frequency domain characteristics of the PCG signal. The ECG and carotid pulse signals are used as timing references for the PCG to identify the first and second heart sounds and to segment the PCG into systole and diastole. The systolic and diastolic energy curves and energy spectra are computed and quantified using the Energy Distribution Coefficient. Typical computation times for the PCG analysis system routines are shown in Table 4.2. These times could be considerably reduced with a faster microprocessor. Upon completion of the analysis routines the EDC values are available to the operator. A routine to display the results is then invoked allowing the operator to view the various output signals on an oscilloscope or strip chart recorder via the D/A converters.

TABLE 4.2**Typical Execution Times of the PCG Analysis System
Routines**

Signal Processing Routine	Typical Execution Time (seconds)
A/D Conversion	1.5
ECG Processing-QRS Complex Detection	1.8
Carotid Processing-Dicrotic Notch	0.6
PCG Processing-Time Domain:	
Systolic Energy Curve and EDC	2.2
Diastolic Energy Curve and EDC	3.5
PCG Processing-Frequency Domain:	
Systolic Energy Spectra and EDC	6.4
Diastolic Energy Spectra and EDC	6.4
TOTAL:	22.3

Chapter V

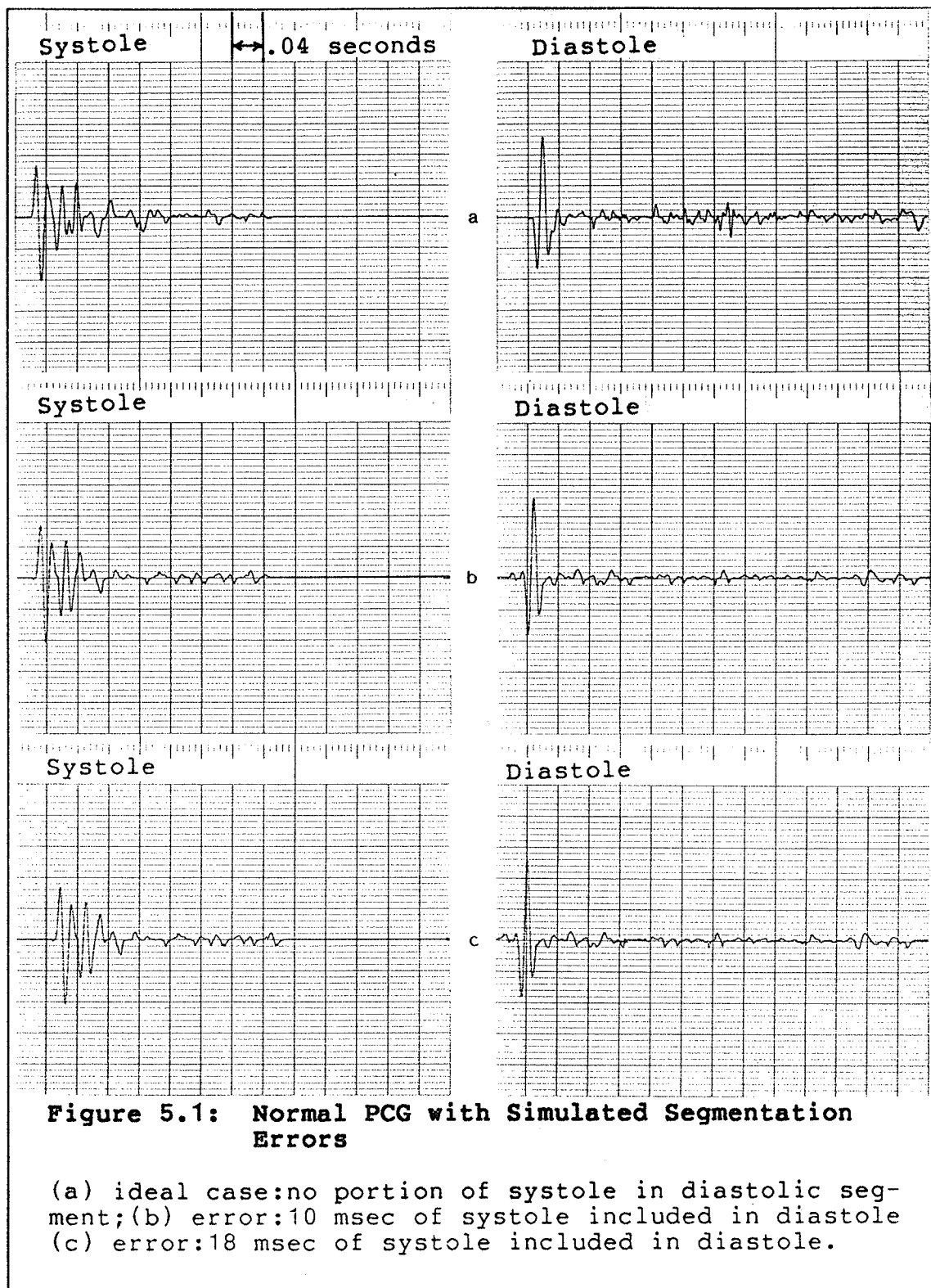
DISCUSSION OF RESULTS

Phonocardiogram signals of 5 healthy, normal subjects and 20 patients with valvular and other cardiovascular defects were taken up for study using the proposed techniques. For a majority of the patients, PCG signals were obtained from various recording sites on the chest wall. This provided a greater number of signals to be tested using the PCG analysis system. The ECG signal and carotid pulse were used as references for selection of the PCG signal over one cardiac cycle and for the segmentation of the PCG into systole and diastole. The energy curves and energy spectra of the systolic and diastolic segments of the PCG signals were obtained, and using these, EDC_{ts} , EDC_{td} , EDC_{fs} , and EDC_{fd} were computed.

An important aspect of PCG segmentation is to ensure minimal error results in the computation of the EDC values. Possible errors in the segmentation procedure include the following:

1. Portion of S2 included in systole.
2. Portion of systole included in diastole.
3. Portion of systole, with a systolic murmur, included in diastole.

The use of the standardized S2-D interval ensures that a portion of S2 is not included in the systolic segment, although the two other cases mentioned above are still possible sources which may affect the EDC values. Figures 5.1 and 5.2 show a normal PCG and a PCG containing a systolic murmur, respectively, with various magnitudes of PCG segmentation error. The PCG signals were initially viewed on a strip chart recording and the exact S2-D delay was used to segment the signal into systole and diastole. Segmentation errors were then introduced by varying the standardized S2-D interval. Referring to Table 4.1 it can be seen that the minimum S2-D delay is 35 msec. Using the standardized S2-D interval of 53 msec, the maximum error which could be expected in segmenting the PCG is 18 msec, i.e., 18 msec of systole will be included in the diastolic segment. This is one of the cases shown in Figures 5.1 and 5.2. The EDC_t and EDC_f values are computed for the case with no error and for the cases with segmentation errors. The results are reflected in Table 5.1. Note that the errors in the EDC values are relatively small, confirming the accuracy of this method. The PCG segmentation method proved to be quite accurate for the PCG analysis performed in this work.



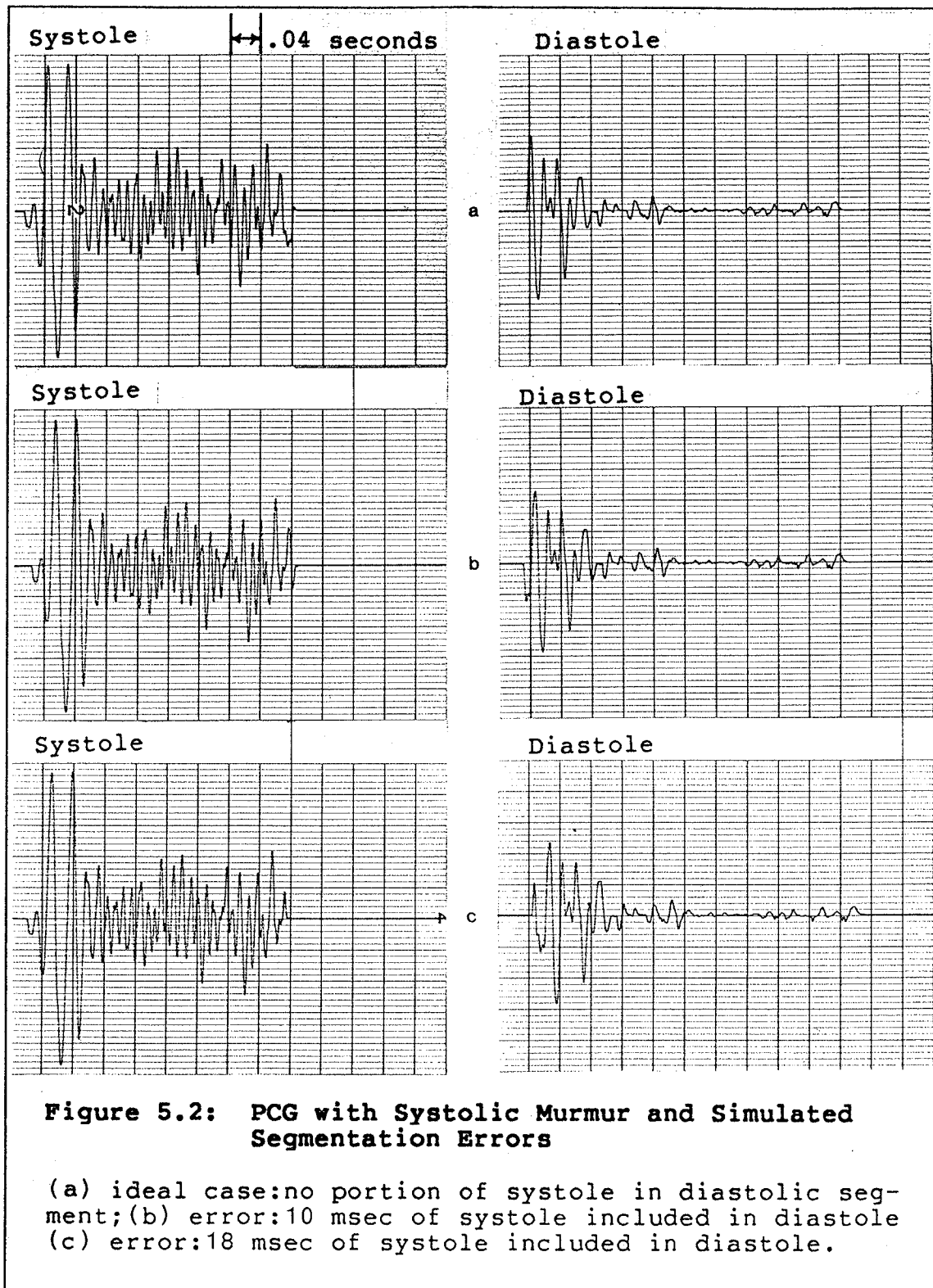


TABLE 5.1
EDC Errors Incurred From Segmentation Errors

PCG	Error	EDC _{ts}	EDC _{td}	EDC _{fs}	EDC _{fd}
Normal (Figure 5.1)	no error	160	123	77	82
	10 msec	163	128	77	80
	18 msec	170	132	77	80
SM (Figure 5.2)	no error	410	119	120	77
	10 msec	416	122	131	75
	18 msec	420	130	133	75

Figure 5.3 shows a PCG signal, segmented into systole and diastole, and the energy curve and energy spectrum of each segment. It can be seen that the energy curves display peaks corresponding to the first and second heart sounds. From the energy spectra it is seen that there is practically no energy beyond 120 Hz. The energy spectrum of the systolic segment contains peaks at approximately 25 Hz, 42 Hz, 58 Hz, and 74 Hz. It is interesting to note that a previous study for spectral decomposition of the first heart sound revealed it consists of a number of peaks in the frequency range 10 - 140 Hz [44]. In the present analysis, the peaks have appeared in the same frequency range. Similarly, the diastolic energy spectrum contains peaks at approximately 35 Hz, 54 Hz, 83 Hz, and 106 Hz, which agree with results attained in [45], in which spectral decomposition of the second heart sound was performed.

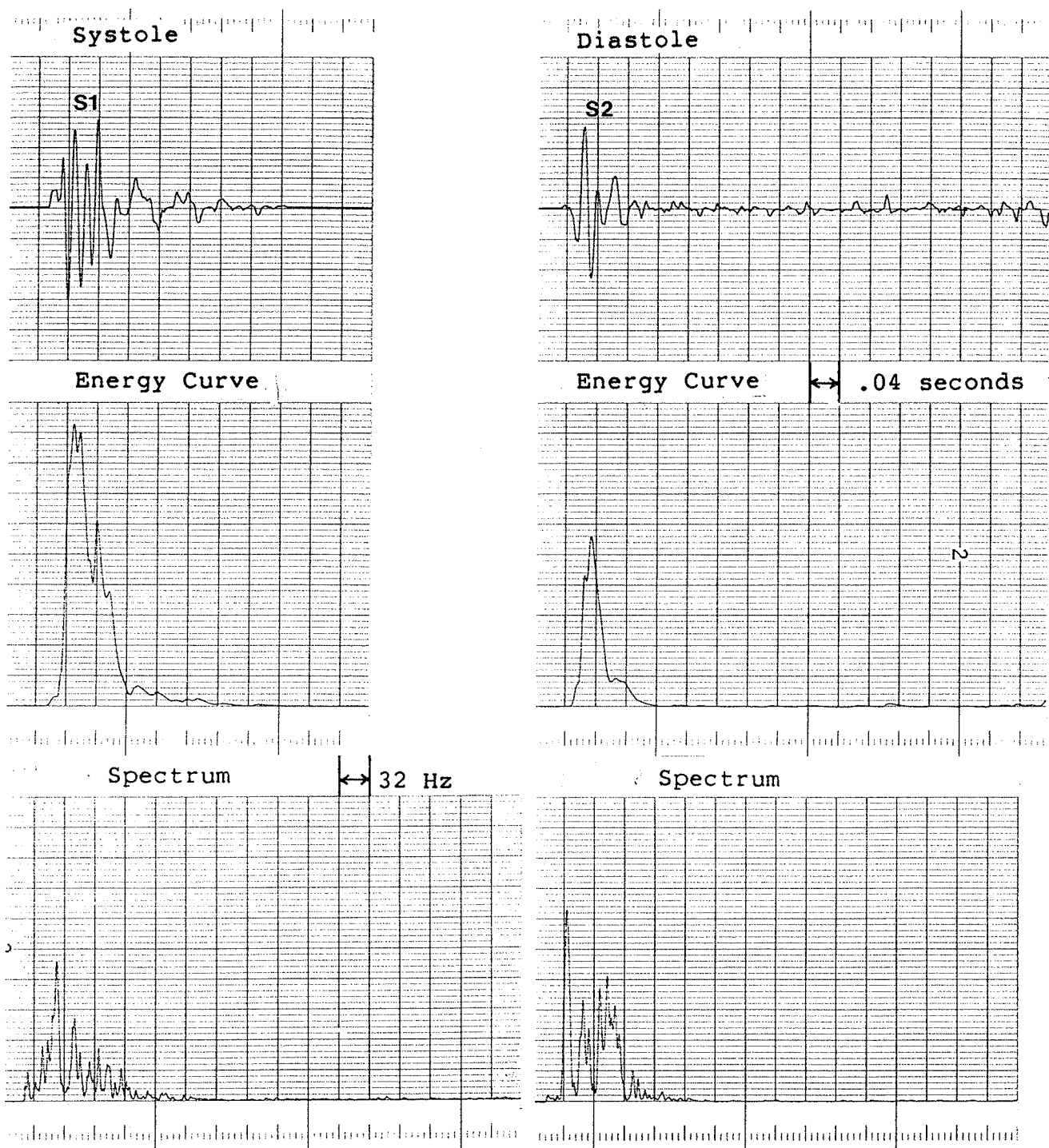


Figure 5.3: Normal PCG and Corresponding Energy Curves and Energy Spectra

The segmented PCG of a subject with ventricular septal defect (VSD) is shown in Figure 5.4. The corresponding energy curves display peaks corresponding to the first heart sound and a split second heart sound. The systolic energy curve shows the presence of a systolic murmur. The systolic energy spectrum indicates significant energy up to approximately 330 Hz, indicating the presence of a high frequency murmur. The diastolic energy curve and energy spectrum show a normal diastole with no murmurs and no significant energy beyond 120 Hz.

PCG signals of subjects with pansystolic ejection murmur (PEM), mitral insufficiency (MI), and aortic stenosis (AS) with corresponding energy curves and energy spectra are shown in Figures 5.5, 5.6, and 5.7. The systolic energy curve and energy spectrum shown in Figure 5.5 indicate the presence of a systolic murmur with energy up to approximately 200 Hz. The diastolic energy curve and energy spectrum indicate normal diastole. The systolic energy curve and the diastolic energy curve shown in Figure 5.6 display peaks corresponding to a systolic and diastolic murmur. However, these murmurs are of low frequency (below 120 Hz) and thus the energy spectra do not indicate significant energy at higher frequencies. The systolic and diastolic energy curves and energy spectra of the patient with AS, shown in Figure 5.7, exhibit the presence of a low frequency systolic murmur and a normal diastole.

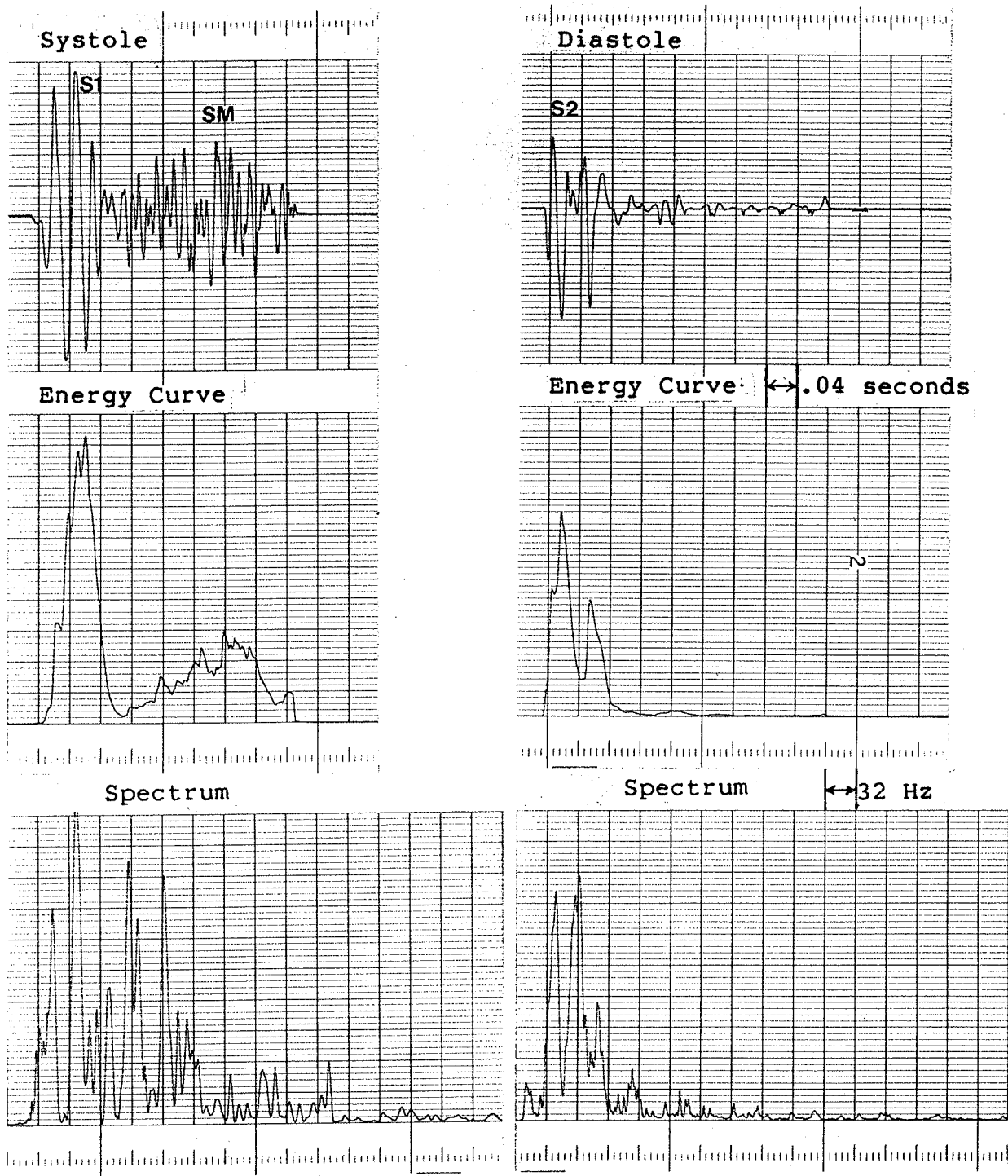


Figure 5.4: PCG with VSD and Corresponding Energy Curves and Energy Spectra.

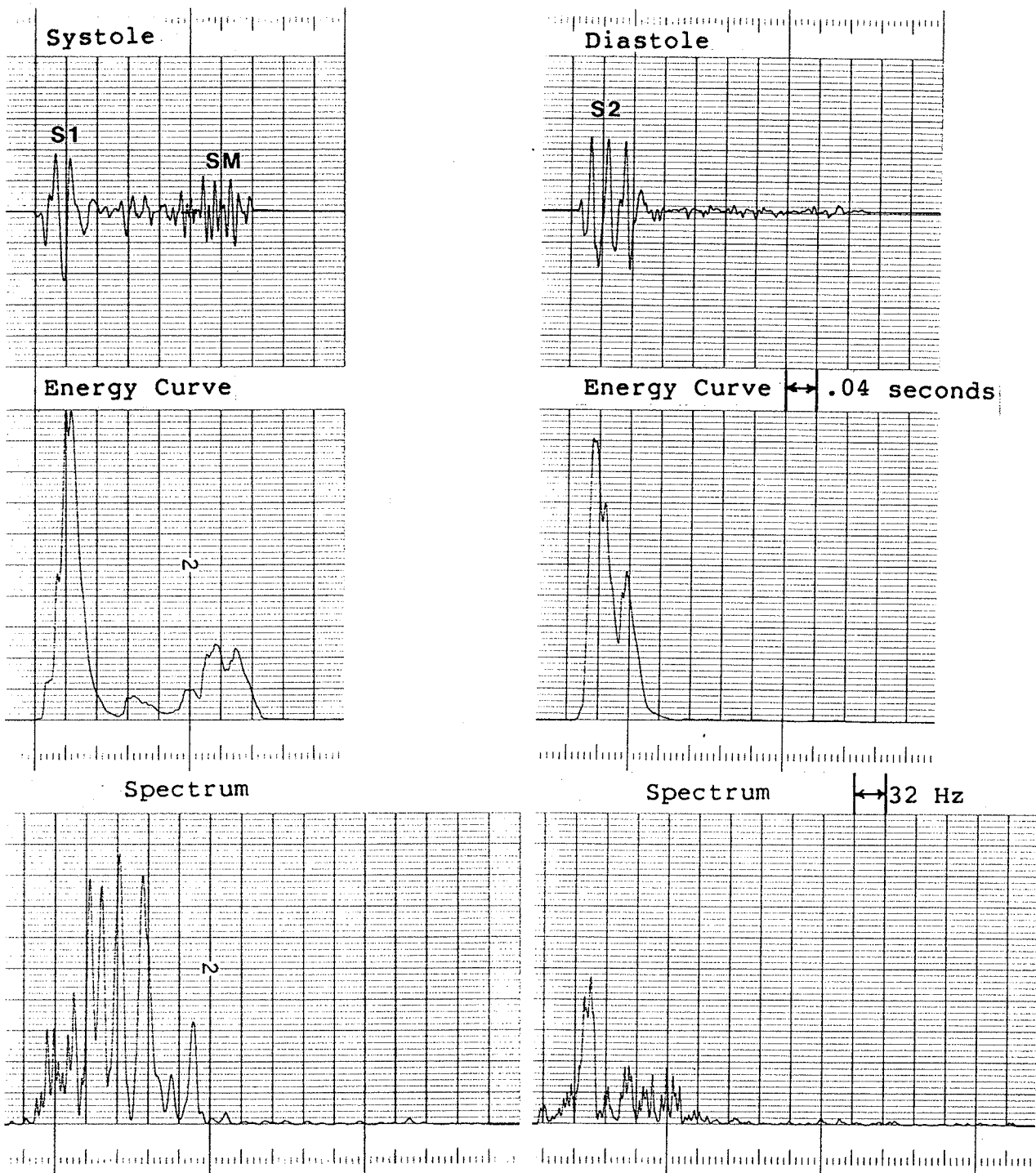


Figure 5.5: PCG with PEM and Corresponding Energy Curves and Energy Spectra

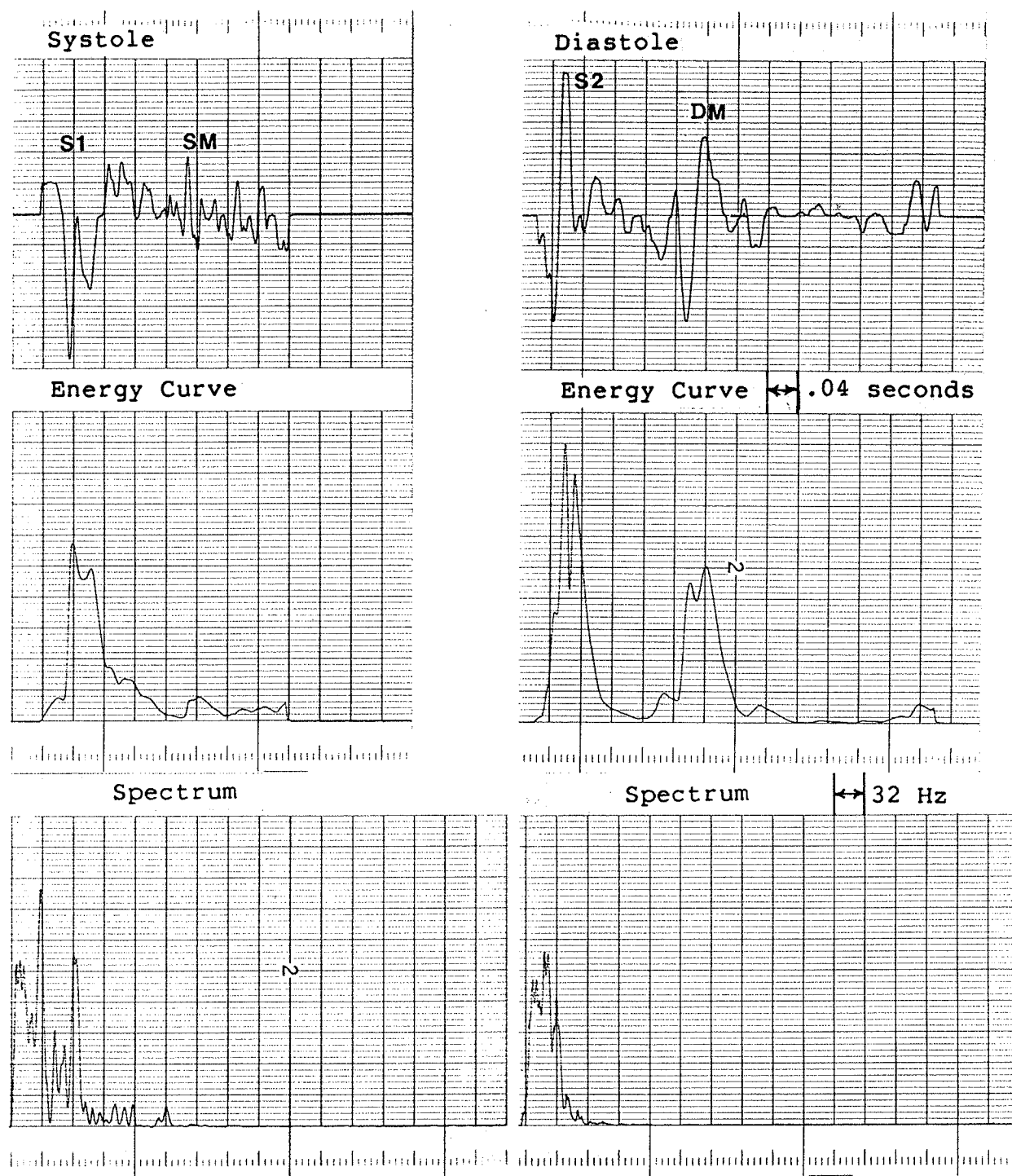


Figure 5.6: PCG with MI and Corresponding Energy Curves and Energy Spectra

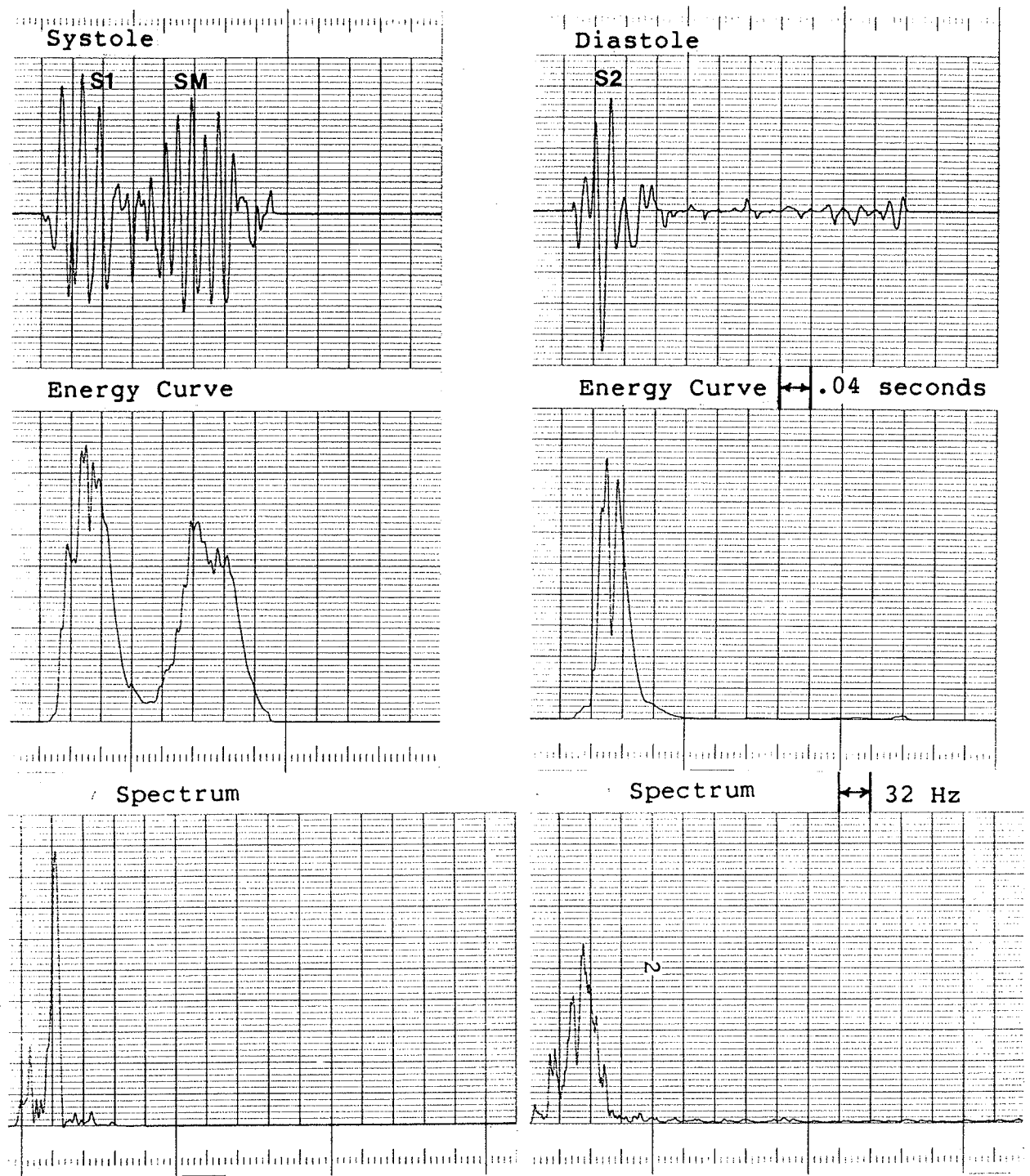


Figure 5.7: PCG with AS and Corresponding Energy Curves and Energy Spectra

To take into account variations of the PCG signal during inspiration and expiration, the average of a minimum of five sets of EDC_{ts} , EDC_{td} , EDC_{fs} , and EDC_{fd} values, obtained from PCG cycles picked up at random from the recordings, were computed for each subject. The average EDC_t and EDC_f values obtained for the 47 signals tested are shown in Table 5.2. The diagnosis of the cardiologist (col.2), the recording site of the PCG (col.3), and the observed features of the signal (col.4) are included in the table. From this table it can be seen that in general, signals with systolic murmurs and/or diastolic murmurs have greater EDC_{ts} and/or EDC_{td} values than for normal cases. Also the EDC_f values for the cases with high frequency murmurs are greater than those for normal cases. A definite classification scheme could not be developed due to the nonavailability of an adequate number of cases belonging to any particular disease category. However, the signals were divided into systole and diastole and further grouped into normal signals and signals with murmurs. The mean and standard deviation of the EDC_t and EDC_f values of each group are computed and reflected in Table 5.3. Here it is seen that the signals with systolic murmurs or diastolic murmurs have larger EDC_{ts} or EDC_{td} values, respectively, than those for normal signals. Murmurs are often graded depending upon their intensity. However, in this work the murmurs were not graded and murmurs of varying intensity are present within a group. This explains the considerably high standard deviations (particularly in the

cases with murmurs). Other factors which could induce variations in the EDC_{td} values include a large or split second heart sound and the presence of a third or fourth heart sound in late diastole.

For systole it can be seen that the EDC_{fs} values are greater for cases with systolic murmurs than for normal cases. However, many of the signals of the pathological cases did not have apparent energy beyond 120 Hz. A few signals had energy extending up to 330 Hz, these resulting in large EDC_{fs} values and thereby increasing the EDC_{fs} mean. For the EDC_{fd} values none of the pathological cases had diastolic murmurs with significant energy over 120 Hz; i.e. all cases had low frequency diastolic murmurs.

With an adequate training set having a sufficiently large number of cases in each category and gradation of murmurs, a pattern recognition technique could be developed with the EDC_t and EDC_f values as parameters for detection and classification of murmurs.

TABLE 5.2
Average EDC_t and EDC_f Values

Patient	Diagnosis	Site	Observed features	EDC _{ts}	EDC _{td}	EDC _{fs}	EDC _{fd}
1	2	3	4	5	6	7	8
A	N	P	N	198	149	61	67
B	N	P	N	169	154	75	80
C	N	P	N	181	151	50	60
1A	MI	P	SM, MDM	223	180	55	56
1B		T		207	172	55	56
2A	MI	P	SM, DM	379	154	52	54
2B		T	SPLS2	205	188	50	52
2C		M		258	273	50	52
3A	VSD	P	SM, SPLS2	540	120	104	100
3B		T	S3	520	188	108	96
4A	MR	P	SM	327	180	54	56
4B		T		205	190	56	54
5	ASD	P	SM, SPLS2	262	196	80	68
6	PAV	P	SM	259	138	70	65
7A	VSD	P	SM, SPLS2	469	172	116	70
7B		T		390	142	125	68
8A	AS	A	SM	340	148	80	74
8B		T		330	130	69	70
9A	VSD	P	SM	245	197	74	56
9B		T		204	156	65	60
10	VSD	T	SM	200	173	60	69
11A	PEM	P	SM	356	144	118	80
11B		C		403	200	95	66
12A	VSD, PS	P	SEM, RA	315	230	74	89
12B		P	RESP	350	230	80	62
12C		M		326	230	86	61
13	VSD	T	SM	412	196	103	55
14A	N	P	N	170	160	50	48
14B		A		175	145	54	50
15A	AS	A	SM	454	186	74	56
15B		M		381	181	74	56
15C		P		360	143	60	58
16A	VSD	P	PSM	430	176	109	75
16B		T		458	143	103	60
16C		T		421	159	105	65
17	ASD, PS	T	SM, DM	253	266	82	80
18	N	T	N	168	149	56	54
19A	VSD, PS	P	SM	490	237	112	70
19B		T		433	183	108	68
20	PS	A	MSM	230	144	68	75
21	PDA	P	SM, DM	346	318	58	69

1	2	3	4	5	6	7	8
22A	N	P	N	205	148	80	82
22B		T		187	166	76	80
22C		M		179	157	75	78
23A	TA, PS	A	SM, DM	416	364	76	80
24A	AR	P	SM, DM	224	155	84	76
24B		M		246	263	73	82

Legend: col.2: N-normal, AS-aortic stenosis

ASD-atrial septal defect

MI-mitral insufficiency, MR-mitral regurgitation

PAV-prosthetic aortic valve

PDA-patent ductus arteriosus

PEM-pulmonary ejection murmur

PS-pulmonary stenosis, TA-tricuspid artesia

VSD-ventricular septal defect

col.3: P-pulmonary area A-aortic area

T-tricuspid area M-mitral area

C-clavicular

col.4: N-normal, SM-systolic murmur

DM-diastolic murmur

MDM/SM-middiastolic/systolic murmur

PSM-pansystolic murmur

RESP-respiration pulse

SPLS2-split second heart sound

S3-third heart sound

TABLE 5.3
Mean and SD of EDC_t and EDC_f Values

Systole	Number of cases	EDC _{ts}	SD	EDC _{fs}	SD
Normal	9	181.3	12.4	64.1	11.6
SM	38	338.6	97.4	80.7	21.6
Diastole	Number of cases	EDC _{td}	SD	EDC _{fd}	SD
Normal	37	164.7	24.5	67.6	12.1
DM	10	233.2	69.8	65.7	12.2

Chapter VI

CONCLUSIONS AND RECOMMENDATIONS FOR FURTHER STUDY

6.1 CONCLUSIONS

In conclusion a prototype MC68000 microprocessor-based system has been designed to provide quantitative analysis of the phonocardiogram. The system includes 32K bytes RAM, A three-channel data acquisition section, an arithmetic processing unit, and a set of D/A converters. The system has the provisions to be dedicated to phonocardiographic applications. A detection algorithm for the first and second heart sounds, which is one of the most important problems in an automatic phonocardiogram diagnosis system, has been developed. The ECG and carotid pulse signals are used to segment the phonocardiogram into systole and diastole. A method has been presented to quantify the systolic and diastolic segments of the phonocardiogram into four parameters representing their time and frequency domain characteristics. Tests on 47 phonocardiogram signals show that the method can lead to an interesting and potentially useful method for detection and classification of murmurs. Studies with a large number of signals could lead to an elaborate classification scheme. A system performing such classification would be extremely useful for screening purposes and routine diagnosis.

6.2 RECOMMENDATIONS

1. A large number of signals in each disease category should be tested using the PCG analysis system and the methods presented in this work. To improve classification the murmurs should be graded according to their intensity. Furthermore, when recording the PCG signals, the transducer should be placed on the area of the chest at which the intensity of the murmur is maximized. The signals should be recorded in an acoustically quiet room, if possible. A pattern classification technique could then be developed using the EDC values as parameters for the detection and classification of murmurs.
2. The PCG analysis system could be used to investigate other areas of heart sound research such as:
 - a) applying passive sonar techniques to PCG signals recorded at multiple locations on the thorax to estimate the location of heart sounds in 3D. This work would involve identification of corresponding events in the different signals by cross-correlation and coherence techniques; estimation of time delay between arrival of the events at different locations; and, ranging to determine the locations of sources.

- b) testing the functional and structural integrity of cardiac prosthetic valves using the sounds produced by the valves.
3. Modifications to the hardware could be undertaken to increase the efficiency of the PCG analysis system. In particular, a direct memory access controller could be added to increase the speed of APU operations. In addition, the system RAM could be increased in order to store longer durations of signal. The added RAM would also provide the additional memory required to allow the signals to be digitized at a higher sampling rate.

REFERENCES

- [1] H. Garret deYoung, "State of the heart", High Technology, Vol.4, pp.33-41, May, 1984.
- [2] A. Macovski, Medical Imaging Systems. Englewood Cliffs, New Jersey: Prentice Hall, 1983.
- [3] R.F. Rushmer, Cardiovascular Dynamics, 4th Ed. Philadelphia: W.B. Saunders Company, 1976.
- [4] J.K. Lewis and W. Dock, "The origin of heart sounds and their variations in myocardial disease", Journal of the American Medical Association, Vol.110, pp.271-275, January, 1938.
- [5] H.A. Sacks and R.C. Roberts, "Heart sounds in young adults", American Heart Journal, Vol.18, pp.303-307, September, 1939.
- [6] A.A. Luisada, C.K. Liu, C. Aravanis, M. Testelli, and J. Morris, "On the mechanism of production of heart sounds", American Heart Journal, Vol.55, pp.383-399, March, 1958.
- [7] D.J. Coleman, "On the origin of the second heart sound", American Heart Journal, Vol.65, pp.237-239, February, 1963.
- [8] G. Di Bartolo, D. Nunez-Dey, G. Muiesan, D.M. MacCanon, and A.A. Luisada, "Hemodynamic correlates of the first heart sound", American Journal of Physiology, Vol.201, pp.888-892, November, 1961.
- [9] P.M. Shah, M. Mori, D.M. MacCanon, and A.A. Luisada, "Hemodynamic correlates of the various components of the first heart sound", Circulation Research, Vol.12, pp.386-392, April, 1963.
- [10] T. Sakamoto, R. Kusukawa, D.M. MacCanon, and A.A. Luisada, "Hemodynamic determinants of the amplitude of the first heart sound", Circulation Research, Vol.16, pp.45-57, January, 1965.
- [11] T.E. Piemme, G.O. Barnett, and L. Dexter, "Relationship of heart sounds to acceleration of blood flow", Circulation Research, Vol.18, pp.303-315, March, 1966.

- [12] A.A. Luisada, D.M. MacCanon, B. Coleman, and L.P. Feigen, "New studies on the first heart sound", American Journal of Cardiology, Vol.28, pp.140-149, August, 1971.
- [13] A.A. Luisada, "The second heart sound in normal and abnormal conditions", American Journal of Cardiology, Vol.28, pp.150-161, August, 1971.
- [14] A.A. Luisada and D.M. MacCanon, "The phases of the cardiac cycle", American Heart Journal, Vol.83, pp.705-711, May, 1972.
- [15] A.A. Luisada, D.M. MacCanon, S. Kumar, and L.P. Feigen, "Changing views on the mechanism of the first and second heart sounds", American Heart Journal, Vol.88, pp.503-514, October, 1974.
- [16] H.N. Sabbah and P.D. Stein, "Investigation of the theory and mechanism of the origin of the second heart sound", Circulation Research, Vol. 39, pp.874-882, December, 1976.
- [17] P.D. Stein and H.N. Sabbah, "Origin of the second heart sound: clinical relevance of new observations", American Journal of Cardiology, Vol.41, pp.108-110, January, 1978.
- [18] K.O. Lim, Y-C Liew, and C-H Oh, "Analysis of mitral and aortic valve vibrations and their role in the production of the first and second heart sounds", Physics in Medicine and Biology, Vol.25, pp.727-733, July, 1980.
- [19] A.A. Luisada and F. Portaluppi, The Heart Sounds: New Facts and Their Clinical Applications. New York: Praeger Publishers, 1982.
- [20] L.-G. Durand and R. Guardo, "A computer model for the study of left ventricular wall contributions to the first heart sound", pp. 445-448 in Computers in Cardiology, IEEE, New York, 1982.
- [21] L.P. Feigen, "Physical characteristics of sound and hearing", American Journal of Cardiology, Vol.28, pp.130-133, August, 1971.
- [22] J.S. Butterworth and E.H. Reppert, "Auscultatory acumen in the general medical population", Journal of the American Medical Association, Vol.174, pp.32-34, September, 1960.
- [23] R.J. Dobrow, J.B. Calatayud, and S. Abraham, "A study of physician variation in heart sound interpretation", Medical Annals District of Columbia, Vol.33, pp.305-308, July, 1964.

- [24] J.F. Green, Fundamental Cardiovascular and Pulmonary Physiology: An Integrated Approach for Medicine. Philadelphia: Lea and Febiger, 1982.
- [25] M.E. Tavel, Clinical Phonocardiography and External Pulse Recording, 3rd Ed. Chicago: Year Book Medical Publishers Inc., 1978.
- [26] E. Van Vollenhoven, N. Suzumura, D.N. Ghista, J. Mazumdar, and T. Hearn, "Phonocardiography: Analyses of instrumentation, and vibration of heart structures to determine their constitutive properties", pp.68-118 in Advances in Cardiovascular Physics, Vol.2, Karger, Basel, Switzerland, 1979.
- [27] Application Note AN732, "Phonocardiography and external pulse recording", Hewlett Packard, 1973.
- [28] J.G. Webster, Editor, Medical Instrumentation: Application and Design. Boston: Houghton Mifflin Company, 1978.
- [29] L. Karpman, J. Cage, C. Hill, A.D. Forbes, V. Karpman, and K. Cohn, "Sound envelope averaging and the differential diagnosis of systolic murmurs", American Heart Journal, Vol.90, pp.600-606, November, 1975.
- [30] A.A. Sarkady, R.R. Clark, and R. Williams, "Computer analysis techniques for phonocardiogram diagnosis", Computers and Biomedical Research, Vol.9, pp.349-363, August, 1976.
- [31] D.S. Gerbarg, F.W. Holcomb, J.J. Hofler, C.E. Bading, G.L. Schultz, and R.E. Sears, "Analysis of phonocardiogram by a digital computer", Circulation Research, Vol.11, pp.569-576, September, 1962.
- [32] M. Yokoi, Z. Uozumi, N. Okamoto, Y. Mizuno, T. Iwatsuka, H. Takahashi, Y. Watanabe, and S. Yashui, "Clinical evaluation on 5 years' experience of automated PCG analysis", Japan Heart Journal, Vol.18, pp.482-490, July, 1977.
- [33] E. Van Vollenhoven, A. Van Rotterdam, T. Dorenbos, and F.G. Schlesinger, "Frequency analysis of heart murmurs", Medical and Biological Engineering, Vol.7, pp.227-233, March, 1969.
- [34] D.S. Gerbarg, "Computer analysis of phonocardiogram", Progress in Cardiovascular Disease, Vol.5, pp.393-405, January, 1963.

- [35] N.S. Blackman, S. Blumenthal, K.D. Brownell, J. Wolfson, and D. Harris, "Cardiac screening by computerized auscultation", American Journal on Public Health, Vol.59, pp.1177-1187, July,1969.
- [36] W. Litwon and F. Begon, "Digital processing of phonocardiograms: first results", International Journal of Biomedical Engineering, Vol.5, pp.58-69, January,1974.
- [37] V.A. McKusick, S.A. Talbot, and G.N. Webb, "Spectral phonocardiography", "Spectral phonocardiography", Bulletin of the Johns Hopkins Hospital, Vol.94, p.187-198, 1954.
- [38] D.E. Winer, L.W. Perry, and C.A. Caceres, "Heart sound analysis: A three dimensional approach", American Journal of Cardiology, Vol.16, pp.547-551, October,1965.
- [39] R.J. Adolph, J.F. Stephens, and K. Tanaka, "The clinical value of frequency analysis of the first heart sound in myocardial infarction", Circulation, Vol.41, pp.1003-1014, June,1970.
- [40] A. Sakai, L.P. Feigen, and A.A. Luisada, "Frequency distribution of the heart sounds in normal man", Cardiovascular Research, Vol.5, pp.358-363, July,1971.
- [41] W.B. Clarke, S.M. Austin, P.M. Shah, P.M. Griffen, J.T. Dove, J. McCullough, and B.F. Schreiner, "Spectral energy of the first heart sound in acute myocardial ischemia", Circulation, Vol.57, pp.593-598, March,1978.
- [42] E.L. Frome and E.L. Frederickson, "Digital spectrum analysis of the first and second heart sounds", Computers and Biomedical Research, Vol.7, pp.421-431, October,1974.
- [43] A.P. Yoganathan, R. Gupta, and W.H. Corcoran, "Fast Fourier transform in the analysis of biomedical data", Medical and Biological Engineering, Vol.14, pp.239-244, March,1976.
- [44] A.P. Yoganathan, R. Gupta, F.E. Udwadia, J.W. Miller, W.H. Corcoran, R. Sarma, J.L. Johnson, and R.J. Bing, "Use of the fast Fourier transform for frequency analysis of the first heart sound in normal man", Medical and Biological Engineering, Vol.14, pp.69-73, January,1976.
- [45] A.P. Yoganathan, R. Gupta, F.E. Udwadia, W.H. Corcoran, R. Sarma, and R.J. Bing, "Use of the fast Fourier transform in the frequency analysis of the second heart sound in normal man", Medical and Biological Engineering, Vol.14, pp.455-459, July,1976.

- [46] K.J. Blinowska, M.A. Czermińska, O.A. Chomicki, and T. Gorowski, "Computer analysis of the frequency spectrum of a phonothyreogram", Medical and Biological Engineering and Computing, Vol.17, pp.207-210, March, 1979.
- [47] P. Pinna Pintor, E. Piccolo, S. Bartolozzi, and V. Fontana, "The FFT in the study of the fourth heart sound", pp.369-372 in Computers in Cardiology, Sept. 26-28, 1979, Geneva, IEEE, New York, 1979.
- [48] C. Longhini, F. Portaluppi, E. Arslen, F. Pedrelli, "The FFT in the analysis of the normal phonocardiogram", Japan Heart Journal, Vol.20, pp.333-339, 1979.
- [49] D. Nandagopal and J. Mazumdar, "A study of temporal variation in heart sound frequency spectra using fast Fourier transform", Australasian Physical and Engineering Sciences in Medicine, Vol.4, pp.47-50, 1981.
- [50] T.C. Hearn, J. Mazumdar, and L.J. Mahar, "First heart sound spectra in relation to anterior mitral-leaflet closing velocity", Medical and Biological Engineering and Computing, Vol.20, pp.466-472, July, 1982.
- [51] H. Weed, M. Sauter, R. Roberts, G. Vossius, and H. Kwee, "Relationship of acoustic heart sound frequency shift to heart function", pp. 386-389 in IEEE 1981 Frontiers in Engineering in Health Care, ed. B.A. Cohen, IEEE, New York, 1981.
- [52] D. Nandagopal, J. Mazumdar, G. Karolyi, and T. Hearn, "An instrumentation system and analysis procedure for phonocardiographic studies", Australian Journal of Biomedical Engineering, Vol.2, pp.16-20, March, 1981.
- [53] A. Iwata, N. Suzumura, and K. Ikegaya, "Pattern classification of the phonocardiogram using linear prediction analysis", Medical and Biological Engineering and Computing, Vol.15, pp.407-412, July, 1977.
- [54] A. Iwata, N. Ishii, N. Suzumura, and K. Ikegaya, "Algorithm for detecting the first and second heart sounds by spectral tracking", Medical and Biological Engineering and Computing, Vol.18, pp.19-26, January, 1980.
- [55] D. Nandagopal, J. Mazumdar, R.E. Bogner, and E. Goldblatt, "Spectral analysis of the second heart sound in normal children by selective linear prediction coding", Medical and Biological Engineering and Computing, Vol.22, pp.229-239, May, 1984.
- [56] M. Okada, "Chest wall maps of heart sounds and murmurs", Computers and Biomedical Research, Vol.15, pp.281-294, June, 1982.

- [57] R. Beyar, S. Braun, S. Levkovitch, and Y. Palti, "A new statistical approach to heart-sound processing", pp.376-380 in IEEE Frontiers of Engineering and Computing in Health Care, Columbus, Ohio, 1983.
- [58] R. Beyar, S. Levkovitz, S. Braun, and Y. Palti, "Heart-sound processing by average and variance calculation - physiologic basic and clinical implications", IEEE Transactions on Biomedical Engineering, Vol. BME-31, pp.591-596, September, 1984.
- [59] D.W. Suobank, A.P. Yoganathan, E.C. Harrison, and W.H. Corcoran, "A quantitative method for the in vitro study of sounds produced by prosthetic aortic heart valves I: analytical considerations." Medical and Biological Engineering and Computing, Vol.22, pp.32-39, January, 1984.
- [60] D.W. Suobank, A.P. Yoganathan, E.C. Harrison, W.H. Corcoran, "A quantitative method for the in vitro study of sounds produced by prosthetic aortic heart valves II: An experimental, comparative study of the sounds produced by a normal and simulated-abnormal Starr-Edwards series 2400 aortic prosthesis", Medical and Biological Engineering and Computing, Vol.22, pp.40-47, January, 1984.
- [61] D.W. Suobank, A.P. Yoganathan, E.C. Harrison, W.H. Corcoran, "A quantitative method for the in vitro study of sounds produced by prosthetic aortic heart valves III: An experimental, comparative study of the sounds produced by normal and simulated-abnormal Smeloff aortic prostheses", Medical and Biological Engineering and Computing, Vol.22, pp.48-54, January, 1984.
- [62] J.C. Hylen, F.E. Kloster, R.H. Herr, P.Q. Hull, A.W. Ames, A. Starr, and H.E. Griswold, "Phonocardiographic diagnosis of aortic ball variance", Circulation, Vol.38, pp.90-102, July, 1968.
- [63] J.T. Willerson, J.A. Kastor, R.E. Dinsmore, E. Mundth, and M.J. Buckley, W.G. Austen, and C.A. Sanders, "Non-invasive assessment of prosthetic mitral paravalvular and intravalvular regurgitation", British Heart Journal, Vol.34, pp.561-568, June, 1972.
- [64] E.N. Mercer, B.D. McCallister, E.R. Giuliani, R.S. Zitnick, "Aortic opening to closing ratio on phonocardiograms of patients with Starr-Edwards aortic valve prosthesis", Mayo Clinic Proceedings, Vol.47, pp.42-47, January, 1972.

- [65] O.W. Boicurt, J.D. Bristow, A. Starr, H.E. Griswold, "A phonocardiographic study of patients with multiple Starr-Edwards prosthetic valves", British Heart Journal, Vol.28, pp.531-538, April, 1966.
- [66] R.J. Romanoff, H.W. Seipp,Jr., L.C. Amsler, E.H. Johnson, and C.L. McIntosh, "Computer-assisted detection of prosthetic aortic heart valve dysfunction", Computers and Biomedical Research, Vol.10, pp.35-44. February, 1977.
- [67] P.D. Stein, H.N. Sabbah, J.B. Lakier, and S. Goldstein, "Frequency spectrum of the aortic component of the second heart sound in patients with normal valves, aortic stenosis and aortic porcine xenografts", American Journal of Cardiology, Vol.46, pp.48-52, July, 1980.
- [68] P.D. Stein, H.N. Sabbah, J.B. Lakier, D.J. Magilligan,Jr., and S. Goldstein, "Frequency of the first heart sound in the assessment of stiffening of mitral bioprosthetic valves", Circulation, Vol.63, pp.200-203, January, 1981.
- [69] T.H. Joo, J.H. McClellan, R.A. Foale, G.S. Myers, and R.S. Lees, "Pole-zero modeling and classification of phonocardiograms", IEEE Transactions on Biomedical Engineering, Vol.BME-30, pp.110-117, February, 1983.
- [70] L.-G. Durand, J. de Guise, and R. Guardo, "FFT techniques for the spectral analysis of prosthetic heart valve sounds", pp.1105-1111 in Proceedings of the 4th Annual Symposium on Computer Applications in Medical Care, IEEE, Washington, D.C., 1980.
- [71] L.G. Durand, M. Brais, M. Blanchard, M. Guerin, M Sleger, J. de Guise, and R. Guardo, "Fourier analysis of Ionescu-Shiley prosthetic closing sounds", p. 150 in Proceedings of the 37th Annual Conference on Engineering in Medicine and Biology, Los Angeles, California, 1984.
- [72] M.R. Rangaraj and I.S.N. Murthy, "Analysis and modelling of phonocardiogram", pp.8-53 to 8-56 in Proceedings of the 1st Mediterranean Conference on Medical and Biological Engineering, Sorrento, 1977.
- [73] M.R. Rangaraj and I.S.N. Murthy, "Cepstral filtering of phonocardiogram signal", pp.118-119 in Digest of the International Symposium and Workshop on Biomedical Engineering, Indian Institute of Technology, New Delhi, 1978.
- [74] M.R. Rangaraj, Digital Analysis of the ECG, PCG, and EMG Signals, Department of Electrical Engineering, Indian Institute of Science, Ph.D. Thesis, Bangalore, 1979.

- [75] M.R. Rangaraj and I.S.N. Murthy, "New techniques for phonocardiogram analysis", Medical and Life Sciences Engineering, Vol.5, pp.6-17, 1979.
- [76] M.R. Rangaraj and I.S.N. Murthy, "Classification of PCG via pole-zero modelling", pp.S7-26 to S7-29 in Proceedings of the 7th All India Symposium on Biomedical Engineering, Hyderabad, 1978.
- [77] M.R. Rangaraj and I.S.N. Murthy, "Quantitative analysis of the phonocardiogram for detection of murmurs", Journal of Biomedical Engineering, Vol.1, pp.247-252, 1979.
- [78] R.J. Lehner, A Microprocessor Based Heart Sound Analyzer, Department of Electrical Engineering, University of Manitoba, B.Sc. Thesis, Winnipeg, 1983.
- [79] R.J. Lehner and R.M Rangayyan, "A microcomputer system for quantitative analysis of the phonocardiogram", in Proceedings MEDCOMP-83, IEEE, Athens, Ohio, 1983.
- [80] M.R. Rangaraj and D.N. Dutt, "Speech processing techniques for the analysis of heart sounds", pp.S4-9 to S4-12 in Proceedings of the 7th All India Symposium on Biomedical Engineering, Hyderabad, 1978.
- [81] H.V. Pippberger, R.A. Dunn, A.S. Berson, "Computer methods in electrocardiography", Annual Review of Biophysics and Bioengineering, Vol.4, pp.15-42, 1975.
- [82] J.M. Jenkins, "Computerized electrocardiography", CRC Critical Reviews on Bioengineering, pp.307-350, November, 1981.
- [83] M. Okada, "3-dimensional graphic display of electrocardiograms", Japan Circulation Journal, Vol.40, pp.167-175, 1976.
- [84] L.J. Thomas, K.W. Clark, C.N. Mead, K.L. Ripley, B.F. Spenger, and G.C. Oliver, "Automated cardiac dysrhythmia analysis", Proceedings of the IEEE, Vol.67, pp.1322-1337, September, 1979.
- [85] Y. Yamashita, "Theoretical studies on the inverse problem in electrocardiography and the uniqueness of the solution", IEEE Transaction on Biomedical Engineering, Vol.BME-29, pp.719-725, November, 1982.
- [86] K. Yajima, S. Kinoshita, H. Tanaka, T. Ihara, and T. Furukawa, "Body surface potential mapping system equipped with a microprocessor for the dynamic observation of potential patterns", Medical and Biological Engineering and Computing, Vol.21, pp.83-90, January, 1983.

- [87] J.R. Cox,Jr., F.M. Nolle, and R.M. Arthur, "Digital analysis of the electroencephalogram, the blood pressure, and the electrocardiogram", Proceedings of the IEEE, Vol.60, pp.1137-1164, October,1972.
- [88] I.S.N. Murthy and M.R. Rangaraj, "New concepts for PVC detection", IEEE Transactions on Biomedical Engineering, Vol.BME-26, pp.409-415, July,1979.
- [89] P.H. Pan and A.W. Bennet, "Improved transform techniques for electrocardiogram analysis", p.92 in 33rd Annual Conference on Engineering in Medicine and Biology, Washington, D.C., 1980.
- [90] H.A. Fozzard, P. Kinias, and A.L. Pai, "Algorithms for analysis of online pressure signals", in Computers in Cardiology, IEEE, pp.77-80, 1974.
- [91] T.A. Pryor, "Some techniques for extraction of useful features from biological signals", pp.1-3 in Proceedings of the 5th Hawaii International Conference on Systems, Sciences - Computers in Biomedicine, 1972.
- [92] J.R. Cox, F.M. Nolle, H.A. Fozzard, and G.G. Oliver,Jr., "AZTEC, a preprocessing program for real-time ECG rhythm analysis", IEEE Transactions on Biomedical Engineering, Vol.BME-15, pp.128-129, April,1968.
- [93] M.E. DeBakey and D.H. Glaeser, "Waveform analysis of the central arterial pressure using a technique of data compression", Journal of the Association for the Advancement of Medical Instrumentation, Vol.6, pp.60-64, January,1972.
- [94] M.C. Kyle, J.D. Klingeman, and E.D. Freis, "Computer identification of brachial arterial pulse waves", Computers and Biomedical Research, Vol.2, pp.151-159, October,1968.
- [95] E.D. Freis and M.C. Kyle, "Computer analysis of carotid and brachial pulse waves: effects of age in normal subjects", American Journal of Cardiology, Vol.22, pp.691-695, November,1968.
- [96] G. Stockman, L. Kanal, and M.C. Kyle, "Structural pattern recognition of carotid pulse waves using a general waveform parsing system", Communications of the Association of Computing Machines, Vol.19, pp.688-695, December,1976.
- [97] P. Kinias, H.A. Fozzard, and M.J. Norusis, "A real-time pressure algorithm", Computers and Biomedical Research, Vol.11, pp.211-220, April,1981.

- [98] C.F. Starmer, P.A. McHale, and J.C. Greenfield, Jr., "Processing of arterial pressure waves with a digital computer", Computers and Biomedical Research, Vol.6, pp.90-96, February, 1973.
- [99] K. Skrabie, Ed., MC68000 16-bit Microprocessor User's Manual, 4th Ed. Englewood Cliffs, New Jersey: Prentice-Hall, 1982.
- [100] MC68000 Educational Computer Board User's Manual, 2nd Ed. Tempe, Arizona: Motorola, 1982.
- [101] MC68230 Parallel Interface/Timer. Austin, Texas: Motorola, 1975.
- [102] MC68000 Cross Assembler Reference Manual, 3rd Ed. Tempe, Arizona: Motorola, 1983.
- [103] R.J. Lehner, Use of the Carotid Pulse for Identification of the Second Heart Sound. Digital Signal Processing project, Department of Electrical Engineering, University of Manitoba, 1984.
- [104] R.J. Lehner and R.M. Rangayyan, "Use of the carotid pulse for detection of the second heart sound", in Proceedings of IEEE International Conference on Computers, Systems, and Signal Processing, Bangalore, India, December, 1984.
- [105] M.B. Rappaport and H.B. Sprague, "Physiologic and physical laws that govern auscultation and their clinical application", American Heart Journal, Vol.21, pp.257-318, March, 1941.
- [106] R.W. Schafer and L.R. Rabiner, "Digital representations of speech signals", Proceedings of IEEE, Vol.63, pp.662-677, April, 1975.
- [107] A.W. Oppenheim and R.W. Schafer, Digital Signal Processing. Englewood Cliffs, New Jersey: Prentice-Hall, Inc, 1975.
- [108] L.G. Durand (Clinical Research Institute of Montreal, Quebec), Discrete Fourier transform Subroutine. private communication.
- [109] F.J. Taylor, Digital Filter Design Handbook. New York: Marcel Dekker, Inc, 1983.

Appendix A
SAAB SCHEMATIC DIAGRAMS

TABLE A.1
Device Reference

Reference	Type	GND	+5V	-5V	+12V	-12V
U1	74LS20	7	14			
U2	74LS05	7	14			
U3	74LS00	7	14			
U4	74LS245	10	20			
U5	74LS245	10	20			
U6	74LS241	10	20			
U7	74LS241	10	20			
U8	74LS373	10	20			
U9	74LS373	10	20			
U10	74C109	7	14			
U11	74C109	7	14			
U12	74LS175	8	16			
U13	74C109	7	14			
U14	74LS138	8	16			
U15	74LS20	7	14			
U16	74LS93	10	5			
U17	ADC1210	21	22	20		
U18	74LS74	7	14			
U19	LM555	1	8			
U20	74LS04	7	14			
U21	74121	7	14			
U22	MC1741				7	14
U23	MC14051B	8	16	7		
U24	7400	7	14			
U25	74LS175	8	16			
U26	LF398				1	4
U27	LF398	7			1	4
U28	LF398	7			1	4
U29	MC1741				7	4
U30	MC1741				7	4
U31	MC1741				7	4
U32	MC1741				7	4
U33	MC1741				7	4
U34	MC1741				7	4
U35	74LS04	7	14			
U36	74LS175	8	16			
U37	74LS138	8	16			
U38	DAC1210LCD	3,12		24		
U39	DAC1210LCD	3,12		24		
U40	DAC1210LCD	3,12		24		

TABLE A.2
Device Reference

Reference	Type	GND	+5V	-5V	+12V	-12V
U41	MC1741	3			7	4
U42	MC1741	3			7	4
U43	MC1741	3			7	4
U44	74LS74	7	14			
U45	74LS175	8	16			
U46	74LS93	10	5			
U47	8231A	1	2		16	
U48	74LS245	10	20			
U49	74LS04	7	14			
U50	74LS00	7	14			
U51	74LS00	7	14			
U52	74LS175	8	16			
U53	2764	14	1,27,28			
U54	2764	14	1,27,28			

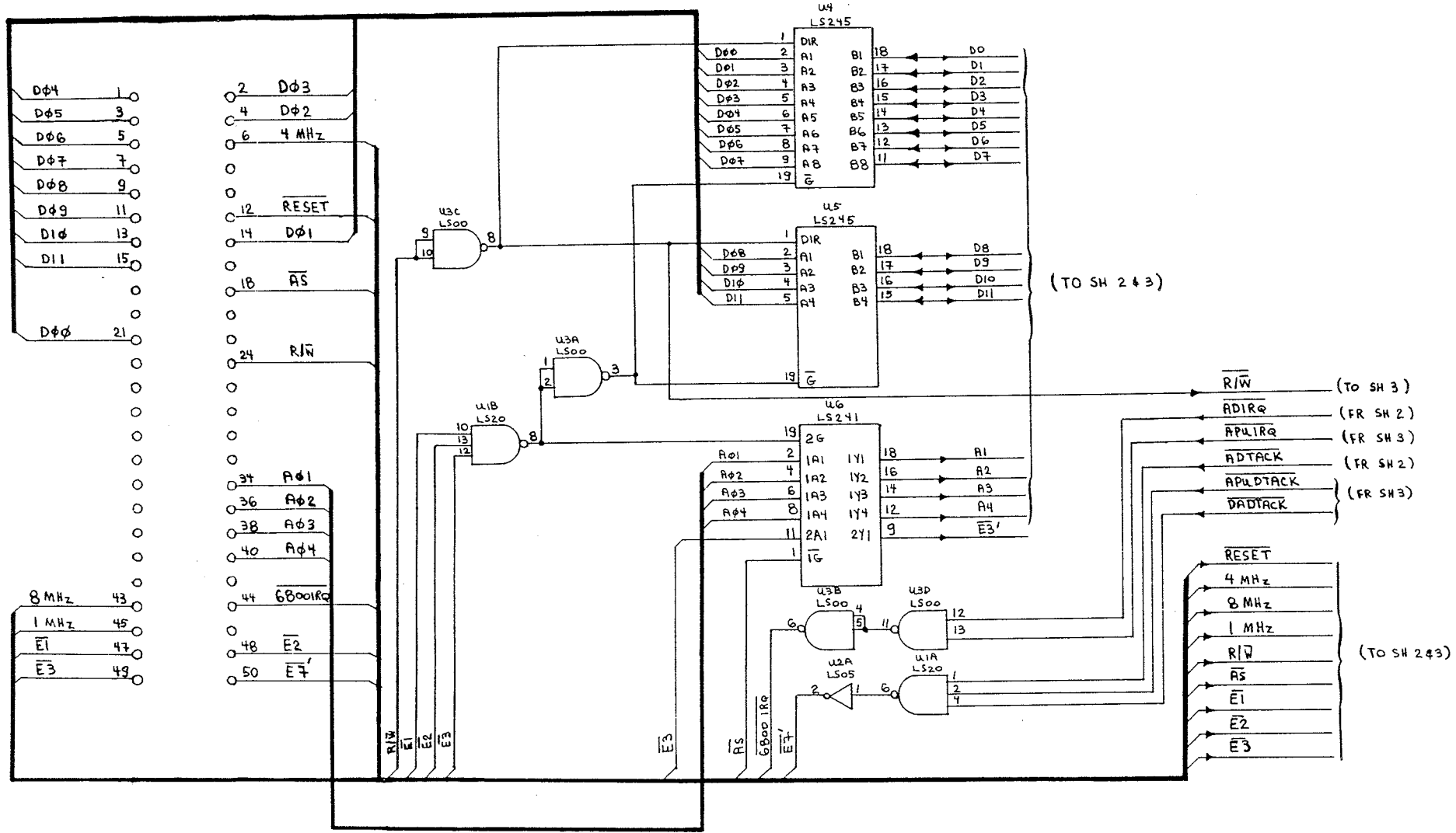


Figure A.1: SAAB Schematic Diagram (sheet 1 of 3)

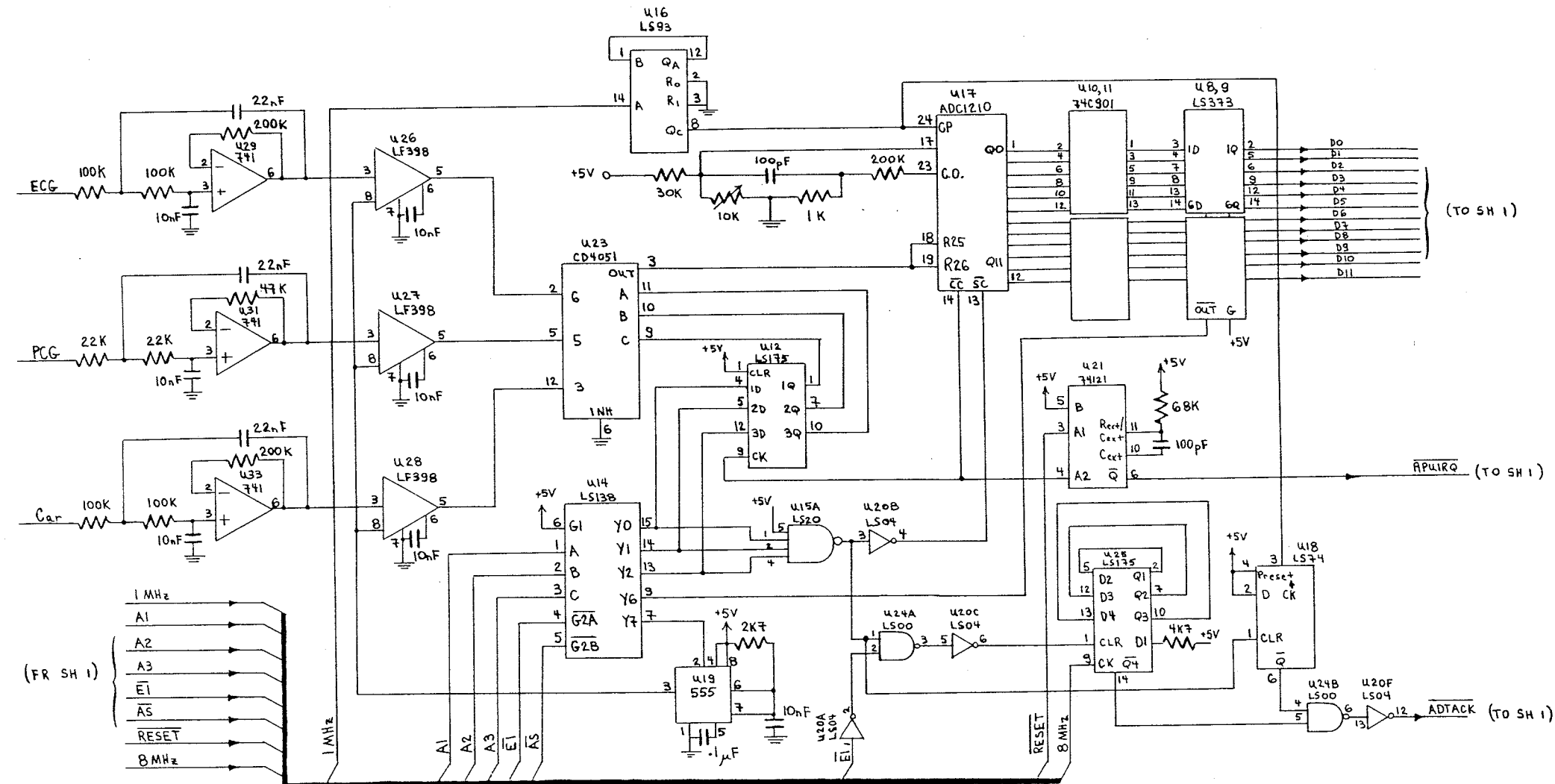


Figure A.2: SAAB Schematic Diagram (sheet 2 of 3)

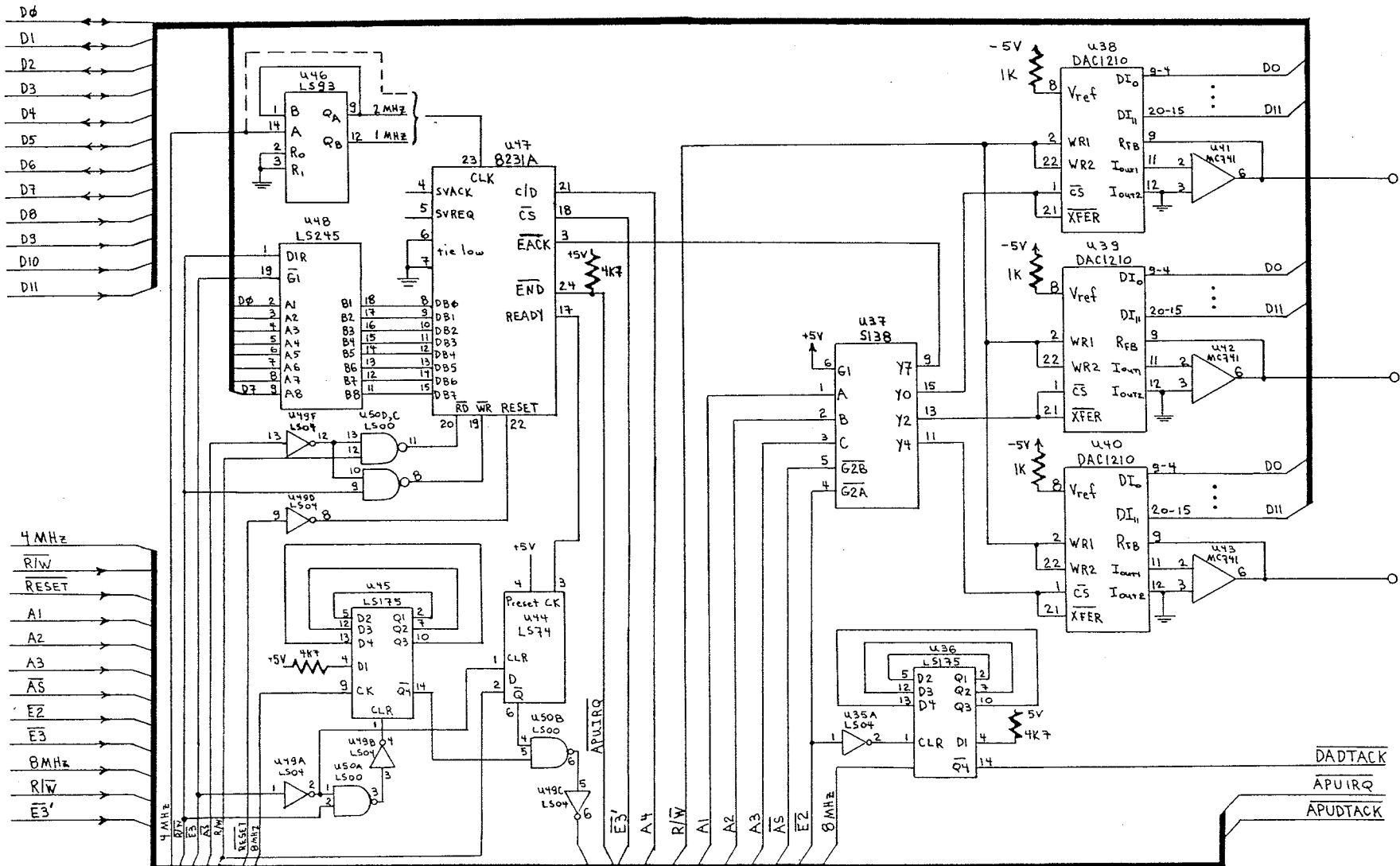


Figure A.3: SAAB Schematic Diagram (sheet 3 of 3)

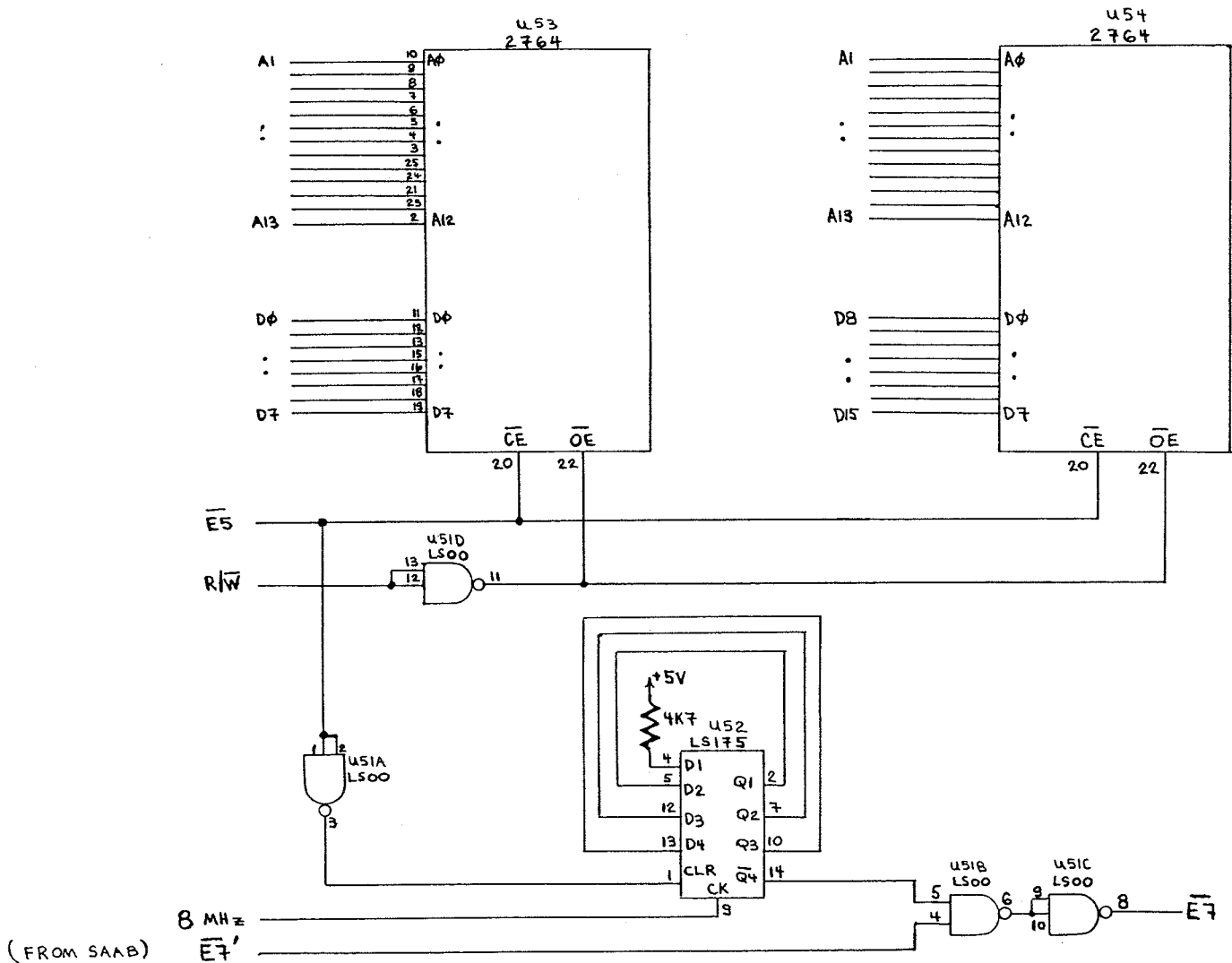


Figure A.4: USER ROM Schematic Diagram

Appendix B
SOFTWARE LISTING

```

1      * NAM THESIS PROJECT, YOU KNOW! !
3 00000900 MEMST EQU $0900 START OF RAM
4 00005FFE MEMEND EQU $5FFE END OF RAM
5 00000900 ECGSTRT SET $0900 STARTING ADDRESS OF ECG SAMPLES
6 00001500 ECGEND SET $1500 ENDING ADDRESS OF ECG SAMPLES
7 00001500 CARSTRT SET $1500 STARTING ADDRESS OF PCG SAMPLES
8 00002100 CAREND SET $2100 ENDING ADDRESS OF PCG SIGNALS
9 00002100 PCGSTRT SET $2100 STARTING ADDRESS OF CAROTID SAMPLES
10 00002D00 PCGEND SET $2D00 ENDING ADDRESS OF CAROTID SAMPLES
11 00001B00 TRECGST EQU $1B00 STARTING ADDRESS OF TRANSFORMED ECG
12 000020FC TRECGEN EQU $20FC ENDING ADDRESS OF TRANSFORMED ECG
13 00002100 TRCARST EQU $2100 STARTING ADDRESS OF TRANSFORMED CAROTID
14 00002300 TRCAREN EQU $2300 ENDING ADDRESS OF TRANSFORMED CAROTID
15 00002300 PCGENST EQU $2300 STARTING ADDRESS OF PCG ENERGY CURVE
16 00003700 TMPSTA EQU $3700 TEMPORARY STORAGE OF CONVOLVED SAMPLES
17 00003700 XRST EQU $3700 STARTING ADDRESS OF REAL PART OF PCG
18 00003EFC XRENH EQU $3EFC HALFWAY POINT REAL ARRAY
19 00004700 XREN EQU $4700 ENDING ADDRESS OF REAL PART OF ECG
20 00004700 XIIST EQU $4700 STARTING ADDRESS OF IMAGINARY PART OF PCG
21 00005700 XIEN EQU $5700 ENDING ADDRESS OF IMAGINARY PART OF PCG
22 00005700 TMPSTB EQU $5700 TEMPORARY STORAGE OF POWER SPECTRUM DATA
23 00005EFC TMPENB EQU $5EFC END OF TEMPORARY STORAGE
24 00004700 TMPSTC EQU $4700 STARTING ADDRESS OF POWER SPECTRUM CONV.
25
26      * I/O DEVICE ADDRESSES
27
28 00010021 TCR EQU $10021 PI/T TIMER CONTROL REGISTER
29 00010025 CPR EQU $10025 PI/T COUNTER PRELOAD REGISTER
30 0001002D CNTR EQU $1002D PI/T COUNTER
31 00010035 TSR EQU $10035 PI/T TIMER STATUS REGISTER
32 00020001 ADCH1 EQU $20001 A/D CHANNEL 1
33 00020003 ADCH2 EQU $20003 A/D CHANNEL 2
34 00020005 ADCH3 EQU $20005 A/D CHANNEL 3
35 0002000C ADREAD EQU $2000C READ A/D CONVERTER
36 0002000E HOLD EQU $2000E START SAMPLE-HOLDS
37 00040000 DACH1 EQU $40000 D/A CHANNEL 1 WRITE AND LATCH
38 00040004 DACH2 EQU $40004 D/A CHANNEL 2 WRITE AND LATCH
39 00040008 DACH3 EQU $40008 D/A CHANNEL 3 WRITE AND LATCH
40 0004000E APUEACK EQU $4000E APU INTERRUPT ACKNOWLEDGE
41 00050001 APUOPER EQU $50001 COMMAND TO W/R OPERANDS TO/FROM APU
42 00050011 APUCOM EQU $50011 SEND COMMAND TO APU
43
44      * VARIOUS DATA REGISTERS USED BY ROUTINES
45
46 000000 00FF DS.B 255 AREA OF MEMORY USED FOR DATA REGISTERS
47 00007F00 VDR EQU $7F00
48 00007F00 QRS1 EQU VDR NUMBER OF BYTES TO QRS1
49 00007F02 QRS2 EQU VDR+2 NUMBER OF BYTES TO QRS2
50 00007F04 T2PEAK EQU VDR+4 NUMBER OF BYTES TO DICROTIC NOTCH USING
51          * T2 PEAK OF CAROTID TRANSFORM.
52 00007F06 DCRTC EQU VDR+6 NUMBER OF BYTES TO DICROTIC NOTCH USING
53          * CDCRTC ROUTINE.
54 00007F08 PCGS1A EQU VDR+8 NUMBER OF BYTES TO S1
55 00007F0A PCGS1B EQU VDR+10 NUMBER OF BYTES TO SECOND S1 (QRS2)
56 00007F0C PCGS2 EQU VDR+12 NUMBER OF BYTES BETWEEN S1 AND S2
57 00007F0E PCGENSE EQU VDR+14 END OF SYSTOLIC PCG ENERGY CURVE
58 00007F10 PCGENDE EQU VDR+16 END OF DIASTOLIC PCG ENERGY CURVE
59 00007F12 SEQNUM EQU VDR+18
60 00007F16 EDCTSYS EQU VDR+22 TIME DOMAIN EDC FOR SYSTOLIC SEGMENT
61 00007F18 EDCTDIA EQU VDR+24 TIME DOMAIN EDC FOR DIASTOLIC SEGMENT
62 00007F1A EDCFSYS EQU VDR+26 FREQ DOMAIN EDC FOR SYSTOLIC SEGMENT

```

```

63 00007F1E EDCFDIA EQU VDR+30 FREQ DOMAIN EDC FOR DIASTOLIC SEGMENT
64 00007F2A L EQU VDR+42
65 00007F2C LE EQU VDR+44
66 00007F2E LE1 EQU VDR+46
67 00007F30 I EQU VDR+48
68 00007F32 J EQU VDR+50
69 00007F34 WR EQU VDR+52
70 00007F38 WI EQU VDR+56
71 00007F3C UR EQU VDR+60
72 00007F40 UI EQU VDR+64
73 00007F44 QUOT EQU VDR+68
74 00007F48 COUNTER EQU VDR+72
75 *
76 *
77 * A/D AND APU CONSTANTS, COMMANDS, AND REGISTERS
78 *
79 *
80 0000007A ADSMPL EQU 122 COUNTER VALUE - 1024 HZ SAMPLING RATE
81 000001E8 ADWNSMP EQU 488 COUNTER VALUE - 256 HZ SAMPLING RATE
82 00000001 SRTIMR EQU $01 START TIMER
83 00000000 HALTIMR EQU $00 HALT TIMER
84 00000070 ADEXADD EQU $70 A/D EXCEPTION ADDRESS
85 00000070 APUEKAD EQU $70 APU EXCEPTION ADDRESS
86 *
87 *
88 * ECG, CAROTID, PCG ADDRESSES AND FFT CONSTANTS
89 *
90 *
91 00000900 ECGSNEW EQU $0900 NEW ECG START ADDRESS
92 00000C00 ECGENEW EQU $0C00 NEW ECG END ADDRESS
93 00000C00 CARSNEW EQU $0C00 NEW CAROTID START ADDRESS
94 00000F00 CARENEW EQU $0F00 NEW CAROTID END ADDRESS
95 00000F00 PCGSNEW EQU $0F00 NEW PCG START ADDRESS
96 00001B00 PCGENEW EQU $1B00 NEW PCG END ADDRESS
97 00000008 ECGDWN EQU $08 ECG DOWNSAMPLE FACTOR (/2)
98 00000008 CARDWN EQU $08 CAROTID DOWNSAMPLE FACTOR
99 00000002 PCGDWN EQU $02 PCG DOWNSAMPLE FACTOR (/2)
100 00000010 EGGCNV EQU 16 ECG CONVOLVE WINDOW WIDTH
101 00000010 CARCNV EQU 16 CAR CONVOLVE WINDOW WIDTH
102 00000020 PCGCNV EQU 32 PCG CONVOLVE WINDOW WIDTH
103 00000098 T1TOT2 EQU 152 MOVE AHEAD THIS MANY BYTES TO LOOK FOR T2
104 0000001B DS2DEL EQU 27 DELAY BETWEEN S2 AND DICROTIC NOTCH (53 MS
105 0000000A LNN EQU 10
106 00000400 N EQU 1024 N=2**LNN
107 00000200 NV2 EQU N/2 NV2=N/2
108 000003FF NM1 EQU N-1 NM1=N-1
109 008A3D70 HAM54 EQU $008A3D70 .54 FLOATING POINT
110 7FEB851E HAM46 EQU $7FEB851E .46 FLOATING POINT
111 *
112 *
113 * APU COMMANDS
114 *
115 *
116 00000006 ACOS EQU $06 32-BIT FLOATING-POINT INVERSE COSINE
117 00000005 ASIN EQU $05 32-BIT FLOATING-POINT INVERSE SINE
118 00000007 ATAN EQU $07 32-BIT FLOATING-POINT INVERSE TANGENT
119 00000034 CHSD EQU $34 32-BIT FIXED-POINT SIGN CHANGE
120 00000015 CHSF EQU $15 32-BIT FLOATING-POINT SIGN CHANGE
121 00000074 CHSS EQU $74 16-BIT FIXED-POINT SIGN CHANGE
122 00000003 COS EQU $03 32-BIT FLOATING-POINT COSINE
123 0000002C DADD EQU $2C 32-BIT FIXED-POINT ADD

```

124 0000002F	DDIV	EQU \$2F	32-BIT FIXED-POINT DIVIDE
125 0000002E	DMUL	EQU \$2E	32-BIT FIXED-POINT MULTIPLY, LOWER
126 00000036	DMUU	EQU \$36	32-BIT FIXED-POINT MULTIPLY, UPPER
127 0000002D	DSUB	EQU \$2D	32-BIT FIXED-POINT SUBTRACT
128 0000000A	EXP	EQU \$0A	32-BIT FLOATING POINT EXP(X)
129 00000010	FADD	EQU \$10	32-BIT FLOATING POINT ADD
130 00000013	FDIV	EQU \$13	32-BIT FLOATING-POINT DIVIDE
131 0000001E	FIXD	EQU \$1E	32-BIT FLOATING-POINT TO 32-BIT FIXED POINT
132 0000001F	FIXS	EQU \$1F	32-BIT FLOATING-POINT TO 16-BIT FIXED-POINT
133 0000001C	FLTD	EQU \$1C	32-BIT FIXED-POINT TO 32-BIT FLOATING-POINT
134 0000001D	FLTS	EQU \$1D	16-BIT FIXED-POINT TO 32-BIT FLOATING-POINT
135 00000012	FMUL	EQU \$12	32-BIT FLOATING-POINT MULTIPLY
136 00000011	FSUB	EQU \$11	32-BIT FLOATING-POINT SUBTRACT
137 00000008	LOG	EQU \$08	32-BIT FLOATING-POINT COMMON LOG
138 00000009	LN	EQU \$09	32-BIT FLOATING-POINT NATURAL LOG
139 00000000	NOPAPU	EQU \$00	NO OPERATION
140 00000038	POPD	EQU \$38	32-BIT STACK POP
141 00000018	POPF	EQU \$18	32-BIT STACK POP (SAME AS POPD)
142 00000078	POPS	EQU \$78	16-BIT STACK POP
143 00000037	PTOD	EQU \$37	PUSK 32-BIT TOS ONTO STACK
144 00000017	PTOF	EQU \$17	PUSH 32-BIT TOS ONTO STACK (SAME AS PTOD)
145 00000077	PTOS	EQU \$77	PUSH 16-BIT TOS ONTO STACK
146 0000001A	PUPI	EQU \$1A	PUSH 32-BIT FLOATING-POINT PI
147 0000000B	PWR	EQU \$0B	32-BIT FLOATING-POINT X(Y)
148 0000006C	SADD	EQU \$6C	16-BIT FIXED-POINT ADD
149 0000006F	SDIV	EQU \$6F	16-BIT FIXED-POINT DIVIDE
150 00000002	SIN	EQU \$02	32-BIT FLOATING-POINT SINE
151 0000006E	SMUL	EQU \$6E	16-BIT FIXED-POINT MULTIPLY, LOWER
152 00000076	SMUU	EQU \$76	16-BIT FIXED-POINT MULTIPLY, UPPER
153 00000001	SQRT	EQU \$01	32-BIT FLOATING-POINT SQUARE ROOT
154 0000006D	SSUB	EQU \$6D	16-BIT FIXED-POINT SUBTRACT
155 00000004	TAN	EQU \$04	32-BIT FLOATING-POINT TANGENT
156 00000039	XCHD	EQU \$39	EXCHANGE 32-BIT STACK OPERANDS
157 00000019	XCHF	EQU \$19	EXCHANGE 32-BIT STACK OPERANDS (SAME AS XCHD)
158 00000079	XCHS	EQU \$79	EXCHANGE 16-BIT STACK OPERANDS
159	*		
160	*		
161	*	TRAP 14 FUNCTION CODES	
162	*		
163	*		
164 000000FD	LINKIT	EQU 253	APPEND USER TABLE TO TRAP 14 TABLE
165 000000F8	OUTCH	EQU 248	OUTPUT SINGLE CHARACTER TO PORT 1
166 000000F7	INCHE	EQU 247	INPUT SINGLE CHARACTER FROM PORT 1
167 000000F3	OUTPUT	EQU 243	OUTPUT STRING TO PORT1
168 000000EC	HEX2DEC	EQU 236	CONVERT HEX TO ASCII
169 000000EA	PUTHEX	EQU 234	CONVERT 1 HEX DIGIT ---> ASCII
170 000000E9	PNT2HX	EQU 233	" 2 " " ---> "
171 000000E8	PNT4HX	EQU 232	" 4 " " ---> "
172 000000E7	PNT6HX	EQU 231	" 6 " " ---> "
173 000000E6	PNT8HX	EQU 230	" 8 " " ---> "
174 000000E5	START	EQU 229	RESTART TUTOR
175 000000E4	TUTOR	EQU 228	GO TO TUTOR
176 000000E3	OUT1CR	EQU 227	OUTPUT STRING PLUS 'CR', 'LF' TO PORT 1
177 000000E2	GETNUMA	EQU 226	CONVERT ASCII ENCODED HEX TO HEX
178 000000E1	GETNUMD	EQU 225	CONVERT ASCII CODED DECIMAL TO HEX
179 00000000	ERROR1	EQU 0	ERROR #1 MESSAGE: QRS COMPLEXES
180	*		

```

182 *#####
183 * MACRO LIST
184 *#####
185 *
186 CALLCNVL MACRO
187 *
188 * SETS POINTER FOR AND CALLS CONVOLVE ROUTINE FOR ECG AND
189 * CAROTID TRANSFORMS AND PCG ENERGY CURVE.
190 * MACRO CALL IS 'TRANSFORM START,CONVOLVE FACTOR,TRANSFORM END
191 *
192 MOVE.W #\1,A0      STARTING ADDRESS OF TRANSFORMED SIGNAL
193 MOVE.W #\2,D0      CONVOVLE WINDOW WIDTH
194 MOVE.W #\3,A1      ENDING ADDRESS OF TRANSFORMED SIGNAL
195 JSR CNVLV         GOTO CONVOLVE SUBROUTINE
196 ENDM
197 *#####
198 CLDATA2 MACRO
199 *
200 * CLEARS TWO DATA REGISTERS
201 *
202 CLR.\0 \1
203 CLR.\0 \2
204 ENDM
205 *#####
206 CLDATA3 MACRO
207 *
208 * CLEARS THREE DATA REGISTERS
209 *
210 CLR.\0 \1
211 CLR.\0 \2
212 CLR.\0 \3
213 ENDM
214 *#####
215 CLDATA8 MACRO
216 *
217 * CLEARS EIGHT DATA REGISTERS
218 *
219 CLR.\0 D0
220 CLR.\0 D1
221 CLR.\0 D2
222 CLR.\0 D3
223 CLR.\0 D4
224 CLR.\0 D5
225 CLR.\0 D6
226 CLR.\0 D7
227 ENDM
228 *#####
229 CONVERT MACRO
230 *
231 * USED FOR A/D CONVERSION. DUMMY WRITE TO TIE PROPER MUX INPUT
232 * CHANNEL TO OUTPUT CHANNEL AND TO START A/D CONVERTER. THEN
233 * WAIT FOR INTERRUPT. AFTER INTERRUPT INCREMENT CHANNEL COUNT
234 * MACRO CALL IS 'A/D CHANNEL EA,COUNTER DATA REG'
235 *
236 MOVE.B #0,\1      MUX IN<-->OUT AND START A/D
237 STOP #\$2300       WAIT UNTIL CONVERSION IS FINISHED.
238 *                  PUT PROCESSOR IN SUPERVISOR STATE WITH
239 *                  INTERRUPT PRIORITY LEVEL 0.
240 ADDI.B #1,\2       INCREMENT A/D CHANNEL COUNTER
241 ENDM
242 *#####

```

```

243      DATAMV MACRO
244      *
245      * MOVES A BLOCK OF DATA FROM ONE LOCATION TO ANOTHER W/DOWNSAM
246      * MACRO CALL IS 'ORIGINAL STARTING ADDRESS,ADDRESS REGISTER,
247      * ORIGINAL END ADDRESS,ADDRESS REGISTER,NEW START,NEW END,
248      * ADDRESS REGISTER,DOWNSAMPLE FACTOR'
249      *
250          STPOIN2 \1,\2,\3,\4      OLD ECG DATA POINTER
251          \1 SET \5
252          \3 SET \6      SET NEW START AND END ADDRESSES
253          MOVE.W #\1,\7      NEW DATA POINTER (DOWNSAMPLED DATA)
254          \@ MOVE.W (\2),(\7)+  MOVE DATA
255          ADD.W #\8,\2      DOWNSAMPLE
256          CMP.W \4,\2
257          BLT.S \@      CONTINUE UNTIL ALL DATA MOVED
258          ENDM
259          ##### DATIMER MACRO #####
260
261          *
262          * INITIALIZE PI/T REGISTERS AND START COUNTING. ALL PARAMETERS
263          * HAVE BEEN SET UP FOR D/A ROUTINES. NEED SAMPLING PERIOD IN
264          * DO.
265          *
266          STPOIN2.L CNTR,A5,CPR,A6  COUNTER,PRELOAD ADDRESS
267          MOVE.L D0,D7      SAMPLING PERIOD; NOTE THAT THERE IS
268          *                  PRESCALER (/32); WITH THE CLK=4MHZ,
269          *                  A COUNTER VALUE OF 1 EQUALS 8 US.
270          MOVEP.L D7,0(A6)      SAMPLING PERIOD --> PRELOAD REGISTE
271          MOVE.B #1,TSR      RESET TSR
272          MOVE.B #STRTIMR,TCR      START TIMER USING TCR RUN CODE
273          ENDM
274          ##### DELAY MACRO #####
275
276          *
277          * CAUSES A TIME DELAY. A DELAY VALUE OF '1' CORRESPONDS TO
278          * APPROXIMATELY 4.5 USEC.
279          * MACRO CALL IS 'DELAY VALUE IM,DATA REGISTER'
280          *
281          MOVE.W #\1,\2
282          \@ DBRA \2,\@      ENDM
283          *##### DSPLOPT MACRO #####
284
285
286          *
287          * DISPLAY D/A OPTIONS ON TERMINAL.
288          * MACRO CALL IS 'START ADDRESS OF MESSAGE EA,END ADDRESS EA'
289          *
290          LEA \1,A5
291          LEA \2,A6
292          TRP14 OUT1CR
293          ENDM
294          *##### GETADD MACRO #####
295          GETADD MACRO
296
297          *
298          * COMPUTES ADDRESS FROM NUMBER OF BYTES AND STARTING ADDRESS.
299          * MACRO CALL IS 'NUMBER OF BYTES EA,ADDRESS REGISTER,STARTING
300          * ADDRESS'
301          *
302          MOVE.W \1,\2
303          ADD.W #\3,\2
            ENDM

```

```

304 *#####
305 ML3216 MACRO
306 *
307 * THIS MACRO MULTIPLIES A 32 BIT NUMBER BY A 16 BIT NUMBER.
308 * RESULT (48 BITS) IS RETURNED IN MULTIPLICAND (LOWER 32 BITS)
309 * AND TEMP DR2 (UPPER 16 BITS).
310 * MACRO CALL IS 'MULTIPLIER (16 BITS) EA,MULTIPLICAND (32 BITS
311 * TEMP DR1,TEMP DR2,TEMP DR3'
312 *
313 CLR.L \4
314 MOVE.W \2,\3 LOWER WORD OF MULTIPLICAND INTO TEMP
315 MULU.W \1,\3 MULTIPLY TEMP BY MULTIPLIER
316 SWAP \2 UPPER WORD OF MULTIPLICAND INTO LOWER WORD
317 MULU.W \1,\2 MULTIPLY LOWER WORD BY MULTIPLIER
318 MOVE.B #15,\5
319 @ LSL.L #1,\2
320 ROXL.L #1,\4
321 DBRA \5,\@ ADD TO GET LOWER 32 BITS
322 ADD.L \3,\2
323 CLR.L \5 ADD TO GET UPPER 16 BITS
324 ADDX.L \5,\4
325 ENDM
326 *#####
327 SPACE MACRO
328 *
329 * OUTPUTS BLANK LINE TO TERMINAL.
330 *
331 LEA SPAC,A5
332 LEA SPCE,A6
333 TRP14 OUT1CR
334 ENDM
335 *#####
336 STPOIN2 MACRO
337 *
338 * SETS TWO POINTERS. MUST INDICATE WHETHER B,W,LW.
339 * MACRO CALL IS 'VALUE IM,ADDRESS REGISTER' * 2
340 *
341 MOVE.\0 #\1,\2
342 MOVE.\0 #\3,\4
343 ENDM
344 *#####
345 STPOIN3 MACRO
346 *
347 * SETS THREE POINTERS. MUST INDICATE WHETHER B,W,LW.
348 * MACRO CALL IS 'VALUE IM,ADDRESS REGISTER' * 3
349 *
350 MOVE.\0 #\1,\2
351 MOVE.\0 #\3,\4
352 MOVE.\0 #\5,\6
353 ENDM
354 *#####
355 SQUARE MACRO
356 *
357 * THIS MACRO SQUARES A WORD AND STORES IT AS A LONG WORD.
358 * MACRO CALL IS 'DATA REGISTER (WORD),DATA REGISTER (LW),
359 * ADDRESS REGISTER (MEMORY POINTER)'
360 *
361 MOVE.W \1,\2
362 MULS.W \1,\2 SQUARE NUMBER
363 MOVE.L \2,(3)+ STORE QUANTITY AS LONG WORD
364 ENDM

```

```

365 *#####
366 TEMPMOVE MACRO
367 *
368 * MOVES DATA FROM TEMPORARY MEMORY (FROM CONVOLVE S/R) TO
369 * ACTUAL TRANSFORM MEMORY.
370 * MACRO CALL IS 'TRANSFROM START,MEMORY POINTER'
371 *
372 STPOIN2 \1,A0,TMPSTA,A1
373 \@ MOVE.L (A1)+,(A0)+      MOVE FROM TEMP TO TRANSFORM
374     CMP.W #\2,A0
375     BLT \@
376     ENDM
377 *#####
378 TIMER MACRO
379 *
380 * INITIALIZE PI/T REGISTERS AND START COUNTING.
381 * MACRO CALL IS 'COUNTER ADDRESS REGISTER,PRELOAD ADDRESS
382 * REGISTER,SAMPLING PERIOD,PERIOD DATA REGISTER'
383 *
384     STPOIN2.L CNTR,\1,CPR,\2 COUNTER,PRELOAD ADDRESS
385     MOVE.L #\3,\4 SAMPLING PERIOD; NOTE THAT THERE IS
386     * PRESCALER (/32); WITH THE CLK=4MHZ,
387     * A COUNTER VALUE OF 1 EQUALS 8 US.
388     MOVEP.L \4,0(\2) SAMPLING PERIOD --> PRELOAD REGISTE
389     MOVE.B #1,TSR RESET TSR
390     MOVE.B #$TRTIMR,TCR START TIMER USING TCR RUN CODE
391     ENDM
392 *#####
393 TRP14 MACRO
394 *
395 * USED TO INVOKE TUTOR TRAP 14 HANDLER.
396 * MACRO CALL IS 'FUNCTION NUMBER IM'.
397 *
398     MOVE.B #\1,D7
399     TRAP #14
400     ENDM
401 *#####
402 TRUNCAT MACRO
403 *
404 * THIS MACRO TRUNCATES A 32 BIT LONG WORD TO 12 BITS.
405 * MACRO CALL IS 'SIGNAL POINTER REGISTER,DATA REGISTER'
406 *
407     MOVE.L (\1)+,\2
408     SWAP \2
409     LSR.W #4,\2
410     ENDM
411 *#####
412 TSTIMR MACRO
413 *
414 * TEST TSR TO DETERMINE IF TIMER HAS COUNTED DOWN TO ZERO.
415 * AFTER COUNTING DOWN DETERMINE IF ALL DATA HAS BEEN PROCESSED
416 * MACRO CALL IS 'END ADDRESS REGISTER,SIGNAL POINTER REGISTER'
417 *
418 \@ CMP.B #0,TSR
419     BEQ \@
420     MOVE.B #1,TSR
421     CMP.W \1,\2
422     ENDM
423 *

```

```

425      ######
426      ######
427      ##
428      ##
429      ##          APU & FFT MACROS
430      ##
431      ##
432      #####
433      #####
434      ##
435      *
436      APU MACRO
437      *
438      * ISSUE A COMMAND TO MANIPULATE DATA ON APU STACK.
439      * MACRO CALL IS 'COMMAND IM'
440      *
441      MOVE.B #\1,APUCOM
442      STOP #$2300
443      ENDM
444      ######
445      APUSGRD MACRO
446      *
447      * READ 32-BIT WORD FROM APU TO SIGNAL ARRAY
448      * MACRO CALL 'SIGNAL AR,ARRAY SCRIPT DR,APU ADDRESS AR'
449      *
450      MOVE.W #$3,D7
451      \@ ROL.L #$8,D6
452      MOVE.B (\3),D6
453      DBRA D7,\@
454      MOVE.L D6,0(\1,\2)
455      ENDM
456      ######
457      APUSGWR MACRO
458      *
459      * MOVE A 32-BIT NUMBER FROM SIGNAL ARRAY TO APU
460      * MACRO CALL IS 'SIGNAL POINTER AR,ARRAY SCRIPT DR,APU ADDRES
461      *
462      MOVE.L 0(\1,\2),D6
463      MOVE.W #$3,D7
464      \@ MOVE.B D6,(\3)
465      ROR.L #$8,D6
466      DBRA D7,\@
467      ENDM
468      ######
469      APURD MACRO
470      *
471      * READ 32-BIT NUMBER FROM APU.
472      * MACRO CALL IS 'APU OPERAND ADDRESS AR,DATA DR'
473      *
474      MOVE.W #$3,D7
475      \@ ROL.L #$8,\2
476      MOVE.B (\1),\2
477      DBRA D7,\@
478      ENDM
479      ######
480      APUWR MACRO
481      *
482      * MOVE A 32-BIT NUMBER FROM MEMORY TO APU
483      * MACRO CALL IS 'VALUE DR,APU ADDRESS AR'
484      *
485      MOVE.W #$3,D7

```

```

486      \@ MOVE.B \1,(\2)
487      ROR.L #$8,\1
488      DBRA D7,\@  

489      ENDM
490      *#####
491      APUWR16 MACRO
492      *
493      * MOVE A 16-BIT NUMBER FROM MEMORY TO APU
494      * MACRO CALL IS 'VALUE DR,APU ADDRESS AR'
495      *
496      MOVE.W #$1,D7
497      \@ MOVE.B \1,(\2)
498      ROR.L #$8,\1
499      DBRA D7,\@  

500      ROR.L #$8,\1
501      ROR.L #$8,\1
502      ENDM
503      *#####
504      POW2TOA MACRO
505      *
506      * CALCULATES 2**A. MACRO CALL IS 'A EA'
507      *
508      MOVE.W \1,D7
509      SUBI.W #1,D7
510      MOVE.W #1,D6
511      \@ MULU.W #2,D6
512      DBRA D7,\@  

513      ENDM
514      *#####
515      REORDER MACRO
516      *
517      * MACRO CALL IS ADDRESS AR,J DR,T DR,I DR
518      *
519      MOVE.L 0(\1,\2),\3
520      MOVE.L 0(\1,\4),0(\1,\2)
521      MOVE.L \3,0(\1,\4)
522      ENDM
523      *
524      *

```

```

526      ##### MAINLINE
527      *##### MAINLINE CALLS THE FOLLOWING SUBROUTINES:
528      *##### USRFNCS: SET UP USER TRAP 14 TABLE
529      *##### ADCONV: PERFORM A/D CONVERSION
530      *##### ECG: PERFORM ECG PROCESSING
531      *##### CAR: PERFORM CAROTID PROCESSING
532      *##### PCGT: PERFORM PCG PROCESSING (TIME DOMAIN)
533      *##### PCGF: PERFORM PCG PROCESSING (FREQ DOMAIN)
534      *##### DAFIX: DISPLAY SIGNALS USING D/A CONVERTERS
535      *##### FIN: END PROGRAM
536      *#####
537      *#####
538      *#####
539      *#####

540 00006000 ORG $006000
541 006000 4280 CLR.L D0
542 006002 307C0900 MOVE.W #MEMST,A0
543 006006 20C0 MEMCLR MOVE.L D0,(A0)+ CLEAR MEMORY
544 006008 B0FC5FFE CMP.W #MEMEND,A0
545 00600C 6FFF8 BLE.S MEMCLR
546 00600E 343C001E MOVE.W #30,D2
547 006012 4EB872D4 MAIN JSR BLANK CLEAR SCREEN
548 006016 51CAFFFA DBRA D2,MAIN
549 00601A 4EB860CE JSR USRFNCS
550 00601E 4EB86126 JSR ADCONV
551 006022 21FC00006240
      0070 MOVE.L #APISR,APUEXAD
552 00602A 4EB8624A JSR ECG
553 00602E 4EB863CA JSR CAR
554 006032 4EB865A0 JSR PCGT
555 006036 4EB86F02 JSR PCGF
556 00603A 4EB872D4 JSR BLANK
557      DSPLOPT QUIT,QUITE
557 00603E 4BF86064 LEA QUIT,A5
557 006042 4DF8608C LEA QUITE,A6
557      TRP14 OUT1CR
557 006046 1E3C00E3 MOVE.B #OUT1CR,D7
557 00604A 4E4E TRAP #14
558      TRP14 INCHE
558 00604C 1E3C00F7 MOVE.B #INCHE,D7
558 006050 4E4E TRAP #14
559 006052 0C000051 CMP.B $$51,D0
560 006056 6704 BEQ.S GOFIN
561 006058 4EB87206 JSR DAFIX
562 00605C 4EB872D4 GOFIN JSR BLANK
563 006060 4EB87A8E JSR FIN
564 006064 4F QUIT DC.W 'OPTION: QUIT (Q) OR DISPLAY RESULTS <R>'
565 00608C 20 QUITE DC.W '
566      *
567      *

```

```

569      **** CONVOLVE SUBROUTINE ****
570      * CALLED BY: ECNVNL, CCNVNL, PTCNVS, PTCNVD
571      ****
572      * A0 ==> A2 <--> TRANSFORMED SIGNAL POINTER
573      * A1 <--> END OF TRANSFORMED SIGNAL
574      * A3 <--> CONVOLVE POINTER
575      * A4 <--> TEMPORARY RESULT POINTER
576      * D0 <--> CONVOLVE WINDOW WIDTH (M)
577      * D1 <--> C(N) = SUMMATION .....
578      * D2 <--> WINDOW WIDTH DOWN COUNTER
579      * D3 <--> TRANSFORM VALUE
580      * D4,D5,D6 <--> TEMPORARY DATA STORAGE
581      ****
582      * CALL FOLLOWING MACROS:
583      * ML3216
584      ****
585      * CONVOLVE SUBROUTINE USED BY ECG AND CAROTID TO SMOOTH ECG
586      * AND CAROTID TRANSFORM. USED BY PCG TO SMOOTH THE ENERGY CUR
587      * SET POINTERS. BLOCK OF MEMORY STARTING AT TMPSTA IS USED TO
588      * STORE THE CONVOLVED SIGNAL.
589      *
590
591 00608E 3448 CNVLV MOVE.W A0,A2          TRANSFORMED SIGNAL POINTER
592 006090 387C3700 MOVE.W #TMPSTA,A4        TEMPORARY MEMORY POINTER
593 006094 584A ADDQ.W #4,A2                INCREMENT BY ONE LONG WORD
594      *
595      * SET POINTERS FOR INNER LOOP CALCULATIONS
596      *
597 006096 364A CNVLV1 MOVE.W A2,A3          CONVOLVE INNER LOOP POINTER
598 006098 4281 CLR.L D1                    C(N)=0
599 00609A 3400 MOVE.W D0,D2                NUMBER OF SAMPLES IN WINDOW
600      *
601      * COMPUTE C(N) FOR SPECIFIC N ,I.E., C(N)=SUMMATION.
602
603 00609C 2623 CNVLV2 MOVE.L -(A3),D3      DECREMENT, THEN LOAD DATA
604 00609E B6C8 CMP.W A0,A3
605 0060A0 6D22 BLT.S CNVLV3
606      *
607      ML3216 D2,D3,D4,D5,D6
607 0060A2 4285 CLR.L D5
607 0060A4 3803 MOVE.W D3,D4
607 0060A6 C8C2 MULU.W D2,D4
607 0060A8 4843 SWAP D3
607 0060AA C6C2 MULU.W D2,D3
607 0060AC 1C3C000F MOVE.B #15,D6
607 0060B0 E38B @003 LSL.L #1,D3
607 0060B2 E395 ROXL.L #1,D5
607 0060B4 51CEFFFA DBRA D6,@003
607 0060B8 D684 ADD.L D4,D3
607 0060BA 4286 CLR.L D6
607 0060BC DB86 ADDX.L D6,D5
608 0060BE D283 ADD.L D3,D1
609 0060C0 51CAFFDA DBRA D2,CNVLV2
610 0060C4 28C1 CNVLV3 MOVE.L D1,(A4)+    C(N) SUMMATION
611 0060C6 584A ADDQ.W #4,A2
612 0060C8 B4C9 CMP.W A1,A2
613 0060CA 6DCA BLT.S CNVLV1
614 0060CC 4E75 RTS
615      *
616      *

```

```

618 *#####
619 *#####
620 *#####
621 *##### DEFINE TABLE FOR TRAP 14 USER FUNCTIONS #####
622 *#####
623 *#####
624 *#####
625 *##### AO <--> START OF NEW TABLE, AFTER TRP14 AO CONTAINS #####
626 *##### THE POINTER TO THE OLD TABLE #####
627 *#####
628 *#####
629 *#####
630 *##### CALL FOLLOWING MACROS: #####
631 *##### TRP14 #####
632 *#####
633 *#####
634 *#####
635 *#####
636 *#####
637 *##### THIS SUBROUTINE SETS UP THE LOOKUP TABLE OF THE STARTING #####
638 *##### ADDRESSES OF USER-DEFINED FUNCTIONS CALLED BY THE TUTOR TRA #####
639 *##### 14 HANDLER. THE FORMAT FOR ENTRIES IN THIS TABLE IS $UUSSSS #####
640 *##### WHERE $UU IS THE FUNCTION NUMBER AND $SSSSSS IS THE STARTIN #####
641 *##### ADDRESS OF THE FUCNTION. #####
642 *#####
643 *#####
644 0060CE 41F860DE USRFNCS LEA NEWTBL,A0 REGISTER A0 POINTS TO NEW TA
645 TRP14 LINKIT
645 0060D2 1E3C00FD MOVE.B #LINKIT,D7
645 0060D6 4E4E TRAP #14
646 0060D8 21C860E2 MOVE.L A0,ENDTBL A0 POINTS TO OLD TABLE
647 0060DC 4E75 RTS
648 0060DE 0000 NEWTBL DC.W $0000
649 0060E0 60E6 DC.W UTRER1 ERROR #1-QRS PEAK DETECT ERROR
650 0060E2 0000 ENDTBL DC.W $0000
651 0060E4 0000 DC.W $0000
652 *#####
653 *#####
654 *##### ERROR HANDLING ROUTINES #####
655 *##### CALLED BY TRAP 14 #####
656 *#####
657 *##### ERROR #1: UNSUCCESSFUL ATTEMPT AT FINDING TWO CONSECUTIVE #####
658 *##### QRS PEAKS. OUTPUT ERROR MESSAGE TO TERMINAL, THE #####
659 *##### GO TO TUTOR. #####
660 *#####
661 *#####
662 0060E6 4EB872D4 UTRER1 JSR BLANK
663 DSPLOPT E1,E1E OUTPUT ERROR MESSAGE
663 0060EA 4BF86100 LEA E1,A5
663 0060EE 4DF86124 LEA E1E,A6
663 TRP14 OUT1CR
663 0060F2 1E3C00E3 MOVE.B #OUT1CR,D7
663 0060F6 4E4E TRAP #14
664 TRP14 TUTOR CONTROL TO TUTOR
664 0060F8 1E3C00E4 MOVE.B #TUTOR,D7
664 0060FC 4E4E TRAP #14
665 0060FE 4E75 RTS
666 006100 45 E1 DC.W 'ERROR #1: 2 QRS COMPLEXES NOT FOUND'
667 006124 20 E1E DC.W '
668 *

```

```

670      *#####
671      *#####
672      *
673      *          A/D CONVERSION
674      *
675      *#####
676      *
677      *      A0 <--> ECG POINTER
678      *      A1 <--> PCG POINTER
679      *      A2 <--> CAROTID POINTER
680      *      A3 <--> PI/T COUNTER ADDRESS
681      *      A4 <--> PI/T PRELOAD ADDRESS
682      *      A5,A6 <--> USED BY TRAP 14 HANDLER
683      *      D0 <--> SAMPLING PERIOD
684      *      D1 <--> S/H DELAY
685      *      D2 <--> A/D CHANNEL COUNTER REGISTER
686      *
687      *#####
688      *
689      *      CALLS FOLLOWING MACROS:
690      *      CONVERT     ''      DELAY
691      *      STPOIN3      TIMER->STPOIN2
692      *      TRP14     ''
693      *
694      *#####
695      *#####
696      *
697      *
698      *      SET ECG, PCG, CAROTID POINTERS AND ISR, COUNTER, PRELOAD
699      *      ADDRESSES. NOTE: INTERRUPTING DEVICE IS THE M6800 TYPE IRQ
700      *      ISR IS AUTOVECTOR 28.
701      *
702      *
703      ADCONV DSPLOPT ADST,ADSTE DISPLAY START OF A/D
703 006126 4BF861EA    LEA ADST,A5
703 00612A 4DF86202    LEA ADSTE,A6
703           TRP14 OUT1CR
703 00612E 1E3C00E3    MOVE.B #OUT1CR,D7
703 006132 4E4E        TRAP #14
704      *
705 006134 21FC0000621C
    0070    MOVE.L #ADCISR,ADEXADD
706           STPOIN3.W ECGstrt,A0,PCGstrt,A1,CARstrt,A2
706 00613C 307C0900    MOVE.W #ECGstrt,A0
706 006140 327C2100    MOVE.W #PCGstrt,A1
706 006144 347C1500    MOVE.W #CARstrt,A2
707      *
708      *
709      *      INITIALIZE TIMER. THE COUNTER IS SET WITH THE SAMPLING PERI
710      *      AND IS DECREMENTED. WHEN THE COUNTER REACHES ZERO, THE ZERO
711      *      DETECT BIT IN THE TSR WILL BE SET. THIS INDICATES THE END O
712      *      A SAMPLING PERIOD.
713      *
714      *
715      *      TIMER A3,A4,ADSMPL,D0
715      *      STPOIN2.L CNTR,A3,CPR,A4
715 006148 267C0001002D MOVE.L #CNTR,A3
715 00614E 287C00010025 MOVE.L #CPR,A4
715 006154 707A    MOVE.L #ADSMPL,D0
715 006156 01CC0000    MOVEP.L D0,0(A4)
715 00615A 13FC0001
    00010035 MOVE.B #1,TSR

```

```

715 006162 13FC0001
    00010021 MOVE.B #STRTIMR,TCR
716   *
717   *
718   * PERFORM A DUMMY WRITE TO INITIATE THE HOLD STATE IN THE
719   * S/H DEVICES. A DELAY IS THEN INCURRED TO ALLOW THE S/H
720   * DEVICES TO ACQUIRE THE SIGNALS.
721   *
722   *
723 00616A 4202 ADCONT CLR.B D2      CLEAR SIGNAL COUNTER
724 00616C 13FC0000
    0002000E MOVE.B #0,HOLD      DUMMY WRITE -- START HOLD STATE
725           DELAY 8,D1      DELAY FOR SAMPLE-HOLD (37 USEC)
725 006174 323C0008 MOVE.W #8,D1
725 006178 51C9FFFE @010 DBRA D1,@010
726   *
727   *
728   * DIGITIZE THE ECG, PCG, CAROTID. A DUMMY WRITE IS PERFORMED
729   * TO TIE THE PROPER MUX INPUT TO THE OUTPUT AND TO START THE
730   * A/D CONVERTER. A WAIT STATE IS THEN ENTERED UNTIL THE
731   * PROCESSOR RECEIVES AN INTERRUPT INDICATING THE END OF
732   * CONVERSION. D2 IS USED AS A SIGNAL COUNTER TO INDICATE WHICH
733   * SIGNAL IS CURRENTLY BEING DIGITIZED.
734   *
735   *
736   CONVERT ADCH1,D2      CONVERT ECG
736 00617C 13FC0000
    00020001 MOVE.B #0,ADCH1
736 006184 4E722300 STOP #$2300
736 006188 06020001 ADDI.B #1,D2
737   *
738   *
739   CONVERT ADCH2,D2      CONVERT CAROTID
739 00618C 13FC0000
    00020003 MOVE.B #0,ADCH2
739 006194 4E722300 STOP #$2300
739 006198 06020001 ADDI.B #1,D2
740   *
741   *
742   CONVERT ADCH3,D2      CONVERT PCG
742 00619C 13FC0000
    00020005 MOVE.B #0,ADCH3
742 0061A4 4E722300 STOP #$2300
742 0061A8 06020001 ADDI.B #1,D2
743   *
744   *
745   * WAIT UNTIL THE SAMPLING PERIOD HAS TERMINATED. WHEN THE ZER
746   * DETECT BIT IN THE TSR EQUALS ONE THE PERIOD IS OVER.
747   *
748   *
749 0061AC 0C390000
    00010035 ADWAIT CMP.B #$0,TSR
750 0061B4 67F6 BEQ ADWAIT
751   *
752   *

```

```

754      *
755      *
756      * AFTER THE PERIOD IS OVER, THE CONTENTS OF THE CPR ARE
757      * TRANSFERRED TO THE CNTR AND THE CNTR STARTS DECREMENTING
758      * AGAIN. RESET THE TSR BY WRITING A $1 TO THE REGISTER. THEN
759      * DETERMINE WHETHER 1.5 SECONDS OF DATA HAS BEEN ACQUIRED. IF
760      * ALL THE DATA HAS NOT YET BEEN ACQUIRED CONTINUE WITH THIS S
761      *
762      *
763 0061B6 13FC0001      MOVE.B #1,TSR          RESET TSR
764 0061BE B0FC1500      CMP.W #ECGEND,A0
765 0061C2 6FA6      BLE ADCONT        DETERMINE IF ALL DATA ACQUIRED
766 0061C4 13FC0000      MOVE.B #HLTMR,TCR      HALT TIMER USING TCR HALT CODE
767      *
768      *
769      * CLEAR MOST SIGNIFICANT NIBBLE IN EACH WORD. THE RANGE OF
770      * VALUES IS: -2.5V = 0000; 0.0V = 0800; 2.5V = 0FFF.
771      *
772      *
773 0061CC 307C0900      MOVE.W #ECGSTRT,A0
774 0061D0 02580FFF      ADCNVRT ANDI.W #$0FFF,(A0)+  CLEAR MOST SIGNIFICANT NIB
775 0061D4 B0FC2D00      CMPI.W #PCGEND,A0
776 0061D8 6FF6      BLE.S ADCNVRT
777      *
778      DSPLOPT ADFIN,ADFINE      DISPLAY END OF A/D
778 0061DA 4BF86204      LEA ADFIN,A5
778 0061DE 4DF8621A      LEA ADFINE,A6
778      TRP14 OUT1CR
778 0061E2 1E3C00E3      MOVE.B #OUT1CR,D7
778 0061E6 4E4E      TRAP #14
779      *
780 0061E8 4E75      RTS
781 0061EA 53      ADST DC.W 'START OF A/D CONVERSION'
782 006202 20      ADSTE DC.W '
783 006204 45      ADFIN DC.W 'END OF A/D CONVERSION'
784 00621A 20      ADFINE DC.W '
785      *
786      *

```

```

788 *#####
789 *      A/D INTERRUPT SERVICE ROUTINE
790 *      APU INTERRUPT SERVICE ROUTINE
791 *#####
792 *
793 *      A0 <--> ECG POINTER
794 *      A1 <--> PCG POINTER
795 *      A2 <--> CAROTID POINTER
796 *
797 *#####
798 *
799 *
800 *      THIS ISR SERVICES THE INTERRUPT CAUSED BY THE END OF CONVER-
801 * SION SIGNAL FROM THE A/D CONVERTER. THE SAMPLE VALUE IS REA-
802 * FROM THE A/D BUFFER, THEN STORED IN SYSTEM RAM. THE S/R ALSO
803 * KEEPS TRACK OF WHICH SIGNAL IS BEING DIGITIZED AND INCREMENT-
804 * THE ECG,PCG,CAROTID POINTERS. ECG=SIGNAL#0, PCG=SIGNAL#1,
805 * CAROTID=SIGNAL#2.
806 *
807 *
808 00621C 0C020000 ADCISR CMPI.B #0,D2
809 006220 6E08 BGT.S AD1
810 006222 30F90002000C MOVE.W ADREAD,(A0)+      STORE ECG DATA AND INCREMENT
811 006228 6014 BRA.S ADEND
812 00622A 0C020001 AD1 CMPI.B #1,D2
813 00622E 6E08 BGT.S AD2
814 006230 32F90002000C MOVE.W ADREAD,(A1)+      STORE PCG DATA AND INCREMENT
815 006236 6006 BRA.S ADEND
816 006238 34F90002000C AD2 MOVE.W ADREAD,(A2)+      STORE CAROTID DATA & INCREME
817 00623E 4E73 ADEND RTE
818 *
819 *      THIS ISR HANDLES THE INTERRUPT RECEIVED FROM THE APU. AN
820 * INTERRUPT ACKNOWLEDGEMENT IS SENT TO THE APU BY WRITING TO
821 * ADDRESS APUEACK.
822 *
823 006240 33FC00FF
     0004000E APISR MOVE.W #$FF,APUEACK DUMMY WRITE-SEND INTERRUPT ACKNOWLE
824 006248 4E73 RTE
825 *
826 *

```

```

828      *#####
829      *#####
830      *
831      *          ECG PROCESSING
832      *
833      *#####
834      *
835      * THE ECG PROCESSING ROUTINE IS COMPRISED OF THE FOLLOWING
836      * MODULES:
837      *
838      * EMOVE: DOWNSAMPLE ECG,CAROTID AND MOVE DATA TO BOTTOM OF
839      * MEMORY.
840      * EDFSQ: DIFFERENTIATE AND SQUARE ECG SIGNAL
841      * ECNVL: CONVOLVE ECG
842      * EQRS: FIND CONSECUTIVE QRS PEAKS
843      *
844      *#####
845      *#####
846      *
847      *
848      * A QRS COMPLEX DETECTION ROUTINE BASED ON A SMOOTHED DIFFEREN
849      * OF THE DIGITIZED ECG SIGNAL IS USED TO DETERMINE THE RR
850      * INTERVAL. WITH X(N) REPRESENTING THE DIGITIZED ECG, THE FIRS
851      * DIFFERENCE IS COMPUTED USING
852      * D(N)=X(N+1)-X(N).
853      * THE FOLLOWING TRANSFORMATION IS THEN APPLIED TO SMOOTH THE
854      * ENERGY OF THE DIFFERENCE SIGNAL
855      *          M    2
856      *          G(N)= E   D (N-K)W(K)
857      *          K=1
858      * WHERE W(K) IS A WEIGHTING SEQUENCE WHICH SELECTS A SEGMENT O
859      * D(N) AND M IS THE NUMBER OF SAMPLES IN WINDOW, AND N IS THE
860      * RUNNING INDEX OF THE SIGNAL AND ITS TRANSFORM.
861      *
862      *
863      *
864 00624A 4EB872D4      ECG JSR BLANK
865      DSPLOPT ECST,ECEN
865 00624E 4BF8626E      LEA ECST,A5
865 006252 4DF86294      LEA ECEN,A6
865      TRP14 OUT1CR
865 006256 1E3C00E3      MOVE.B #OUT1CR,D7
865 00625A 4E4E      TRAP #14
866 00625C 4EB86296      JSR EMOVE
867 006260 4EB862D4      JSR EDFSQ
868 006264 4EB862F2      JSR ECNVL
869 006268 4EB86314      JSR EQRS
870 00626C 4E75      RTS
871 00626E 45      ECST DC.W 'ECG PROCESSING - QRS COMPLEX DETECTION'
872 006294 20      ECEN DC.W ''
873      *
874      *

```

```

876 ****
877 *
878 *
879 * EMOVE
880 ****
881 *
882 * A0 <--> SIGNAL POINTER
883 * A1 <--> END OF SIGNAL DATA
884 * A2 <--> NEW SIGNAL POINTER
885 *
886 ****
887 *
888 * CALL FOLLOWING MACROS:
889 DATAMV->STPOIN2 ''
890 *
891 ****
892 *
893 *
894 * THIS MODULE DOWNSAMPLES THE ECG AND CAROTID BY 4 TO GIVE AN
895 * EFFECTIVE SAMPLING RATE OF 256 Hz. ALL DATA INCLUDING THE P
896 * ARE THEN RELOCATED TO THE BOTTOM OF USER MEMORY.
897 *
898 *
899 EMOVE DATAMV ECGSTRT,A0,ECGEND,A1,ECGSNEW,ECGENEW,A2,ECGDWN
899 STPOIN2 ECGSTRT,A0,ECGEND,A1
899 006296 307C0900 MOVE #ECGSTRT,A0
899 00629A 327C1500 MOVE #ECGEND,A1
899 00000900 ECGSTRT SET ECGSNEW
899 00000C00 ECGEND SET ECGENEW
899 00629E 347C0900 MOVE.W #ECGSTRT,A2
899 0062A2 34D0 @016 MOVE.W (A0),(A2)+ MOVE DATA
899 0062A4 5048 ADD.W #ECGDWN,A0
899 0062A6 B0C9 CMP.W A1,A0
899 0062A8 6DF8 BLT.S @016
900 DATAMV CARSTRT,A0,CARENDA1,CARSNEW,CARENEW,A2,CARDWN
900 STPOIN2 CARSTRT,A0,CARENDA1
900 0062AA 307C1500 MOVE #CARSTRT,A0
900 0062AE 327C2100 MOVE #CARENDA1
900 00000C00 CARSTRT SET CARSNEW
900 00000F00 CAREND SET CARENEW
900 0062B2 347C0C00 MOVE.W #CARSTRT,A2
900 0062B6 34D0 @017 MOVE.W (A0),(A2)+ MOVE DATA
900 0062B8 5048 ADD.W #CARDWN,A0
900 0062BA B0C9 CMP.W A1,A0
900 0062BC 6DF8 BLT.S @017
901 DATAMV PCGSTRT,A0,PCGEND,A1,PCGSNEW,PCGENEW,A2,PCGDWN
901 STPOIN2 PCGSTRT,A0,PCGEND,A1
901 0062BE 307C2100 MOVE #PCGSTRT,A0
901 0062C2 327C2D00 MOVE #PCGEND,A1
901 00000F00 PCGSTRT SET PCGSNEW
901 00001B00 PCGEND SET PCGENEW
901 0062C6 347C0F00 MOVE.W #PCGSTRT,A2
901 0062CA 34D0 @018 MOVE.W (A0),(A2)+ MOVE DATA
901 0062CC 5448 ADD.W #PCGDWN,A0
901 0062CE B0C9 CMP.W A1,A0
901 0062D0 6DF8 BLT.S @018
902 0062D2 4E75 RTS
903 *
904 *

```

```

906 ****
907 * EDF SQU ****
908 ****
909 * A0 <--> ECG POINTER
910 * A1 <--> TRANSFORMED ECG POINTER
911 * D0 <--> N
912 * D1 <--> X(N+1)-X(N)
913 * D2 <--> X(N+1)-X(N)**2
914 ****
915 * CALLS FOLLOWING MACROS:
916 * STPOIN2 SQUARE
917 ****
918 *
919 * TAKE FIRST DIFFERENCE OF DIGITIZED ECG SIGNAL AND SQUARE.
920 *
921 EDF SQU STPOIN2 ECGSTRT,A0,TRECGST,A1
921 0062D4 307C0900 MOVE #ECGSTRT,A0
921 0062D8 327C1B00 MOVE #TRECGST,A1
922 0062DC 4299 CLR.L (A1)+ SET 1ST TRANSFORMED ECG SAMPLE TO 0
923 0062DE 3018 EDF SQ MOVE.W (A0)+,D0
924 0062E0 3210 MOVE.W (A0),D1
925 0062E2 9240 SUB.W D0,D1
926 * SQUARE D1,D2,A1
926 0062E4 3401 MOVE.W D1,D2
926 0062E6 C5C1 MULS.W D1,D2
926 0062E8 22C2 MOVE.L D2,(A1)+ MOVE DATA
927 0062EA B0FC0C00 CMP.W #ECGEND,A0
928 0062EE 6DEE BLT.S EDF SQ CONTINUE TIL ALL SAMPLES TRANSFORM
929 0062F0 4E75 RTS
930 *
931 ****
932 * ECNVL ****
933 ****
934 * A0 <--> TRANSFORMED ECG START
935 * A1 <--> TRANSFORMED ECG END
936 * D0 <--> CONVOLVE WINDOW WIDTH
937 * A1 <--> TEMPORARY STORGE POINTER
938 ****
939 * CALLS FOLLOWING MACROS: SUBROUTINES:
940 * CALLCNVL TEMPMOVE CNVLV
941 ****
942 *
943 * CALL CONVOLVE ROUTINE TO SMOOTH TRANSFORMED ECG
944 *
945 ECNVL CALLCNVL TRECGST,ECGCNV,TRECGEN
945 0062F2 307C1B00 MOVE.W #TRECGST,A0
945 0062F6 303C0010 MOVE.W #ECGCNV,D0
945 0062FA 327C20FC MOVE.W #TRECGEN,A1
945 0062FE 4EB8608E JSR CNVLV
946 TEMPMOVE TRECGST,TRECGEN
946 STPOIN2 TRECGST,A0,TMPSTA,A1
946 006302 307C1B00 MOVE #TRECGST,A0
946 006306 327C3700 MOVE #TMPSTA,A1
946 00630A 20D9 @022 MOVE.L (A1)+,(A0)+ MOVE DATA
946 00630C B0FC20FC CMP.W #TRECGEN,A0
946 006310 6DF8 BLT @022
947 006312 4E75 RTS
948 *
949 *

```

```

951 ****
952 *
953 * EQRS
954 *   A0 <--> TRANSFORMED ECG POINTER
955 *   A1 <--> TRANSFORMED ECG SUBPOINTER FOR PEAK DETECT LOOP
956 *   D0 <--> TEMPORARY DATA STORAGE
957 *   D1 <--> MAXIMUM TRANSFORMED ECG VALUE, THEN THRESHOLD
958 *   D2 <--> COUNTER FOR PEAK DETECT LOOP
959 *   D3 <--> NUMBER OF PEAKS DETECTED COUNTER
960 *   D4 <--> PEAK LOCATION COUNTER
961 *   D5 <--> CURRENT TESTING FOR PEAK VALUE
962 *   D6 <--> NUMBER OF SAMPLES TO QRS PEAK #1
963 *   D7 <--> NUMBER OF SAMPLES TO QRS PEAK #2
964 ****
965 * FIRST SET POINTERS. THE PEAK LOCATION COUNTER IS FIRST SET
966 * 36 (BYTES). THIS IS DONE SINCE THE SEARCH FOR THE FIRST QRS
967 * PEAK STARTS AT THE TENTH TRANSFORM SAMPLE. THE QRS PEAK
968 * COUNTER IS SET TO ONE. ONCE THE COUNTER REACHES -1 BOTH QRS
969 * COMPLEXES HAVE BEEN FOUND.
970 *
971 006314 4281 EQRS CLR.L D1      CLEAR CURRENT MAXIMUM
972 006316 383C0024 MOVE.W #36,D4    COUNTER
973 00631A 163C0001 MOVE.B #1,D3    SET QRS PEAK DOWN COUNTER
974 00631E 307C1B00 MOVE.W #TRECGST,A0  STARTING ADDRESS OF SEARCH FOR MAXI
975 *
976 * THE TRANSFORMED ECG VALUES ARE SCANNED AND A THRESHOLD IS SE
977 * AT THREE QUARTERS THE MAXIMUM VALUE.
978 *
979 006322 B290 EQRS1 CMP.L (A0),D1  COMPARE CURRENT MAXIMUM TO NEW VAL
980 006324 6C02 BGE.S EQRS2          IF (A0)<D1, NO MAXIMUM
981 006326 2210 MOVE.L (A0),D1        D1<(A1) THUS STORE NEW CURRENT MAX
982 006328 5848 EQRS2 ADDQ.W #4,A0
983 000020F0 TRECCHK EQU TRECGEN-12
984 00632A B0FC20F0 CMP.W #TRECCHK,A0
985 00632E 6DF2 BLT.S EQRS1          SEARCH ENTIRE DATA
986 006330 E489 LSR.L #2,D1
987 006332 2001 MOVE.L D1,D0
988 006334 D081 ADD.L D1,D0
989 006336 D081 ADD.L D1,D0      SET THRESHOLD AT 3/4 * MAX
990 *
991 *
992 * THE TRANSFORMED VALUES ARE SCANNED A SECOND TIME. IF THE SAM
993 * VALUE IS BELOW THE THRESHOLD, THE SAMPLE IS THROWN OUT. NOTE
994 * IF THE ENTIRE TRANSFORM HAS BEEN SCANNED WITHOUT THE DETECTI
995 * OF TWO QRS COMPLEXES, AN ERROR MESSAGE IS DISPLAYED. IF THE
996 * SAMPLE VALUE IS GREATER THAN THE THRESHOLD, THEN CHECK FOR A
997 * PEAK, CORRESPONDING TO QRS COMPLEX.
998 *
999 *
1000 006338 307C1B00 MOVE.W #TRECGST,A0  STARTING ADDRESS OF TRANSFORMED ECG
1001 00633C D0FC0024 ADD.W #36,A0      START LOOKING FOR PEAKS AT 10TH LW
1002 006340 5848 EQRS3 ADDQ.W #4,A0      INCREMENT POINTER TO NEXT LONG WORD
1003 006342 B0FC20FC CMP.W #TRECGEN,A0
1004 006346 6E46 BGT.S ECGERR         IF ENTIRE TRANSFORMED ECG BUFFER HA
1005 * BEEN CHECKED W/O 2 PEAKS THEN ERROR
1006 006348 5844 ADDQ.W #4,D4        PEAK LOCATION COUNTER (IN BYTES)
1007 00634A B290 CMP.L (A0),D1        COMPARE (A0) TO THRESHOLD. IF LESS
1008 00634C 6EF2 BGT EQRS3          THEN GO TO NEXT SAMPLE
1009 *
1010 *
1011 * A PEAK IS FOUND BY COMPARING THE SAMPLE VALUE WITH THE TEN

```

1012 * PREVIOUS AND TEN NEXT SAMPLE VALUES. IF THE SAMPLE VALUE IS
 1013 * GREATER THAN THESE TWENTY SAMPLES, A PEAK, CORRESPONDING TO
 1014 * THE END OF THE QRS COMPLEX, HAS BEEN FOUND. THIS IS CONTINUE
 1015 * UNTIL TWO PEAKS ARE FOUND.
 1016 *
 1017 *
 1018 00634E 343C000A MOVE.W #10,D2
 1019 006352 3248 MOVE.W A0,A1
 1020 006354 2A10 MOVE.L (A0),D5
 1021 006356 BAA1 EQRS4 CMP.L -(A1),D5
 1022 006358 6DE6 BLT EQRS3
 1023 00635A 51CAFFFA DBRA D2,EQRS4
 1024 *
 1025 *
 1026 00635E 343C000A MOVE.W #10,D2
 1027 006362 3248 MOVE A0,A1
 1028 006364 BA99 EQRS5 CMP.L (A1)+,D5
 1029 006366 6DD8 BLT EQRS3
 1030 006368 51CAFFFA DBRA D2,EQRS5
 1031 *
 1032 *
 1033 * PEAK FOUND! DETERMINE IF BOTH QRS PEAKS HAVE BEEN FOUND.
 1034 * IF NOT, CONTINUE SEARCH FOR NEXT QRS PEAK.
 1035 *
 1036 *
 1037 00636C 3E04 MOVE.W D4,D7
 1038 00636E 04030001 SUBI.B #1,D3
 1039 006372 6D0C BLT.S EQRS6
 1040 006374 3C07 MOVE.W D7,D6
 1041 006376 06440190 ADD.W #400,D4
 1042 00637A D0FC0190 ADD.W #400,A0
 1043 00637E 60C0 BRA EQRS3
 1044 *
 1045 *
 1046 * BOTH QRS PEAKS HAVE BEEN FOUND. THE ECG HAS BEEN DOWNSAMPLED
 1047 * BY FACTOR OF 4. TAKING INTO ACCOUNT THAT THE TRANSFORM
 1048 * IS REPRESENTED BY LONG WORDS (4 BYTES), THE NUMBER OF BYTES
 1049 * TO QRS1 AND QRS2 CAN BE FOUND BY DIVIDING D6,D7 BY 2.
 1050 *
 1051 *
 1052 006380 E24E EQRS6 LSR.W #1,D6
 1053 006382 31C67F00 MOVE.W D6,QRSS1
 1054 * NUMBER OF BYTES TO QRS1 (2 BYTES=1 SAMPLE)
 1055 006386 E24F LSR.W #1,D7
 1056 006388 31C77F02 MOVE.W D7,QRSS2
 1057 * NUMBER OF BYTES TO QRS2 (2 BYTES=1 SAMPLE)
 1058 00638C 4E75 RTS
 1059 ECGERR TRP14 ERROR1
 1059 00638E 1E3C0000 MOVE.B #ERROR1,D7
 1059 006392 4E4E TRAP #14
 1060 * ERROR-TRAP 14
 1061 *

```

1063 ****
1064 * FINDMAX SUBROUTINE
1065 * CALLED BY: CT1T2
1066 ****
1067 * A0 <--> SIGNAL POINTER
1068 * A1 <--> END OF SIGNAL
1069 * D0 <--> CURRENT MAXIMUM
1070 * D1 <--> LOCATION OF MAXIMUM IN BYTES
1071 * D2 <--> COUNTER
1072 ****
1073 * CALLS FOLLOWING MACROS:
1074 * CLDATA3
1075 ****
1076 *
1077 * FINDMAX SUBROUTINE. FINDS MAXIMUM VALUE IN A SET OF DATA
1078 * AND COUNTS THE NUMBER OF BYTES TO THAT MAXIMUM.
1079 *
1080 FINDMAX CLDATA3.L D0,D1,D2
1080 006394 4280 CLR.L D0
1080 006396 4281 CLR.L D1
1080 006398 4282 CLR.L D2
1081 00639A B090 FINDMX CMP.L (A0),D0      COMPARE TRANSFORM VALUE WITH CURRENT
1082 00639C 6C04 BGE.S FMAX      IF MAX>VALUE <--> NO NEW MAX
1083 00639E 2010 MOVE.L (A0),D0      IF VALUE>MAX <--> NEW CURRENT MAX
1084 0063A0 3202 MOVE.W D2,D1      LOCATION OF CURRENT MAX IN BYTES
1085 0063A2 5848 FMAX ADDQ.W #4,A0      INCREMENT SIGNAL POINTER
1086 0063A4 5842 ADDQ.W #4,D2      INCREMENT COUNTER
1087 0063A6 B0C9 CMP.W A1,A0      ALL TRANSFORM VALUES CHECKED?
1088 0063A8 6DF0 BLT FINDMX      IF NOT CONTINUE
1089 0063AA 4E75 RTS
1090 *
1091 *
1092 ****
1093 * TWO'S COMPLEMENT SUBROUTINE
1094 * CALLED BY: C2DFSQ, PTSQU, PFMSYS
1095 ****
1096 * A0 <--> STARTING ADDRESS AND SIGNAL POINTER
1097 * A1 <--> ENDING ADDRESS OF SIGNAL
1098 * D0 <--> SAMPLE VALUE TO BE CONVERTED
1099 ****
1100 *
1101 * CONVERTS 12-BIT NUMBER TO 16-BIT TWO'S COMPLEMENT REPRESENT
1102 *
1103 0063AC 3010 TWOCOMP MOVE.W (A0),D0
1104 0063AE 06400800 ADDI.W #$800,D0
1105 0063B2 0880000C BCLR #12,D0
1106 0063B6 0800000B BTST #11,D0
1107 0063BA 67000006 BEQ TWOCOMA
1108 0063BE 0040F000 OR.W #$F000,D0
1109 0063C2 30C0 TWOCOMA MOVE.W D0,(A0)+      MOVE DATA
1110 0063C4 B0C9 CMP.W A1,A0
1111 0063C6 6FE4 BLE.S TWOCOMP
1112 0063C8 4E75 RTS
1113 *
1114 *

```

```

1116      *#####
1117      *#####
1118      *
1119      *          CAROTID PROCESSING
1120      *
1121      *#####
1122      *
1123      *          THE CAROTID PROCESSING ROUTINE IS COMPRISED OF THE FOLLOWIN
1124      * MODULES:
1125      *
1126      *          C2DFSQ: SECOND DERIVATIVE AND SQUARE CAROTID
1127      *          CCNVL: CONVOLVE CAROTID
1128      *          CT1T2: FIND PEAKS IN CAROTID TRANSFORM CORRESPONDING TO
1129      *          ONSET OF EJECTION AND DICROTIC NOTCH
1130      *          CDCRTC: FIND DICROTIC NOTCH IN CAROTID PULSE
1131      *
1132      *#####
1133      *
1134      *
1135      *          THE DICROTIC NOTCH OF THE CAROTID PULSE IS SEARCHED FOR IN
1136      *          REGION STARTING AT QRS1 (P1 ON CAROTID PULSE) TO A POINT 50
1137      *          MSEC AFTER P1. THE DICROTIC NOTCH IS DEFINED AS THE POINT O
1138      *          MINIMUM PRESSURE OCCURRING IN THE REGION OF THE MAXIMUM SEC
1139      *          DERIVATIVE. A LEAST SQUARES ESTIMATE OF THE SECOND DEIVATIV
1140      *          IS OBTAINED FROM
1141      *           $P(N) = 2Y(N-2)-Y(N-1)-2Y(N)-Y(N+1)+2Y(N+2)$ 
1142      *          WHERE Y(N) IS THE DIGITIZED CAROTID PULSE AND P(N) IS THE
1143      *          SECOND DERIVATIVE EVALUATED AT THE NTH DATA POINT. THE
1144      *          FOLLOWING TRANSFORMATION IS THEN USED TO OBTAIN A SMOOTHED
1145      *          ENERGY CURVE OF THE 2ND DERIVATIVE
1146      *           $S(N) = \sum_{k=1}^M p(N-k)w(k)$ 
1147      *
1148      *
1149      *          WHERE W(K) IS A WINDOW WHICH SELECTS A SEGMENT OF P(N), M I
1150      *          THE NUMBER OF SAMPLES IN WINDOW AND N IS THE RUNNING INDEX
1151      *          THE SIGNAL AND TRANSFORM. THE WINDOW W(K) WAS SELECTED SUCH
1152      *          THAT W(K)=(M-K+1).
1153      *
1154      *
1155 0063CA 4EB872D4      CAR JSR BLANK
1156          DSPLOPT CAST,CAEN
1156 0063CE 4BF863EE      LEA CAST,A5
1156 0063D2 4DF8641C      LEA CAEN,A6
1156          TRP14 OUT1CR
1156 0063D6 1E3C00E3      MOVE.B #OUT1CR,D7
1156 0063DA 4E4E          TRAP #14
1157 0063DC 4EB8641E      JSR C2DFSQ
1158 0063E0 4EB86470      JSR CCNVL
1159 0063E4 4EB864A0      JSR CT1T2
1160 0063E8 4EB864CA      JSR CDCRTC
1161 0063EC 4E75          RTS
1162 0063EE 43          CAST DC.W 'CAROTID PROCESSING - DICROTIC NOTCH DETECTION'
1163 00641C 20          CAEN DC.W ''
1164      *
1165      *

```

```

1167 ****
1168 *
1169 *
1170 *
1171 ****
1172 * A0 <--> TRANSFORMED CAROTID POINTER
1173 * A1 <--> START OF CAROTID PULSE CORRESPONDING TO QRS1
1174 * A2 <--> SUBPOINTER IN CALCULATION OF SECOND DIFFERENCE
1175 * A3 <--> END OF TRANSFORMED CAROTID PULSE
1176 * D1 <--> TEMPORARY DATA REGISTER
1177 * D2 <--> TEMPORARY DATA REGISTER
1178 ****
1179 * CALL THE FOLLOWING MACROS:      SUBROUTINES:
1180 *          GETADD      STPOIN2      TWOCOMP
1181 *          SQUARE
1182 ****
1183 * TAKE SECOND DIFFERENCE OF CAROTID PULSE, SQUARE TRANSFORMED
1184 * VALUES IN A REGION STARTING AT QRS1 AND CONTAINING 500 MSEC
1185 * OF DATA.
1186 *
1187 00641E 307C0C00 C2DFSQ MOVE.W #CARSTRT,A0
1188 006422 327C0F00 MOVE.W #CARENDE,A1
1189 006426 4EB863AC JSR TWOCOMP      CONVERT CAROTID TO TWOS COMPLEMENT
1190 00642A 307C2100 MOVE #TRCARST,A0
1190 00642E 367C2300 MOVE #TRCAREN,A3
1191          GETADD QRS1,A1,CARSTRT
1191 006432 32787F00 MOVE.W QRS1,A1
1191 006436 D2FC0C00 ADD.W #CARSTRT,A1
1192 00643A 4298 CLR.L (A0)+      CLEAR REGISTER
1193 00643C 4298 CLR.L (A0)+      FIRST TWO LOCATIONS ARE ZERO
1194 00643E 4293 CLR.L (A3)
1195 006440 42A3 CLR.L -(A3)
1196 006442 42A3 CLR.L -(A3)      LAST TWO LOCATIONS ARE ZERO
1197 006444 3449 C2DFSQ1 MOVE A1,A2      USE A2 AS SUBPOINTER
1198 006446 5449 ADDQ.W #2,A1      INCREMENT CAROTID POINTER
1199 006448 321A MOVE.W (A2)+,D1
1200 00644A 5C4A ADDQ.W #6,A2
1201 00644C E349 LSL.W #1,D1      COMPUTE 2 * Y(N-2)
1202 00644E 925A SUB.W (A2)+,D1      - Y(N-1)
1203 006450 5C4A ADDQ.W #6,A2
1204 006452 341A MOVE.W (A2)+,D2
1205 006454 5C4A ADDQ.W #6,A2
1206 006456 E34A LSL.W #1,D2
1207 006458 9242 SUB.W D2,D1      -2 * Y(N)
1208 00645A 925A SUB.W (A2)+,D1      - Y(N+1)
1209 00645C 5C4A ADDQ.W #6,A2
1210 00645E 3412 MOVE.W (A2),D2
1211 006460 E34A LSL.W #1,D2
1212 006462 D242 ADD.W D2,D1      + 2 * Y(N+2)
1213          SQUARE D1,D2,A0      P(N)**2
1213 006464 3401 MOVE.W D1,D2
1213 006466 C5C1 MULS.W D1,D2
1213 006468 20C2 MOVE.L D2,(A0)+      MOVE DATA
1214 00646A B0CB CMPA.W A3,A0
1215 00646C 6DD6 BLT C2DFSQ1      CONTINUE UNTIL 500 MSEC OF PULSE
1216 00646E 4E75 RTS
1217 *
1218 *

```

```

1220 ****
1221 *
1222 * CCNVL
1223 *
1224 ****
1225 *
1226 * A0 <--> TRANSFORMED CAROTID START
1227 * A1 <--> TRANSFORMED CAROTID END
1228 * D0 <--> CONVOLVE WINDOW WIDTH
1229 * A1 <--> TEMPORARY MEMORY STORAGE
1230 *
1231 ****
1232 *
1233 * CALLS FOLLOWING MACROS:
1234 * CALLCNVL
1235 * TEMPMOVE
1236 *
1237 * CALLS FOLLOWING SUBROUTINES:
1238 * CONVOLVE
1239 *
1240 ****
1241 *
1242 *
1243 * CALL CONVOLVE ROUTINE TO SMOOTH TRANSFORMED CAROTID
1244 *
1245 CCNVL CALLCNVL TRCARST,CARCNV,TRCAREN
1245 006470 307C2100 MOVE.W #TRCARST,A0
1245 006474 303C0010 MOVE.W #CARCNV,D0
1245 006478 327C2300 MOVE.W #TRCAREN,A1
1245 00647C 4EB8608E JSR CNVLV
1246 *
1247 *
1248 TEMPMOVE TRCARST,TRCAREN
1248 STPOIN2 TRCARST,A0,TMPSTA,A1
1248 006480 307C2100 MOVE #TRCARST,A0
1248 006484 327C3700 MOVE #TMPSTA,A1
1248 006488 20D9 @030 MOVE.L (A1)+,(A0)+ MOVE DATA
1248 00648A B0FC2300 CMP.W #TRCAREN,A0
1248 00648E 6DF8 BLT @030
1249 *
1250 * CONVERT CAROTID SAMPLES BACK TO 12-BIT REPRESENTATION FOR
1251 * DAC ROUTINES
1252 *
1253 006490 307C0C00 MOVE.W #CARSTRT,A0
1254 006494 06580800 CCNVLA ADD.W #$800,(A0)+ CONVERT TO 12-BIT
1255 006498 B0FC0F00 CMPI.W #CAREND,A0
1256 00649C 6FF6 BLE.S CCNVLA
1257 00649E 4E75 RTS
1258 *
1259 *

```

```

1261 ****
1262 *
1263 *
1264 CT1T2
1265 *
1266 *
1267 *      A0 <--> TRANSFORMED CAROTID POINTER
1268 *      A1 <--> END OF TRANSFORM
1269 *      D0 <--> CURRENT MAXIMUM
1270 *      D1 <--> OUPEAK, DNPEAK (T1 & T2)
1271 *      D2 <--> COUNTER
1272 *
1273 ****
1274 *
1275 *      CALLS FOLLOWING MACROS:
1276 *      GETADD    STPOIN2
1277 *
1278 *      CALLS FOLLOWING SUBROUTINES:
1279 *      FINDMAX
1280 *
1281 ****
1282 *
1283 *
1284 *      FIND PEAK IN CAROTID TRANSFORM CORRESPONDING TO ONSET
1285 *      OF EJECTION AND DICROTIC NOTCH, I.E., T1 & T2.
1286 *
1287 *
1288 CT1T2 STPOIN2 TRCARST,A0,TRCAREN,A1
1288 0064A0 307C2100 MOVE #TRCARST,A0
1288 0064A4 327C2300 MOVE #TRCAREN,A1
1289 0064A8 4EB86394 JSR FINDMAX      FIND MAXIMUM VALUE IN TRANSFORMED CARO
1290 *
1291 *      THE MAXIMUM IN THE CAROTID TRANSFORM CORRESPONDS TO THE ONS
1292 *      OF EJECTION. SET A POINTER TO A POINT 150 MSEC (39 SAMPLES
1293 *      150 BYTES) AHEAD OF T1. THEN SEARCH FOR T2 IN THE AREA FROM
1294 *      THIS POINT TO THE END OF THE TRANSFORMED CAROTID.
1295 *
1296 *      D3 CONTAINS NUMBER OF BYTES TO A POINT
1297 *      GETADD D1,D3,T1TOT2 200 MSEC (T1TOT2) AFTER T1.
1297 0064AC 3601 MOVE.W D1,D3
1297 0064AE 06430098 ADD.W #T1TOT2,D3
1298 *      GETADD D3,A0,TRCARST  POINTER FOR SEARCH OF T1
1298 0064B2 3043 MOVE.W D3,A0
1298 0064B4 D0FC2100 ADD.W #TRCARST,A0
1299 0064B8 4EB86394 JSR FINDMAX
1300 0064BC D243 ADD.W D3,D1          BYTES FROM P1 TO T2
1301 0064BE E249 LSR.W #1,D1        DIVIDE BY 2 TO CONVERT LW TO W
1302 0064C0 D2787F00 ADD.W QRS1,D1
1303 0064C4 31C17F04 MOVE.W D1,T2PEAK   BYTES TO T2 FROM BEGINNING OF C
1304 0064C8 4E75 RTS
1305 *
1306 *

```

```

1308 ****
1309 *
1310 *
1311 CDCRTC
1312 *
1313 ****
1314 * A0 <--> CAROTID POINTER STARTING 10 SAMPLES BEFORE T2
1315 * A1 <--> POINT 10 SAMPLES AFTER T2
1316 * D0 <--> CURRENT MINIMUM
1317 * D5 <--> START OF S2
1318 *
1319 ****
1320 *
1321 * CALLS FOLLOWING MACROS:
1322 GETADD ''
1323 *
1324 ****
1325 *
1326 *
1327 * DEFINE A REGION ON THE CAROTID PULSE CORRESPONDING TO +_ 10
1328 * SAMPLES OF THE T2 PEAK. IN THIS REGION SEARCH FOR A LOCAL
1329 * MINIMUM CORRESPONDING TO THE ACTUAL DICROTIC NOTCH
1330 *
1331 *
1332 CDCRTC GETADD T2PEAK,A0,CARSTR
1332 0064CA 30787F04 MOVE.W T2PEAK,A0
1332 0064CE D0FC0C00 ADD.W #CARSTR,A0
1333 0064D2 90FC0014 SUBA.W #20,A0 POINT 10 SAMPLES BEFORE T2 ON CAROTID
1334 GETADD T2PEAK,A1,CARSTR
1334 0064D6 32787F04 MOVE.W T2PEAK,A1
1334 0064DA D2FC0C00 ADD.W #CARSTR,A1
1335 0064DE D2FC0014 ADD.W #20,A1 POINT 10 SAMPLES AFTER T2 ON CAROTID
1336 *
1337 0064E2 303C7FFF MOVE.W #$7FFF,D0 CURRENT MINIMUM VALUE
1338 0064E6 B050 CDCRTC1 CMP.W (A0),D0 COMPARE PULSE VALUE WITH CURRENT MINI
1339 0064E8 6D000006 BLT CDCRTC2 IF VALUE>MIN, THEN NO CURRENT MINIMUM
1340 0064EC 3010 MOVE.W (A0),D0 IF MIN>VALUE, THEN A NEW MINIMUM
1341 0064EE 3A08 MOVE.W A0,D5 LOCATION OF CURRENT MINIMUM
1342 0064F0 5448 CDCRTC2 ADDQ.W #2,A0 INCREMENT PULSE POINTER
1343 0064F2 B0C9 CMP.W A1,A0 CHECK ALL 10 SAMPLES FOR MINIMUM
1344 0064F4 6DF0 BLT CDCRTC1
1345 0064F6 04450C00 SUB.W #CARSTR,D5 SUBTRACT CARST TO GET NUMBER O
1346 * DICROTIC NOTCH IN CAROTID PULSE
1347 0064FA 31C57F06 MOVE.W D5,DCRTC
1348 0064FE 0445001B SUB.W #DS2DEL,D5 SUBTRACT DELAY TO GET START OF S2
1349 006502 9A787F00 SUB.W QRS1,D5 CALCULATE NUMBER OF BYTES BEWTEEN QRS
1350 * AND START OF S2
1351 006506 E54D LSL.W #2,D5 MULTIPLY BY 4 (PCG SAMPLED AT RATE 4
1352 * CAROTID
1353 006508 31C57F0C MOVE.W D5,PCGS2 NUMBER OF BYTES BETWEEN S1 AND S2
1354 00650C 4E75 RTS
1355 *
1356 *

```

```

1358 ****
1359 * ENERGY DISTRIBUTION COEFFICIENT COMPUTATION S/R
1360 ****
1361 * A0 <--> START OF SEGMENT
1362 * A1 <--> END OF SEGMENT
1363 * D3,D2 <--> EDC DENOMINATOR
1364 * D1,D0 <--> EDC NUMERATOR
1365 * D5,D6,D7 <--> TEMP DATA REGISTERS FOR MULTIPLICATION
1366 ****
1367 * CALLS FOLLOWING MACROS: SUBROUTINES:
1368 * CLDATA8 ML3216 DVD6464
1369 ****
1370 *
1371 * COMPUTE ENERGY DISTRIBUTION COEFFICIENT. PERFORM PRECORRECTI
1372 * ON EDC BY MULTIPLYING BY 1024.
1373 *
1374 EDC CLDATA8.L
1374 00650E 4280 CLR.L D0
1374 006510 4281 CLR.L D1
1374 006512 4282 CLR.L D2
1374 006514 4283 CLR.L D3
1374 006516 4284 CLR.L D4
1374 006518 4285 CLR.L D5
1374 00651A 4286 CLR.L D6
1374 00651C 4287 CLR.L D7
1375 00651E 42B87F12 CLR.L SEQNUM
1376 006522 2818 EDC1 MOVE.L (A0)+,D4
1377 006524 D484 ADD.L D4,D2
1378 006526 D787 ADDX.L D7,D3 EDC DENOMINATOR
1379 006526 SEQNUM,D4,D5,D6,D7 E(N)*H(N)
1379 006528 4286 CLR.L D6
1379 00652A 3A04 MOVE.W D4,D5
1379 00652C CAF87F12 MULU.W SEQNUM,D5
1379 006530 4844 SWAP D4
1379 006532 C8F87F12 MULU.W SEQNUM,D4
1379 006536 1E3C000F MOVE.B #15,D7
1379 00653A E38C @037 LSL.L #1,D4
1379 00653C E396 ROXL.L #1,D6
1379 00653E 51CFFFFA DBRA D7,@037
1379 006542 D885 ADD.L D5,D4
1379 006544 4287 CLR.L D7
1379 006546 DD87 ADDX.L D7,D6
1380 006548 D084 ADD.L D4,D0
1381 00654A D386 ADDX.L D6,D1. EDC NUMERATOR
1382 00654C 067800017F12 ADDI.W #1,SEQNUM INCREMENT SEQUENCE
1383 006552 B0C9 CMPA.W A1,A0
1384 006554 6DCC BLT EDC1
1385 006556 4EB86564 JSR DVD6464
1386 00655A 20387F44 MOVE.L QUOT,D0
1387 00655E EB88 LSL.L #5,D0
1388 006560 EB88 LSL.L #5,D0 MULTIPLY BY 1024 (PRE-EDC CORRECTI
1389 006562 4E75 RTS
1390 *
1391 *

```

```

1393 ****
1394 *
1395 ***** DVD6464 ****
1396 * D1,D0 <--> DIVIDEND
1397 * D3,D2 <--> DIVISOR
1398 * D5,D4;D7,D6 <--> PARTIAL DIVIDEND; TEMP PART DIVIDEND
1399 ****
1400 * THIS ROUTINE PERFORMS 16 BIT BY 16 BIT DIVISION. RESULT IS 3
1401 * BIT QUOTIENT.
1402 *
1403 006564 42B87F44 DVD6464 CLR.L QUOT CLEAR QUOTIENT
1404 006568 4284 CLR.L D4
1405 00656A 4285 CLR.L D5
1406 00656C 11FC00407F48 MOVE.B #64,COUNTER NUMBER OF BYTES IN DIVIDEND
1407 006572 E388 D6464A LSL.L #1,0
1408 006574 E391 ROXL.L #1,D1
1409 006576 E394 ROXL.L #1,D4
1410 006578 E395 ROXL.L #1,D5
1411 00657A 2E387F44 MOVE.L QUOT,D7 SHIFT DIVIDEND INTO PARTIAL DIVIDEN
1412 00657E E38F LSL.L #1,D7 SHIFT QUOTIENT
1413 006580 21C77F44 MOVE.L D7,QUOT
1414 006584 2C04 MOVE.L D4,D6
1415 006586 2E05 MOVE.L D5,D7
1416 006588 9C82 SUB.L D2,D6
1417 00658A 9F83 SUBX.L D3,D7
1418 00658C 6D00000A BLT D6464B
1419 006590 2806 MOVE.L D6,D4
1420 006592 2A07 MOVE.L D7,D5 SAVE NEW PARTIAL DIVIDEND
1421 006594 52B87F44 ADDQ.L #1,QUOT INCREMENT QUOTIENT
1422 006598 53387F48 D6464B SUBQ.B #1,COUNTER DECREMENT COUNTER
1423 00659C 66D4 BNE D6464A
1424 00659E 4E75 RTS
1425 *
1426 *

```

```

1428      *#####
1429      *#####
1430      *
1431      *          PCG PROCESSING - TIME DOMAIN
1432      *
1433      *#####
1434      *
1435      *          THE PCG PROCESSING ROUTINE IS COMPRISED OF THE FOLLOWING
1436      *          MODULES:
1437      *
1438      *          PTSQU:   SQUARE PCG SAMPLES TO OBTAIN PCG ENERGY CURVE
1439      *          PTCNVS:  SMOOTH SYSTOLIC PCG ENERGY CURVE
1440      *          PTCNVD:  SMOOTH DIASTOLIC PCG ENERGY CURVE
1441      *          PTEDC:   COMPUTE PCG SYSTOLIC AND DIASTOLIC EDC
1442      *
1443      *#####
1444      *#####
1445      *
1446      *
1447 0065A0 4EB872D4      PCGT JSR BLANK
1448          DSPLOPT PCST,PCEN
1448 0065A4 4BF865EE      LEA PCST,A5
1448 0065A8 4DF8660A      LEA PCEN,A6
1448          TRP14 OUT1CR
1448 0065AC 1E3C00E3      MOVE.B #OUT1CR,D7
1448 0065B0 4E4E          TRAP #14
1449 0065B2 4EB86660      JSR PTSQU
1450          DSPLOPT PCSST,PCSEN
1450 0065B6 4BF8660C      LEA PCSST,A5
1450 0065BA 4DF86626      LEA PCSEN,A6
1450          TRP14 OUT1CR
1450 0065BE 1E3C00E3      MOVE.B #OUT1CR,D7
1450 0065C2 4E4E          TRAP #14
1451 0065C4 4EB866AE      JSR PTCNVS
1452          DSPLOPT PCDST,PCDEN
1452 0065C8 4BF86628      LEA PCDST,A5
1452 0065CC 4DF86644      LEA PCDEN,A6
1452          TRP14 OUT1CR
1452 0065D0 1E3C00E3      MOVE.B #OUT1CR,D7
1452 0065D4 4E4E          TRAP #14
1453 0065D6 4EB866DC      JSR PTCNVD
1454          DSPLOPT PCEST,PCEEN
1454 0065DA 4BF86646      LEA PCEST,A5
1454 0065DE 4DF8665E      LEA PCEEN,A6
1454          TRP14 OUT1CR
1454 0065E2 1E3C00E3      MOVE.B #OUT1CR,D7
1454 0065E6 4E4E          TRAP #14
1455 0065E8 4EB866FE      JSR PTEDC
1456 0065EC 4E75          RTS
1457 0065EE 50          PCST DC.W 'PCG PROCESSING - TIME DOMAIN'
1458 00660A 20          PCEN DC.W ' '
1459 00660C 20          PCSST DC.W ' ' ' SYSTOLIC ENERGY CURVE'
1460 006626 20          PCSEN DC.W ' ' ' DIASTOLIC ENERGY CURVE'
1461 006628 20          PCDST DC.W ' ' ' COMPUTE EDC VALUES'
1462 006644 20          PCDEN DC.W ' ' '
1463 006646 20          PCEST DC.W ' ' '
1464 00665E 20          PCEEN DC.W ' ' '
1465      *
1466      *

```

```

1468 ****
1469      * PTSQU
1470 ****
1471      * A0 <--> PCG POINTER STARTING AT QRS1
1472      * A2 <--> PCG ENERGY CURVE POINTER
1473      * A1 <--> PCG END CORRESPONDING TO QRS2
1474      * D0 <--> X(N)
1475      * D1 <--> X(N)**2
1476 ****
1477      * CALLS FOLLOWING MACROS:
1478      * GETADD ' ' ' SQUARE
1479 ****
1480      *
1481      * SQUARE ENTIRE PCG SIGNAL TO GET ENERGY CURVE OF SIGNAL. USE
1482      * TWO'S COMPLEMENT REPRESENTATION. OBTAIN START AND END OF ON
1483      * CYCLE OF PCCG CORRESPONDING TO QRS1 AND QRS2.
1484      *
1485      *
1486 006660 30387F00    PTSQU MOVE.W QRS1,D0
1487 006664 E548 LSL.W #2,D0
1488 006666 31C07F08    MOVE.W D0,PCGS1A
1489 00666A 30387F02    MOVE.W QRS2,D0
1490 00666E E548 LSL.W #2,D0
1491 006670 31C07F0A    MOVE.W D0,PCGS1B      FIND START AND END OF PCG CYCLE
1492      * CORRESPNDING TO QRS1 AND QRS2. TAKE
1493      * INTO ACCOUNT PCG SAMPLING RATE.
1494      GETADD PCGS1A,A0,PCGSTRT
1494 006674 30787F08    MOVE.W PCGS1A,A0
1494 006678 D0FC0F00    ADD.W #PCGSTRT,A0
1495      GETADD PCGS1B,A1,PCGSTRT
1495 00667C 32787F0A    MOVE.W PCGS1B,A1
1495 006680 D2FC0F00    ADD.W #PCGSTRT,A1
1496 006684 4EB863AC   JSR TWOCOMP
1497      GETADD PCGS1A,A0,PCGSTRT
1497 006688 30787F08    MOVE.W PCGS1A,A0
1497 00668C D0FC0F00    ADD.W #PCGSTRT,A0
1498      GETADD PCGS1B,A1,PCGSTRT
1498 006690 32787F0A    MOVE.W PCGS1B,A1
1498 006694 D2FC0F00    ADD.W #PCGSTRT,A1
1499 006698 347C2300    MOVE.W #PCGENST,A2 PCG ENERGY CURVE POINTER
1500 00669C 3018 PTSQ1 MOVE.W (A0)+,D0      GET PCG SAMPLE
1501      SQUARE D0,D1,A2
1501 00669E 3200 MOVE.W D0,D1
1501 0066A0 C3C0 MULS.W D0,D1
1501 0066A2 24C1 MOVE.L D1,(A2) +
1502 0066A4 B0C9 CMP.W A1,A0      MOVE DATA
1503 0066A6 6DF4 BLT PTSQ1      CHECK IF ALL VALUES SQUARED
1504 0066A8 31CA7F10    MOVE A2,PCGENDE      IF NOT, CONTINUE WITH THIS ROUTINE
1505 0066AC 4E75 RTS      END OF DIASTOLIC ENERGY CURVE
1506      *
1507      *

```

```

1509 ****
1510 *
1511 PTCNVS
1512 *      A0 <--> START OF SQUARED PCG SIGNAL
1513 *      A1 <--> END OF SYSTOLIC SEGMENT
1514 *      D0 <--> CONVOLVE WINDOW WIDTH
1515 *      A1 <--> TEMPORARY STORAGE POINTER
1516 ****
1517 *      CALLS FOLLOWING MACROS:
1518 *          GETADD      STPOIN2   '
1519 *      CALLS FOLLOWING SUBROUTINES:
1520 *          CNVLV
1521 ****
1522 *      CALL CONVOLVE ROUTINE TO SMOOTH ENERGY CURVE OF SYSTOLIC
1523 *      SEGMENT OF PCG SIGNAL
1524 *
1525     PTCNVS STPOIN2 PCGENST,A0,PCGCNV,D0
1525 0066AE 307C2300 MOVE #PCGENST,A0
1525 0066B2 303C0020 MOVE #PCGCNV,D0
1526 0066B6 32387F0C MOVE.W PCGS2,D1
1527 0066BA E349 LSL.W #1,D1
1528     GETADD D1,A1,PCGENST
1528 0066BC 3241 MOVE.W D1,A1
1528 0066BE D2FC2300 ADD.W #PCGENST,A1
1529 0066C2 31C97F0E MOVE A1,PCENSE END OF SYSTOLIC ENERGY CURVE
1530 0066C6 4EB8608E JSR CNVLV GOTO CONVOLVE SUBROUTINE
1531     STPOIN2 PCGENST,A0,TMPSTA,A1
1531 0066CA 307C2300 MOVE #PCGENST,A0
1531 0066CE 327C3700 MOVE #TMPSTA,A1
1532 0066D2 20D9 PTCS1 MOVE.L (A1)+,(A0)+ MOVE CONVOLVE TEMP TO PCG ENERGY
1533 0066D4 B0F87F0E CMP.W PCGENSE,A0
1534 0066D8 6DF8 BLT PTCS1
1535 0066DA 4E75 RTS
1536 *
1537 ****
1538 *
1539 PTCNVD
1540 *      A0 <--> START OF DIASTOLIC SEGMENT OF PCG SIGNAL
1541 *      A1 <--> END OF DIASTOLIC SEGMENT
1542 *      D0 <--> CONVOLVE WINDOW WIDTH
1543 *      A1 <--> TEMPORARY STORAGE POINTER
1544 ****
1545 *      CALLS FOLLOWING SUBROUTINES:
1546 *          CNVLV
1547 ****
1548 *      CALL CONVOLVE ROUTINE TO SMOOTH ENERGY CURVE OF DIASTOLIC
1549 *      SEGMENT OF PCG SIGNAL
1550 *
1551 0066DC 30787F0E PTCNVD MOVE.W PCGENSE,A0
1552 0066E0 303C0020 MOVE.W #PCGCNV,D0 CONVOLVE WINDOW WIDTH
1553 0066E4 32787F10 MOVE.W PCGENDE,A1 END OF DIASTOLIC SEGMENT
1554 0066E8 4EB8608E JSR CNVLV GOTO CONVOLVE SUBROUTINE
1555 0066EC 30787F0E MOVE.W PCGENSE,A0
1556 0066F0 327C3700 MOVE.W #TMPSTA,A1
1557 0066F4 20D9 PTCD1 MOVE.L (A1)+,(A0)+ MOVE CONVOLVE TEMP TO PCG ENERGY
1558 0066F6 B0F87F10 CMP.W PCGENDE,A0
1559 0066FA 6DF8 BLT PTCD1
1560 0066FC 4E75 RTS
1561 *
1562 *

```

```

1564 ****
1565 * PTEDC
1566 ****
1567 * A0 <--> START OF SEGMENT
1568 * A1 <--> END OF SEGMENT
1569 * D0 <--> EDC - RETURNED FROM EDC S/R
1570 * D2 <--> NUMBER OF SAMPLES IN SEGMENT
1571 ****
1572 * CALLS FOLLOWING SUBROUTINES:
1573 * EDC
1574 ****
1575 *
1576 * COMPUTE EDCTSYS
1577 *
1578 0066FE 307C2300 PTEDC MOVE.W #PCGENST,A0
1579 006702 32787F0E MOVE.W PCGENSE,A1
1580 006706 4EB8650E JSR EDC
1581 *
1582 * SYSTOLIC EDC IN D0. CORRECT THE EDC BY DIVIDING BY THE NUMBE
1583 * OF SAMPLES IN THE SYSTOLIC SEGMENT.
1584 *
1585 00670A 323C2300 MOVE.W #PCGENST,D1
1586 00670E 34387F0E MOVE.W PCGENSE,D2
1587 006712 9441 SUB.W D1,D2
1588 006714 E44A LSR.W #2,D2
1589 006716 80C2 DIVU D2,D0
1590 006718 31C07F16 MOVE.W D0,EDCTSYS
1591 *
1592 * COMPUTE EDCTDIA
1593 *
1594 00671C 30787F0E MOVE.W PCGENSE,A0
1595 006720 32787F10 MOVE.W PCGENDE,A1
1596 006724 4EB8650E JSR EDC
1597 *
1598 * DIASTOLIC EDC IN D0. CORRECT DIASTOLIC EDC BY DIVIDING BY TH
1599 * NUMBER OF SAMPLES IN SEGMENT.
1600 *
1601 006728 32387F0E MOVE.W PCGENSE,D1
1602 00672C 34387F10 MOVE.W PCGENDE,D2
1603 006730 9441 SUB.W D1,D2
1604 006732 E44A LSR.W #2,D2
1605 006734 80C2 DIVU D2,D0
1606 006736 31C07F18 MOVE.W D0,EDCTDIA
1607 *
1608 GETADD PCGS1A,A0,PCGSTRT CONVERT BACK TO 12-BIT NUMBER
1608 00673A 30787F08 MOVE.W PCGS1A,A0
1608 00673E D0FC0F00 ADD.W #PCGSTRT,A0
1609 GETADD PCGS1B,A1,PCGSTRT
1609 006742 32787F0A MOVE.W PCGS1B,A1
1609 006746 D2FC0F00 ADD.W #PCGSTRT,A1
1610 00674A 06580800 PTEDC1 ADD.W #$800,(A0)+ ADD DATA
1611 00674E B0C9 CMP.W A1,A0
1612 006750 6FF8 BLE.S PTEDC1
1613 006752 4E75 RTS
1614 *
1615 *

```

```

1617 ****
1618 * APU/FFT SUBROUTINES
1619 ****
1620 *
1621 * THE FOLLOWING SUBROUTINES ARE USED BY FFT:
1622 *
1623 * CALCW: COMPUTE W=CMPLX(COS(PI/LE1),-SIN(PI/LE1))
1624 * CALCT: COMPUTE T=F(IP)*U
1625 * CALCFIM: COMPUTE IMAGINARY F(IP)=F(I)-T;F(I)=F(I)+T
1626 * CALCFRL: COMPUTE REAL F(IP)=F(I)-T;F(I)=F(I)+T
1627 * CALCU: COMPUTE U=U*W
1628 *
1629 ****
1630 *
1631 * CALLS FOLLOWING MACROS:
1632 * APU APURD APUWR APUWR16
1633 *
1634 ****
1635 *
1636 * COMPUTE W=CMPLX(COS(PI/LE1),-SIN(PI/LE1))
1637 * REAL: WR=COS(PI/LE1)
1638 * IMAG: WI=-SIN(PI/LE1)
1639 *
1640 CALCW APU PUPI PUSH PI ON TO STACK -> TOS
1640 006754 13FC001A
  00050011 MOVE.B #PUPI,APUCOM
1640 00675C 4E722300 STOP #$2300
1641 006760 3C387F2E MOVE.W LE1,D6 MOVE LE1 TO TOS
1642          APUWR16 D6,A0
1642 006764 3E3C0001 MOVE.W #$1,D7
1642 006768 1086 @053 MOVE.B D6,(A0)
1642 00676A E09E ROR.L #$8,D6
1642 00676C 51CFFFFA DBRA D7,@053
1642 006770 E09E ROR.L #$8,D6
1642 006772 E09E ROR.L #$8,D6
1643          APU FLTS CONVERT LE1 TO 32-BIT FLOATING POINT
1643 006774 13FC001D
  00050011 MOVE.B #FLTS,APUCOM
1643 00677C 4E722300 STOP #$2300
1644          APU FDIV PI/LE1 -> TOS
1644 006780 13FC0013
  00050011 MOVE.B #FDIV,APUCOM
1644 006788 4E722300 STOP #$2300
1645          APU PTOD PUSH TOS -> NOS; TOS UNCHANGED
1645 00678C 13FC0037
  00050011 MOVE.B #PTOD,APUCOM
1645 006794 4E722300 STOP #$2300
1646          APU COS COS(PI/LE1) -> TOS
1646 006798 13FC0003
  00050011 MOVE.B #COS,APUCOM
1646 0067A0 4E722300 STOP #$2300
1647          APU XCHD EXCHANGE TOS AND NOS
1647 0067A4 13FC0039
  00050011 MOVE.B #XCHD,APUCOM
1647 0067AC 4E722300 STOP #$2300
1648          APU SIN SIN(PI/LE1) -> TOS
1648 0067B0 13FC0002
  00050011 MOVE.B #SIN,APUCOM
1648 0067B8 4E722300 STOP #$2300
1649          APU CHSF -SIN(PI/LE1) -> TOS
1649 0067BC 13FC0015
  00050011 MOVE.B #CHSF,APUCOM

```

```

1649 0067C4 4E722300      STOP #$2300
1650          APURD A0,D6
1650 0067C8 3E3C0003      MOVE.W #$3,D7
1650 0067CC E19E @061 ROL.L #$8,D6
1650 0067CE 1C10 MOVE.B (A0),D6
1650 0067D0 51CFFFFA      DBRA D7,@061
1651 0067D4 21C67F38      MOVE.L D6,WI
1652          APURD A0,D6
1652 0067D8 3E3C0003      MOVE.W #$3,D7
1652 0067DC E19E @062 ROL.L #$8,D6
1652 0067DE 1C10 MOVE.B (A0),D6
1652 0067E0 51CFFFFA      DBRA D7,@062
1653 0067E4 21C67F34      MOVE.L D6,WR      STORE WR AND WI 32-BIT FL-P VALUES
1654 0067E8 4E75      RTS
1655          *
1656          * COMPUTE T=F(IP)*U:
1657          * REAL: TR=(FR(IP)*UR)-(FI(IP)*UI)
1658          * IMAG: TI=(FI(IP)*UR)+(FR(IP)*UR)
1659          *
1660          CALCT APUSGWR A3,D1,A0      MOVE FI(IP) & FR(IP) TO APU STACK
1660 0067EA 2C331000      MOVE.L 0(A3,D1),D6
1660 0067EE 3E3C0003      MOVE.W #$3,D7
1660 0067F2 1086 @063 MOVE.B D6,(A0)
1660 0067F4 E09E ROR.L #$8,D6
1660 0067F6 51CFFFFA      DBRA D7,@063
1661          APUSGWR A2,D1,A0
1661 0067FA 2C321000      MOVE.L 0(A2,D1),D6
1661 0067FE 3E3C0003      MOVE.W #$3,D7
1661 006802 1086 @064 MOVE.B D6,(A0)
1661 006804 E09E ROR.L #$8,D6
1661 006806 51CFFFFA      DBRA D7,@064
1662          APUWR D2,A0      MOVE UR TO APU STACK
1662 00680A 3E3C0003      MOVE.W #$3,D7
1662 00680E 1082 @065 MOVE.B D2,(A0)
1662 006810 E09A ROR.L #$8,D2
1662 006812 51CFFFFA      DBRA D7,@065
1663          APU FMUL      (FR(IP)*UR) -> TOS
1663 006816 13FC0012      00050011 MOVE.B #FMUL,APUCOM
1663 00681E 4E722300      STOP #$2300
1664          APU XCHD      EXCHANGE TOS AND NOS
1664 006822 13FC0039      00050011 MOVE.B #XCHD,APUCOM
1664 00682A 4E722300      STOP #$2300
1665          APUWR D3,A0      MOVE UI TO APU STACK
1665 00682E 3E3C0003      MOVE.W #$3,D7
1665 006832 1083 @068 MOVE.B D3,(A0)
1665 006834 E09B ROR.L #$8,D3
1665 006836 51CFFFFA      DBRA D7,@068
1666          APU FMUL      (FI(IP)*UI) -> TOS
1666 00683A 13FC0012      00050011 MOVE.B #FMUL,APUCOM
1666 006842 4E722300      STOP #$2300
1667          APU FSUB      (FR(IP)*UR)-(FI(IP)*UI)=TR -> TOS
1667 006846 13FC0011      00050011 MOVE.B #FSUB,APUCOM
1667 00684E 4E722300      STOP #$2300
1668          APUSGWR A3,D1,A0      MOVE FI(IP) & FR(IP) TO APU STACK
1668 006852 2C331000      MOVE.L 0(A3,D1),D6
1668 006856 3E3C0003      MOVE.W #$3,D7
1668 00685A 1086 @071 MOVE.B D6,(A0)

```

```

1668 00685C E09E ROR.L #$8,D6
1668 00685E 51CFFFFA DBRA D7,@071
1669 APUSGWR A2,D1,A0
1669 006862 2C321000 MOVE.L 0(A2,D1),D6
1669 006866 3E3C0003 MOVE.W #$3,D7
1669 00686A 1086 @072 MOVE.B D6,(A0)
1669 00686C E09E ROR.L #$8,D6
1669 00686E 51CFFFFA DBRA D7,@072
1670 APUWR D3,A0 MOVE UI TO APU STACK
1670 006872 3E3C0003 MOVE.W #$3,D7
1670 006876 1083 @073 MOVE.B D3,(A0)
1670 006878 E09B ROR.L #$8,D3
1670 00687A 51CFFFFA DBRA D7,@073
1671 APU FMUL (FR(IP)*UI) -> TOS
1671 00687E 13FC0012
    00050011 MOVE.B #FMUL,APUCOM
1671 006886 4E722300 STOP #$2300
1672 APU XCHD EXCHANGE TOS AND NOS
1672 00688A 13FC0039
    00050011 MOVE.B #XCHD,APUCOM
1672 006892 4E722300 STOP #$2300
1673 APUWR D2,A0 MOVE UR TO APU STACK
1673 006896 3E3C0003 MOVE.W #$3,D7
1673 00689A 1082 @076 MOVE.B D2,(A0)
1673 00689C E09A ROR.L #$8,D2
1673 00689E 51CFFFFA DBRA D7,@076
1674 APU FMUL (FI(IP)*UR) -> TOS
1674 0068A2 13FC0012
    00050011 MOVE.B #FMUL,APUCOM
1674 0068AA 4E722300 STOP #$2300
1675 APU FADD (FR(IP)*UI)+(FI(IP)*UR)=TI -> TOS
1675 0068AE 13FC0010
    00050011 MOVE.B #FADD,APUCOM
1675 0068B6 4E722300 STOP #$2300
1676 0068BA 4E75 RTS
1677 *
    * COMPUTE IMAGINARY PART OF F(IP)=F(I)-T;F(I)=F(I)+T:
1678     * FI(IP)=FI(I)-TI;FI(I)=FI(I)+TI
1679     *
1680     *
1681 CALCFIM APU PTOD PUSH TOS->NOS; TOS UNCHANGED
1681 0068BC 13FC0037
    00050011 MOVE.B #PTOD,APUCOM
1681 0068C4 4E722300 STOP #$2300
1682 APUSGWR A3,D0,A0 MOVE F(I) TO APU STACK
1682 0068C8 2C330000 MOVE.L 0(A3,D0),D6
1682 0068CC 3E3C0003 MOVE.W #$3,D7
1682 0068D0 1086 @080 MOVE.B D6,(A0)
1682 0068D2 E09E ROR.L #$8,D6
1682 0068D4 51CFFFFA DBRA D7,@080
1683 APU XCHD EXCHANGE TOS AND NOS
1683 0068D8 13FC0039
    00050011 MOVE.B #XCHD,APUCOM
1683 0068E0 4E722300 STOP #$2300
1684 APU FSUB FI(I)-TI=FI(IP)
1684 0068E4 13FC0011
    00050011 MOVE.B #FSUB,APUCOM
1684 0068EC 4E722300 STOP #$2300
1685 APU XCHD EXCHANGE TOS AND NOS
1685 0068F0 13FC0039
    00050011 MOVE.B #XCHD,APUCOM
1685 0068F8 4E722300 STOP #$2300

```

```

1686          APUSGWR A3,D0,A0      MOVE F(I) TO APU STACK
1686 0068FC 2C330000  MOVE.L 0(A3,D0),D6
1686 006900 3E3C0003  MOVE.W #$3,D7
1686 006904 1086 @084 MOVE.B D6,(A0)
1686 006906 E09E ROR.L #$8,D6
1686 006908 51CFFFFA DBRA D7,@084
1687          APU FADD             FI(I)+TI=FI(I)
1687 00690C 13FC0010
1687          00050011 MOVE.B #FADD,APUCOM
1687 006914 4E722300 STOP #$2300
1688          APUSGRD A3,D0,A0
1688 006918 3E3C0003  MOVE.W #$3,D7
1688 00691C E19E @086 ROL.L #$8,D6
1688 00691E 1C10 MOVE.B (A0),D6
1688 006920 51CFFFFA DBRA D7,@086
1688 006924 27860000 MOVE.L D6,0(A3,D0)
1689          APUSGRD A3,D1,A0
1689 006928 3E3C0003  MOVE.W #$3,D7
1689 00692C E19E @087 ROL.L #$8,D6
1689 00692E 1C10 MOVE.B (A0),D6
1689 006930 51CFFFFA DBRA D7,@087
1689 006934 27861000 MOVE.L D6,0(A3,D1)
1690 006938 4E75 RTS
1691          *
1692          * COMPUTE REAL PART OF F(IP)=F(I)-T;F(I)=F(I)+T;
1693          * FR(IP)=FR(I)-TR;FR(I)=FR(I)+TR
1694          *
1695          CALCFLR APU PTOD      PUSH TOS->NOS; TOS UNCHANGED
1695 00693A 13FC0037
1695          00050011 MOVE.B #PTOD,APUCOM
1695 006942 4E722300 STOP #$2300
1696          APUSGWR A2,D0,A0      MOVE FR(I) TO APU STACK
1696 006946 2C320000  MOVE.L 0(A2,D0),D6
1696 00694A 3E3C0003  MOVE.W #$3,D7
1696 00694E 1086 @089 MOVE.B D6,(A0)
1696 006950 E09E ROR.L #$8,D6
1696 006952 51CFFFFA DBRA D7,@089
1697          APU XCHD             EXCHANGE TOS AND NOS
1697 006956 13FC0039
1697          00050011 MOVE.B #XCHD,APUCOM
1697 00695E 4E722300 STOP #$2300
1698          APU FSUB             FR(I)-TR=FR(IP)
1698 006962 13FC0011
1698          00050011 MOVE.B #FSUB,APUCOM
1698 00696A 4E722300 STOP #$2300
1699          APU XCHD             EXCHANGE TOS AND NOS
1699 00696E 13FC0039
1699          00050011 MOVE.B #XCHD,APUCOM
1699 006976 4E722300 STOP #$2300
1700          APUSGWR A2,D0,A0      MOVE FR(I) TO APU STACK
1700 00697A 2C320000  MOVE.L 0(A2,D0),D6
1700 00697E 3E3C0003  MOVE.W #$3,D7
1700 006982 1086 @093 MOVE.B D6,(A0)
1700 006984 E09E ROR.L #$8,D6
1700 006986 51CFFFFA DBRA D7,@093
1701          APU FADD             FR(I)+TR=FR(I)
1701 00698A 13FC0010
1701          00050011 MOVE.B #FADD,APUCOM
1701 006992 4E722300 STOP #$2300
1702          APUSGRD A2,D0,A0
1702 006996 3E3C0003  MOVE.W #$3,D7

```

```

1702 00699A E19E @095 ROL.L #$8,D6
1702 00699C 1C10 MOVE.B (A0),D6
1702 00699E 51CFFFFA DBRA D7,@095
1702 0069A2 25860000 MOVE.L D6,0(A2,D0)
1703 APUSGRD A2,D1,A0
1703 0069A6 3E3C0003 MOVE.W #$3,D7
1703 0069AA E19E @096 ROL.L #$8,D6
1703 0069AC 1C10 MOVE.B (A0),D6
1703 0069AE 51CFFFFA DBRA D7,@096
1703 0069B2 25861000 MOVE.L D6,0(A2,D1)
1704 0069B6 4E75 RTS
1705 *
1706 * COMPUTE U=U*W
1707 * REAL: UR=(UR*WR)-(UI*WI)
1708 * IMAG: UI=(UI*WR)+(UR*WI)
1709 *
1710 CALCU APUWR D2,A0 MOVE UI & WI TO APU STACK
1710 0069B8 3E3C0003 MOVE.W #$3,D7
1710 0069BC 1082 @097 MOVE.B D2,(A0)
1710 0069BE E09A ROR.L #$8,D2
1710 0069C0 51CFFFFA DBRA D7,@097
1711 0069C4 2C387F34 MOVE.L WR,D6
1712 APUWR D6,A0
1712 0069C8 3E3C0003 MOVE.W #$3,D7
1712 0069CC 1086 @098 MOVE.B D6,(A0)
1712 0069CE E09E ROR.L #$8,D6
1712 0069D0 51CFFFFA DBRA D7,@098
1713 APU FMUL (UI*WI) -> TOS
1713 0069D4 13FC0012
    00050011 MOVE.B #FMUL,APUCOM
1713 0069DC 4E722300 STOP #$2300
1714 APUWR D3,A0 MOVE UR & WR TO APU STACK
1714 0069E0 3E3C0003 MOVE.W #$3,D7
1714 0069E4 1083 @100 MOVE.B D3,(A0)
1714 0069E6 E09B ROR.L #$8,D3
1714 0069E8 51CFFFFA DBRA D7,@100
1715 0069EC 2C387F38 MOVE.L WI,D6
1716 APUWR D6,A0
1716 0069F0 3E3C0003 MOVE.W #$3,D7
1716 0069F4 1086 @101 MOVE.B D6,(A0)
1716 0069F6 E09E ROR.L #$8,D6
1716 0069F8 51CFFFFA DBRA D7,@101
1717 APU FMUL (UR*WR) -> TOS
1717 0069FC 13FC0012
    00050011 MOVE.B #FMUL,APUCOM
1717 006A04 4E722300 STOP #$2300
1718 APU FSUB (UR*WR)-(UI*WI)=UR->TOS
1718 006A08 13FC0011
    00050011 MOVE.B #FSUB,APUCOM
1718 006A10 4E722300 STOP #$2300
1719 APUWR D3,A0 MOVE UI & WR TO APU STACK
1719 006A14 3E3C0003 MOVE.W #$3,D7
1719 006A18 1083 @104 MOVE.B D3,(A0)
1719 006A1A E09B ROR.L #$8,D3
1719 006A1C 51CFFFFA DBRA D7,@104
1720 006A20 2C387F34 MOVE.L WR,D6
1721 APUWR D6,A0
1721 006A24 3E3C0003 MOVE.W #$3,D7
1721 006A28 1086 @105 MOVE.B D6,(A0)
1721 006A2A E09E ROR.L #$8,D6
1721 006A2C 51CFFFFA DBRA D7,@105

```

```

1722          APU FMUL           (UI*WR) -> TOS
1722 006A30 13FC0012
1722          00050011 MOVE.B #FMUL,APUCOM
1722 006A38 4E722300 STOP #$2300
1723          APUWR D2,A0      MOVE UR & WI TO APU STACK
1723 006A3C 3E3C0003 MOVE.W #$3,D7
1723 006A40 1082 @107 MOVE.B D2,(A0)
1723 006A42 E09A ROR.L #$8,D2
1723 006A44 51CFFFFA DBRA D7,@107
1724 006A48 2C387F38 MOVE.L WI,D6
1725          APUWR D6,A0
1725 006A4C 3E3C0003 MOVE.W #$3,D7
1725 006A50 1086 @108 MOVE.B D6,(A0)
1725 006A52 E09E ROR.L #$8,D6
1725 006A54 51CFFFFA DBRA D7,@108
1726          APU FMUL           (UR*WI) -> TOS
1726 006A58 13FC0012
1726          00050011 MOVE.B #FMUL,APUCOM
1726 006A60 4E722300 STOP #$2300
1727          APU FADD           (UI*WR)+(UR*WI)=UI->TOS
1727 006A64 13FC0010
1727          00050011 MOVE.B #FADD,APUCOM
1727 006A6C 4E722300 STOP #$2300
1728          APURD A0,D3      NEW UR & UI VALUES
1728 006A70 3E3C0003 MOVE.W #$3,D7
1728 006A74 E19B @111 ROL.L #$8,D3
1728 006A76 1610 MOVE.B (A0),D3
1728 006A78 51CFFFFA DBRA D7,@111
1729          APURD A0,D2
1729 006A7C 3E3C0003 MOVE.W #$3,D7
1729 006A80 E19A @112 ROL.L #$8,D2
1729 006A82 1410 MOVE.B (A0),D2
1729 006A84 51CFFFFA DBRA D7,@112
1730 006A88 4E75 RTS

```

```

1732 ****
1733 * FFT SUBROUTINE
1734 ****
1735 * A0 <--> APU OPERAND ADDRESS
1736 * A1 <--> APU COMMAND/STATUS ADDRESS
1737 ****
1738 * CALLS FOLLOWING MACROS: STPOIN2
1739 ****
1740 *
1741 FFT DSPLOPT HAM,HAME
1741 006A8A 4BF86E9C LEA HAM,A5
1741 006A8E 4DF86EB4 LEA HAME,A6
1741 TRP14 OUT1CR
1741 006A92 1E3C00E3 MOVE.B #OUT1CR,D7
1741 006A96 4E4E TRAP #14
1742 STPOIN2.L APUOPER,A0,APUCOM,A1
1742 006A98 207C00050001 MOVE.L #APUOPER,A0
1742 006A9E 227C00050011 MOVE.L #APUCOM,A1
1743 *
1744 * CONVERT VALUES IN REAL AND IMAGINARY ARRAYS FROM 16-BIT
1745 * FIXED POINT TO 32-BIT FLOATING POINT. MULTIPLY SIGNAL
1746 * BY HAMMING WINDOW W(N), WHERE W(N)=.54+.46(COS(2*PI*N/M))
1747 *
1748 STPOIN2.W XRST,A2,XIST,A3 START OF REAL AND IMAGINARY
1748 006AA4 347C3700 MOVE.W #XRST,A2
1748 006AA8 367C4700 MOVE.W #XIST,A3
1749 *
1750 * CONVERT 16-BIT NUMBERS IN REAL AND IMAGINARY ARRAYS
1751 * TO 32-BIT FLOATING POINT
1752 *
1753 006AAC 2012 FFT0 MOVE.L (A2),D0 PUT 16-BIT NUMBER INTO DR
1754 APUWR16 D0,A0 WRITE NUMBER TO STACK
1754 006AAE 3E3C0001 MOVE.W #$1,D7
1754 006AB2 1080 @116 MOVE.B D0,(A0)
1754 006AB4 E098 ROR.L #$8,D0
1754 006AB6 51CFFFFA DBRA D7,@116
1754 006ABA E098 ROR.L #$8,D0
1754 006ABC E098 ROR.L #$8,D0
1755 APU FLTS CONVERT TO FLOATING POINT
1755 006ABE 13FC001D
1755 00050011 MOVE.B #FLTS,APUCOM
1755 006AC6 4E722300 STOP #$2300
1756 APURD A0,D0 READ CONVERTED NUMBER
1756 006ACA 3E3C0003 MOVE.W #$3,D7
1756 006ACE E198 @118 ROL.L #$8,D0
1756 006AD0 1010 MOVE.B (A0),D0
1756 006AD2 51CFFFFA DBRA D7,@118
1757 006AD6 24C0 MOVE.L D0,(A2)+ STORE BACK INTO ARRAY
1758 006AD8 B4FC5700 CMP.W #XIEN,A2
1759 006ADC 6DCE BLT FFT0 CONTINUE UNTIL ENTIRE ARRAYS CONVERTE
1760 *
1761 * MULTIPLY BY HAMMING WINDOW
1762 *
1763 006ADE 2A3C00000400 HAMM MOVE.L #1024,D5 NUMBER OF SAMPLES IN SIGNAL
1764 006AE4 223CFFFFE01 MOVE.L #-511,D1 START OF HAMMING WINDOW
1765 006AEA 263C008A3D70 MOVE.L #HAM54,D3
1766 006AF0 283C7FEB851E MOVE.L #HAM46,D4
1767 APU PUPI
1767 006AF6 13FC001A
1767 00050011 MOVE.B #PUPI,APUCOM
1767 006AFE 4E722300 STOP #$2300

```

```

1768 006B02 7002 MOVE.L #$2,D0
1769          APUWR D0,A0
1769 006B04 3E3C0003 MOVE.W #$3,D7
1769 006B08 1080 @120 MOVE.B D0,(A0)
1769 006B0A E098 ROR.L #$8,D0
1769 006B0C 51CFFFFA DBRA D7,@120
1770          APU FLTD
1770 006B10 13FC001C
    00050011 MOVE.B #FLTD,APUCOM
1770 006B18 4E722300 STOP #$2300
1771          APU FMUL
1771 006B1C 13FC0012
    00050011 MOVE.B #FMUL,APUCOM
1771 006B24 4E722300 STOP #$2300
1772          APUWR D5,A0
1772 006B28 3E3C0003 MOVE.W #$3,D7
1772 006B2C 1085 @123 MOVE.B D5,(A0)
1772 006B2E E09D ROR.L #$8,D5
1772 006B30 51CFFFFA DBRA D7,@123
1773          APU FLTD
1773 006B34 13FC001C
    00050011 MOVE.B #FLTD,APUCOM
1773 006B3C 4E722300 STOP #$2300
1774          APU FDIV
1774 006B40 13FC0013
    00050011 MOVE.B #FDIV,APUCOM
1774 006B48 4E722300 STOP #$2300
1775          APURD A0,D2      D2 = 2*PI/1024
1775 006B4C 3E3C0003 MOVE.W #$3,D7
1775 006B50 E19A @126 ROL.L #$8,D2
1775 006B52 1410 MOVE.B (A0),D2
1775 006B54 51CFFFFA DBRA D7,@126
1776          STPOIN2.W XRST,A2,XREN,A3
1776 006B58 347C3700 MOVE.W #XRST,A2
1776 006B5C 367C4700 MOVE.W #XREN,A3
1777          HAMM1 APUWR D1,A0
1777 006B60 3E3C0003 MOVE.W #$3,D7
1777 006B64 1081 @128 MOVE.B D1,(A0)
1777 006B66 E099 ROR.L #$8,D1
1777 006B68 51CFFFFA DBRA D7,@128
1778          APU FLTD
1778 006B6C 13FC001C
    00050011 MOVE.B #FLTD,APUCOM
1778 006B74 4E722300 STOP #$2300
1779          APUWR D2,A0
1779 006B78 3E3C0003 MOVE.W #$3,D7
1779 006B7C 1082 @130 MOVE.B D2,(A0)
1779 006B7E E09A ROR.L #$8,D2
1779 006B80 51CFFFFA DBRA D7,@130
1780          APU FMUL      2PI/1024 * N
1780 006B84 13FC0012
    00050011 MOVE.B #FMUL,APUCOM
1780 006B8C 4E722300 STOP #$2300
1781          APU COS      COS(2PI*N/1024)
1781 006B90 13FC0003
    00050011 MOVE.B #COS,APUCOM
1781 006B98 4E722300 STOP #$2300
1782          APUWR D4,A0
1782 006B9C 3E3C0003 MOVE.W #$3,D7
1782 006BA0 1084 @133 MOVE.B D4,(A0)
1782 006BA2 E09C ROR.L #$8,D4

```

```

1782 006BA4 51CFFFFA      DBRA D7,@133
1783          APU FMUL           .46COS(2PI*N/1024)
1783 006BA8 13FC0012
    00050011 MOVE.B #FMUL,APUCOM
1783 006BB0 4E722300      STOP #$2300
1784          APUWR D3,A0
1784 006BB4 3E3C0003      MOVE.W #$3,D7
1784 006BB8 1083 @135 MOVE.B D3,(A0)
1784 006BBA E09B ROR.L #$8,D3
1784 006BBC 51CFFFFA      DBRA D7,@135
1785          APU FADD          .54+(.46COS(2PI*N/1024))
1785 006BC0 13FC0010
    00050011 MOVE.B #FADD,APUCOM
1785 006BC8 4E722300      STOP #$2300
1786 006BCC 2012      MOVE.L (A2),D0
1787          APUWR D0,A0
1787 006BCE 3E3C0003      MOVE.W #$3,D7
1787 006BD2 1080 @137 MOVE.B D0,(A0)
1787 006BD4 E098 ROR.L #$8,D0
1787 006BD6 51CFFFFA      DBRA D7,@137
1788          APU FMUL          X(N) * W(N)
1788 006BDA 13FC0012
    00050011 MOVE.B #FMUL,APUCOM
1788 006BE2 4E722300      STOP #$2300
1789          APURD A0,D0
1789 006BE6 3E3C0003      MOVE.W #$3,D7
1789 006BEA E198 @139 ROL.L #$8,D0
1789 006BEC 1010 MOVE.B (A0),D0
1789 006BEE 51CFFFFA      DBRA D7,@139
1790 006BF2 24C0 MOVE.L D0,(A2)+      MOVE DATA
1791 006BF4 5281 ADD.L #$1,D1
1792 006BF6 B4CB CMP.W A3,A2
1793 006BF8 6F00FF66      BLE HAMM1
1794          *
1795          ****
1796          *     A2 <--> START OF REAL PART OF SIGNAL
1797          *     A3 <--> START OF IMAGINARY PART OF SIGNAL
1798          *     D0 <--> J; D1 <--> I; D2 <--> T; D3 <--> K
1799          *     D4 <--> (J-1)*4 ARRAY POINTER
1800          *     D5 <--> (I-1)*4 ARRAY POINTER
1801          *
1802          *     CALLS FOLLOWING MACROS:
1803          *     STPOIN2 '' CLDATA2 REORDER ''
1804          *
1805          *
1806          *     FFT SUBROUTINE ---- DO 3 LOOP
1807          *
1808          DSPLOPT FFTM,FFTME
1808 006BFC 4BF86EB6      LEA FFTM,A5
1808 006C00 4DF86EC4      LEA FFTME,A6
1808          TRP14 OUT1CR
1808 006C04 1E3C00E3      MOVE.B #OUT1CR,D7
1808 006C08 4E4E TRAP #14
1809 006C0A 207C00050001 MOVE.L #APUOPER,A0
1810 006C10 347C3700      MOVE.W #XRST,A2 START OF REAL ARRAY
1811          CLDATA2.W D4,D5
1811 006C14 4244 CLR.W D4
1811 006C16 4245 CLR.W D5
1812          STPOIN2 1,D0,1,D1      J=1;I=1
1812 006C18 303C0001      MOVE #1,D0
1812 006C1C 323C0001      MOVE #1,D1

```

```

1813      *
1814      * DO 3 I = 1,NM1
1815      *
1816 006C20 B240 FFT3LP CMP.W D0,D1
1817 006C22 6C1C BGE.S FFT1           IF (I .GE. J) GOTO 1
1818          REORDER A2,D4,D2,D5   T=F(J);F(J)=F(I);F(I)=T:*REAL*
1818 006C24 24324000 MOVE.L 0(A2,D4),D2
1818 006C28 25B250004000 MOVE.L 0(A2,D5),0(A2,D4)
1818 006C2E 25825000 MOVE.L D2,0(A2,D5)
1819          REORDER A3,D4,D2,D5 :*IMAGINARY*
1819 006C32 24334000 MOVE.L 0(A3,D4),D2
1819 006C36 27B350004000 MOVE.L 0(A3,D5),0(A3,D4)
1819 006C3C 27825000 MOVE.L D2,0(A3,D5)
1820 006C40 363C0200 FFT1 MOVE.W #NV2,D3   K=NV2
1821 006C44 B640 FFT2 CMP.W D0,D3
1822 006C46 6C06 BGE.S FFT3           IF (K .GE. J) GOTO 3
1823 006C48 9043 SUB.W D3,D0   J=J-K
1824 006C4A E24B LSR.W #1,D3   K=K/2
1825 006C4C 60F6 BRA.S FFT2   GOTO 2
1826 006C4E D043 FFT3 ADD.W D3,D0   J=J+K
1827 006C50 5241 ADDQ.W #1,D1   I=I+1
1828 006C52 5845 ADDQ.W #$4,D5   I ARRAY POINTER
1829 006C54 3800 MOVE.W D0,D4
1830 006C56 5344 SUBQ.W #$1,D4
1831 006C58 E54C LSL.W #$2,D4   J ARRAY POINTER
1832 006C5A 0C4103FF CMP.W #NM1,D1
1833 006C5E 6FC0 BLE.S FFT3LP   3 CONTINUE
1834      *
1835      *
1836      *
1837      *
1838 ****
1839      *      A0,A1 <--> APU OPERAND ADDRESS, APU COMMAND ADDRESS
1840      *      A2,A3 <--> REAL AND IMAGINARY SIGNAL START
1841      *      D0,D1 <--> I ARRAY SUBSCRIPT (LW), IP ARRAY SCRIPT (LW)
1842      *      D2,D3 <--> UR,UI 32-BIT FLOATING POINT VALUES
1843      *      D6,D7 <--> SCRATCH
1844      ****
1845      *
1846      *      DO 5 OUTSIDE LOOP
1847      *
1848      STPOIN2 XRST,A2,XIST,A3  START OF REAL AND IMAGINARY SIGNAL
1848 006C60 347C3700 MOVE #XRST,A2
1848 006C64 367C4700 MOVE #XIST,A3
1849      *
1850      * DO 5 L=1,LN
1851      *
1852 006C68 31FC00017F2A MOVE.W #1,L   L=1
1853          FFTOLP5 POW2TOA L
1853 006C6E 3E387F2A MOVE.W L,D7
1853 006C72 04470001 SUBI.W #1,D7
1853 006C76 3C3C0001 MOVE.W #1,D6
1853 006C7A CCFC0002 @146 MULU.W #2,D6
1853 006C7E 51CFFFFA DBRA D7,@146
1854 006C82 31C67F2C MOVE.W D6,LE   LE=2**L
1855 006C86 E24E LSR.W #1,D6
1856 006C88 31C67F2E MOVE.D6,LE1   LE1=LE/2
1857 006C8C 42B87F3C CLR.L UR
1858 006C90 06B800000001
1859 006C98 7F3C ADDI.L #1,UR
1859 006C98 42B87F40 CLR.L UI   U=(1.0,0.0)

```

```

1860 006C9C 2C387F3C      MOVE.L UR,D6      MOVE UR & UI TO APU STACK
1861          APUWR D6,A0
1861 006CA0 3E3C0003      MOVE.W #$3,D7
1861 006CA4 1086 @147 MOVE.B D6,(A0)
1861 006CA6 E09E ROR.L #$8,D6
1861 006CA8 51CFFFFA      DBRA D7,@147
1862 006CAC 2C387F40      MOVE.L UI,D6
1863          APUWR D6,A0
1863 006CB0 3E3C0003      MOVE.W #$3,D7
1863 006CB4 1086 @148 MOVE.B D6,(A0)
1863 006CB6 E09E ROR.L #$8,D6
1863 006CB8 51CFFFFA      DBRA D7,@148
1864          APU FLTD
1864 006CBC 13FC001C      00050011 MOVE.B #FLTD,APUCOM
1864 006CC4 4E722300      STOP #$2300
1865          APU XCHD
1865 006CC8 13FC0039      00050011 MOVE.B #XCHD,APUCOM
1865 006CD0 4E722300      STOP #$2300
1866          APU FLTD
1866 006CD4 13FC001C      00050011 MOVE.B #FLTD,APUCOM
1866 006CDC 4E722300      STOP #$2300
1867          APURD A0,D2
1867 006CE0 3E3C0003      MOVE.W #$3,D7
1867 006CE4 E19A @152 ROL.L #$8,D2
1867 006CE6 1410 MOVE.B (A0),D2
1867 006CE8 51CFFFFA      DBRA D7,@152
1868          APURD A0,D3
1868 006CEC 3E3C0003      MOVE.W #$3,D7
1868 006CF0 E19B @153 ROL.L #$8,D3
1868 006CF2 1610 MOVE.B (A0),D3
1868 006CF4 51CFFFFA      DBRA D7,@153
1869          *
1870          * COMPUTE W=CMPLX(COS(PI/LE1),-SIN(PI/LE1))
1871          *
1872 006CF8 4EB86754      JSR CALCW
1873          *
1874          * DO 5 J=1,LE1
1875          *
1876 006CFC 31FC00017F32  MOVE.W #1,J      J=1
1877          *
1878          * DO 4 I=J,N,LE
1879          *
1880 006D02 31F87F327F30 FFTLP5 MOVE.W J,I I=J
1881 006D08 30387F30      FFTLP4 MOVE.W I,D0
1882 006D0C 04400001      SUBI.W #1,D0
1883 006D10 E548 LSL.W #2,D0
1884 006D12 32387F30      MOVE.W I,D1
1885 006D16 D2787F2E      ADD.W LE1,D1
1886 006D1A 04410001      SUBI.W #1,D1
1887 006D1E E549 LSL.W #2,D1
1888          *
1889          * COMPUTE T=F(IP)*U:
1890          *
1891 006D20 4EB867EA      JSR CALCT
1892          *
1893          * TI -> TOS; TR -> NOS
1894          * COMPUTE F(IP)=F(I)-T
1895          * F(I)=F(I)+T

```

```

1896      *
1897 006D24 4EB868BC      JSR CALCFIM
1898 006D28 4EB8693A      JSR CALCFRL
1899 006D2C 3C387F2C      FFT4 MOVE.W LE,D6
1900 006D30 DD787F30      ADD.W D6,I      I=I+LE
1901 006D34 0C7804007F30  CMP.W #N,I
1902 006D3A 6FCC      BLE FFTLP4      CONTINUE UNTIL LOOP 4 UNTIL I>N
1903      *
1904      * COMPUTE U=U*W:
1905      *
1906 006D3C 4EB869B8      JSR CALCUL
1907      *
1908 006D40 067800017F32  FFT5 ADDI.W #1,J  J=J+1
1909 006D46 3C387F32      MOVE.W J,D6
1910 006D4A BC787F2E      CMP.W LE1,D6
1911 006D4E 6FB2      BLE FFTLP5      CONTINUE INNER LOOP 5 UNTIL J>LE1
1912 006D50 067800017F2A  FFT05 ADDI.W #1,L
1913 006D56 0C78000A7F2A  CMPI.W #LNIN,L
1914 006D5C 6F00FF10      BLE FFTOLP5      CONTINUE OUTER LOOP 5 UNTIL L>LN
1915      *
1916      * COMPUTE POWER SPECTRUM BY SQUARING POSITIVE PART OF
1917      * MAGNITUDE
1918      *
1919      DSPLOPT PS,PSE
1919 006D60 4BF86EC6      LEA PS,A5
1919 006D64 4DF86EDE     LEA PSE,A6
1919      TRP14 OUT1CR
1919 006D68 1E3C00E3      MOVE.B #OUT1CR,D7
1919 006D6C 4E4E      TRAP #14
1920 006D6E 207C00050001  MOVE.L #APUOPER,A0
1921      STPOIN2.W XRST,A2,XIST,A3
1921 006D74 347C3700      MOVE.W #XRST,A2
1921 006D78 367C4700      MOVE.W #XIST,A3
1922 006D7C 303C0000      MOVE.W #$0,D0
1923      FFT6 APUSGWR A2,D0,A0      WRITE REAL PART TO STACK
1923 006D80 2C320000      MOVE.L 0(A2,D0),D6
1923 006D84 3E3C0003      MOVE.W #$3,D7
1923 006D88 1086 @156 MOVE.B D6,(A0)
1923 006D8A E09E      ROR.L #$8,D6
1923 006D8C 51CFFFFA      DBRA D7,@156
1924 006D90 13FC0037      APU PTOD      PUSH TOS
1924 00050011 MOVE.B #PTOD,APUCOM
1924 006D98 4E722300      STOP #$2300
1925 006D9C 13FC0012      APU FMUL      SQUARE REAL PART
1925 00050011 MOVE.B #FMUL,APUCOM
1925 006DA4 4E722300      STOP #$2300
1926      APUSGWR A3,D0,A0      WRITE IMAGINARY PART TO STACK
1926 006DA8 2C330000      MOVE.L 0(A3,D0),D6
1926 006DAC 3E3C0003      MOVE.W #$3,D7
1926 006DB0 1086 @159 MOVE.B D6,(A0)
1926 006DB2 E09E      ROR.L #$8,D6
1926 006DB4 51CFFFFA      DBRA D7,@159
1927 006DB8 13FC0037      APU PTOD
1927 00050011 MOVE.B #PTOD,APUCOM
1927 006DC0 4E722300      STOP #$2300
1928 006DC4 13FC0012      APU FMUL      SQUARE IMAGINARY PART
1928 00050011 MOVE.B #FMUL,APUCOM

```

```

1928 006DCC 4E722300      STOP #$2300
1929          APU FADD          ADD XR**2 TO XI**2
1929 006DD0 13FC0010
    00050011 MOVE.B #FADD,APUCOM
1929 006DD8 4E722300      STOP #$2300
1930          APUSGRD A2,D0,A0      STORE POWER SPECTRUM SAMPLE IN XREAL
1930 006DDC 3E3C0003      MOVE.W #$3,D7
1930 006DE0 E19E @163 ROL.L #$8,D6
1930 006DE2 1C10 MOVE.B (A0),D6
1930 006DE4 51CFFFFA      DBRA D7,@163
1930 006DE8 25860000      MOVE.L D6,0(A2,D0)
1931 006DEC 06400004      ADDI.W #$4,D0
1932 006DF0 0C401000      CMPI.W #4096,D0
1933 006DF4 6D8A      BLT FFT6
1934 006DF6 4E75      RTS      SKIP CONVOLUTION ROUTINE FOR NOW
1935          *      CAN USE ROUTINE BY REMOVING THIS RTS.
1936          *
1937          *      CONVOLUTION ROUTINE TO SMOOTH POWER SPECTRA
1938          *
1939          DSPLOPT SMP$,SMP$E
1939 006DF8 4BF86EE0      LEA SMP$,A5
1939 006DFC 4DF86F00     LEA SMP$E,A6
1939          TRP14 OUT1CR
1939 006E00 1E3C00E3      MOVE.B #OUT1CR,D7
1939 006E04 4E4E      TRAP #14
1940 006E06 207C00050001      MOVE.L #APUOPER,A0
1941 006E0C 7008      MOVE.L #8,D0      CONVOLVE WINDOW WIDTH
1942 006E0E 347C3700      MOVE.W #XRST,A2      START OF POWER SPECTRUM
1943 006E12 387C4700      MOVE.W #TMPSTC,A4      TEMPORARY STORAGE POINTER
1944 006E16 584A      ADDQ.W #$4,A2      INCREMENT POWER SPECTRA POINTER
1945          *
1946          *
1947 006E18 364A      FLCN1 MOVE.W A2,A3      CONVOLVE INNER LOOP POINTER
1948 006E1A 4281      CLR.L D1      C(N)=0
1949 006E1C 2400      MOVE.L D0,D2      # OF SAMPLES IN WINDOW
1950          *
1951 006E1E 2623      FLCN2 MOVE.L -(A3),D3      DECREMENT, THEN LOAD DATA
1952 006E20 B6FC3700      CMP.W #XRST,A3      ENSURE WINDOW NOT BEFORE XRST.
1953 006E24 6D00005A      BLT FLCN3      X(N-K)
1954          APUWR D3,A0
1954 006E28 3E3C0003      MOVE.W #$3,D7      W(K)
1954 006E2C 1083 @165 MOVE.B D3,(A0)
1954 006E2E E09B      ROR.L #$8,D3
1954 006E30 51CFFFFA      DBRA D7,@165
1955          APUWR D2,A0
1955 006E34 3E3C0003      MOVE.W #$3,D7
1955 006E38 1082 @166 MOVE.B D2,(A0)
1955 006E3A E09A      ROR.L #$8,D2
1955 006E3C 51CFFFFA      DBRA D7,@166
1956          APU FLTD
1956 006E40 13FC001C
    00050011 MOVE.B #FLTD,APUCOM
1956 006E48 4E722300      STOP #$2300
1957          APU FMUL      X(N-K)W(K)
1957 006E4C 13FC0012
    00050011 MOVE.B #FMUL,APUCOM
1957 006E54 4E722300      STOP #$2300
1958          APUWR D1,A0
1958 006E58 3E3C0003      MOVE.W #$3,D7
1958 006E5C 1081 @169 MOVE.B D1,(A0)
1958 006E5E E099      ROR.L #$8,D1

```

1958 006E60 51CFFFFA DBRA D7,@169
 1959 APU FADD C(N) SUMMATION
 1959 006E64 13FC0010
 00050011 MOVE.B #FADD,APUCOM
 1959 006E6C 4E722300 STOP #\$2300
 1960 APURD A0,D1
 1960 006E70 3E3C0003 MOVE.W #\$3,D7
 1960 006E74 E199 @171 ROL.L #\$8,D1
 1960 006E76 1210 MOVE.B (A0),D1
 1960 006E78 51CFFFFA DBRA D7,@171
 1961 006E7C 51CAFFA0 DBRA D2,FLCN2 CONTINUE FOR ENTIRE WINDOW
 1962 *
 1963 006E80 28C1 FLCN3 MOVE.L D1,(A4)+ C(N) FOR SPECIFIC N
 1964 006E82 584A ADDQ.W #\$4,A2 INCREMENT POINTER
 1965 006E84 B4FC3EFC CMP.W #XRENH,A2
 1966 006E88 6D8E BLT FLCN1
 1967 *
 1968 * MOVE DATA BACK TO XRST
 1969 *
 1970 006E8A 307C3700 MOVE.W #XRST,A0
 1971 006E8E 327C4700 MOVE.W #TMPSTC,A1
 1972 006E92 20D9 FLCNE MOVE.L (A1)+,(A0)+ MOVE DATA
 1973 006E94 B0FC3EFC CMP.W #XRENH,A0
 1974 006E98 6DF8 BLT FLCNE
 1975 006E9A 4E75 RTS
 1976 006E9C 20 HAM DC.W ' HAMMING WINDOW'
 1977 006EB4 20 HAME DC.W ' FFT'
 1978 006EB6 20 FFTM DC.W ' FFT'
 1979 006EC4 20 FFTME DC.W ' POWER SPECTRUM'
 1980 006EC6 20 PS DC.W ' POWER SPECTRUM'
 1981 006EDE 20 PSE DC.W ' SMOOTH POWER SPECTRUM'
 1982 006EE0 20 SMPS DC.W ' SMOOTH POWER SPECTRUM'
 1983 006F00 20 SMPSE DC.W ' SMOOTH POWER SPECTRUM'
 1984 *
 1985 *

```

1987      *#####
1988      *#####
1989      *
1990      *          PCG PROCESSING - FREQ DOMAIN
1991      *
1992      *#####
1993      *          THE PCG PROCESSING ROUTINE IS COMPRISED OF THE FOLLOWING
1994      *          MODULES:
1995      *
1996      *          PFMSYS: MOVE PCG SYSTOLE INTO COMPLEX ARRAY
1997      *          FFT: COMPUTE POWER SPECTRUM OF SYSTOLE
1998      *          PPFSYS: MOVE SYSTOLE POWER SPECTRUM TO TEMP
1999      *          PFMDIA: MOVE DIASTOLE INTO COMPLEX ARRAY
2000      *          FFT: COMPUTE POWER SPECTRUM OF DIASTOLE
2001      *          PFEDC: COMPUTE ENERGY DISTRIBUTION COEFFICIENTS
2002      *#####
2003      *#####
2004      *

2005 006F02 4EB872D4      PCGF JSR BLANK
2006      DSPLOPT PFST,PFEN
2006 006F06 4BF86F58      LEA PFST,A5
2006 006F0A 4DF86F7A      LEA PFEN,A6
2006      TRP14 OUT1CR
2006 006F0E 1E3C00E3      MOVE.B #OUT1CR,D7
2006 006F12 4E4E      TRAP #14
2007      DSPLOPT PFSFT,PFSFTE
2007 006F14 4BF86F7C      LEA PFSFT,A5
2007 006F18 4DF86F8E      LEA PFSFTE,A6
2007      TRP14 OUT1CR
2007 006F1C 1E3C00E3      MOVE.B #OUT1CR,D7
2007 006F20 4E4E      TRAP #14
2008 006F22 4EB86FBE      JSR PFMSYS
2009 006F26 4EB86A8A      JSR FFT
2010      DSPLOPT PFDFT,PFDFT
2010 006F2A 4BF86F90      LEA PFDFT,A5
2010 006F2E 4DF86FA2      LEA PFDFT,A6
2010      TRP14 OUT1CR
2010 006F32 1E3C00E3      MOVE.B #OUT1CR,D7
2010 006F36 4E4E      TRAP #14
2011 006F38 4EB8700C      JSR PPFSYS
2012 006F3C 4EB87022      JSR PFMDIA
2013 006F40 4EB86A8A      JSR FFT
2014      DSPLOPT PFEST,PFEEN
2014 006F44 4BF86FA4      LEA PFEST,A5
2014 006F48 4DF86FBC      LEA PFEEN,A6
2014      TRP14 OUT1CR
2014 006F4C 1E3C00E3      MOVE.B #OUT1CR,D7
2014 006F50 4E4E      TRAP #14
2015 006F52 4EB87062      JSR PFEDC
2016 006F56 4E75      RTS
2017 006F58 50      PFST DC.W 'PCG PROCESSING - FREQUENCY DOMAIN'
2018 006F7A 20      PFEN DC.W '
2019 006F7C 20      PFSFT DC.W '      SYSTOLIC FFT'
2020 006F8E 20      PFSFTE DC.W '      DIASTOLIC FFT'
2021 006F90 20      PFDFT DC.W '      COMPUTE EDC VALUES'
2022 006FA2 20      PFDFT DC.W '
2023 006FA4 20      PFEST DC.W '
2024 006FBC 20      PFEEN DC.W '

```

```

2026 ****
2027 * PFMSYS
2028 ****
2029 *
2030 * A0 <--> START OF SYSTOLE
2031 * A1 <--> END OF SYSTOLE
2032 * A2 <--> START OF REAL ARRAY;IMAGINARY ARRAY
2033 * D0 <--> SCRATCH
2034 *
2035 ****
2036 *
2037 * CALL FOLLOWING MACROS:
2038 * GETADD '
2039 *
2040 ****
2041 *
2042 * THIS ROUTINE MOVES THE SYSTOLIC SEGMENT OF THE PCG INTO THE
2043 * REAL ARRAY. THE ARRAY IS APPENDED WITH ZEROS. THE IMAGINARY
2044 * ARRAY IS SET TO ZERO.
2045 *
2046 *
2047 PFMSYS GETADD PCGS1A,A0,PCGSTRT
2047 006FBE 30787F08 MOVE.W PCGS1A,A0
2047 006FC2 D0FC0F00 ADD.W #PCGSTRT,A0
2048 GETADD PCGS1B,A1,PCGSTRT
2048 006FC6 32787F0A MOVE.W PCGS1B,A1
2048 006FCA D2FC0F00 ADD.W #PCGSTRT,A1
2049 006FCE 4EB863AC JSR TWOCOMP      CONVERT PCG TO TWOS COMPLEMENT
2050 GETADD PCGS1A,A0,PCGSTRT      START OF SYSTOLE
2050 006FD2 30787F08 MOVE.W PCGS1A,A0
2050 006FD6 D0FC0F00 ADD.W #PCGSTRT,A0
2051 006FDA 3248 MOVE.W A0,A1
2052 006FDC D2F87F0C ADD.W PCGS2,A1      END OF SYSTOLE
2053 006FE0 347C3700 MOVE.W #XRST,A2      START OF XREAL ARRAY
2054 006FE4 4280 CLR.L D0
2055 006FE6 3018 PFMSYS1 MOVE.W (A0)+,D0      MOVE SYSTOLE IN REAL ARRAY
2056 006FE8 24C0 MOVE.L D0,(A2)+      MOVE DATA
2057 006FEA B0C9 CMP.W A1,A0
2058 006FEC 6DF8 BLT PFMSYS1
2059 006FEE 24FC00000000 PFMSYS2 MOVE.L #0,(A2)+      APPEND WITH ZEROS
2060 006FF4 B4FC4700 CMP.W #XREN,A2
2061 006FF8 6DF4 BLT PFMSYS2
2062 006FFA 347C4700 MOVE.W #XIST,A2
2063 006FFE 24FC00000000 PFMSYS3 MOVE.L #0,(A2)+      SET IMAGINARY ARRAY TO ZERO
2064 007004 B4FC5700 CMP.W #XIEN,A2
2065 007008 6DF4 BLT PFMSYS3
2066 00700A 4E75 RTS
2067 *
2068 *

```

```

2070 ****
2071 * PFPSYS
2072 ****
2073 *
2074 *      A2 <--> START OF REAL ARRAY;POWER SPECTRUM
2075 *      A3 <--> TEMPORARY STORAGE
2076 *      DO <--> COUNTER
2077 *
2078 ****
2079 *
2080 *      CALL FOLLOWING MACROS:
2081 *          STPOIN2
2082 *
2083 ****
2084 *
2085 *
2086 *      THE SYSTOLIC POWER SPECTRUM IS RETURNED IN THE FIRST HALF OF
2087 *      REAL ARRAY. THIS ROUTINE MOVES THE POWER SPECTRUM TO TEMPORA
2088 *      STORAGE.
2089 *
2090 *
2091 PFPSYS STPOIN2.W XRST,A2,TMPSTB,A3
2091 00700C 347C3700 MOVE.W #XRST,A2
2091 007010 367C5700 MOVE.W #TMPSTB,A3
2092 007014 303C0200 MOVE.W #512,D0
2093 007018 26DA PFPSYS1 MOVE.L (A2)+,(A3)+      MOVE DATA
2094 00701A 51C8FFFC DBRA D0,PFPSYS1
2095 00701E 6DF8 BLT PFPSYS1
2096 007020 4E75 RTS
2097 *
2098 *

```

```

2100 ****
2101 * PFMDIA
2102 ****
2103 *
2104 * A0 <--> START OF DIASTOLE
2105 * A1 <--> END OF DIASTOLE
2106 * A2 <--> START OF REAL ARRAY;IMAGINARY ARRAY
2107 *
2108 ****
2109 *
2110 * CALL FOLLOWING MACROS:
2111 * GETADD ''
2112 *
2113 ****
2114 *
2115 * THIS ROUTINE MOVES THE DIASTOLIC SEGMENT OF THE PCG INTO THE
2116 * REAL ARRAY. THE ARRAY IS APPENDED WITH ZEROS. THE IMAGINARY
2117 * ARRAY IS SET TO ZERO.
2118 *
2119 *
2120 PFMDIA GETADD PCGS1A,A0,PCGSTRT START OF SYSTOLE
2120 007022 30787F08 MOVE.W PCGS1A,A0
2120 007026 D0FC0F00 ADD.W #PCGSTRT,A0
2121 00702A D0F87F0C ADD.W PCGS2,A0
2122 * GETADD PCGS1B,A1,PCGSTRT START OF DIASTOLE
2122 * END OF DIASTOLE
2122 00702E 32787F0A MOVE.W PCGS1B,A1
2122 007032 D2FC0F00 ADD.W #PCGSTRT,A1
2123 007036 347C3700 MOVE.W #XRST,A2 START OF XREAL ARRAY
2124 00703A 4280 CLR.L D0
2125 00703C 3018 PFMDIA1 MOVE.W (A0)+,D0 MOVE DIASTOLE IN REAL ARRAY
2126 00703E 24C0 MOVE.L D0,(A2)+ MOVE DATA
2127 007040 B0C9 CMP.W A1,A0
2128 007042 6DF8 BLT PFMDIA1
2129 007044 24FC00000000 PFMDIA2 MOVE.L #0,(A2)+ APPEND WITH ZEROS
2130 00704A B4FC4700 CMP.W #XREN,A2
2131 00704E 6DF4 BLT PFMDIA2
2132 007050 347C4700 MOVE.W #XIIST,A2
2133 007054 24FC00000000 PFMDIA3 MOVE.L #0,(A2)+ SET IMAGINARY ARRAY TO ZERO
2134 00705A B4FC5700 CMP.W #XIEN,A2
2135 00705E 6DF4 BLT PFMDIA3
2136 007060 4E75 RTS
2137 *
2138 *

```

```

2140 **** PFEDC ****
2141 * PFEDC
2142 **** PFEDC ****
2143 *
2144 * A2 <--> START OF SIGNAL
2145 * D6 <--> EDC VALUE IS RETURNED IN THIS REGISTER
2146 *
2147 **** PFEDC ****
2148 *
2149 * CALL FOLLOWING MACROS:      SUBROUTINES:
2150 * EDC
2151 *
2152 **** PFEDC ****
2153 *
2154 *
2155 * COMPUTE EDC VALUES OF SYSTOLIC AND DIASTOLIC SEGMENTS
2156 *
2157 *
2158 007062 347C5700 PFEDC MOVE.W #TMPSTB,A2
2159 007066 4EB87094 JSR FLEDC
2160 00706A 21C67F1A MOVE.L D6,EDCFSYS
2161 00706E 347C3700 MOVE.W #XRST,A2
2162 007072 4EB87094 JSR FLEDC
2163 007076 21C67F1E MOVE.L D6,EDCFDIA
2164 *
2165 GETADD PCGS1A,A0,PCGSTRT CONVERT BACK TO 12-BIT NUMBER
2165 00707A 30787F08 MOVE.W PCGS1A,A0
2165 00707E D0FC0F00 ADD.W #PCGSTRT,A0
2166 GETADD PCGS1B,A1,PCGSTRT
2166 007082 32787F0A MOVE.W PCGS1B,A1
2166 007086 D2FC0F00 ADD.W #PCGSTRT,A1
2167 00708A 06580800 PFEDC1 ADD.W $$800,(A0)+ ADD DATA
2168 00708E B0C9 CMP.W A1,A0
2169 007090 6FF8 BLE.S PFEDC1
2170 007092 4E75 RTS
2171 *
2172 *

```

```

2174 ****
2175 * FLEDC
2176 ****
2177 *
2178 * A0 <--> APU OPERAND ENTRY ADDRESS
2179 * A1 <--> APU COMMAND ENTRY ADDRESS
2180 * A2 <--> START OF SIGNAL. WHEN ROUTINE CALLED START OF
2181 * SIGNAL MUST BE IN A2
2182 * D0 <--> N (MULTIPLIER IN NUMERATOR)
2183 * D3 <--> SQUARE ROOT OF VALUE
2184 * D6 <--> FINAL EDC VALUE 32-BIT FIXED POINT
2185 *
2186 ****
2187 *
2188 * CALL FOLLOWING MACROS:
2189 * STPOIN2 APUWR '' APUSGWR '' APURD APU
2190 *
2191 ****
2192 *
2193 *
2194 * THIS ROUTINE COMPUTES THE FLOATING POINT EDC VALUE. PARAMETE
2195 * ARE ENTERED AS 32-BIT FLOATING POINT. EDC VALUES COMPUTED FO
2196 * POSITIVE SIDE OF POWER SPECTRUM. RETURNED VALUE (EDC) IS
2197 * CONVERTED TO 32 FIXED POINT AND RESIDES IN DATA REGISTER D6.
2198 *
2199 *
2200 FLEDC STPOIN2.L APUOPER,A0,APUCOM,A1
2200 007094 207C00050001 MOVE.L #APUOPER,A0
2200 00709A 227C00050011 MOVE.L #APUCOM,A1
2201 0070A0 7000 MOVE.L #$0,D0
2202 APUWR D0,A0
2202 0070A2 3E3C0003 MOVE.W #$3,D7
2202 0070A6 1080 @185 MOVE.B D0,(A0)
2202 0070A8 E098 ROR.L #$8,D0
2202 0070AA 51CFFFFA DBRA D7,@185
2203 APUWR D0,A0 MOVE NUMERATOR AND DENOMINATOR ON
2203 0070AE 3E3C0003 MOVE.W #$3,D7
2203 0070B2 1080 @186 MOVE.B D0,(A0)
2203 0070B4 E098 ROR.L #$8,D0
2203 0070B6 51CFFFFA DBRA D7,@186
2204 * STACK (INITIALLY ZERO).
2205 0070BA 4241 CLR.W D1 SIGNAL ARRAY POINTER
2206 0070BC 7401 MOVE.L #$1,D2 MULTIPLIER (N) IN EDC COMPUTATION
2207 FLEDC1 APUSGWR A2,D1,A0 WRITE POWER SPECTRA SAMPLE TO STA
2207 0070BE 2C321000 MOVE.L 0(A2,D1),D6
2207 0070C2 3E3C0003 MOVE.W #$3,D7
2207 0070C6 1086 @187 MOVE.B D6,(A0)
2207 0070C8 E09E ROR.L #$8,D6
2207 0070CA 51CFFFFA DBRA D7,@187
2208 APU FADD UPDATE DENOMINATOR
2208 0070CE 13FC0010
2208 00050011 MOVE.B #FADD,APUCOM
2208 0070D6 4E722300 STOP #$2300
2209 APU XCHF EXCHANGE NUM AND DEN ON STACK
2209 0070DA 13FC0019
2209 00050011 MOVE.B #XCHF,APUCOM
2209 0070E2 4E722300 STOP #$2300
2210 APUWR D2,A0 WRITE N TO STACK
2210 0070E6 3E3C0003 MOVE.W #$3,D7
2210 0070EA 1082 @190 MOVE.B D2,(A0)
2210 0070EC E09A ROR.L #$8,D2

```

```

2210 0070EE 51CFFFFA      DBRA D7,@190
2211          APU FLTD           FLOATING POINT
2211 0070F2 13FC001C
    00050011 MOVE.B #FLTD,APUCOM
2211 0070FA 4E722300      STOP #$2300
2212          APUSGWR A2,D1,A0
2212 0070FE 2C321000      MOVE.L 0(A2,D1),D6
2212 007102 3E3C0003      MOVE.W #$3,D7
2212 007106 1086  @192 MOVE.B D6,(A0)
2212 007108 E09E   ROR.L #$8,D6
2212 00710A 51CFFFFA      DBRA D7,@192
2213          APU FMUL
2213 00710E 13FC0012
    00050011 MOVE.B #FMUL,APUCOM
2213 007116 4E722300      STOP #$2300
2214          APU FADD
2214 00711A 13FC0010
    00050011 MOVE.B #FADD,APUCOM
2214 007122 4E722300      STOP #$2300
2215          APU XCHF
2215 007126 13FC0019
    00050011 MOVE.B #XCHF,APUCOM
2215 00712E 4E722300      STOP #$2300
2216 007132 5282  ADD.L #$1,D2
2217 007134 5841  ADD.W #$4,D1
2218 007136 0C410800      CMP.W #2048,D1
2219 00713A 6D82  BLT FLEDC1
2220          APU FDIV
2220 00713C 13FC0013
    00050011 MOVE.B #FDIV,APUCOM
2220 007144 4E722300      STOP #$2300
2221          APU FIXD
2221 007148 13FC001E
    00050011 MOVE.B #FIXD,APUCOM
2221 007150 4E722300      STOP #$2300
2222          APURD A0,D6
2222 007154 3E3C0003      MOVE.W #$3,D7
2222 007158 E19E  @198 ROL.L #$8,D6
2222 00715A 1C10  MOVE.B (A0),D6
2222 00715C 51CFFFFA      DBRA D7,@198
2223 007160 4E75   RTS
2224          *
2225          *

```

WRITE POWER SPECTRA VALUE TO STAC

N * S(N)

UPDATE NUMERATOR

EXCHANGE NUMAND DEN

INCREMENT MULTIPLIER

INCREMENT SIGNAL ARRAY POINTER

CONTINUE UNTIL ENTIRE SPECTRA COM
NUMERATOR/DENOMINATOR = EDC

CONVERT TO 32-BIT FIXED

D6 CONATINS EDC VALUE

```

2227      #####*
2228      *
2229      *          D/A CONVERSION ROUTINES
2230      *
2231      *          1) NORMALIZE ALL TRANSFORM DATA TO BE CONVERTED
2232      *          WITH 12 BIT D/A.
2233      *          2) DISPLAY OPTIONS MENU
2234      *          3) SELECT OPTION
2235      *          4) PERFORM CONVERSION
2236      *          5) GO TO 2)
2237      *
2238      #####*
2239      *
2240      *
2241      *
2242      *          FIND MAXIMUM VALUE IN ARRAY... MAX RETURNED IN D0
2243      *          A2 <--> START      A3 <--> END
2244      *
2245 007162 4280 DAMAX CLR.L D0           CLEAR INITIAL MAXIMUM
2246 007164 221A DAMAX1 MOVE.L (A2)+,D1
2247 007166 B081 CMP.L D1,D0           CHECK CURRENT VALUE AGAINST MAX
2248 007168 6C02 BGE.S DAMAX2
2249 00716A 2001 MOVE.L D1,D0           UPDATE CURRENT MAX
2250 00716C B4CB DAMAX2 CMP.W A3,A2
2251 00716E 6FF4 BLE.S DAMAX1           SEARCH ENTIRE ARRAY
2252 007170 4E75 RTS
2253      *
2254      *
2255      *          NORMALIZE ALL DATA IN ARRAY TO MAXIMUM VALUE OF 4095 (FFF)
2256      *          A0,A1 <--> APU ADDRESSES   A2,A3 <--> START AND END
2257      *          D0 <--> MAXIMUM VALUE IN ARRAY
2258      *
2259      *
2260      DANORM APUWR D0,A0
2260 007172 3E3C0003 MOVE.W #$3,D7
2260 007176 1080 @199 MOVE.B D0,(A0)
2260 007178 E098 ROR.L #$8,D0
2260 00717A 51CFFFFA DBRA D7,@199
2261          APU FLTD
2261 00717E 13FC001C MOVE.B #FLTD,APUCOM
2261 00050011 MOVE.B #FLTD,APUCOM
2261 007186 4E722300 STOP #$2300
2262          APURD A0,D0           MAX VALUE - FLOATING POINT
2262 00718A 3E3C0003 MOVE.W #$3,D7
2262 00718E E198 @201 ROL.L #$8,D0
2262 007190 1010 MOVE.B (A0),D0
2262 007192 51CFFFFA DBRA D7,@201
2263 007196 223C0CFFF000 MOVE.L #$0CFFF000,D1    4095 - FLOATING POINT
2264 00719C 2412 DANORM1 MOVE.L (A2),D2    SAMPLE VALUE
2265          APUWR D2,A0
2265 00719E 3E3C0003 MOVE.W #$3,D7
2265 0071A2 1082 @202 MOVE.B D2,(A0)
2265 0071A4 E09A ROR.L #$8,D2
2265 0071A6 51CFFFFA DBRA D7,@202
2266          APU FLTD
2266 0071AA 13FC001C MOVE.B #FLTD,APUCOM
2266 00050011 MOVE.B #FLTD,APUCOM
2266 0071B2 4E722300 STOP #$2300
2267          APUWR D0,A0
2267 0071B6 3E3C0003 MOVE.W #$3,D7
2267 0071BA 1080 @204 MOVE.B D0,(A0)

```

```

2267 0071BC E098 ROR.L #$8,D0
2267 0071BE 51CFFFFA DBRA D7,@204
2268 APU FDIV VALUE/MAX
2268 0071C2 13FC0013
    00050011 MOVE.B #FDIV,APUCOM
2268 0071CA 4E722300 STOP #$2300
2269 APUWR D1,A0
2269 0071CE 3E3C0003 MOVE.W #$3,D7
2269 0071D2 1081 @206 MOVE.B D1,(A0)
2269 0071D4 E099 ROR.L #$8,D1
2269 0071D6 51CFFFFA DBRA D7,@206
2270 APU FMUL (VALUE/MAX)*4095
2270 0071DA 13FC0012
    00050011 MOVE.B #FMUL,APUCOM
2270 0071E2 4E722300 STOP #$2300
2271 APU FIXED FIXED POINT
2271 0071E6 13FC001E
    00050011 MOVE.B #FIXD,APUCOM
2271 0071EE 4E722300 STOP #$2300
2272 APURD A0,D2
2272 0071F2 3E3C0003 MOVE.W #$3,D7
2272 0071F6 E19A @209 ROL.L #$8,D2
2272 0071F8 1410 MOVE.B (A0),D2
2272 0071FA 51CFFFFA DBRA D7,@209
2273 0071FE 24C2 MOVE.L D2,(A2)+ MOVE DATA
2274 007200 B4CB CMP.W A3,A2
2275 007202 6F98 BLE DANORM1 NORMALIZE ENTIRE ARRAY
2276 007204 4E75 RTS
2277 *
2278 *
2279 * NORMALIZE ECG, CAROTID, AND PCG TRANSFORMS... DIVIDE
2280 * ALL SAMPLES BY THE MAX AND MULTIPLY BY 4095.
2281 * A0,A1 <--> APU ADDRESSES
2282 * A2,A3 <--> START AND END OF ARRAY
2283 *
2284 *
2285 DAFIX STPOIN2.L APUOPER,A0,APUCOM,A1
2285 007206 207C00050001 MOVE.L #APUOPER,A0
2285 00720C 227C00050011 MOVE.L #APUCOM,A1
2286 STPOIN2.W TREGST,A2,TRECGCHK,A3
2286 007212 347C1B00 MOVE.W #TREGST,A2
2286 007216 367C20F0 MOVE.W #TRECGCHK,A3
2287 00721A 4EB87162 JSR DAMAX
2288 00721E 347C1B00 MOVE.W #TREGST,A2
2289 007222 4EB87172 JSR DANORM
2290 STPOIN2.W TRCARST,A2,TRCAREN,A3
2290 007226 347C2100 MOVE.W #TRCARST,A2
2290 00722A 367C2300 MOVE.W #TRCAREN,A3
2291 00722E 4EB87162 JSR DAMAX
2292 007232 347C2100 MOVE.W #TRCARST,A2
2293 007236 4EB87172 JSR DANORM
2294 00723A 347C2300 MOVE.W #PCGENST,A2
2295 00723E 36787F10 MOVE.W PCGENDE,A3
2296 007242 4EB87162 JSR DAMAX
2297 007246 347C2300 MOVE.W #PCGENST,A2
2298 00724A 4EB87172 JSR DANORM
2299 00724E 6000003C BRA DAFIXB
2300 *
2301 *
2302 * TAKE SQUARE ROOT OF POWER SPECTRUM -> FOURIER TRANSFORM
2303 * IN 32-BIT FIXED POINT (FOR DISPLAY PURPOSES)

```

```

2304      *
2305 007252 2412 PSTOFT MOVE.L (A2),D2
2306          APUWR D2,A0
2306 007254 3E3C0003 MOVE.W #$3,D7
2306 007258 1082 @213 MOVE.B D2,(A0)
2306 00725A E09A ROR.L #$8,D2
2306 00725C 51CFFFFA DBRA D7,@213
2307          APU SQRT
2307 007260 13FC0001
          00050011 MOVE.B #SQRT,APUCOM
2307 007268 4E722300 STOP #$2300
2308          APU FIXD
2308 00726C 13FC001E
          00050011 MOVE.B #FIXD,APUCOM
2308 007274 4E722300 STOP #$2300
2309          APURD A0,D2
2309 007278 3E3C0003 MOVE.W #$3,D7
2309 00727C E19A @216 ROL.L #$8,D2
2309 00727E 1410 MOVE.B (A0),D2
2309 007280 51CFFFFA DBRA D7,@216
2310 007284 24C2 MOVE.L D2,(A2)+           MOVE DATA
2311 007286 B4CB CMP.W A3,A2
2312 007288 6FC8 BLE PSTOFT
2313 00728A 4E75 RTS
2314      *
2315      * NORMALIZE FREQUENCY DOMAIN DATA. TAKE SQUARE ROOT OF POWER
2316      * SPECTRUM TO GET FT - CONVERT TO 32-BIT FIXED POINT. THE
2317      * NORMALIZE DATA.... DIVIDE SAMPLES BY MAX AND MULTIPLY BY
2318      * 4095. A0,A2 <--> APU ADDRESSES, A2,A3 <--> START AND END
2319      *
2320          DAFIXB STPOIN2.L APUOPER,A0,APUCOM,A1
2320 00728C 207C00050001 MOVE.L #APUOPER,A0
2320 007292 227C00050011 MOVE.L #APUCOM,A1
2321          STPOIN2.W XRST,A2,XRENH,A3
2321 007298 347C3700 MOVE.W #XRST,A2
2321 00729C 367C3EFC MOVE.W #XRENH,A3
2322 0072A0 4EB87252 JSR PSTOFT
2323 0072A4 347C3700 MOVE.W #XRST,A2
2324 0072A8 4EB87162 JSR DAMAX
2325 0072AC 347C3700 MOVE.W #XRST,A2
2326 0072B0 4EB87172 JSR DANORM
2327          STPOIN2.W TMPSTB,A2,TMPENB,A3
2327 0072B4 347C5700 MOVE.W #TMPSTB,A2
2327 0072B8 367C5EFC MOVE.W #TMPENB,A3
2328 0072BC 4EB87252 JSR PSTOFT
2329 0072C0 347C5700 MOVE.W #TMPSTB,A2
2330 0072C4 4EB87162 JSR DAMAX
2331 0072C8 347C5700 MOVE.W #TMPSTB,A2
2332 0072CC 4EB87172 JSR DANORM
2333 0072D0 600000016 BRA DA
2334      *
2335      *
2336      * CLEAR SCREEN
2337      *
2338          BLANK SPACE
2338 0072D4 4BF872E4 LEA SPAC,A5
2338 0072D8 4DF872E6 LEA SPCE,A6
2338          TRP14 OUT1CR
2338 0072DC 1E3C00E3 MOVE.B #OUT1CR,D7
2338 0072E0 4E4E TRAP #14
2339 0072E2 4E75 RTS

```

```

2340 0072E4 20    SPAC DC.W   '
2341 0072E6 20    SPCE DC.W   '
2342      *
2343 0072E8 33FC0800
                  00040000 DA MOVE.W #$800,DACH1
2344 0072F0 33FC0000
                  00040004 MOVE.W #0,DACH2
2345 0072F8 13FC0000
                  00010021 MOVE.B #HLTIMR,TCR      HALT TIMER USING TCR HALT CODE
2346 007300 343C001E      MOVE.W #30,D2
2347      DAMEN SPACE
2347 007304 4BF872E4      LEA SPAC,A5
2347 007308 4DF872E6      LEA SPCE,A6
2347      TRP14 OUT1CR
2347 00730C 1E3C00E3      MOVE.B #OUT1CR,D7
2347 007310 4E4E      TRAP #14
2348 007312 51CAFFFO      DBRA D2,DAMEN
2349      *
2350      * DISPLAY OPTIONS
2351      *
2352      DAOPT DSPLOPT MSG,MSGE
2352 007316 4BF875F6      LEA MSG,A5
2352 00731A 4DF87628      LEA MSGE,A6
2352      TRP14 OUT1CR
2352 00731E 1E3C00E3      MOVE.B #OUT1CR,D7
2352 007322 4E4E      TRAP #14
2353 007324 4EB872D4      JSR BLANK
2354 007328 4EB872D4      JSR BLANK
2355      DSPLOPT OPT1,OPT1E
2355 00732C 4BF8762A      LEA OPT1,A5
2355 007330 4DF8765E      LEA OPT1E,A6
2355      TRP14 OUT1CR
2355 007334 1E3C00E3      MOVE.B #OUT1CR,D7
2355 007338 4E4E      TRAP #14
2356      DSPLOPT OPT2,OPT2E
2356 00733A 4BF87660      LEA OPT2,A5
2356 00733E 4DF8769A      LEA OPT2E,A6
2356      TRP14 OUT1CR
2356 007342 1E3C00E3      MOVE.B #OUT1CR,D7
2356 007346 4E4E      TRAP #14
2357      DSPLOPT OPT3,OPT3E
2357 007348 4BF8769C      LEA OPT3,A5
2357 00734C 4DF876D6      LEA OPT3E,A6
2357      TRP14 OUT1CR
2357 007350 1E3C00E3      MOVE.B #OUT1CR,D7
2357 007354 4E4E      TRAP #14
2358      DSPLOPT OPT4,OPT4E
2358 007356 4BF876D8      LEA OPT4,A5
2358 00735A 4DF87718      LEA OPT4E,A6
2358      TRP14 OUT1CR
2358 00735E 1E3C00E3      MOVE.B #OUT1CR,D7
2358 007362 4E4E      TRAP #14
2359      DSPLOPT OPT5,OPT5E
2359 007364 4BF8771A      LEA OPT5,A5
2359 007368 4DF8775C      LEA OPT5E,A6
2359      TRP14 OUT1CR
2359 00736C 1E3C00E3      MOVE.B #OUT1CR,D7
2359 007370 4E4E      TRAP #14
2360      DSPLOPT OPT6,OPT6E
2360 007372 4BF8775E      LEA OPT6,A5
2360 007376 4DF8779C      LEA OPT6E,A6

```

```

2360           TRP14 OUT1CR
2360 00737A 1E3C00E3      MOVE.B #OUT1CR,D7
2360 00737E 4E4E   TRAP #14
2361           DSPLLOPT OPT7,OPT7E
2361 007380 4BF8779E      LEA OPT7,A5
2361 007384 4DF877E0      LEA OPT7E,A6
2361           TRP14 OUT1CR
2361 007388 1E3C00E3      MOVE.B #OUT1CR,D7
2361 00738C 4E4E   TRAP #14
2362           DSPLLOPT OPT8,OPT8E
2362 00738E 4BF877E2      LEA OPT8,A5
2362 007392 4DF87826      LEA OPT8E,A6
2362           TRP14 OUT1CR
2362 007396 1E3C00E3      MOVE.B #OUT1CR,D7
2362 00739A 4E4E   TRAP #14
2363           DSPLLOPT OPT9,OPT9E
2363 00739C 4BF87828      LEA OPT9,A5
2363 0073A0 4DF87862      LEA OPT9E,A6
2363           TRP14 OUT1CR
2363 0073A4 1E3C00E3      MOVE.B #OUT1CR,D7
2363 0073A8 4E4E   TRAP #14
2364           DSPLLOPT OPTA,OPTAE
2364 0073AA 4BF87864      LEA OPTA,A5
2364 0073AE 4DF87898      LEA OPTAE,A6
2364           TRP14 OUT1CR
2364 0073B2 1E3C00E3      MOVE.B #OUT1CR,D7
2364 0073B6 4E4E   TRAP #14
2365           DSPLLOPT OPTB,OPTBE
2365 0073B8 4BF8789A      LEA OPTB,A5
2365 0073BC 4DF878D4      LEA OPTBE,A6
2365           TRP14 OUT1CR
2365 0073C0 1E3C00E3      MOVE.B #OUT1CR,D7
2365 0073C4 4E4E   TRAP #14
2366           DSPLLOPT OPTC,OPTCE
2366 0073C6 4BF878D6      LEA OPTC,A5
2366 0073CA 4DF8790E      LEA OPTCE,A6
2366           TRP14 OUT1CR
2366 0073CE 1E3C00E3      MOVE.B #OUT1CR,D7
2366 0073D2 4E4E   TRAP #14
2367           DSPLLOPT OPTF,OPTFE
2367 0073D4 4BF87910      LEA OPTF,A5
2367 0073D8 4DF87944      LEA OPTFE,A6
2367           TRP14 OUT1CR
2367 0073DC 1E3C00E3      MOVE.B #OUT1CR,D7
2367 0073E0 4E4E   TRAP #14
2368           *
2369           * ENTER OPTION
2370           *
2371 0073E2 4EB872D4      JSR BLANK
2372 0073E6 4EB872D4      JSR BLANK
2373 0073EA 4BF87946      NTROPT LEA ENTR,A5
2374 0073EE 4DF8795C      LEA ENTRE,A6
2375           TRP14 OUTPUT
2375 0073F2 1E3C00F3      MOVE.B #OUTPUT,D7
2375 0073F6 4E4E   TRAP #14
2376           TRP14 INCHE          WAIT FOR SINGLE CHARACTER INPUT
2376 0073F8 1E3C00F7      MOVE.B #INCHE,D7
2376 0073FC 4E4E   TRAP #14
2377           *
2378 0073FE 0C000031      CMP.B #$31,D0
2379 007402 67000068      BEQ ECGCAR

```

```

2380 007406 0C000032      CMP.B #$$32,D0
2381 00740A 670000FC      BEQ PCGETR
2382 00740E 0C000033      CMP.B #$$33,D0
2383 007412 6700007E      BEQ ECGTR
2384 007416 0C000034      CMP.B #$$34,D0
2385 00741A 6700009C      BEQ CARETR
2386 00741E 0C000035      CMP.B #$$35,D0
2387 007422 670000BA      BEQ CARTR
2388 007426 0C000036      CMP.B #$$36,D0
2389 00742A 670000FE      BEQ PCGCTR
2390 00742E 0C000037      CMP.B #$$37,D0
2391 007432 6700011C      BEQ PCGSYS
2392 007436 0C000038      CMP.B #$$38,D0
2393 00743A 6700013C      BEQ PCGDIA
2394 00743E 0C000039      CMP.B #$$39,D0
2395 007442 67000162      BEQ SYSFT
2396 007446 0C000041      CMP.B #$$41,D0
2397 00744A 67000182      BEQ SYSPS
2398 00744E 0C000042      CMP.B #$$42,D0
2399 007452 67000166      BEQ DIAFT
2400 007456 0C000043      CMP.B #$$43,D0
2401 00745A 67000186      BEQ DIAPS
2402 00745E 0C000045      CMP.B #$$45,D0
2403 007462 66000004      BNE NTROPT1
2404 007466 4E75 RTS
2405 007468 6000FE7E      NTROPT1 BRA DA
2406 *
2407 *
2408 *
2409 *
2410 ****
2411 *          D/A DISPLAY ROUTINES
2412 ****
2413 *          A0 <--> STARTING ADDRESS CHANNEL 1
2414 *          A1 <--> STARTING ADDRESS CHANNEL 2
2415 *          A2 <--> ENDING ADDRESS CHANNEL 1
2416 *          A3 <--> ENDING ADDRESS CHANNEL 2
2417 *          D0 <--> SAMPLING PERIOD
2418 *          D1 <--> WORD/LONG WORD INDICATOR
2419 *          D3 <--> SAMPLING CODE (FOR CHANNEL 2)
2420 ****
2421 *          DISPLAY ECG AND CAROTID PULSE ON CHANNELS 1 AND 2
2422 *
2423 00746C 307C0900      ECGCAR MOVE.W #ECGSTRT,A0
2424 007470 327C0C00      MOVE.W #CARSTRT,A1
2425 007474 347C0C00      MOVE.W #ECGEND,A2
2426 007478 367C0F00      MOVE.W #CARENDA3
2427 00747C 203C000001E8  MOVE.L #ADWNSMP,D0
2428 007482 163C0000      MOVE.B #0,D3
2429 007486 123C0000      MOVE.B #$0,D1
2430 00748A 4EB8795E     JSR DA2CH
2431 00748E 6000FE58     BRA DA
2432 *
2433 *          DISPLAY ECG AND ECG TRANSFORM ON CHANNELS 1 AND 2
2434 *
2435 007492 307C0900      ECGTR MOVE.W #ECGSTRT,A0
2436 007496 327C1B00      MOVE.W #TRECGST,A1
2437 00749A 347C0C00      MOVE.W #ECGEND,A2
2438 00749E 367C20F0      MOVE.W #TRECGCHK,A3
2439 0074A2 203C000001E8  MOVE.L #ADWNSMP,D0
2440 0074A8 163C0000      MOVE.B #0,D3

```

```

2441 0074AC 123C0001      MOVE.B #1,D1
2442 0074B0 4EB8795E       JSR DA2CH
2443 0074B4 6000FE32       BRA DA
2444 *
2445 * DISPLAY CAROTID AND ECG TRANSFORM ON CHANNELS 1 AND 2
2446 *
2447 0074B8 307C0C00      CARETR MOVE.W #CARSTRT,A0
2448 0074BC 327C1B00       MOVE.W #TRECGST,A1
2449 0074C0 347C0F00       MOVE.W #CARENDA2
2450 0074C4 367C20F0       MOVE.W #TRECGCHK,A3
2451 0074C8 203C000001E8   MOVE.L #ADWNSMP,D0
2452 0074CE 163C0000       MOVE.B #0,D3
2453 0074D2 123C0001       MOVE.B #1,D1
2454 0074D6 4EB8795E       JSR DA2CH
2455 0074DA 6000FE0C       BRA DA
2456 *
2457 * DISPLAY CAROTID AND CAROTID TRANSFORM ON CHANNELS 1 AND 2
2458 *
2459 0074DE 307C0C00      CARTR MOVE.W #CARSTRT,A0
2460 0074E2 D0F87F00       ADD.W QRS1,A0
2461 0074E6 327C2100       MOVE.W #TRCARST,A1
2462 0074EA 347C0F00       MOVE.W #CARENDA2
2463 0074EE 367C2300       MOVE.W #TRCAREN,A3
2464 0074F2 203C000001E8   MOVE.L #ADWNSMP,D0
2465 0074F8 163C0000       MOVE.B #0,D3
2466 0074FC 123C0001       MOVE.B #1,D1
2467 007500 4EB8795E       JSR DA2CH
2468 007504 6000FDE2       BRA DA
2469 *
2470 * DISPLAY PCG AND ECG TRANSFORM ON CHANNELS 1 AND 2
2471 *
2472 007508 307C0F00      PCGETR MOVE.W #PCGSTRT,A0
2473 00750C 327C1B00       MOVE.W #TRECGST,A1
2474 007510 347C1B00       MOVE.W #PCGEND,A2
2475 007514 367C20F0       MOVE.W #TRECGCHK,A3
2476 007518 707A MOVE.L #ADSMPL,D0
2477 00751A 123C0001       MOVE.B #1,D1
2478 00751E 163C0003       MOVE.B #3,D3
2479 007522 4EB8795E       JSR DA2CH
2480 007526 6000FD00       BRA DA
2481 *
2482 * DISPLAY PCG AND CAROTID TRANSFORM AN CHANNELS 1 AND 2
2483 *
2484 00752A 307C0F00      PCGCTR MOVE.W #PCGSTRT,A0
2485 00752E D0F87F08       ADD.W PCGS1A,A0
2486 007532 327C2100       MOVE.W #TRCARST,A1
2487 007536 347C1B00       MOVE.W #PCGEND,A2
2488 00753A 367C2300       MOVE.W #TRCAREN,A3
2489 00753E 707A MOVE.L #ADSMPL,D0
2490 007540 123C0001       MOVE.B #1,D1
2491 007544 163C0003       MOVE.B #3,D3
2492 007548 4EB8795E       JSR DA2CH
2493 00754C 6000FD9A       BRA DA
2494 *
2495 * DISPLAY SYSTOLIC PCG AND ENERGY ON CHANNELS 1 AND 2
2496 *
2497 007550 307C0F00      PCGSYS MOVE.W #PCGSTRT,A0
2498 007554 D0F87F08       ADD.W PCGS1A,A0
2499 007558 327C2300       MOVE.W #PCGENST,A1
2500 00755C 3448 MOVE.W A0,A2
2501 00755E D4F87F0C       ADD.W PCGS2,A2

```

```

2502 007562 36787F0E      MOVE.W PCGENSE,A3
2503 007566 707A      MOVE.L #ADSMPL,D0
2504 007568 123C0001      MOVE.B #1,D1
2505 00756C 163C0000      MOVE.B #0,D3
2506 007570 4EB8795E      JSR DA2CH
2507 007574 6000FD72      BRA DA
2508      *
2509      * DISPLAY DIASTOLIC PCG AND ENERGY CURVE ON CHANNELS 1 AND 2
2510      *
2511 007578 307C0F00      PCGDIA MOVE.W #PCGSTRT,A0
2512 00757C D0F87F08      ADD.W PCGS1A,A0
2513 007580 D0F87F0C      ADD.W PCGS2,A0
2514 007584 32787F0E      MOVE.W PCGENSE,A1
2515 007588 347C0F00      MOVE.W #PCGSTRT,A2
2516 00758C 36787F10      MOVE.W PCGENDE,A3
2517 007590 D4F87F0A      ADD.W PCGS1B,A2
2518 007594 707A      MOVE.L #ADSMPL,D0
2519 007596 123C0001      MOVE.B #1,D1
2520 00759A 163C0000      MOVE.B #0,D3
2521 00759E 4EB8795E      JSR DA2CH
2522 0075A2 6000FD44      BRA DA
2523      *
2524      * DISPLAY SYSTOLE FOURIER TRANSFORM ON CHANNEL 1
2525      *
2526      SYSFT STPOIN2.W TMPSTB,A1,TMPENB,A3
2526 0075A6 327C5700      MOVE.W #TMPSTB,A1
2526 0075AA 367C5EFC      MOVE.W #TMPENB,A3
2527 0075AE 123C0000      MOVE.B #$0,D1
2528 0075B2 4EB879D0      JSR DA2CHFT
2529 0075B6 6000FD30      BRA DA
2530      *
2531      * DISPLAY DIASTOLE FOURIER TRANSFORM ON CHANNEL 1
2532      *
2533      DIAFT STPOIN2.W XRST,A1,XRENH,A3
2533 0075BA 327C3700      MOVE.W #XRST,A1
2533 0075BE 367C3EFC      MOVE.W #XRENH,A3
2534 0075C2 123C0000      MOVE.B #$0,D1
2535 0075C6 4EB879D0      JSR DA2CHFT
2536 0075CA 6000FD1C      BRA DA
2537      *
2538      * DISPLAY SYSTOLE POWER SPECTRUM ON CHANNEL 1
2539      *
2540      SYSPS STPOIN2.W TMPSTB,A1,TMPENB,A3
2540 0075CE 327C5700      MOVE.W #TMPSTB,A1
2540 0075D2 367C5EFC      MOVE.W #TMPENB,A3
2541 0075D6 123C0001      MOVE.B #$1,D1
2542 0075DA 4EB879D0      JSR DA2CHFT
2543 0075DE 6000FD08      BRA DA
2544      *
2545      * DISPLAY DIASTOLE POWER SPECTRUM ON CHANNEL 1
2546      *
2547      DIAPS STPOIN2.W XRST,A1,XRENH,A3
2547 0075E2 327C3700      MOVE.W #XRST,A1
2547 0075E6 367C3EFC      MOVE.W #XRENH,A3
2548 0075EA 123C0001      MOVE.B #$1,D1
2549 0075EE 4EB879D0      JSR DA2CHFT
2550 0075F2 6000FCF4      BRA DA
2551      *
2552 0075F6 20      MSG DC.W ' EDCTS,EDCTD,EDCFS,EDCFD IN $7F16,7F1B,7F1A,7F1E'
2553 007628 20      MSGE DC.W ' '
2554 00762A 20      OPT1 DC.W ' 1. ECG - CHANNEL 1, CAROTID - CHANNEL 2 @ 256 HZ

```

2555 00765E 20 OPT1E DC.W ' ' 1.
2556 007660 20 OPT2 DC.W ' ' 2. PCG - CHANNEL 1, ECG TRANSFORM - CHANNEL 2
2557 007690 20 DC.W ' @ 1024 HZ
2558 00769A 20 OPT2E DC.W ' ' 3.
2559 00769C 20 OPT3 DC.W ' ' ECG - CHANNEL 1, ECG TRANSFORM - CHANNEL 2 @
2560 0076D6 20 OPT3E DC.W ' ' 4.
2561 0076D8 20 OPT4 DC.W ' ' CAROTID - CHANNEL 1, ECG TRANSFORM - CHANNEL 2
2562 00770C 20 DC.W ' @ 256 HZ
2563 007718 20 OPT4E DC.W ' ' 5.
2564 00771A 20 OPT5 DC.W ' ' CAROTID - CHANNEL 1, CAROTID TRANSFORM - CHAN
2565 007752 20 DC.W ' @ 256 HZ
2566 00775C 20 OPT5E DC.W ' ' 6.
2567 00775E 20 OPT6 DC.W ' ' PCG - CHANNEL 1, CAROTID TRANSFORM - CHANNEL
2568 007792 20 DC.W ' @ 1024 HZ
2569 00779C 20 OPT6E DC.W ' ' 7.
2570 00779E 20 OPT7 DC.W ' ' PCG(SYSTOLE) - CHANNEL 1, ENERGY CURVE - CHAN
2571 0077D6 20 DC.W ' @ 1024 HZ
2572 0077E0 20 OPT7E DC.W ' ' 8.
2573 0077E2 20 OPT8 DC.W ' ' PCG(DIASTOLE) - CHANNEL 1, ENERGY CURVE - CHA
2574 00781C 20 DC.W ' @ 1024 HZ
2575 007826 20 OPT8E DC.W ' ' 9.
2576 007828 20 OPT9 DC.W ' ' PCG(SYSTOLE) FOURIER TRANSFORM - CHANNEL 1 @
2577 007862 20 OPT9E DC.W ' ' A. PCG(SYSTOLE) POWER SPECTRUM - CHANNEL 1 500 H
2578 007864 20 OPTA DC.W ' ' B. PCG(DIASTOLE) FOURIER TRANSFORM - CHANNEL 1 @
2579 007898 20 OPTAE DC.W ' ' C. PCG(DIASTOLE) POWER SPECTRUM - CHANNEL 1 @ 50
2580 00789A 20 OPTB DC.W ' ' E. CONTINUE WITH FREQUENCY ANALYSIS/END PROGRAM
2581 0078D4 20 OPTBE DC.W ' ' OPTFE DC.W ' ' ENTR DC.W ' ENTER CHOICE (1-E): '
2582 0078D6 20 OPTC DC.W ' ' ENTRE DC.W ' '

```

2589 ****
2590 * DA2CH
2591 ****
2592 * A0,A2 <--> START,END ADDRESS - CHANNEL 1 DATA
2593 * A1,A3 <--> START,END ADDRESS - CHANNEL 2 DATA
2594 * D0 <--> SAMPLING PERIOD
2595 * D1 <--> WORD/LONG WORD INDICATOR
2596 * D2 <--> SAMPLE VALUE
2597 * D3 <--> SAMPLING CODE
2598 ****
2599 * CALLS FOLLOWING MACROS:
2600 * DATIMER
2601 * TSTIMR
2602 ****
2603 * THIS SUBROUTINE SENDS DATA (12 BITS) TO D/A CHANNELS 1 & 2.
2604 * FOR CASES WHEN TWO SIGNALS WITH DIFFERENT
2605 * SAMPLING RATES ARE DISPLAYED, THE SIGNAL WITH THE LARGER
2606 * SAMPLING PERIOD MUST GO TO CHANNEL 2 USING THE SAMPLING CODE
2607 * THE SAMPLING PERIOD OF THE DATA GOING TO CHANNEL 2 MUST BE
2608 * A FACTOR OF THE SAMPLING PERIOD OF THE DATA GOING TO CHANNEL
2609 * 1. SAMPLING CODE = ((S.P.1./S.P.2)-1).
2610 * D1 IS THE WORD (0)/LONGWORD (1) INDICATOR.
2611 * DA2CH DATIMER INITIALIZATION AND START TIMER
2612 * STPOIN2.L CNTR,A5,CPR,A6 SAMPLING PERIOD MUST BE IN D0
2612 00795E 2A7C0001002D MOVE.L #CNTR,A5
2612 007964 2C7C00010025 MOVE.L #CPR,A6
2612 00796A 2E00 MOVE.L D0,D7
2612 00796C 0FCE0000 MOVEP.L D7,0(A6)
2612 007970 13FC0001
2612 00010035 MOVE.B #1,TSR
2612 007978 13FC0001
2613 00010021 MOVE.B #STRRTIMR,TCR
2613 007980 4204 CLR.B D4
2614 007982 33D800040000 DASIG MOVE.W (A0)+,DACH1
2615 007988 B2CB CMP.W A3,A1
2616 00798A 6D00000A BLT DACA
2617 00798E 343C0000 MOVE.W #$0,D2
2618 007992 6000001E BRA DAC2
2619 007996 0C040000 DACA CMP.B #0,D4
2620 00799A 67000008 BEQ DAC1
2621 00799E 5304 SUBQ.B #1,D4
2622 0079A0 60000010 BRA DAC2
2623 0079A4 1803 DAC1 MOVE.B D3,D4
2624 0079A6 0C010001 CMP.B #$1,D1
2625 0079AA 66000004 BNE DAC3
2626 0079AE 5449 ADD.W #$2,A1
2627 0079B0 3419 DAC3 MOVE.W (A1)+,D2
2628 0079B2 33C200040004 DAC2 MOVE.W D2,DACH2
2629 TSTIMR A2,A0
2629 0079B8 0C390000
2629 00010035 @243 CMP.B #0,TSR
2629 0079C0 67F6 BEQ @243
2629 0079C2 13FC0001
2629 00010035 MOVE.B #1,TSR
2629 0079CA B0CA CMP.W A2,A0
2630 0079CC 6DB4 BLT DASIG
2631 0079CE 4E75 RTS
2632 *

```

```

2634 ****
2635 * DA2CHFT
2636 ****
2637 * A1 <--> START OF FT - CHANNEL 2 DATA; PS
2638 * A3 <--> END OF FT - CHANNEL 2 DATA; PS
2639 * A4 <--> APU OPERAND ENTRY ADDRESS
2640 * D0 <--> SAMPLING PERIOD (800 HZ)
2641 * D1 <--> FT/PS INDICATOR
2642 * D2 <--> SAMPLE VALUE D3 <--> 4095 FLOATING
2643 ****
2644 * CALLS FOLLOWING MACROS:
2645 * DATIMER TSTIMR
2646 ****
2647 *
2648 * DISPLAY FOURIER TRANSFORM ON CHANNEL 2
2649 *
2650 0079D0 287C00050001 DA2CHFT MOVE.L #APUPER,A4
2651 0079D6 263C0CFFF000 MOVE.L #$0CFFF000,D3
2652 0079DC 203C0000009C MOVE.L #156,D0
2653 DATIMER
2653 STPOIN2.L CNTR,A5,CPR,A6
2653 0079E2 2A7C0001002D MOVE.L #CNTR,A5
2653 0079E8 2C7C00010025 MOVE.L #CPR,A6
2653 0079EE 2E00 MOVE.L D0,D7
2653 0079F0 0FCE0000 MOVEP.L D7,0(A6)
2653 0079F4 13FC0001
2653 00010035 MOVE.B #1,TSR
2653 0079FC 13FC0001
2654 00010021 MOVE.B #STRRTIMR,TCR
2654 007A04 2419 DA2CHFT1 MOVE.L (A1)+,D2
2655 007A06 0C010001 CMPB.B #$1,D1
2656 007A0A 66000062 BNE DA2CHFT2
2657 APUWR D2,A4
2657 007A0E 3E3C0003 MOVE.W #$3,D7
2657 007A12 1882 @245 MOVE.B D2,(A4)
2657 007A14 E09A ROR.L #$8,D2
2657 007A16 51CFFFFA DBRA D7,@245
2658 APU FLTD
2658 007A1A 13FC001C
2658 00050011 MOVE.B #FLTD,APUCOM
2658 007A22 4E722300 STOP $$2300
2659 APU PTOD
2659 007A26 13FC0037
2659 00050011 MOVE.B #PTOD,APUCOM
2659 007A2E 4E722300 STOP $$2300
2660 APU FMUL
2660 007A32 13FC0012
2660 00050011 MOVE.B #FMUL,APUCOM
2660 007A3A 4E722300 STOP $$2300
2661 APUWR D3,A4
2661 007A3E 3E3C0003 MOVE.W #$3,D7
2661 007A42 1883 @249 MOVE.B D3,(A4)
2661 007A44 E09B ROR.L #$8,D3
2661 007A46 51CFFFFA DBRA D7,@249
2662 APU FDIV
2662 007A4A 13FC0013
2662 00050011 MOVE.B #FDIV,APUCOM
2662 007A52 4E722300 STOP $$2300
2663 APU FIXD
2663 007A56 13FC001E
2663 00050011 MOVE.B #FIXD,APUCOM

```

```
2663 007A5E 4E722300      STOP #$2300
2664          APURD A4,D2
2664 007A62 3E3C0003      MOVE.W #$3,D7
2664 007A66 E19A @252 ROL.L #$8,D2
2664 007A68 1414 MOVE.B (A4),D2
2664 007A6A 51CFFFFA      DBRA D7,@252
2665 007A6E 33C200040004 DA2CHFT2 MOVE.W D2,DACH2
2666          TSTIMR A3,A1
2666 007A74 0C390000
               00010035 @253 CMP.B #0,TSR
2666 007A7C 67F6 BEQ @253
2666 007A7E 13FC0001
               00010035 MOVE.B #1,TSR
2666 007A86 B2CB CMP.W A3,A1
2667 007A88 6F00FF7A      BLE DA2CHFT1
2668 007A8C 4E75 RTS
2669 *
2670 *
2671 *
2672 *#####
2673 *#####
2674 *#####
2675 ****
2676 *
2677 *
2678 007A8E 4BF87AA2      FIN LEA FINST,A5
2679 007A92 4DF87AB2      LEA FINEND,A6
2680          TRP14 OUT1CR
2680 007A96 1E3C00E3      MOVE.B #OUT1CR,D7
2680 007A9A 4E4E TRAP #14
2681          TRP14 TUTOR
2681 007A9C 1E3C00E4      MOVE.B #TUTOR,D7
2681 007AA0 4E4E TRAP #14
2682 007AA2 54 FINST DC.W 'THATS ALL FOLKS'
2683 007AB2 20 FINEND DC.W '
2684 *
2685 *
```

2687

END

***** TOTAL ERRORS 0-- 0 -- TOTAL LINES 2685

APPROX1680 UNUSED SYMBOL TABLE ENTRIES

@003	0060B0 @010	006178 @016	0062A2 @017	0062B6 @018	0062CA
@022	00630A @030	006488 @037	00653A @053	006768 @061	0067CC
@062	0067DC @063	0067F2 @064	006802 @065	00680E @068	006832
@071	00685A @072	00686A @073	006876 @076	00689A @080	0068D0
@084	006904 @086	00691C @087	00692C @089	00694E @093	006982
@095	00699A @096	0069AA @097	0069BC @098	0069CC @100	0069E4
@101	0069F4 @104	006A18 @105	006A28 @107	006A40 @108	006A50
@111	006A74 @112	006A80 @116	006AB2 @118	006ACE @120	006B08
@123	006B2C @126	006B50 @128	006B64 @130	006B7C @133	006BA0
@135	006BB8 @137	006BD2 @139	006BEA @146	006C7A @147	006CA4
@148	006CB4 @152	006CE4 @153	006CF0 @156	006D88 @159	006DB0
@163	006DE0 @165	006E2C @166	006E38 @169	006E5C @171	006E74
@185	0070A6 @186	0070B2 @187	0070C6 @190	0070EA @192	007106
@198	007158 @199	007176 @201	00718E @202	0071A2 @204	0071BA
@206	0071D2 @209	0071F6 @213	007258 @216	00727C @243	0079B8
@245	007A12 @249	007A42 @252	007A66 @253	007A74 ACOS	000006
AD1	00622A AD2	006238 ADCH1	020001 ADCH2	020003 ADCH3	020005
ADCISR	00621C ADCNVRT	0061D0 ADCONT	00616A ADCONV	006126 ADEND	00623E
ADEXADD	000070 ADFIN	006204 ADFINE	00621A ADREAD	02000C ADSMPL	00007A
ADST	0061EA ADSTE	006202 ADWAIT	0061AC ADWNSMP	0001E8 APISR	006240
APUCOM	050011 APUEACK	04000E APUEXAD	000070 APUOPER	050001 ASIN	000005
ATAN	000007 BLANK	0072D4 C2DFSQ	00641E C2DFSQ1	006444 CAEN	00641C
CALCFIM	0068BC CALCFL	00693A CALCT	0067EA CALCU	0069B8 CALCW	006754
CAR	0063CA CARCNV	000010 CARDWN	000008 CAREND	000F00 CARENEW	000F00
CARETR	0074B8 CARSNEW	000C00 CARSTRT	000C00 CARTR	0074DE CAST	0063EE
CCNVL	006470 CCNVLA	006494 CDCRTC	0064CA CDCRTC1	0064E6 CDCRTC2	0064F0
CHSD	000034 CHSF	000015 CHSS	000074 CNTR	01002D CNVLV	00608E
CNVLV1	006096 CNVLV2	00609C CNVLV3	0060C4 COS	000003 COUNTER	007F48
CPR	010025 CT1T2	0064A0 D6464A	006572 D6464B	006598 DA	0072E8
DA2CH	00795E DA2CHFT	0079D0 DA2CHFT1	007A04 DA2CHFT2	007A6E DAC1	0079A4
DAC2	0079B2 DAC3	0079B0 DACA	007996 DACH1	040000 DACH2	040004
DACH3	040008 DADD	00002C DAFIX	007206 DAFIXB	00728C DAMAX	007162
DAMAX1	007164 DAMAX2	00716C DAMEN	007304 DANORM	007172 DANORM1	00719C
DAOPT	007316 DASIG	007982 DCRTC	007F06 DDIV	00002F DIAFT	0075BA
DIAPS	0075E2 DMUL	00002E DMUU	000036 DS2DEL	00001B DSUB	00002D
DVD6464006564	E1	006100 E1E	006124 ECEN	006294 ECG	00624A
ECGCAR	00746C ECGCNV	000010 ECGDWN	000008 ECGEND	000C00 ECGENEW	000C00
ECGERR	00638E ECGSNEW	000900 ECGSTRT	000900 ECGTR	007492 ECNVL	0062F2
ECST	00626E EDC	00650E EDC1	006522 EDCFDIA	007F1E EDCFSYS	007F1A
EDCTDIA	007F18 EDCTSYS	007F16 EDFSQ	0062DE EDFSQ	0062D4 EMOVE	006296
ENDTBL	0060E2 ENTR	007946 ENTRE	00795C EQRS	006314 EQRS1	006322
EQRS2	006328 EQRS3	006340 EQRS4	006356 EQRS5	006364 EQRS6	006380
ERROR1	000000 EXP	00000A FADD	000010 FDIV	000013 FFT	006A8A
FFT0	006AAC FFT1	006C40 FFT2	006C44 FFT3	006C4E FFT3LP	006C20
FFT4	006D2C FFT5	006D40 FFT6	006D80 FFTLP4	006D08 FFTLP5	006D02
FFTM	006EB6 FFTME	006EC4 FFT05	006D50 FFTOLP5	006C6E FIN	007A8E
FINDMAX	006394 FINDMX	00639A FINEND	007AB2 FINST	007AA2 FIXD	00001E
FIXS	00001F FLCN1	006E18 FLCN2	006E1E FLCN3	006E80 FLCNE	006E92
FLEDC	007094 FLEDC1	0070BE FLTD	00001C FLTS	00001D FMAX	0063A2
FMUL	000012 FSUB	000011 GETNUMA	0000E2 GETNUMD	0000E1 GOFIN	00605C
HAM	006E9C HAM46	EB851E HAM54	8A3D70 HAME	006EB4 HAMM	006ADE
HAMM1	006B60 HEX2DEC	0000EC HLTIIMR	000000 HOLD	02000E I 007F30	
INCHE	0000F7 J 007F32	L 007F2A LE	007F2C LE1	007F2E	
LINKIT	0000FD LN	000009 LNN	00000A LOG	000008 MAIN	006012

MEMCLR	006006	MEMEND	005FFE	MEMST	000900	MSG	0075F6	MSGE	007628
N	000400	NEWTBL	0060DE	NM1	0003FF	NOPAPU	000000	NTROPT	0073EA
NTROPT	1007468	NV2	000200	OPT1	00762A	OPT1E	00765E	OPT2	007660
OPT2E	00769A	OPT3	00769C	OPT3E	0076D6	OPT4	0076D8	OPT4E	007718
OPT5	00771A	OPT5E	00775C	OPT6	00775E	OPT6E	00779C	OPT7	00779E
OPT7E	0077E0	OPT8	0077E2	OPT8E	007826	OPT9	007828	OPT9E	007862
OPTA	007864	OPTAE	007898	OPTB	00789A	OPTBE	0078D4	OPTC	0078D6
OPTCE	00790E	OPTF	007910	OPTFE	007944	OUT1CR	0000E3	OUTCH	0000F8
OUTPUT	0000F3	PCDEN	006644	PCDST	006628	PCEEN	00665E	PCEN	00660A
PCEST	006646	PCGNV	000020	PCGCTR	00752A	PCGDIA	007578	PCGDWN	000002
PCGEND	001B00	PCGENDE	007F10	PCGENEW	001B00	PCGENSE	007F0E	PCGENST	002300
PCGETR	007508	PCGF	006F02	PCGS1A	007F08	PCGS1B	007F0A	PCGS2	007F0C
PCGSNEW	0000F00	PCGSTRT	000F00	PCGSYS	007550	PCGT	0065A0	PCSEN	006626
PCSSST	00660C	PCST	0065EE	PFDFT	006F90	PFDFTE	006FA2	PFEDC	007062
PFEDC1	00708A	PFEEN	006FBC	PFEN	006F7A	PFEST	006FA4	PFMDIA	007022
PFMDIA1	00703C	PFMDIA2	007044	PFMDIA3	007054	PFMSYS	006FBE	PFMSYS1	006FE6
PFMSYS2	0006FEE	PFMSYS3	006FFE	PFPSYS	00700C	PFPSYS1	007018	PFSFT	006F7C
PFSFT	006F8E	PFST	006F58	PNT2HX	0000E9	PNT4HX	0000E8	PNT6HX	0000E7
PNT8HX	0000E6	POPD	000038	POPF	000018	POPS	000078	PS	006EC6
PSE	006EDE	PSTOFT	007252	PTCD1	0066F4	PTCNVD	0066DC	PTCNVS	0066AE
PTCS1	0066D2	PTEDC	0066FE	PTEDC1	00674A	PTOD	000037	PTOF	000017
PTOS	000077	PTSQ1	00669C	PTSQU	006660	PUPI	00001A	PUTHEX	0000EA
PWR	00000B	QRS1	007F00	QRS2	007F02	QUIT	006064	QUITE	00608C
QUOT	007F44	SADD	00006C	SDIV	00006F	SEQNUM	007F12	SIN	000002
SMPS	006EE0	SMPSE	006F00	SMUL	00006E	SMUU	000076	SPAC	0072E4
SPCE	0072E6	SQRT	000001	SSUB	00006D	START	0000E5	STRTRIMR	000001
SYSFT	0075A6	SYSPS	0075CE	T1TOT2	000098	T2PEAK	007F04	TAN	000004
TCR	010021	TMPENB	005EFC	TMPSTA	003700	TMPSTB	005700	TMPSTC	004700
TRCAREN	002300	TRCARST	002100	TRECGCHK	0020F0	TRECGEN	0020FC	TRECGST	001B00
TSR	010035	TUTOR	0000E4	TWOCOMA	0063C2	TWOCOMP	0063AC	UI	007F40
UR	007F3C	USRFNCS	0060CE	UTRER1	0060E6	VDR	007F00	WI	007F38
WR	007F34	XCHD	000039	XCHF	000019	XCHS	000079	XIEN	005700
XIST	004700	XREN	004700	XRENH	003EFC	XRST	003700		